THE ROLE AND REGULATION OF ASTERLESS IN THE CENTROSOME CYCLE



Zsofia A. Novak

Lincoln College

University of Oxford

A thesis submitted for the degree of

Doctor of Philosophy

Trinity Term 2014

ACKNOWLEDGEMENTS

First and foremost I would like to thank my supervisor, Jordan, for being the best mentor anyone could wish for. He has provided me with endless support, excellent advice and suggestions whilst also giving me the freedom to choose and develop my projects. Our discussions have always been fuel for my motivation, and I have learnt so much from him. I have thoroughly enjoyed the whole of my DPhil research and I believe Jordan's guidance has the greatest part in this.

I would like to express my gratitude to Matthew Whitby for his expert guidance during my Diploma and rotation projects. He taught me so much about planning my research, precision, quality work and diligence – I feel that what I learnt from him and his lab have provided the foundation of my DPhil. I would also like to thank Matthew and Francis Barr for their expert advice and help, as my Thesis Committee, during my DPhil project.

I thank the Wellcome Trust for supporting my DPhil with very generous funding. I am very fortunate to have been a part of the Chromosome and Developmental Biology DPhil Programme; for me, joining this programme was a dream come true, and it gave me a DPhil experience that was so much more than a research project. Thank you to the whole Management Committee, especially Matthew, for building such a great Programme.

I have been so fortunate to learn from Paul and Alan. They have taught me all about microscopy, were always there to help me, and our brainstorm sessions were a constant source of advice and motivation to me during these past years!

I would like to thank everyone in the Raff lab for all the help over the years, especially Saroj for organizing everything so amazingly and always being there to help all of us. I would like to say a special thank you to Cat, Janina and Violet for all the helpful discussions and support over the years, which have helped my work so much.

I am so grateful for my amazing friends, Nicole and Annika. They have made my time in Oxford so much fun; they share my best memories from these past years, and have always been there for me in everything. I have been so lucky to be a part of Lincoln College Boat Club; I spent so many happy hours and met wonderful friends here. LCBC will always remain very special to me.

The past four years were a journey together with Dave, Laura, Sharon and Stephen. I am so happy to have met you guys and thank you for all the great times we shared – in and out of labs or seminar rooms!

I am so thankful for having the most loving, supportive, amazing partner in my life. Sam, you have been my constant source of happiness during the past few years, and were always with me during the best parts of my DPhil, and helped me through the harder times. You mean so much to me, I can't thank you enough.

I'm so fortunate to have the never-ending love and support of my beloved family. Edes Mamim, koszonom a draga szeretetedet, a rengeteg gondoskodast, torodest, figyelmesseget amit meg igy felnott letemre is mindig kapok Toled, es ami a legnehezebb reszeit is annyira megkonnyitette az elmult eveknek. Draga Oktu, koszonom hogy mindig mindenben segitesz es szamithatok Rad, es koszonom a sok tudomanyos beszelgetesunk – hiszem, hogy ezeknek oriasi resze volt abban, ahogy a munkam alakult, es abban, hogy erre a dolgozatra most igazan buszke lehetek. Imadlak Titeket, kimondhatatlanul! Edes Mazi es Tomi, koszonom hogy a vilag legjobb testverei vagytok, koszonom Nektek, hogy mindig mindenben szamithatok Ratok – imadlak mindkettotoket es buszke vagyok hogy a testveretek vagyok. Draga Nagyikam es edes Greti Nagymamam, koszonom a rengeteg szeretetteteket, torodeseteket es tamogatasotokat – imadlak Titeket es koszonom, hogy mindig is biztattatok, hittetek bennem!

THESIS SUMMARY

The role and regulation of Asterless in the centrosome cycle

Zsofia A. Novak, Lincoln College
Submitted for degree of Doctor of Philosophy, Trinity Term 2014

Centrosomes are the main microtubule organizing centres in animal cells and are formed by a pair of centrioles together with surrounding pericentriolar material (PCM). Cycling cells duplicate their centrosomes strictly once per cell cycle. This process is driven by the semi-conservative duplication of the centrioles that are found at the centrosome core. During the exit from mitosis the two centrioles within the single inherited centrosome separate, and upon the start of *S*-phase each of these inherited mother centrioles assembles an adjacent daughter at its side. This process results in two complete centrosomes that can form the poles of the mitotic spindle, and thus segregate evenly to the next cell generation.

The formation of a daughter centriole suppresses the initiation of new duplication events from the same templating mother centriole until this daughter separates – disengages – at the end of the cell cycle. This regulation – that acts to repress centriole amplification – is summarized in the 'licensing model of centriole duplication' (Tsou and Stearns, 2006). This model states that centriole disengagement provides the license for the re-duplication of mother centrioles. Importantly, experiments show that while abolishing centriole engagement is sufficient to allow mother centrioles to re-duplicate within the same cycle, it is insufficient to allow daughter centrioles the assembly of a granddaughter before they mature into mothers towards the end of their first cell cycle. The molecular nature of this daughter-to-mother transition remains mysterious.

In this thesis I show that in *Drosophila* embryos the essential centriole duplication protein Asl is not incorporated into daughter centrioles as they assemble during *S*-phase, but is only incorporated once mother and daughter separate at the end of mitosis. The initial incorporation of Asterless (Asl) is irreversible, and is dependent on centriolar DSas-4. Crucially, Asl incorporation is essential for daughter centrioles to mature into mothers that can support centriole duplication. I propose that Asl acts as a permanent *primary license* that allows new centrioles to duplicate for the first time. Once acquired, this primary license is not lost but rather further regulation is taken over by the re-duplication licensing mechanism, disengagement. This work extends the previously proposed licensing model to also explain how new centrioles are licensed for their first duplication event.

TABLE OF CONTENTS

Chapter 1: Introduction 1

1.1 Centrioles, centrosomes and cilia 1

1.1.1 The structure of centrioles 1

1.1.2 The centrosome 6

1.1.2.1 Centrosome organization and assembly 7

1.1.2.2 The importance of centrosomes 10

1.1.3 Cilia 12

1.1.4 Centrosomes and cilia in human disease 15

1.2 The centrosome cycle 18

1.2.1 The molecular assembly of centrioles 20

1.2.1.1 ZYG-1/Sak/Plk4: the triggers of centriole assembly 21

1.2.1.2 The SAS-6, SAS-5 and SAS-4 protein families 22

1.2.1.3 Asterless/Cep152 26

1.2.2 Regulation of the centrosome cycle 30

1.2.2.1 Temporal regulation/Cell cycle control 32

1.2.2.2 Numerical regulation 34

1.2.2.3 The licensing model of centrosome duplication 36

1.3 The syncytial blastoderm stage *Drosophila* embryo 39

1.3.1 The early embryonic development of Drosophila 39

1.3.2 The importance of centrosomes during the early development of Drosophila 41

1.3.3 The centrosome cycle of the syncytial blastoderm stage Drosophila embryo 42

1.4 Live imaging of the centrosome cycle in the syncytial blastoderm stage *Drosophila* embryo 44

1.5 Thesis outline 47

Chapter 2: Materials and Methods 48

2.1 Fly husbandry 48

2.1.1 Fly handling 48

2.1.2 Drosophila stocks 48

2.1.2.1 Generation of the asl^{B46} mutant line 50

2.1.2.2 Transgenic lines 50

2.2 Molecular Biology 51

2.2.1 Construction of transformation vectors for the generation of transgenic Drosophila lines 51

2.2.2 Construction of vectors for in vitro RNA production (for RNA-microinjection experiments) 53

2.2.3 Plasmid mutagenesis 54

2.2.4 Purification of genomic DNA from Drosophila 57

2.2.5 Diagnostic PCR reactions 57

2.2.6 DNA sequencing 57
2.2.7 In vitro RNA transcription 58
2.3 Biochemistry 59
2.3.1 Immunoprecipitation of proteins from Drosophila embryo cytoplasm extracts 59
2.3.1.1 Preparation of cytoplasm extracts 59
2.3.1.2 Preparation of pulldown beads 60
2.3.1.3 Immunoprecipitation 60
2.3.2 Preparation of Drosophila embryo and brain lysates for protein expression analysis 61
2.3.3 SDS-PAGE 61
2.3.4 Western blotting 62
2.4 Cell biology 62
2.4.1 Preparation of embryos for live imaging analysis 62
2.4.2 Microinjection of antibodies or RNA into living embryos 63
2.4.3 Fixation and staining of embryos for immunofluorescence analysis 63
2.4.4 Fixation and staining of 3rd instar larval brains for immuno-fluorescence analysis 64
2.5 Microscopy 65
2.5.1 Live confocal imaging of Drosophila embryos 65
2.5.2 Photobleaching 67
2.5.3 Super-resolution imaging of living Drosophila embryos 68
2.5.4 Immunofluorescence imaging of fixed Drosophila embryos and brains 68
2.6 Image analysis and statistics 68
2.6.1 Analysis of live imaging data acquired on the Perkin Elmer ERS Spinning Disc confocal system 68
2.6.2 Analysis of live imaging data acquired on the OMX V3 super-resolution imaging system 71
2.6.3 Image processing for presentation 71
Chapter 3: The dynamic localization of DSas-4-GFP and Asl-GFP at centrosomes in the *Drosophila* embryo 73
3.1 Summary 73
3.2 Results 75
3.2.1 The centrosomal incorporation of DSas-4-GFP 75
3.2.1.1 Generation of a Drosophila line that expresses endogenous levels of DSas-4-GFP 75
3.2.1.2 DSas-4-GFP is incorporated into daughter centrioles as they assemble 75
3.2.1.3 Centrosomal recruitment of DSas-4-GFP is restricted to *S*-phase of the embryonic cell cycle, and by mitosis DSas-4-GFP within daughter centrioles is stably fixed 84
3.2.2 The centrosomal incorporation of Asl-GFP 88
3.2.2.1 Generation of an asl null allele 88
3.2.2.2 Asl-GFP is first recruited to daughter centrioles at around the time they disengage from their mothers 91
3.2.2.3 Half of centrosomal Asl-GFP molecules are in dynamic exchange with cytoplasmic molecules while half are stably associated with the mother centriole 97

3.3 Discussion 99
3.3.1 Physiological expression of DSas-4-GFP and Asl-GFP in living Drosophila embryos 99
3.3.2 The dynamic incorporation of DSas-4-GFP partially resembles that of SAS-4, but also shows several unique features 99
3.3.3 Asl-GFP displays a very surprising dynamic behaviour at centrosomes 102
Chapter 4: DSas-4–dependent incorporation of Asl licenses new centrioles to duplicate for the first time 105
4.1 Summary 105
4.2 Results 107
4.2.1 DSas-4 plays a key role in the initial recruitment of Asl-GFP to new centrioles 107
4.2.2 Multiple molecular mechanisms are responsible for establishing the complete Asl pool at centrosomes 113
4.2.3 Disengaged new centrioles that lack Asl can not form a daughter 117
4.3 Discussion 121
4.3.1 The molecular pathways of Asl recruitment to centrosomes 121
4.3.2 Asl incorporation licenses disengaged daughter centrioles to duplicate for the first time 125
Chapter 5: Investigating the molecular regulation of Asl incorporation at newly disengaged centrioles 131
5.1 Summary 131
5.2 Results 134
5.2.1 DSas-4 and Asl do not efficiently form complexes in the cytoplasm 134
5.2.2 Moderate overexpression of Asl-GFP can drive its early incorporation at engaged daughter centrioles 136
5.2.3 Investigating the potential role of DSas-4 S300 phosphorylation in the initial recruitment of Asl to centrioles 143
5.2.4 Investigating the role of region 198-244 within DSas-4 in the initial recruitment of Asl to centrioles 152
5.3 Discussion 157
5.3.1 Attempts to identify the mechanisms that regulate the initial, DSas-4–dependent, incorporation of Asl at centrioles 157
5.3.2 Moderate overexpression of Asl-GFP leads to its early incorporation into engaged daughter centrioles 161
Chapter 6: Discussion 163
6.1 Summary 163
6.2 Asterless: a primary license of centriole duplication 165
6.3 Future Work 168
6.4 Conclusions 171
References 172
Appendix 185

LIST OF ABBREVIATIONS

3D	three dimensions
3D SIM	3D structured-illumination microscopy
aa	amino acid
Ana	Anastral
Asl	Asterless
bp	base pairs
Cdk	Cyclin dependent kinase
Cep	Centrosomal protein
Cnn	Centrosomin
co-IP	co-immunoprecipitation
CPAP	centrosomal P4.1-associated protein
DNA	deoxyribonucleic acid
D-Plp	*Drosophila* pericentrin-like protein
FRAP	fluorescence recovery after photobleaching
GFP	Green fluorescent protein
k	kilo (1,000)
M	molar
min	minutes
MT	microtubules
MTOC	microtubule organizing centre
NEB	nuclear envelope breakdown
MZT	maternal-to-zygotic transition
PACT	Pericentrin AKAP-450 centrosomal targeting domain
PBS	phosphate buffered saline
PCM	pericentriolar material
PCR	polymerase chain reaction
Plk	Polo-like kinase
RFP	Red fluorescent protein
RT	room temperature
rxn	reaction

s	seconds
SAS/Sas	Spindle assembly abnormal
s.d.	standard deviation of the mean
s.e.m.	standard error of the mean
STIL	SCL/TAL1 interrupting locus
SPD/Spd	Spindle defective
tp	time point
WT	wild-type
ZYG	zygotic defective

LIST OF FIGURES

Figure 1.1: Centriole structure.

Figure 1.2: Centrosome organization and assembly.

Figure 1.3: The structure of cilia.

Figure 1.4: The centriole duplication cycle in vertebrate cells.

Figure 1.5: The sequential role of centriole duplication proteins in procentriole assembly.

Figure 1.6: The molecular interactions and centrosomal localization of Asl/Cep152.

Figure 1.7: Regulation of the centriole duplication cycle.

Figure 1.8: Plk2-dependent phosphorylation of CPAP is required for procentriole assembly.

Figure 1.9: A comparison of DNA replication and centriole duplication licensing.

Figure 1.10: The mitotic cycles of the syncytial blastoderm stage *Drosophila* embryo.

Figure 1.11: The centrosome cycle of the early *Drosophila* embryo.

Figure 1.12: Studying centriole duplication using confocal microscopy in the *Drosophila* embryo: the use of centrosome lineage.

Figure 3.1: Generation of a *Drosophila* line expressing endogenous levels of DSas-4-GFP.

Figure 3.2: Live analyses of centrosomal DSas-4-GFP levels during *S*-phase of the cell cycle.

Figure 3.3: An analysis of DSas-4-GFP recruitment to centrosomes during the cell cycle.

Figure 3.4: DSas-4-GFP is a *bona fide* centriolar protein that does not appear to localize to the PCM in *Drosophila* embryos.

Figure 3.5: Growing daughter centrioles recruit excessive amounts of DSas-4-GFP during their assembly in *S*-phase.

Figure 3.6: DSas-4-GFP is stably fixed in fully-grown centrioles.

Figure 3.7: The model of DSas-4-GFP incorporation during centriole duplication in *Drosophila* embryos.

Figure 3.8: Generation of asl^{B46}, an *asl* null allele.

Figure 3.9: The asl^{B46} allele appears to be a functionally null allele that does not produce any detectable Asl protein.

Figure 3.10: Live analysis of centrosomal Asl-GFP levels during *S*-phase of the cell cycle.

Figure 3.11: The recruitment of Asl-GFP to duplicating centrosomes during the cell cycle.

Figure 3.12: Asl-GFP forms a ring around parental centrioles in living *Drosophila* embryos.

Figure 3.13: The model of Asl-GFP incorporation during centriole duplication in *Drosophila* embryos.

Figure 3.14: Approximately half of the total centrosomal Asl-GFP pool is immobile, while the other half remains in dynamic exchange with cytoplasmic molecules.

Figure 4.1: Testing the functional role of DSas-4 in the initial recruitment of Asl using immuno-inhibition.

Figure 4.2: Immuno-inhibition of DSas-4 blocks the initial incorporation of Asl-GFP into newly assembled centrioles.

Figure 4.3: Immuno-inhibition of cytoplasmic Asl to prevent its centriolar recruitment: the generation of unmodified new centrioles that lack Asl.

Figure 4.4: Immuno-inhibition of the DSas-4 –interacting region of cytoplasmic Asl prevents its incorporation into newly assembled, disengaged centrioles.

Figure 4.5: Immuno-inhibition of DSas-4 does not affect the turnover of Asl-GFP at older centrioles.

Figure 4.6: Immuno-inhibiting the Asl-GFP pool of older centrioles abolishes the turnover of Asl-GFP within centrosomes.

Figure 4.7: Model of the dynamic behaviour and recruitment of Asl-GFP at older centrioles.

Figure 4.8: Asl-negative centrosomes fail to duplicate .

Figure 4.9: Disengaged new centrioles that lack Asl cannot template daughter centrioles.

Figure 4.10: A dual licensing model for centriole duplication in *Drosophila*.

Figure 5.1: Comparison of the centriolar incorporation timings of DSas-4 and Asl during the cell cycle.

Figure 5.2: DSas-4 and Asl molecules do not interact readily in the cytoplasm, suggesting that their interaction is regulated at centrioles.

Figure 5.3: Overexpression of Asl-GFP leads to its more symmetric distribution at old and new centrosomes during early *S*-phase.

Figure 5.4: Overexpression of Asl-GFP can promote its early incorporation into engaged daughter centrioles.

Figure 5.5: Overexpression of Asl-GFP does not promote the formation of cytoplasmic DSas-4 – Asl-GFP complexes, but appears to weakly enhance the self-interaction of Asl molecules.

Figure 5.6: CPAP S595 is conserved across evolution and is positioned within the Cep152-interacting region.

Figure 5.7: Neither mimicking nor abolishing potential phosphorylation at DSas-4 S300 affects the incorporation of DSas-4-GFP into procentrioles, or interferes with efficient centriole duplication.

Figure 5.8: Neither mimicking nor abolishing potential phosphorylation at DSas-4 S300 promotes the interaction between cytoplasmic DSas-4 and Asl.

Figure 5.9: Investigating whether multisite phosphorylation within DSas-4 257-304 might play a role in regulating the initial incorporation of Asl at new centrioles.

Figure 5.10: Potential multisite phosphorylation within DSas-4 257-304 does not appear to play a critical role in its efficient centriolar incorporation or the regulation of Asl recruitment.

Figure 5.11: Investigating whether multisite phosphorylation within DSas-4 198-244 might play a role in regulating the initial incorporation of Asl at new centrioles.

Figure 5.12: DSas-4 198-244 is not essential for its own centriolar incorporation, but plays a crucial role in the initial recruitment of Asl to newly assembled centrioles.

Figure 5.13: DSas-4Δ198-244–GFP expression has an equally severe effect on centriolar Asl recruitment and Asl-dependent processes as immuno-inhibiting of the interaction between DSas-4 and Asl.

LIST OF TABLES

Table 1.1: Key centrosomal proteins and their involvement in human diseases.

Table 2.1: List of *Drosophila* lines that were obtained from other sources.

Table 2.2: List of transgenic *Drosophila* lines that were generated and used in this study.

Table 2.3: List of primers used for cloning the genetic regions of DSas-4, Asl or Sak.

Table 2.4: List of plasmids that were generated and used in this study for the generation of transgenic *Drosophila* lines.

Table 2.5: Primers used for amplifying the *dsas-4* cDNA sequence.

Table 2.6: List of primers used for site directed mutagenesis in this study.

Table 2.7: List of plasmids that were generated and used in this study for *in vitro* RNA production.

Table 2.8: Diagnostic PCRs.

Table 2.9: Primary antibodies used in this study.

Table 2.10: Exposure and laser settings used for live confocal imaging.

Table 2.11: Protocol used for measuring the changes in Asl-GFP or DSas-4-GFP along the mitotic cycle.

CHAPTER 1: INTRODUCTION

1.1 CENTRIOLES, CENTROSOMES AND CILIA

Centrioles are microtubule-based cylindrical structures (Figure 1.1A,B) that play a central role in the assembly of two important organelles: the centrosome and cilia. Although not found in all present-day eukaryotes, the centriole is an ancient structure that was present in the last common ancestor of these (Carvalho-Santos et al. 2011). Its original function is believed to have been the nucleation of cilia/flagella (Marshall 2009), while its role in the assembly of centrosomes, the key microtubule-organizing centres of animal cells, appears to be a more recent evolutionary trait (Azimzadeh 2014). The emergence of centrosomes within the animal lineage is believed to be linked to the coordination of more complex developmental processes (Azimzadeh 2014).

Centrosomes and cilia play a number of important roles in cells; consequently both their dysfunction and numerical aberrations are linked to a plethora of human diseases and developmental disorders (Nigg and Raff 2009; Chavali et al. 2014). It is therefore important to understand how centrioles, the core structure of both centrosomes and cilia, are formed and how their numbers are regulated in dividing cells.

1.1.1 THE STRUCTURE OF CENTRIOLES

Centrioles are found in all eukaryotic species that have cilia at any stage of their life cycle (Marshall 2009). The core centriolar structure is highly conserved across evolution, although a great degree of variation can be seen in the exact architecture, size and formation of centrioles in different species, or even in the different tissues of the same animal (Carvalho-Santos et al. 2011). The diameter of centrioles is usually between 100-250nm, while their length ranges from 100nm to

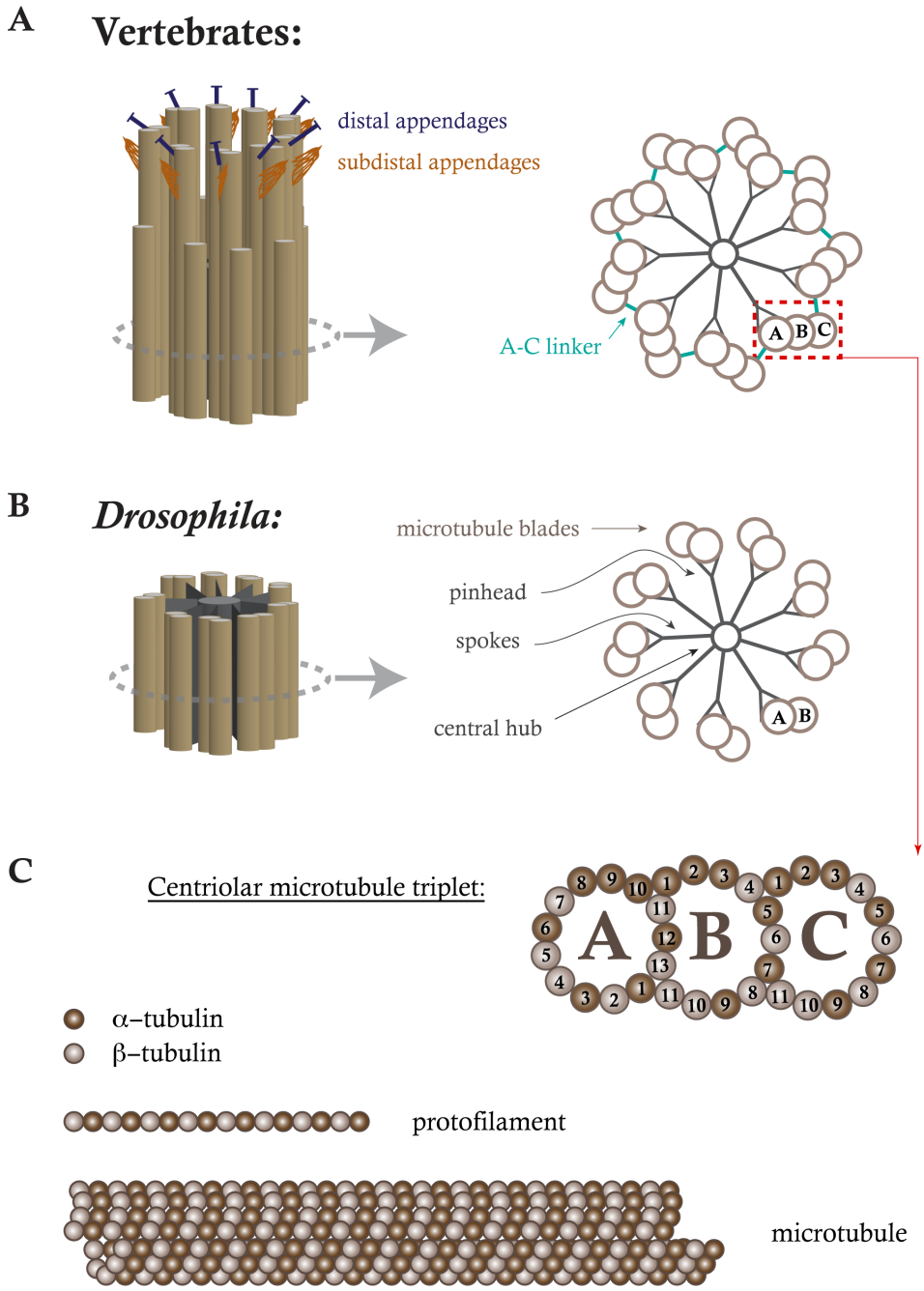


Figure 1.1 Centriole structure.

(A,B) Comparison of centriolar architecture between vertebrate cells (A) and the majority of *Drosophila* cells (B). A cross-section view of centrioles is shown on the right. (C) The organization of centriolar microtubules. Cross-section view shows of the number and arrangement of protofilaments in a microtubule triplet. Below, the composition of protofilaments and microtubules is shown.

500nm in most cell types (Winey and O'Toole 2014), however there are extreme examples of centrioles that are several micrometres long, such as the basal bodies found in *Drosophila* spermatids and *Trichonympha*. The centrioles of *Drosophila* embryos are approximately 200nm long, while vertebrate centrioles are usually about 400nm in length (Gonzalez et al. 1998).

The special, evolutionarily conserved, nine-fold symmetry of centrioles is established by their core cartwheel structure – the earliest detectable intermediate of newly forming centrioles that is generally crucial for their assembly (Hirono 2014). The cartwheel consists of a circular central hub surrounded by nine evenly spaced spokes (Figure 1.1A,B). Each spoke terminates in a pinhead structure (Hirono 2014), which attaches to a microtubule blade; this projects the nine-fold symmetry of the cartwheel spokes to the centriolar microtubules. The core architecture of the centriolar cartwheel is thought to be imposed by the unique oligomerization properties of the SAS-6 protein family (Table 1.1) (Nakazawa et al. 2007; Kitagawa et al. 2011; van Breugel et al. 2011). SAS-6 homologues (described in more detail in section 1.2.1.2) are found in all species that contain centrioles (Carvalho-Santos et al. 2010; Carvalho-Santos et al. 2011) and are one of the first proteins recruited to newly assembling centrioles (Leidel et al. 2005; Rodrigues-Martins et al. 2007a). These proteins have been shown to oligomerize to form nine-fold symmetrical rings (Kitagawa et al. 2011; van Breugel et al. 2011; Guichard et al. 2012; van Breugel et al. 2014) or spirals (Hilbert et al. 2013) – thereby the intricate centriolar cartwheel arrangement is formed simply by a supramolecular assembly of SAS-6. While the self-interaction of SAS-6 molecules primarily dictates the evolutionarily conserved symmetry of centrioles, it is believed that other, so far unspecified, proteins are likely to play a role in enforcing this arrangement *in vivo* (Cottee et al. 2011; Hilbert et al. 2013).

The function and symmetry of the centriolar cartwheel is extremely conserved across eukaryotes. However, interestingly, its size, architecture and stability all show significant variation across different cell types. In most organisms the cartwheel is approximately 100nm long and is found at the proximal end of centrioles (Hirono 2014). In *Drosophil*a *melanogaster* embryos the

approximately 180-200nm long cartwheel occupies the entire length of the centriolar lumen (Callaini et al. 1997; Gonzalez et al. 1998). Possibly the most extreme example of cartwheel length – over 3.5μm – is found in the exceptionally long centrioles of *Trichonympha* species (Hirono 2014). A striking difference from the canonical cartwheel architecture can be seen in *Caenorhabditis. elegans* (*C. elegans* hereafter), where centrioles contain a central tube structure (that lacks long, prominent spokes) instead of a cartwheel. This central tube appears to be formed through a spiralling self-assembly of SAS-6 (Hilbert et al. 2013), instead of the more common stacking of closed SAS-6–rings - the mechanism that assembles the canonical cartwheel structure (Guichard et al. 2012). Remarkably, however, both of these arrangements lead to identical nine-fold symmetry of centrioles. The stability of the centriolar cartwheel also shows strong differences across species. Vertebrate centrioles lose their cartwheel once their assembly is complete, during their first mitosis (Strnad et al. 2007; Hirono 2014). In contrast, the cartwheel forms a permanent structure within centrioles in the majority of *Drosophila* tissues (Gonzalez et al. 1998), and the central tube is also a stable constituent of *C. elegans* centrioles (Leidel et al. 2005).

The most recognizable feature of centrioles is their radial array of nine microtubule blades, which constitute the centriole wall. The number of microtubules in each centriolar blade varies across species (Figure 1.1A,B). Vertebrate centrioles usually contain microtubule triplets, with only the inner two microtubules of each blade extending all the way to the distal tip of the centriole (Gonczy 2012). *Drosophila* centrioles contain doublet microtubules in most, but not all, cell types (ciliated cells, namely spermatids and sensory neurons, contain triplets), while *C. elegans* centrioles display singlet microtubules (Callaini et al. 1997; Winey and O'Toole 2014). The microtubule blades show a characteristic chirality in centrioles containing doublets or triplets: they appear twisted in anti-clockwise direction when viewed from the proximal end of the centriole (Figure 1.1A,B).

Microtubules are hollow, non-covalent polymeric filaments that are formed by the lateral association of 13 protofilaments, each of which is the linear assembly of α- and β-tubulin heterodimer subunits (Conde and Caceres 2009) (Figure 1.1C). Each centriolar microtubule blade

contains a single complete microtubule (formed by 13 protofilaments); this so-called A-tubule is always the one to form a connection with the pinhead structure at the end of each cartwheel spoke. The B- and C-tubules are almost always incomplete: they usually consist of only 11 protofilaments each, and so a part of their wall is formed by the protofilaments of the preceding tubule (Figure 1.1C). In vertebrate centrioles neighbouring microtubule blades are connected to one another through linkers that connect the C-tubule of one triplet to the A-tubule of the following triplet (Gonczy 2012, and also Figure 1.1A). The centriolar microtubules are exceptionally stable compared to their highly dynamic cytoplasmic counterparts; this may be achieved through their extensive post-translational modifications (particularly tubulin glutamylation) and the fusion of microtubule walls within each centriolar blade (Wloga and Gaertig 2010; Winey and O'Toole 2014).

Older centrioles of vertebrate cells (and a variety of other species) harbour distal and subdistal appendages (Figure 1.1A). These appear on centrioles approximately 1.5 cell cycles following the start of their assembly and are the indication of the structural maturity of a centriole (Paintrand et al. 1992; Azimzadeh and Marshall 2010; Hoyer-Fender 2010). Distal appendages are involved in the docking of the centriole/basal body at the plasma membrane, and thereby play an important role in ciliogenesis (Kobayashi and Dynlacht 2011). Similarly to the cartwheel and centriolar microtubules, the arrangement of distal appendages shows nine-fold symmetry. These structures are oriented slightly towards the distal tip of the centriole and, once acquired, persist at centrioles at all stages of the cell cycle (Hoyer-Fender 2010). Distal appendages harbour Cep164, a protein essential for the assembly of primary cilia (Graser et al. 2007), and their formation requires Odf2 and Odf1 (Ishikawa et al. 2005; Singla et al. 2010). Subdistal appendages are found slightly lower, around the region of the centriolar cylinder where the triplet microtubules convert to doublets. These appendages, which function in anchoring microtubules at centrioles, also show nine-fold symmetry, however, unlike distal appendages, they are variable in their thickness, number and distribution. Their formation also requires Odf2 (Ishikawa et al. 2005), and they contain proteins such as ninein, ε-tubulin, centriolin/Cep110 and Cep170 (Hoyer-Fender 2010). Once acquired,

subdistal appendages show a cell cycle dependent localization pattern: they are present at mature mother centrioles during interphase, but always disappear from these during mitosis (Hoyer-Fender 2010).

The localization of appendage proteins at mother centrioles can explain the functional asymmetry of the two centrioles within a centrosome: only mother centrioles can act as basal bodies during ciliogenesis (Hoyer-Fender 2010; Kobayashi and Dynlacht 2011), and they are also predominantly responsible for anchoring most of the microtubules at the centrosome (Piel et al. 2000). The same asymmetric behaviour is, however, also true for *Drosophila* centrioles, which do not display visible appendage structures (Callaini et al. 1997; Nigg and Raff 2009), but contain homologues of several appendage proteins (Hodges et al. 2010; Carvalho-Santos et al. 2011). Thus, it appears that the asymmetric localization of a specific subset of proteins must be responsible for the functional distinction between mother and daughter centrioles, rather than the physical appendage structures themselves.

1.1.2 THE CENTROSOME

Centrosomes are the main microtubule organizing centres in animal cells that have key importance in the efficiency of cellular processes such as chromosome segregation, cell division and motility (Bornens 2012). In addition, they also act as a hub for the regulation of a variety of intracellular signalling and regulatory networks (Jackman et al. 2003; Doxsey et al. 2005a; Doxsey et al. 2005b; Arquint et al. 2014). Centrosomes also play important roles in the coordination of developmental events through controlling cell polarity and asymmetric cell division (Rieder et al. 2001; Azimzadeh 2014). It is believed that the emergence of these organelles in the animal lineage is primarily linked to these latter functions: the acquisition of the centrosome probably aided the ability of multicellular organisms to coordinate the complex developmental patterning events required for the evolution of today's higher animals (Azimzadeh 2014). Nevertheless, *Drosophila*

can proceed through most of development without centrosomes (with the exception of the embryonic stages that precede the MZT; centrosome function is indispensable during this period). This demonstrates that these organelles are not absolutely essential for these developmental patterning events, at least in flies (Basto et al., 2006).

1.1.2.1 CENTROSOME ORGANIZATION AND ASSEMBLY

Centrosomes are formed by a pair of centrioles surrounded by a large number of proteins collectively called the pericentriolar material (PCM) (reviewed in Bettencourt-Dias and Glover 2007 and Mennella 2014 and shown in Figure 1.2A). The PCM harbours γ-tubulin complexes, which are responsible for microtubule nucleation (Kuriyama and Borisy 1981; Moritz et al. 1995a; Moritz et al. 1995b; Kollman et al. 2011), as well as various proteins that are involved in the regulation of microtubule formation and stability (Budde et al. 2001; Lee et al. 2001; Giet et al. 2002; Barros et al. 2005). In addition, the PCM contains a huge number of other proteins involved in a variety of cellular processes, such as regulators of cell cycle transitions or components of the DNA damage response network (Jackman et al. 2003; Takada et al. 2003; Doxsey et al. 2005a; Doxsey et al. 2005b; Arquint et al. 2014). All of these proteins localize within the PCM by binding to the PCM scaffold (Conduit et al. 2014b).

Functional centrosomes are formed through the hierarchical recruitment of PCM proteins by mother centrioles (Conduit et al. 2010; Wang et al. 2011; Conduit et al. 2014b). Interestingly, although centrosomes contain hundreds of different proteins (Andersen et al. 2003), the actual formation centrosomes only requires a very few (Azimzadeh 2014; Conduit et al. 2014b). In *Drosophila*, the mother centriole–specific protein Asl is crucial for initiating PCM recruitment (Conduit et al. 2014b) (Figure 1.2B). Asl promotes the sequential recruitment of DSpd-2 and Cnn, two key proteins that cooperate in establishing the PCM scaffold (Conduit et al. 2014b) (Figure 1.2B). All three of these proteins have functionally conserved human homologues (Cep152: Asl;

Cep192: DSpd-2; CDK5RAP2: Cnn) (Gomez-Ferreria et al. 2007; Lucas and Raff 2007; Blachon et al. 2008; Fong et al. 2008; Gomez-Ferreria and Sharp 2008), suggesting that a similar mechanism could drive PCM assembly in human cells.

Upon binding around centrioles, Cnn molecules (and most likely DSpd-2 as well — Paul Conduit, personal communication) are phosphorylated by Polo kinase to self-associate, and at the same time surrender their centriole-proximal binding sites to unmodified molecules (Conduit et al. 2014a). This results in the formation of a protein scaffold of DSpd-2 and Cnn that is formed at the centriole surface and then constantly fluxes outwards to provide binding sites that recruit other proteins that collectively form the functional mitotic PCM (Conduit et al. 2014a; Conduit et al. 2014b).

For a long time it was believed that the PCM is an unstructured assembly of a vast number of different proteins. It is now clear that, at least during interphase, the PCM has an evolutionarily conserved, precisely organized arrangement, where individual proteins are restricted to specific domains (Fu and Glover 2012; Lawo et al. 2012; Mennella et al. 2012; Sonnen et al. 2012; Mennella et al. 2014). Super-resolution fluorescence microscopic studies have revealed at least two distinct, concentric PCM layers surrounding centrioles in interphase: the centriole-proximal PCM fibres and the outer PCM matrix (reviewed in Mennella 2014 and shown in Figure 1.2C). The PCM fibres contain elongated coiled-coil proteins that form a border between the surface of the mother centriole and the PCM matrix. PCM fibre proteins, including Asl/Cep152 and D-Plp/Pericentrin, are characterized by a strict directional orientation: one end of the protein is anchored at the centriole wall, while the other extends outwards into the PCM matrix. The PCM matrix domain includes DSpd-2/Cep192, Cnn/CDK5RAP2 and γ-tubulin together with a large number of other proteins. Each of these proteins occupies a characteristic region within the matrix (Fu and Glover 2012; Mennella et al. 2012). During mitosis, this ordered arrangement is lost as DSpd-2 and Cnn form a scaffold that expands the PCM dramatically, leading to a much larger PCM matrix that displays a more even localization of its components than its interphase equivalent (Conduit 2014a, Conduit 2014b).

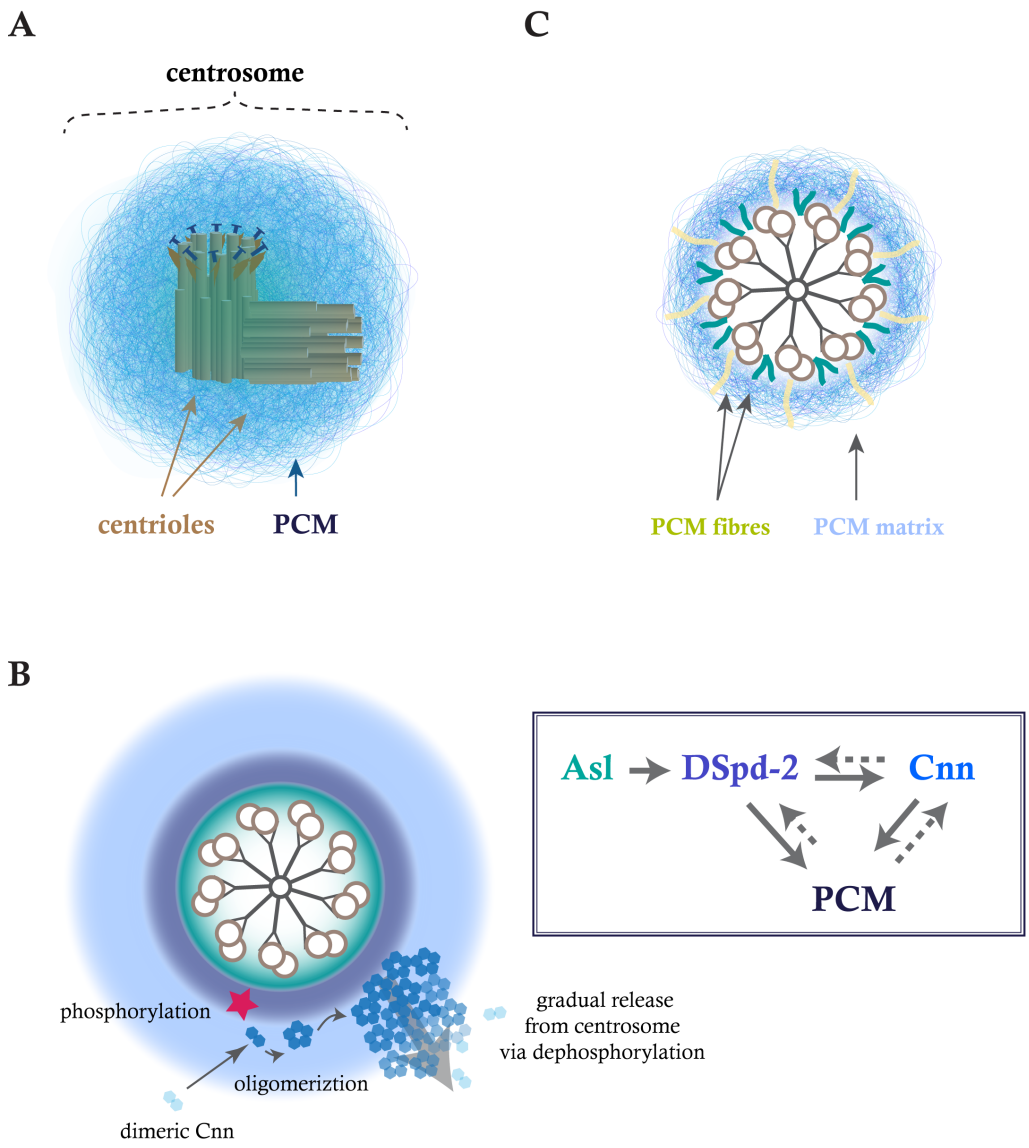


Figure 1.2 Centrosome organization and assembly.

(A) Schematic showing the organization of a centrosome. A pair of orthogonally arranged centrioles (*brown*) is found at the centrosome core. These are surrounded by a meshwork of proteins that are collectively called the pericentriolar material, or PCM (*blue*). (B) Centrosome formation in *Drosophila* requires the hierarchical recruitment of PCM scaffold proteins, DSpd-2 and Cnn, to parental centrioles through Asl (based on Conduit 2014b). The formation of the PCM scaffold involves phosphorylation-dependent oligomerization of Cnn near the centriole surface, which results in the formation of a 'Cnn-meshwork' surrounding the centriole (Conduit 2014a). A similar mechanism is likely to promote the self-interaction of DSpd-2 (Paul Conduit, personal communication). (C) Organization of the PCM during interphase. The PCM can be divided into two main subdomains: the centriole-proximal PCM fibres and the more peripheral PCM matrix. These two main domains are primarily distinguished by the arrangement of their components: the PCM fibres contain extended coiled-coil proteins with a strict molecular orientation at the centrosome, while the PCM matrix proteins show no clear molecular directionality (based on Mennella 2014).

The PCM is a highly dynamic network of proteins; its levels and microtubule-nucleating activity are continuously regulated to match the requirements of the cell. A clear example of this is the robust increase in PCM recruitment and microtubule nucleation in preparation to form the mitotic spindle; a process called centrosome maturation (Khodjakov and Rieder 1999). This process is primarily driven by two main mitotic serine-threonine kinases, Polo/Plk1 (Bettencourt-Dias et al. 2004; Conduit et al. 2014a) and Aurora A (Hannak et al. 2001; Berdnik and Knoblich 2002; Hirota et al. 2003). Both of these kinases play dual roles in centrosome maturation: they elicit the robust growth of the PCM scaffold to promote the recruitment of further microtubule nucleating and regulating complexes (Terada et al. 2003; Haren et al. 2009; Conduit et al. 2014a), but also promote microtubule dynamicity by modulating the activity of key microtubule stabilizing/destabilizing factors (Budde et al. 2001; Giet et al. 2002; Barros et al. 2005).

1.1.2.2 THE IMPORTANCE OF CENTROSOMES

As main centres of microtubule nucleation, centrosomes play important roles in processes such as mitotic spindle assembly, accurate chromosome segregation, cell division and motility. Centrosomes are no doubt important for the efficiency of these events, and centrosome abnormalities that lead to errors in these processes have been shown to cause aneuploidy and invasive cellular behaviour – hallmarks of human cancers (Ganem et al. 2009; Pihan 2013; Godinho and Pellman 2014; Godinho et al. 2014). However, despite the obvious importance of centrosomes in these cellular processes, from an evolutionary perspective centrosomes are not essential for them (Debec et al. 2010); these processes are completed successfully in species that completely lack centrosomes (the majority of non-metazoan taxa). Furthermore, centrosomes are often absent from certain cells of organisms that generally do contain them, and the requirement of centrosome function strongly varies between different tissues. These facts raise the question: why did centrosomes really evolve?

Rieder et al. suggest an increasingly popular hypothesis, which is that "centrosomes are more important for proper development and maintenance of organism viability than for cell viability' (Rieder et al. 2001; Bornens 2012; Azimzadeh 2014). Centrosomes play crucial roles in establishing and maintaining cellular polarity (Cowan and Hyman 2004; Bienkowska and Cowan 2012; Tang and Marshall 2012), which is not only essential for the developmental patterning and correct organogenesis of multicellular animals, but also indispensable for the proper function of adult organs (Siegrist and Doe 2007).

While centrosome function is not essential for the formation of the mitotic spindle in most animal cells, it appears to be essential for properly controlling its orientation. The reason for this is that centrosomes are indispensable for astral microtubules, which interact with cortical cues to anchor the spindle in a specific plane (Rebollo et al. 2007; Kotak and Gonczy 2013). As a result, centrosomes are crucial for the asymmetric division of stem cells that rely on the uneven distribution of cell fate determinants, as opposed to niche-regulated fate determination (Betschinger and Knoblich 2004; Basto et al. 2006; Knoblich 2008). This process is crucial at various stages of development - from early embryonic cleavage divisions (Gonczy and Rose 2005) to the complex organogenesis of higher animals (Sun and Hevner 2014) – as well as the proper homeostasis of adult tissues (Goulas et al. 2012).

An interesting theory suggests that in vertebrates a key task of centrosomes is the faithful segregation of centrioles to daughter cells during cell division, to ensure that future cells form no less and no more than a single primary cilium (Friedlander and Wahrman 1970; Rieder et al. 2001). This speculation provides an elegant explanation why centrioles should reside at spindle poles (considering that, as discussed above, this is not a required for spindle formation *per se*), as primary cilia are absolutely crucial for vertebrate development (Mahjoub 2013; Fry et al. 2014). Importantly, however, centrioles are found at the spindle poles in lower animals too, the development of which does not depend on primary cilia (Basto et al. 2006; Gerdes et al. 2009). This strongly suggests that the faithful maintenance of centriole/basal body numbers over

successive cell generations is unlikely to be the main reason why centrosomes originally evolved, although it has, without doubt, become one of their most important roles during vertebrate evolution.

In conclusion, it is possible that during the evolution of the metazoan lineage the PCM was originally coupled to centrioles to allow its accurate replication, distribution and numerical control, which are crucial for its roles in cellular polarity and asymmetric cell division. This, in turn, however, linked centrioles to spindle poles and assured their even segregation – a great benefit for regulating cellular centriole numbers, which most likely opened the opportunity to use primary cilia for more efficient control of key developmental events.

1.1.3 CILIA

Eukaryotic cilia and flagella are centriole-derived, polarized organelles that appear as protrusions of the cellular membrane in quiescent cells. Cilia emerged early during eukaryotic evolution, and as a result they are found in all major clades – albeit not in all species. The ancient roles of cilia are linked to cellular motility and sensing (Mitchell 2007), while during the evolution of multicellular organisms these functions became greatly extended to fulfil essential roles in developmental patterning, tissue- and organogenesis, as well as correct organ function (Fry et al. 2014). Based on both their structural and functional features, there are two main types of cilia: primary (non-motile) and motile.

Cilia are generally formed by 3 main structural elements: the basal body, transition zone and the axoneme (Figure 1.3). The basal body is formed by a modified mother centriole that is anchored at the plasma membrane through its distal appendage proteins. The basal body acts as the origin of cilia assembly as well as the structural base of fully formed cilia. The extension of the basal body forms the axoneme, a microtubule-based structure that is coated by specialized membrane (Rohatgi

and Snell 2010). Primary and motile cilia differ in the structure of their axoneme: this is simply composed of 9 radially arranged microtubule doublets (the extensions of the centriolar A&B-tubules) in the case of primary cilia (9+0), while motile cilia contain an additional two microtubules in the centre of their axoneme (9+2) and possess dynein arms on their peripheral doublets (Satir et al. 2010) (Figure 1.3). The region where the basal body converts into the axoneme is called the transition zone. This part of the cilium contains a complex set of proteins that function in anchoring the basal body at the cell surface, connecting the microtubule doublets to the ciliary membrane, regulating the composition of the ciliary membrane, and controlling protein traffic between the ciliary and cytoplasmic compartments (Reiter et al. 2012).

Motile cilia function in cellular motility and sensory reception in both unicellular species and higher organisms (Mitchell 2007; Bloodgood 2010). Certain vertebrate epithelial cell types (e.g. those lining the cerebral ventricles, respiratory tracks, Fallopian tubes) contain hundreds of motile cilia that function in generating fluid flow that is key for correct organ development and/or function (Ibanez-Tallon et al. 2003; Ibanez-Tallon et al. 2004).

Primary cilia are restricted to certain cell types in invertebrate species, where they mostly fulfil diverse sensory roles (including chemo-, mechano-, thermo- and hygroreception) (Keil 2012). In contrast, they are found almost ubiquitously on the various cell types of vertebrates (Gerdes et al. 2009). Here, their basic sensory functions (Singla and Reiter 2006) have been extended with responding to and transmitting crucial developmental signals (Goetz and Anderson 2010): Hedgehog (Huangfu et al. 2003) signalling became functionally coupled with primary cilia, while Wnt signalling is partially mediated through this organelle (Gerdes et al. 2007; Corbit et al. 2008). As a result, primary cilia have evolved to become indispensable for vertebrate development (Goetz and Anderson 2010).

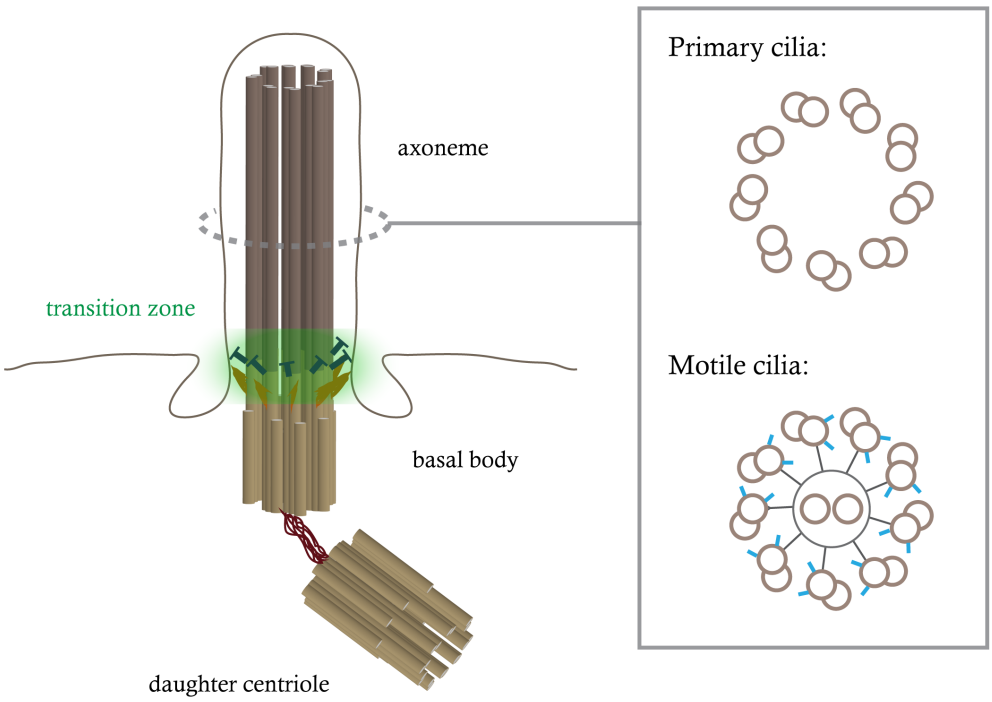


Figure 1.3 The structure of cilia.

Schematic showing the main structural elements of cilia: the basal body, the transition zone and the axoneme. The axonemal architectures of primary and motile cilia are shown on the right. 9 microtubule doublets form the axoneme of primary cilia (9+0 arrangement); these are the extensions of the centriolar A- and B-tubules. The axoneme of motile cilia also contains two central microtubules (9+2) arrangement, radial spokes, as well as dynein arms on the peripheral doublets.

1.1.4 CENTROSOMES AND CILIA IN HUMAN DISEASE

Functional or numerical abnormalities of both centrosomes and cilia form the underlying cause of a wide range of human developmental disorders as well as adulthood disease (Nigg and Raff 2009; Bettencourt-Dias et al. 2011). Interestingly, although the majority of our cells contain these organelles, both centrosome and cilia defects often cause pathologies that affect certain tissues but not others. This highlights how the functional requirement of these organelles varies between different cell types of the same body. In this section I use the human gene nomenclature within the text for referring to disease-linked genes, but indicate the *Drosophila* homologues of these in Table 1.1.

Table 1.1. Key centrosomal proteins and their involvement in human diseases.

***Drosophila* protein**	**Human protein**	**Localization**	**Disease (locus) in human**
Sak	Plk4	Centriole wall	
DSas-6	HsSas-6	Centriolar cartwheel	
Ana2	STIL	Centriolar cartwheel	MCPH7
Cep135/Bld10	Cep135	Cartwheel pinhead	MCPH8
DSas-4	CPAP	Centriole wall	MCPH6, SCKL4
Asl	Cep152	Centriole wall/PCM	MCPH9, SCKL5
-	Cep63	Centriole wall/PCM	SCKL6
DSpd-2	Cep192	Centriole wall/PCM	
Cnn	CDK5RAP2	PCM	MCPH3
D-Plp	PCNT	Centriole wall/PCM	MOPD2 (microcephaplic osteodysplastic PD II)

Ciliary defects usually cause more severe pathologies than those of the centrosome, due to their crucial role in developmental signalling. Genetic mutations in a large variety of ciliary components are linked to a number of pleiotropic disorders that are collectively called ciliopathies (Goetz and Anderson 2010). Ciliopathies, which can be caused by the defective formation or function of either primary or motile cilia, can show a broad spectrum of severity, depending on which proteins are affected (Tobin and Beales 2009). The common symptoms of multiple ciliopathies include polydactyly, cystic kidneys, *situs inversus* and obesity, while certain rare mutations of some ciliary genes lead to developmental defects that are invariably lethal (Tobin and Beales 2009).

Autosomal primary recessive microcephaly (MCPH) is a genetic neurodevelopmental disorder thought to be a *bona fide* centrosomal disease (Chavali et al. 2014). So far mutations in nine genes have been linked to MCPH, five of which are genes of key centriole and centrosome components (STIL, CPAP, CEP135, CEP152, CDK5RAP2), while the remaining four gene products are also associated with the spindle poles, or participate in the spindle assembly checkpoint (Chavali et al. 2014). Although these proteins function in nearly all tissues, interestingly MCPH appears to exclusively affect the cerebral cortex. Its main characteristics are reduced head circumference together with variable degree of mental retardation (Mahmood et al. 2011). MCPH symptoms are present at birth and are non-progressive after (Mahmood et al. 2011), showing that the disorder specifically affects embryonic, but not postnatal development. It is believed that MCPH results from abnormal divisions of polar neural progenitors during the development of the cerebral cortex, which leads to a reduced number of neurons in an otherwise structurally normal brain (Bettencourt-Dias et al. 2011). Neurogenesis is normally dependent on the controlled orientation of cell division, as neural progenitor pools must initially be amplified through symmetric divisions, followed by actual neurogenesis as a result of their asymmetric divisions. As described earlier, centrosomes are crucial for the controlled orientation of the mitotic spindle; consequently, abnormal centrosome function is thought to interfere with either the amplification of neural progenitors or neurogenesis in the developing brain. It is also possible that centrosome defects contribute to MCPH through

affecting neuronal migration, or by causing mitotic delay (Novorol et al. 2013) during proliferative and neurogenic divisions (Chavali et al. 2014).

Mutations in a few, but not all, MCPH genes can cause a broader spectrum of disease, collectively called microcephalic primordial dwarfism (PD), where microcephaly is accompanied by progressive overall growth failure. So far over 14 genes have been linked to PD (Chavali et al. 2014); these are predominantly genes of cell cycle regulators and proteins involved in DNA replication (ORC subunits, ATR, ATRIP and CtIP) together with 4 centrosomal proteins, namely, CPAP, CEP152, CEP63 and PCNT (Chavali et al. 2014). It is an interesting question whether PD is simply a more severe manifestation of MCPH, or it is linked to a protein interaction network that is functionally distinct from that of MCPH?

Numerical abnormalities of both centrosomes and cilia have been implicated in cancer. Already a century ago, Boveri had suggested centrosome amplification as a source of aneuploidy and consequent tumorigenesis. Since then it has become clear that centrosome amplification is a common hallmark of cancer (Chan 2011), however it is still debated whether it acts as a cause or consequence during malignant transformation (Nigg 2002). It has been shown that although, in contrast to previous hypotheses, centrosome amplification rarely results is multipolar mitosis in somatic cells, it leads to aneuploidy as a result of merotelic kinetochore attachments that form during a transient multipolar intermediate that precedes centrosomal clustering and formation of the pseudo-bipolar spindle (Ganem et al. 2009). Merotelic attachments lead to lagging chromosomes during anaphase, which often result in chromosome segregation errors (Ganem et al. 2009). Centrosome amplifications can also contribute to tumorigenesis independently of its effects on chromosome segregation. Recently it has been shown that increased microtubule nucleation as a result of centrosome amplification can promote cellular invasion through enhancing Rac1 activity, which leads to a loss of cell-cell adhesions (Godinho et al. 2014). This may explain why extra centrosomes can provide an advantage for tumour cells, although they are generally poorly tolerated in untransformed cells (Sluder and Nordberg 2004). In addition to their amplification, the

abnormal function of centrosomes is also believed to be linked to cancer, by mis-regulating asymmetric divisions and thereby allowing the expansion of stem cell pools (Zyss and Gergely 2009).

As the organelles mediating Hedgehog signalling, cilia have a clear link to cancer (Hassounah et al. 2012). Studies show that upon oncogenic induction of the Hedgehog pathway cilia can be both protective against tumorigenesis or act to promote that, depending on the nature of the activating signal (Han et al. 2009; Wong et al. 2009). In addition, ciliary function can also impact on tumorigenesis through other signalling pathways that control cell cycle progression, by sending sensory information to the mTOR pathway, or through the response to cancer therapeutics via its sensory and signalling roles (Seeger-Nukpezah et al. 2013).

1.2 THE CENTROSOME CYCLE

Proliferating cells duplicate their centrosomes in a highly controlled manner during the cell cycle. Similarly to chromosomes, the centrosome must be duplicated once and only once per cell cycle; this ensures that mitotic cells contain two centrosomes that form the poles of the spindle apparatus, and consequently each daughter cell inherits a single centrosome. Both the failure and excess of centrosome duplication can lead to mitotic delay and the propagation of harmful effects to subsequent cell generations, or elimination of the cell through apoptosis. In this section I describe the canonical centrosome duplication cycle using the example of vertebrate cells, and later in section 1.3.3 I highlight the few characteristics of this process that are specific to *Drosophila* embryos, the main experimental system I have used in my studies.

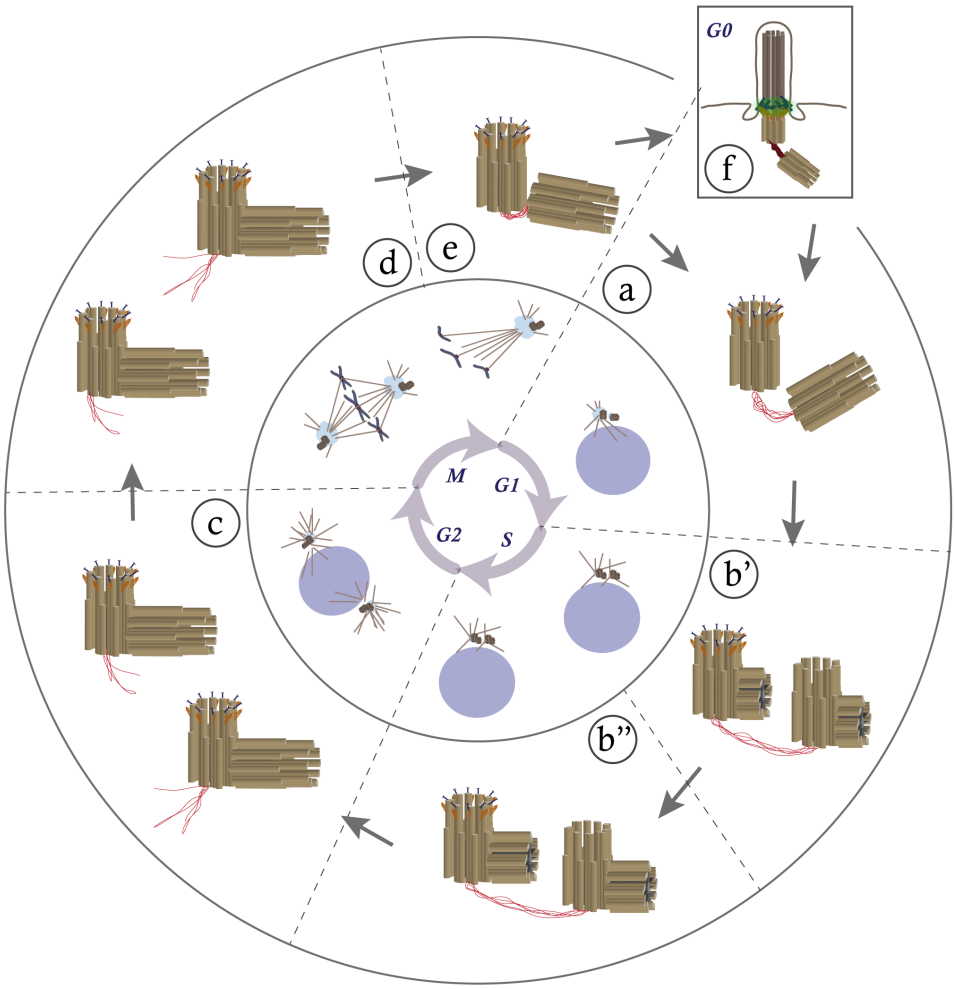


Figure 1.4 The centriole duplication cycle in vertebrate cells.

Schematic shows the events of centriole duplication (PCM not shown) in vertebrate cells during the cell cycle. *G1* (and *G0*)-stage cells contain a single centrosome comprising a pair of disengaged centrioles (a). Upon entry into *S*-phase each of the original, parental or mother, centrioles start to assemble a new centriole, called procentriole or daughter centriole, on its side (b'). The procentrioles elongate during *S*-phase (b") and reach their full length by *G2* phase (c). During *G2* the younger of the parental centrioles acquires its appendages. The two fully duplicated centrosomes loose their physical attachment and move to opposite sides of the nucleus in preparation to form the mitotic spindle (d). During the metaphase-anaphase transition mother and daughter centrioles disengage (e) within each centrosome. Upon completion of mitosis the two centrosomes, each containing a pair of disengaged centrioles, segregate to daughter cells. The new-born cells either enter quiescence – the centrosome can then move to the plasma membrane where the older centriole forms the basal body of the primary cilium – or continue to proliferate, in which case the cycle starts again.

Centrosome duplication is driven by the semiconservative replication of the centrioles (Figure 1.4). As a cell exits mitosis, it inherits a single centrosome comprising a pair of centrioles (Figure 1.4a). During *S*-phase each of these two inherited centrioles acts as a template and assembles a new *daughter* centriole at its side (Figure 1.4b'). Daughter centrioles, which can also be called *procentrioles* during their growth phase, form at a strict perpendicular angle to their parental, or *mother*, centriole and are tightly associated, or *engaged*, with it. Procentrioles elongate throughout *S*-phase (Figure 1.4b") until they reach their full length in *G2* (Figure 1.4c). The centriole replication process results in two centrosomes, each containing a pair of centrioles. In late *G2* the younger of the two mother centrioles acquires appendages, which mark its full structural maturity (Figure 1.4c). Just prior to mitotic entry the two centrosomes (which were so far located in close proximity to each other) separate and migrate to opposing sides of the nucleus, while both parental centrioles initiate robust PCM recruitment leading to centrosome maturation. The increased microtubule-nucleating capacity allows the establishment of the mitotic spindle (Figure 1.4d). During anaphase the tight engagement of mother and daughter centrioles within each of the two centrosomes is lost; the centriole pairs disengage, but remain close together, tethered to each other by a fibrous linker (Figure 1.4e). As mitosis draws to completion the two centrosomes, each containing a disengaged centriole pair, segregate to the two daughter cells. If cellular proliferation continues, the centrosome cycle starts again (Figure 1.4a-e). If cells leave the cycle to enter *G0* phase, the centrosome can move to the plasma membrane where the older centriole acts as a basal body to form the primary cilium (Figure 1.4f).

1.2.1 THE MOLECULAR ASSEMBLY OF CENTRIOLES

Centrioles are formed by a small number of proteins, which are recruited to the side of mother centrioles in a hierarchical manner during the process of procentriole assembly (Delattre et al. 2006). The core molecular pathway of procentriole formation was largely deciphered through the pioneering studies carried out in *C. elegans*, which showed that centriole assembly requires the

orderly recruitment of only five key proteins, SPD-2, ZYG-1, SAS-6, SAS-5, and SAS-4 (Figure 1.5) (O'Connell et al. 2001; Kirkham et al. 2003; Leidel and Gonczy 2003; Dammermann et al. 2004; Delattre et al. 2004; Kemp et al. 2004; Pelletier et al. 2004; Leidel et al. 2005). Subsequent studies in *Drosophila* and vertebrate cells showed that this pathway is highly conserved throughout evolution (Figure 1.5), but also identified Asterless/Cep152, a protein originally described as being crucial for PCM recruitment (Bonaccorsi et al. 1998; Varmark et al. 2007), as the only essential centriole duplication factor in fly and vertebrate cells that is not present in *C. elegans*. In this section I describe the function of the essential centriolar proteins together with a few other proteins that are important, but not crucial, for centriole assembly, and also provide a comparison of their roles in worms, flies and vertebrates.

1.2.1.1 ZYG-1/SAK/PLK4: THE TRIGGERS OF CENTRIOLE ASSEMBLY

Procentriole formation is initiated upon the recruitment and localized activity of ZYG-1 (*C. elegans*), Sak (*Drosophila*) or Plk4 (vertebrates) at the proximal wall of mother centrioles (O'Connell et al. 2001; Bettencourt-Dias et al. 2005; Habedanck et al. 2005; Zitouni et al. 2014). ZYG-1, Sak and Plk4 are serine-threonine protein kinases, each of which comprises an N-terminal kinase domain, a C-terminal polo box (PB) and a central domain called the cryptic PB (CPB) (Zitouni et al. 2014).

The CPB is responsible for recruiting ZYG-1/Sak/Plk4 to mother centrioles, through its direct interaction with SPD-2 (*C. elegans*), Asl (*Drosophila*), or the homologues of both these proteins, Cep192 and Cep152 (vertebrates) (Leung et al. 2002; Slevin et al. 2012; Shimanovskaya et al. 2014). Once localized to the wall of a parental centriole, these kinases catalyse the assembly of the core structure (the central tube or cartwheel) of a new daughter centriole (Delattre et al. 2006; Pelletier et al. 2006; Kleylein-Sohn et al. 2007). Overexpression of Sak/Plk4 leads to centriole

amplification through the simultaneous formation of multiple daughter centrioles around parental centrioles (Kleylein-Sohn et al. 2007; Cunha-Ferreira et al. 2009).

In *C. elegans*, ZYG-1 recruits SAS-6–SAS-5 complexes to the site of procentriole assembly through its direct molecular interaction with SAS-6 (Lettman et al. 2013). This recruitment step does not depend on the kinase activity of ZYG-1, although this is crucial for the assembly of the central tube (Lettman et al. 2013). It is currently thought that the centriolar substrate of this family of kinases is not SAS-6, but rather SAS-5/Ana2/STIL (Lettman et al. 2013; Dzhindzhev et al. 2014). The human homologue of SAS-4, called CPAP, has also been shown to be phosphorylated by Plk4 *in vitro*, although the significance of this is unclear (Chang et al. 2010). In conclusion, the essential, early role of these kinases in procentriole assembly is dual: they recruit core centriolar components through direct molecular interaction and also perform the enzymatic catalysis of central tube/cartwheel assembly (Lettman et al. 2013).

ZYG-1, Sak and Plk4 are auto-regulating kinases (Guderian et al. 2010; Holland et al. 2010) that form homodimeric complexes through the association of their CPB domains (Slevin et al. 2012; Shimanovskaya et al. 2014) and regulate their own stability through *trans*-autophosphorylation (Guderian et al. 2010; Holland et al. 2010). The autodestruction of ZYG-1/Sak/Plk4 upon reaching a certain threshold of kinase activity is an important component of the control mechanisms that restrain centriole amplification (Holland et al. 2010), which I detail later in section 1.2.2.

1.2.1.2 THE SAS-6, SAS-5 AND SAS-4 PROTEIN FAMILIES

Pioneering studies in *C. elegans* showed that SAS-6, SAS-5 and SAS-4 are core centriolar proteins recruited downstream of ZYG-1 to the sites of procentriole assembly (Leidel and Gonczy 2003; Dammermann et al. 2004; Delattre et al. 2004; Leidel et al. 2005; Delattre et al. 2006). Since then, homologues of all three proteins have been identified in different species (Hung et al. 2000; Leidel et al. 2005; Basto et al. 2006; Stevens et al. 2010; Tang et al. 2011; Arquint et al. 2012); SAS-6 and

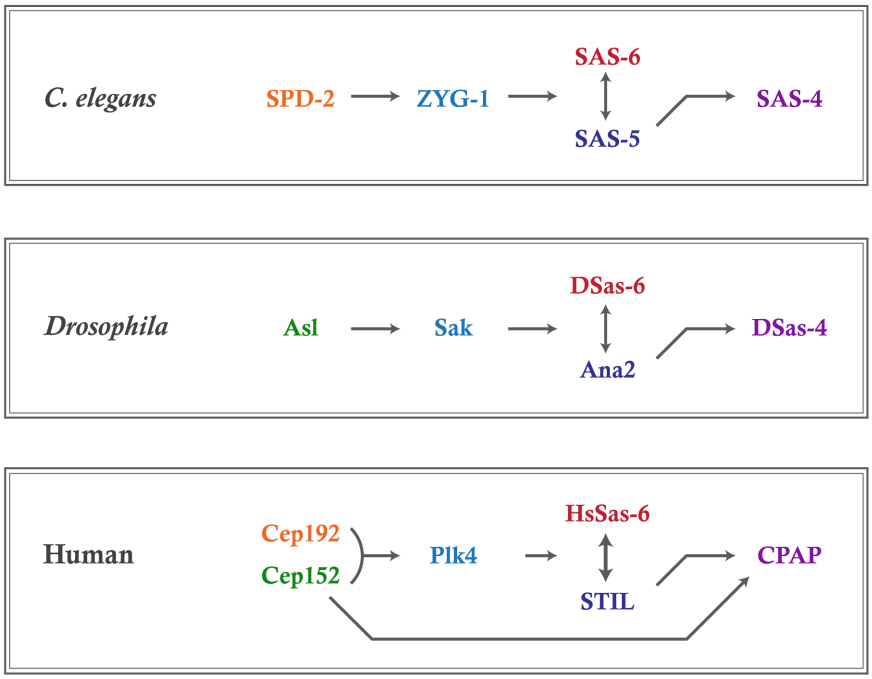


Figure 1.5 The sequential role of centriole duplication proteins in procentriole assembly.

The highly conserved procentriole assembly pathway requires the orderly action of only a few key proteins, as indicated in the diagram. Homologous proteins are shown in the same colour.

SAS-4 are conserved across a wide range of eukaryotic species while SAS-5 appears to be restricted to the metazoan lineage (Carvalho-Santos et al. 2010). The various homologues of all three proteins show extremely conserved function across evolution, but significant differences can be seen in their molecular behaviour in different species. The three proteins form a physical and functional interaction network to generate the core central cartwheel/tube structure of centrioles, and due to their highly interlinked roles I describe these proteins together in this section.

The self oligomerization properties of SAS-6 homologues have been proposed to be responsible for establishing the nine-fold symmetry of the centriolar cartwheel (Nakazawa et al. 2007; Kitagawa et al. 2011; van Breugel et al. 2011). SAS-6–like molecules contain a highly conserved globular N-terminal domain followed by a long coiled coil and a poorly conserved C-terminal region (Leidel et al. 2005). They oligomerize through two interaction interfaces: homodimers form through the parallel interaction of two coiled coil domains, while these dimers can associate into rings through the interaction of their N-terminal globular domains (Kitagawa et al. 2011; van Breugel et al. 2011; Gonczy 2012). Although SAS-6 homologues can consistently self-assemble into nine-fold symmetrical structures, interestingly they appear to achieve this through non-identical oligomeric arrangements in different species. *C. elegans* SAS-6 molecules form a nine-fold symmetrical spiral structure (Hilbert et al. 2013), while SAS-6 molecules in *Trichonympha* (and most likely in many other species too) form closed rings, several of which stack on each other to form the 3D centriolar cartwheel (Guichard et al. 2012).

SAS-5-like proteins are also crucial for procentriole assembly (Delattre et al. 2004; Stevens et al. 2010; Tang et al. 2011; Arquint et al. 2012), however, unlike SAS-6 and SAS-4, relatively little is known about their exact molecular function. *C. elegans* SAS-5 interacts with SAS-6 in a direct manner (Leidel et al. 2005; Qiao et al. 2012) and the two proteins are recruited to sites of procentriole assembly as a complex (Delattre et al. 2006; Pelletier et al. 2006; Lettman et al. 2013); the interaction between them appears to facilitate the oligomerization of SAS-6 to form the central tube structure (Qiao et al. 2012). The *Drosophila* homologue of SAS-5, Ana2, also interacts

directly with DSas-6 (Stevens et al. 2010) – this does not appear to be true, however, for the human homologues, STIL and HsSas-6 (Tang et al. 2011; Arquint et al. 2012), despite the fact that the functional interaction between the two proteins is highly conserved (Stevens et al. 2010; Arquint et al. 2012). In contrast, SAS-5 proteins interact directly with SAS-4 homologues not only in *C. elegans* and flies (Cottee et al. 2013), but in human cells as well (Tang et al. 2011). Taken together, it is clear that SAS-5-like proteins function together with SAS-6 and SAS-4 homologues to establish the core structure of centrioles, however their exact molecular role is yet to be clarified.

C. elegans SAS-4 has been first described from this family of proteins as an essential centriole duplication factor (Kirkham et al. 2003; Leidel and Gonczy 2003) that is required for the addition of centriolar microtubules to the central tube structure of growing procentrioles (Pelletier et al. 2006). The conserved, essential role of SAS-4 homologues in centriole formation was verified when the *Drosophila* and human homologues – DSas-4 and CPAP, respectively – were also shown to be indispensable for this process (Basto et al. 2006; Tang et al. 2009). Overexpression studies of DSas-4 and CPAP showed that these proteins also play a key role in stabilizing centriolar microtubules: these elongate significantly in response to excessive cellular levels of DSas-4/CPAP (albeit in flies this is more strongly restrained by the centriole capping protein CP110 than in human cells) (Kohlmaier et al. 2009; Schmidt et al. 2009; Tang et al. 2009; Franz et al. 2013). In line with this role, DSas-4/CPAP localize at the centriole wall, peripherally to DSas-6/HsSas-6 (Fu and Glover 2012; Lawo et al. 2012; Mennella et al. 2012) although a fraction of centrosomal CPAP appears to localize within the PCM as well (Sonnen et al. 2012).

SAS-6, SAS-5 and SAS-4 homologues are incorporated into procentrioles in a sequential manner during their assembly. SAS-6/HsSas-6 and SAS-5/STIL are co-dependent in their recruitment to the site of procentriole assembly (Delattre et al. 2006; Pelletier et al. 2006; Tang et al. 2011; Lettman et al. 2013), while SAS-5/STIL is required for the subsequent recruitment of SAS-4/CPAP (Delattre et al. 2006; Pelletier et al. 2006; Kohlmaier et al. 2009; Tang et al. 2011). This also appears to be the case in *Drosophila*, where the overexpression of each DSas-6 and Ana2, but not

DSas-4, can drive centriole overduplication, suggesting that DSas-4 functions downstream of the other two core centriolar proteins (Peel et al. 2007).

As the most fundamental procentriolar constituents, SAS-6, SAS-5 and SAS-4 homologues are targets of strict cell cycle–dependent regulation, to ensure the timely duplication of centrioles whilst restraining their amplification. I describe the regulation of these proteins in section 1.2.2, as part of mechanisms that are responsible for the temporal and numerical control of the centrosome cycle.

1.2.1.3 ASTERLESS/CEP152

Drosophila Asterless (Asl) and vertebrate Cep152 are large (120kDa and 152kDa, respectively), highly coiled-coil proteins predicted to be involved in protein-protein interactions, comprising no known enzymatic activity (Varmark et al. 2007). Asl had been well documented to play a key role in PCM recruitment in flies (Bonaccorsi et al. 1998; Varmark et al. 2007), thus it was a great surprise when Asl was discovered to be essential for centriole duplication as well (Blachon et al. 2008; Dobbelaere et al. 2008). Blachon et al. showed that the hypomorph asl^{mecD} mutation leads to an uncoordinated phenotype in adult *Drosophila*, which is characteristic of flies that completely lack centrioles (Basto et al. 2006) and the knockdown of *cep152* in zebrafish embryos also resulted in a phenotype characteristic of ciliary defects. A large number of studies have now shown that knockdown of Cep152 interferes with normal centriole duplication in every vertebrate cell line analysed to date (Blachon et al. 2008; Cizmecioglu et al. 2010; Dzhindzhev et al. 2010; Hatch et al. 2010; Kim et al. 2013; Sonnen et al. 2013)

The PCM had been implicated in the regulation of centriole duplication (Dammermann et al. 2004; Loncarek et al. 2008); however, the role of Asl/Cep152 was soon proved to be far more specific than that of a general concentrator of procentriolar components. Asl/Cep152 were shown to play

the key role of recruiting Sak/Plk4 to centrosomes to initiate procentriole assembly (Cizmecioglu et al. 2010; Dzhindzhev et al. 2010; Hatch et al. 2010). This central role in the centriole duplication process was certainly surprising, primarily because most of our understanding of the highly conserved core duplication pathway is built on the pioneering studies performed in *C. elegans* - which lacks an Asl/Cep152 homologue.

Three independent studies, carried out in *Drosophila* cells (Dzhindzhev et al. 2010), *Xenopus* egg extracts (Hatch et al. 2010) and human cells (Cizmecioglu et al. 2010; Dzhindzhev et al. 2010), showed that Asl/Cep152 interacts with Sak/Plk4 *in vivo* and *in vitro* (Figure 1.6A). All three studies showed that Asl/Cep152 still localized at centrosomes following the knockdown of Plk4, while Dzhindzhev et al. showed that the knockdown of Asl – or overexpression of its mutated form that is unable to interact with Sak – prevents the recruitment of Sak to centrioles. These assays unequivocally placed Asl/Cep152 upstream of Sak/Plk4 in the centriole assembly pathway. However the role of Cep152 in the centrosomal recruitment of Plk4 in humans did not appear as simple as in flies: although expression of a Plk4-binding mutant form of Cep152 effectively depleted Plk4 from centrosomes (Cizmecioglu et al. 2010; Hatch et al. 2010), knockdown of Cep152 had little affect on Plk4 localization (Cizmecioglu et al. 2010; Dzhindzhev et al. 2010; Hatch et al. 2010). These results suggested that although Cep152 is involved in the centrosomal recruitment of Plk4, in contrast to Asl, it does not fulfil this role alone. Recently this was shown to be the case, when Cep192 – the vertebrate homologue of another PCM protein, SPD-2/DSpd-2 – was found to cooperate with Cep152 in the centrosomal recruitment of Plk4 in human cells (Kim et al. 2013; Sonnen et al. 2013). The region of Cep192 that interacts with Plk4 is not found in DSpd-2 (Sonnen et al. 2013), explaining why Sak recruitment is entirely dependent on Asl in flies (Dzhindzhev et al. 2010). Thus, in *C. elegans* and flies, SPD-2 or Asl, respectively, recruit ZYG-1/Sak to centrosomes alone (Delattre et al. 2006; Pelletier et al. 2006; Dzhindzhev et al. 2010), while vertebrates have developed a layered mechanism of Plk4 recruitment that relies on the sequential action of both proteins (Kim et al. 2013; Sonnen et al. 2013).

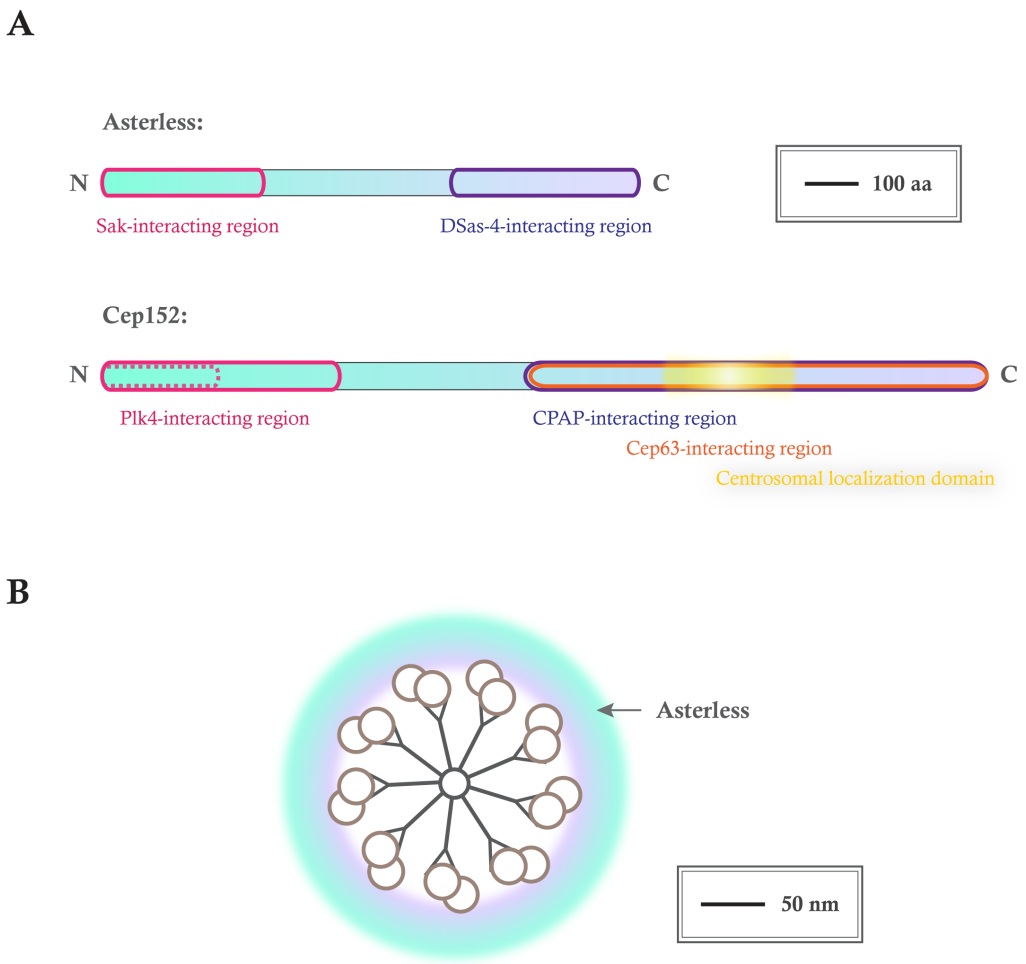


Figure 1.6 The molecular interactions and centrosomal localization of Asl/Cep152.

(A) Schematics illustrate the molecular regions of Asl and Cep152 that are required for their interaction with Sak/Plk4 (*pink*), DSas-4/CPAP (*dark purple*), and Cep63 (*orange*, Cep152 only). The centrosomal localization domain has been mapped for Cep152 (shown in *yellow*), but not for Asl. The schematics are drawn to scale, and are based on Dzhindzhev 2010, Hatch 2010, Brown 2013. Dzhindzhev *et al*. mapped the extended Plk4-interaction region show (solid *pink* line) while Hatch *et al.* mapped the shorter region (dashed *pink* line). (B) Asl localizes at the wall of parental centrioles and shows a strict directional orientation. The C-terminal region of Asl (*light purple*) localizes tight at the centriole wall while the N-terminal region (*light blue*) extends outwards towards the PCM (not shown). Based on Mennella 2012.

Asl/Cep152 also interacts with another of the core centriolar proteins, DSas-4/CPAP, in an evolutionarily conserved manner (Figure 1.6A) (Cizmecioglu et al. 2010; Dzhindzhev et al. 2010). Asl/Cep152 and DSas-4/CPAP were found to interact both *in vivo* and *in vitro*, and knockdown of Cep152, but not Asl, resulted in the loss of CPAP/DSas-4 from centrosomes (Cizmecioglu et al. 2010; Dzhindzhev et al. 2010). Based on these effects, and the direct *in vitro* interaction between the two proteins, it was proposed that Asl acts as a scaffold between DSas-4 and Sak to promote centriole duplication (Dzhindzhev et al. 2010), while the recruitment dependencies have changed in vertebrates in a way that Cep152 mediates the recruitment of both CPAP and Plk4 during procentriole assembly (Cizmecioglu et al. 2010; Dzhindzhev et al. 2010).

While it is currently unknown how Asl/Cep152 is incorporated at the centrosome, it was recently shown that in vertebrate cells Cep63 is a key player in the correct centrosomal localization of Cep152 (Sir et al. 2011; Lukinavicius et al. 2013). Cep63 is a non-essential centriole duplication protein that has a key role in the efficiency of centriole duplication in cells that have shorter doubling times (Sir et al. 2011). It is important for the efficient localization of Cep152 to the centrosome, and thus, it has been proposed that Cep63 ensures the timely centrosomal accumulation of Cep152 to promote the initiation of procentriole assembly in a potentially short window of opportunity (Sir et al. 2011). Cep63 and Cep152 are co-dependent in their centrosomal localization and are recruited there together, as a complex (Brown et al. 2013; Lukinavicius et al. 2013). Newly formed daughter centrioles first start to incorporate Cep63 and Cep152 in late mitosis, which continues after cytokinesis during the following *G1* phase. Intriguingly, Cep63 deficiency was shown to only partially disrupt the centrosomal localization of Cep152 during interphase, however completely abolish it during mitosis (Sir et al. 2011) – thus, it appears that Cep63 has a more marked affect on the centrosomal maintenance of Cep152 than its initial recruitment (Sir et al. 2011). Cep63 homologues appear to be restricted to vertebrates, and so far no homologue of this protein has been identified in flies.

Asl/Cep152 localize as a ring around parental centrioles and thereby occupies a border region between centrioles and their associated PCM (Sir et al. 2011; Fu and Glover 2012; Lawo et al. 2012; Mennella et al. 2012; Sonnen et al. 2012; Lukinavicius et al. 2013). Asl coats the entire surface of the relatively short centrioles found in *Drosophila* (Fu and Glover 2012; Mennella et al. 2012), while Cep152 is restricted to the proximal end of longer vertebrate centrioles (Sir et al. 2011; Lawo et al. 2012; Sonnen et al. 2012; Lukinavicius et al. 2013). Both in flies and humans Asl/Cep152 shows a clear directional orientation, with its C-terminal, DSas-4/CPAP (and Cep63)–interacting region found closer to the centriole wall, and its N-terminal Sak/Plk4–interacting region extending outwards towards the PCM (Figure 1.6A,B) (Mennella et al. 2012; Sonnen et al. 2012).

Despite its key role in centriole duplication it is currently unclear how Asl/Cep152 is initially recruited to newly assembled centrioles. Furthermore, even though the molecular interactions and functions of Asl/Cep152 have been extensively characterized in recent years, we still know little about how it really acts in centriole duplication. These questions will form the starting point of my studies presented in this thesis.

1.2.2 REGULATION OF THE CENTROSOME CYCLE

Similarly to chromosomal replication, centrosome duplication is also regulated at two levels during the cell cycle: duplication must occur once and only once per cell cycle, and during this process one and only one copy must be made of each template (Nigg 2007). I first describe the mechanisms that control the temporal and numerical aspects of centrosome duplication (Figure 1.7), and then join these two together by introducing the licensing model of centrosome duplication. Finally, I draw a brief comparison between centrosome duplication licensing and the highly analogous process of DNA replication licensing, using this to point out where our knowledge of centrosome duplication licensing is still incomplete.

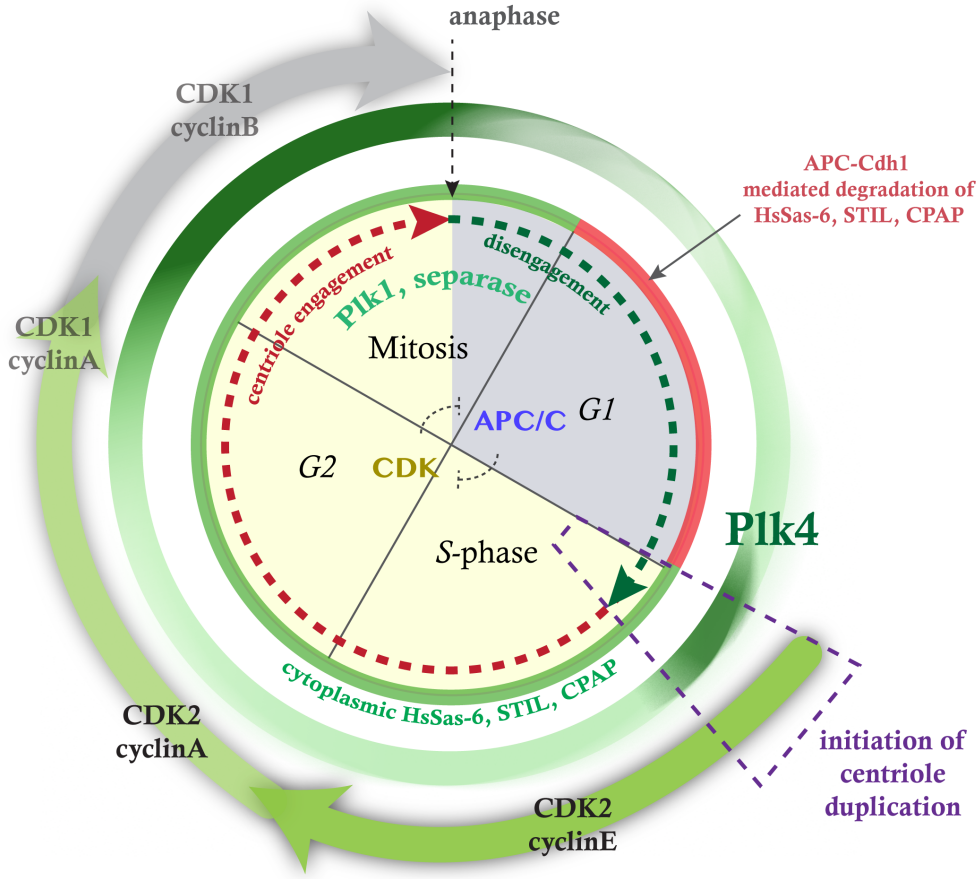


Figure 1.7 Regulation of the centriole duplication cycle.

Schematic summarizes the various cues that control centriole duplication (PCM maturation not shown). The initiation of procentriole assembly (highlighted as *purple* box) requires the temporal overlap of four key factors: (a) Plk4 activity, (b) Cdk2 activity, (c) disengaged parental centrioles and (d) the cytoplasmic availability of core duplication proteins. See main text for details.

1.2.2.1 TEMPORAL REGULATION/CELL CYCLE CONTROL

The key events of centrosome duplication are tightly connected to specific stages of the cell cycle. The initiation of centriole duplication in cycling cells is tied to the start of *S*-phase, as it generally requires the temporal overlap of two key kinase activities: Plk4 and Cdk2 (Figure 1.7). Cdk2 is the master regulator of the *G1*/*S* transition (Cdk2/cyclin E) as well as *S*-phase progression (Cdk2/cyclin A). Multiple studies have shown that both normal centrosome duplication, as well as re-duplication, is dependent on the activity of these complexes (Hinchcliffe et al. 1999; Lacey et al. 1999; Matsumoto et al. 1999; Meraldi et al. 1999; Tsou and Stearns 2006b). The molecular mechanisms by which Cdk2 enables centriole duplication is yet to be confirmed, however a likely possibility is that – through inactivating APC/Cdh1 – Cdk2 activity stabilizes the core centriolar proteins HsSas-6, STIL and CPAP (all of which are destabilized during late mitosis/*G1* in an APC/C–dependent manner) (Strnad et al. 2007; Tang et al. 2009; Arquint and Nigg 2014).

Plk4 and its homologues are required to initiate the recruitment of core centriolar components to the wall of mother centrioles. The levels of Plk4 peak in mitosis, prior to the initiation of centriole duplication (Rogers et al. 2009). Plk4 is a suicide kinase: in addition to phosphorylating its substrates, it also targets itself through regulated multisite *trans*-autophosphorylation, resulting in its degradation through the SCF-Slimb/βTrCP-E3 ubiquitin ligase (Cunha-Ferreira et al. 2009; Rogers et al. 2009; Guderian et al. 2010; Cunha-Ferreira et al. 2013). The multisite nature of Plk4 autophosphorylation is thought to provide a window of time for it to act on its substrates (Cunha-Ferreira et al. 2013), and the overlap of this period with Cdk2 activity sets the initiation of procentriole assembly. The autophosphorylation of Plk4 is counteracted by protein phosphatase 2A: this enzyme acts to stabilize Plk4 during mitosis, but in the absence of its regulatory subunits Tws/B55, leaves it to be degraded during interphase (Brownlee et al. 2011; Zitouni et al. 2014).

The cytoplasmic levels of the core centriolar proteins HsSas-6, STIL and CPAP are also regulated during the cell cycle, with levels gradually increasing from early *S*-phase until mitosis, and then

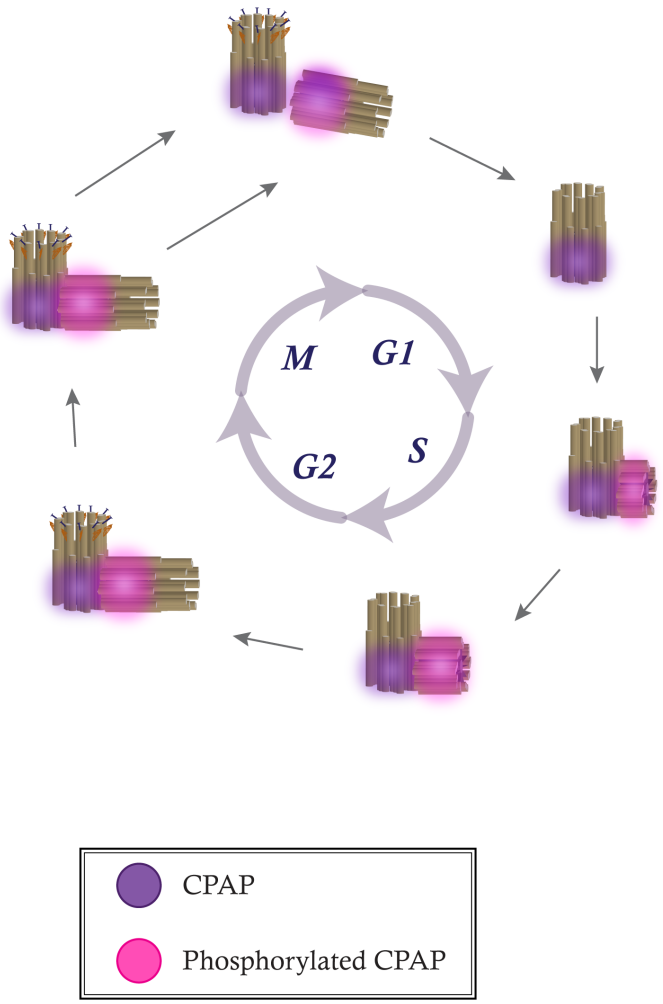


Figure 1.8 Plk2-dependent phosphorylation of CPAP is required for procentriole assembly.

Chang *et al*. (2010) showed that Plk2 phosphorylates CPAP molecules that are incorporated into procentrioles, and this modification is important for procentriole assembly. During mitosis the phosphate groups, however, are removed from newly formed daughter centrioles. Thus this modification is specifically required for the efficient assembly of new centrioles but is not needed for their maintenance (schematics based on Chang 2010).

falling during late mitosis/*G1* via degradation through the recognition of their KEN-box by the APC-Cdh1 complex (STIL is additionally targeted by APC-Cdc20) (Strnad et al. 2007; Tang et al. 2009; Arquint and Nigg 2014). The regulated degradation of these proteins is important for restraining centriole amplification (Strnad et al. 2007; Arquint and Nigg 2014), and mutations that interfere with the APC/C-depedent degradation of STIL are linked to microcephaly in humans (Arquint and Nigg 2014).

In vertebrate cells centriole duplication is also regulated through the activity of Plk2 (Warnke et al. 2004), a kinase that is important for the *G1/S* transition in higher animals but has no homologue in flies (Barr et al. 2004; Zitouni et al. 2014). Plk2 localizes at centrosomes during *G1* and *S* phases, and it has recently been shown to phosphorylate CPAP upon *S*-phase entry to promote procentriole assembly and elongation (Chang et al. 2010). The Plk2-dependent phosphorylation pattern of CPAP appears to be important for the formation, but not the maintenance, of daughter centrioles (Figure 1.8): CPAP molecules are dephosphorylated at the end of the cell cycle, when daughter centrioles are fully grown, and remain unmodified within older centrioles thereafter (Chang et al. 2010).

1.2.2.2 NUMERICAL REGULATION

The number of daughter centrioles formed per mother centriole in a single cycle is determined by two main mechanisms. The first is the correct maintenance of engagement with the daughter centriole until late mitosis. The second is the maintenance of adequate cytoplasmic levels of the proteins that act most upstream in procentriole assembly – Plk4, HsSas-6 and STIL – during the cell cycle.

The re-duplication of mother centrioles within the same cell cycle is blocked through a centrosome-intrinsic mechanism (Wong and Stearns 2003). It was shown that centriole re-

duplication can not be provoked by cell fusion experiments – thus the initiation of second or further duplication events is not restrained by the progression through the cell cycle, but rather a certain intrinsic difference between centrosomes that have already duplicated and those that are yet to do so (Wong and Stearns 2003). This model was supported when Tsou & Stearns (2006) later described that the engagement of the first daughter centriole represses the formation of any further ones around the same mother until centriole disengagement at the end of the cell cycle. Centriole disengagement normally occurs at the metaphase-anaphase transition (Vidwans et al. 1999; Tsou and Stearns 2006a) and requires the activity of Plk1 and separase (Tsou and Stearns 2006a; Tsou et al. 2009; Loncarek et al. 2010; Wang et al. 2011). It has also been shown that laser ablation of the daughter centriole (Loncarek et al. 2008) as well as early disengagement provoked by ectopic expression of active Plk1 (Loncarek et al. 2010) is sufficient to induce centriole re-duplication.

Studies have shown that the overexpression of Sak/Plk4, DSas-6/HsSas-6, Ana2/STIL or their impaired cell-cycle dependent degradation leads to centriole amplification (Kleylein-Sohn et al. 2007; Peel et al. 2007; Rodrigues-Martins et al. 2007b; Strnad et al. 2007; Stevens et al. 2010; Arquint et al. 2012). In contrast to centriole re-duplication (which is induced by premature disengagement of mother and daughter centrioles, allowing the assembly of a single new daughter at a time) the overexpression of these proteins promotes the simultaneous formation of multiple daughter centrioles around the same mother centriole, thus overriding the normal requirement for centriole disengagement.

It is thought that, rather than acting as a *bona fide* template, the role of parental centrioles in centrosome duplication is to provide a platform for concentrating the regulatory molecules that orchestrate the self-assembly of daughter centrioles (Rodrigues-Martins et al. 2007b). The overexpression of key centriolar components can therefore lead to the formation of multiple foci of centriole assembly.

1.2.2.3 THE LICENSING MODEL OF CENTROSOME DUPLICATION

The licensing model of centrosome duplication, formulated by Tsou & Stearns (2006), summarizes how this process is limited to once per cell cycle. According to this model, the formation of the first daughter centriole *blocks* re-duplication, while centriole disengagement at the end of the cycle relieves the block, and provides the *license* for a new duplication event to occur in the subsequent cycle. The *block* (new structure synthesis) and *license* terms were introduced to emphasize the strong analogy with the regulation of DNA replication.

The accurate control of both the chromosome and centrosome cycles relies on the strict temporal separation of licensing and new structure synthesis: the non-overlapping alteration of these events guarantees a single duplication event per cycle. In both cycles, this temporal separation is achieved through linking new structure synthesis and licensing to the two main mutually exclusive enzyme activities that drive the cell cycle: CDK and APC/C (Figure 1.9). Both DNA replication and centriole duplication are initiated upon entry into *S*-phase in a CDK dependent manner, while licensing of the next round of duplication occurs at/after the metaphase-anaphase transition, as the APC/C becomes activated. As CDKs and APC/C oppose the action of one another, they ensure that new structure synthesis and duplication licensing does not coexist.

The licensing of DNA replication is performed during late mitosis/*G1* through the sequential loading of 'licensing factors' (CDC6, CDT1 and the replicative helicase) onto the origin-recognition complexes (ORC) that are bound to DNA sequences called origins of replication (note that in some species the ORC complexes are maintained bound to the DNA throughout the cell cycle, while in other species they are re-assembled as a part of the licensing process). CDC6 and CDT1 bind to ORCs and load the replicative helicase (MCM), which results in the establishment of the pre-replicative (pre-RC) complex – a licensed origin. Cdk is then activated upon the entry into *S*-phase, converting the inactive pre-RC into an active helicase, leading to the onset of DNA synthesis, while at the same time preventing any further licensing by restraining APC/C and

directly phosphorylating the licensing proteins. During the metaphase/anaphase transition, CDK is inactivated and the APC/C is activated, relieving the block to licensing and so allowing a new licensing event to prime the next round of replication (Siddiqui et al. 2013).

In comparison, centrioles are licensed for a new round of duplication when they disengage from their daughter at the metaphase-anaphase transition (Figure 1.9). Disengagement has been shown to require the activity of both Plk1 and separase (Tsou and Stearns 2006b; Tsou et al. 2009), the activation of the latter being dependent on the APC/C–mediated destruction of securin (Peters 2002). Upon the entry into *S*-phase a single new daughter centriole assembles at the side of each freestanding, licensed parental centriole. As disengagement is tied to the metaphase-anaphase transition, parental centrioles are prevented from assembling further daughters before the subsequent cell cycle.

Although the two duplication processes are highly analogous, there are some differences between them. Possibly the most important is that, in contrast to the complementary strands of DNA, the two centrioles in a pair are not licensed for duplication by identical mechanisms. From the data within the studies examining the various control mechanisms that enforce a single daughter per mother centriole, it is clear that the various perturbations of these regulatory mechanisms invariably allow mother centrioles to re-duplicate, but not their engaged or disengaged daughters (Kleylein-Sohn et al. 2007; Loncarek et al. 2008; Cunha-Ferreira et al. 2009; Wang et al. 2011). Indeed, it has been described recently that, unlike mother centrioles, freestanding (not engaged) daughter centrioles require a certain Plk1-dependent 'modification' to allow their future duplication (Loncarek et al. 2010; Wang et al. 2011). The nature of this change is mysterious. In conclusion, the current licensing model of centrosome duplication is incomplete: it explains how mother centrioles –that have duplicated before – are licensed for a new round of duplication, but does not explain how the very first round of duplication is permitted.

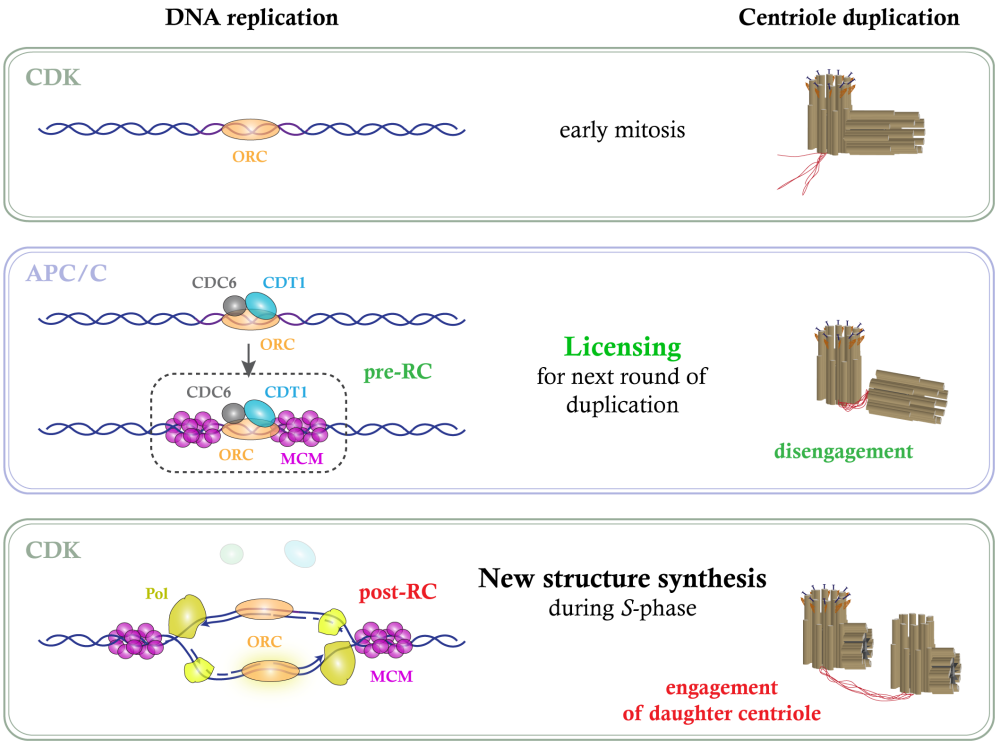


Figure 1.9 A comparison of DNA replication and centriole duplication licensing.

Schematic illustrates the analogous steps of DNA replication (left) and centriole duplication (right). Both duplication cycles can be separated into 'licensing' and 'new structure synthesis' phases, which alternate in a strictly non-overlapping manner. Licensing is only permitted in an APC/C environment (middle panel): the activity of this enzyme complex (as well as the absence of Cdk activity) is required for both DNA replication licensing (to relieve the inactivation of licensing proteins CDC6, CDT1 and MCM helicase) and centriole duplication licensing (as centriole disengagement requires separase activity). New structure synthesis cannot occur during this stage however, as that requires Cdk activity. Once licensed chromosomes/centrioles progress into an *S*-phase environment, further licensing can no longer occur as Cdk activity shuts down APC/C. New structure synthesis takes place. Until the progression into anaphase new structure synthesis is permitted, until the licenses are 'used up': this explains why experimental conditions that re-license DNA/centrioles can promote re-duplication during *S/G2* phases.

1.3 THE SYNCYTIAL BLASTODERM STAGE *DROSOPHILA* EMBRYO

1.3.1 THE EARLY EMBRYONIC DEVELOPMENT OF *DROSOPHILA*

In the first two hours following fertilization the *Drosophila* embryo completes its first 13 mitotic cycles as a syncytium. During this period the nuclear divisions are synchronous (as no cell membranes are formed) and consist of rapidly alternating phases of DNA replication (*S*-phase) and mitosis, without detectable gap phases (*G1, G2*) between. These extremely rapid early cycles, ranging from 8-21 minutes long (Foe and Alberts 1983; Gilbert 2000), are fuelled by an abundant maternal supply of cell cycle components and expedited by the reduced stringency of cell cycle checkpoints.

The first 9 mitotic cycles that follow fertilization constitute the *preblastoderm stage*. For the majority of this period (cycles 1-7) all nuclei multiply within the central region of the embryo. In the 8th cycle most nuclei begin to migrate outwards towards the periphery of the embryo, leaving only the future yolk nuclei behind in the middle (Foe and Alberts 1983). In the early stages of cycle 10 the majority of migrating nuclei reach the periphery of the embryo and form a monolayer just beneath the cortex. This marks the beginning of the *syncytial blastoderm stage* (Figure 1.10), during which the nuclei continue to divide for another four mitotic cycles at a progressively decreasing rate (Foe and Alberts 1983). These cycles are metasynchronous: mitosis usually progresses as two wavefronts across the embryonic nuclei, which originate at the poles of the embryo and meet around the middle about 30 seconds after their initiation (Foe and Alberts 1983). The highly organised cortical cytoskeleton is responsible for the proper distribution of nuclei and correct spindle orientation during these cycles (Figure 1.10). Each peripheral nucleus is associated with its own extensive actin and microtubule network, which are organized by its own centrosomes (Warn et al. 1984; Karr and Alberts 1986; Raff and Glover 1988; Raff and Glover 1989). Both the actin and microtubule cortical cytoskeleton is heavily re-organized during the mitotic cycle to allow efficient and ordered nuclear divisions (Figure 1.10).

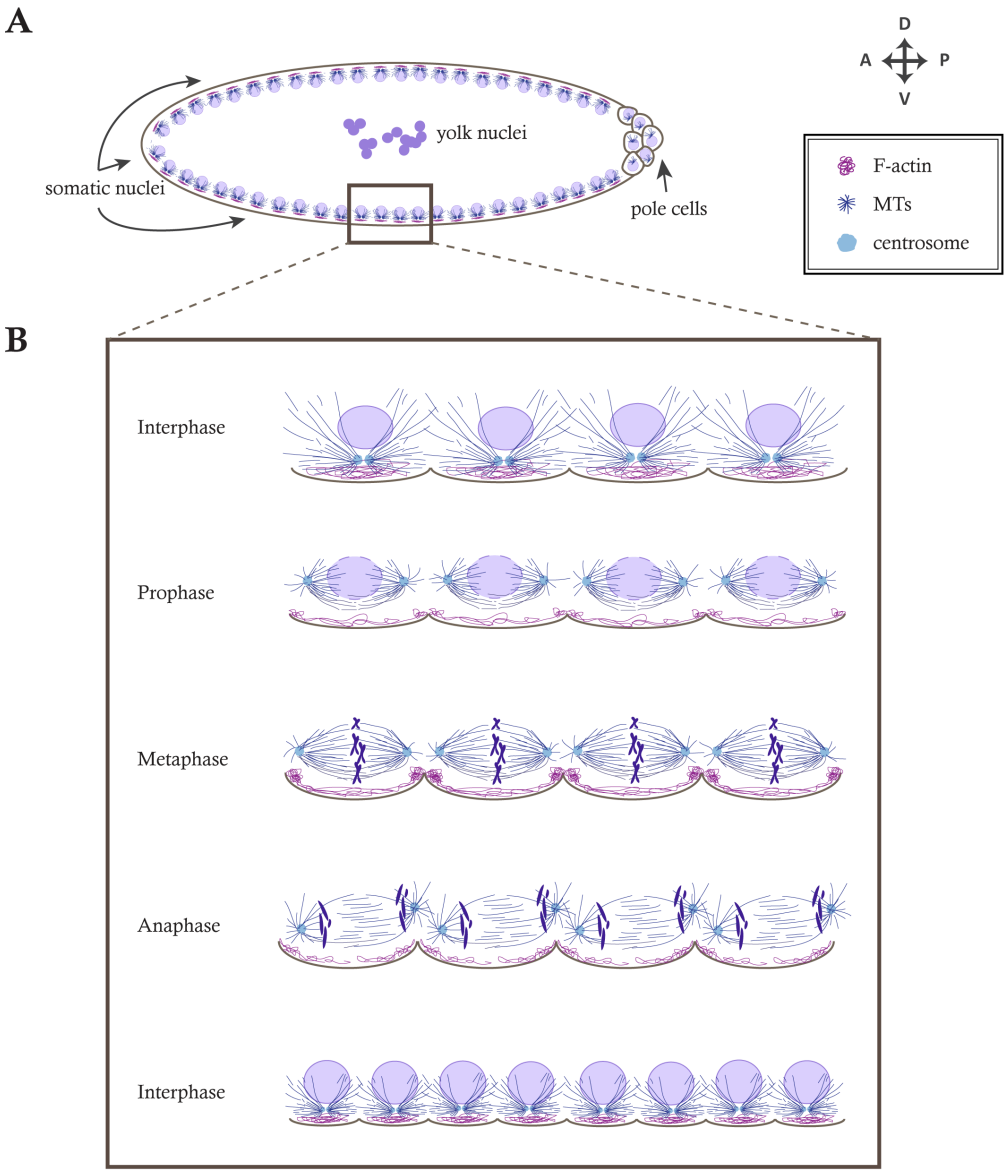


Figure 1.10 The mitotic cycles of the syncytial blastoderm stage *Drosophila* embryo.

(A) Schematic shows the anatomy of the syncytial blastoderm stage fly embryo. Somatic nuclei and their associated centrosomes localize in the cortical region of the embryo, while yolk nuclei are found internally. At the posterior region of the embryo a small number of cellularized nuclei form the pole cells. (B) During the early embryonic mitotic cycles the cortical cytoplasm is heavily reorganized in order to guide the correct division of cortical nuclei within the syncytium. During interphase F-actin caps localize between the plasma membrane and each nucleus. Upon the entry into mitosis and mitotic progression, the actin caps elongate to form physical boundaries between the neighbouring nuclei. The actin caps also divide together with the nuclear material. The embryonic centrosomes are responsible for organizing both the microtubule network and actin network associated with each nucleus.

During the syncytial blastoderm stage the mitotic cycles get progressively slower, due to the gradual elongation of interphase between cycles 10 and 13 (Foe and Alberts 1983). This is most likely due to the lengthier accumulation of mitotic cyclins; the extent of their degradation progressively increases from cycle to cycle with the exponentially growing number of nuclei (Edgar et al. 1994). The elongation of interphase provides time for the initiation of zygotic transcription, which leads to the maternal-to-zygotic transition (MZT) during the interphase of cycle 14 (Foe 1993). This transition is characterized by the degradation of maternal gene products and a burst in zygotic gene expression, leading to complete zygotic control over further developmental events (Tadros and Lipshitz 2009). In *S*-phase of cycle 14 (which is much longer than that of any earlier cycle) the syncytial nuclei cellularize, leading to a monolayer of cortical cells – the *cellular blastoderm stage*. The first apparent embryonic G2 phase is introduced in cycle 14, and at this stage the cells loose their synchrony. In mitosis 14, the first cell cycle event driven by zygotic gene expression, the embryo initiates gastrulation.

1.3.2 THE IMPORTANCE OF CENTROSOMES DURING THE EARLY DEVELOPMENT OF *DROSOPHILA*

Centrioles and centrosomes are not essential for the developmental stages that follow the MZT in *Drosophila* (Basto et al. 2006), however they are indispensable for progression through the preceding syncytial cycles (Stevens et al. 2007). During the first 13 cycles centrosomes play multiple crucial roles that are specific to these early divisions, and failure of any one of these inevitably terminates embryonic development. Conversion of the sperm centriole (that enters the egg during fertilization) into a functioning centrosome is essential for the fusion of the male and female pronuclei. As a result, failure of establishing the sperm aster arrests embryonic development before the very first mitotic cycle (Dix and Raff 2007; Varmark et al. 2007). Centrosomes also play a key role in mitotic progression, through regulating the destruction of cyclin B (Huang and Raff 1999; Wakefield et al. 2000; Rieder et al. 2001). During the preblastoderm stage of *Drosophila* development the degradation of cyclin B occurs locally around the diving nuclei, as opposed to

globally throughout the cytoplasm of the entire embryo (Edgar et al. 1994; Su et al. 1998; Huang and Raff 2002; Raff et al. 2002). As a result, the efficient local regulation of cyclin B degradation by centrosomes is crucial for progression through the preblastoderm stage. Embryos that are unable to duplicate their centrosomes arrest during one of their first nuclear divisions by failing to complete mitosis (Stevens et al. 2007).

Following the preblastoderm stage, centrosome function becomes crucial for a different reason: the proper spatial organization of the peripheral nuclei within the syncytial blastoderm. Prior to the establishment of cell borders the successful division of increasingly crowded nuclei becomes more and more of a challenge, and relies heavily on the cortical cytoskeleton, in particular the cortical microfilaments, organized by the centrosomes. Impaired centrosome function can result in defective organization of these crucial cytoskeletal elements, leading to spindle collisions, nuclear loss and, eventually, arrest of further development (Sullivan and Theurkauf 1995; Vaizel-Ohayon and Schejter 1999).

1.3.3 THE CENTROSOME CYCLE OF THE SYNCYTIAL BLASTODERM STAGE *DROSOPHILA* EMBRYO

The key events of syncytial centriole duplication, and the cell cycle-dependent initiation of these, appear very similar to the canonical process. The individual events, however, are each compressed in time and follow one another much faster than normally, due to the rapid progression of the mitotic divisions (Figure 1.11). At the start of each cycle, the newly disengaged centrioles initiate duplication immediately upon the transition from telophase into early *S*-phase, due to the absence of a detectable *G1* phase. Daughter centrioles grow at the side of each parental centriole during *S*-phase and by metaphase they are structurally indistinguishable from their mother centriole (Figure 1.11) (Callaini and Riparbelli 1990). As in the canonical pathway, mother and daughter centrioles disengage during anaphase (Callaini and Riparbelli 1990). Only a few seconds later, however, they have already entered *S*-phase and started a new round of duplication (Figure 1.11).

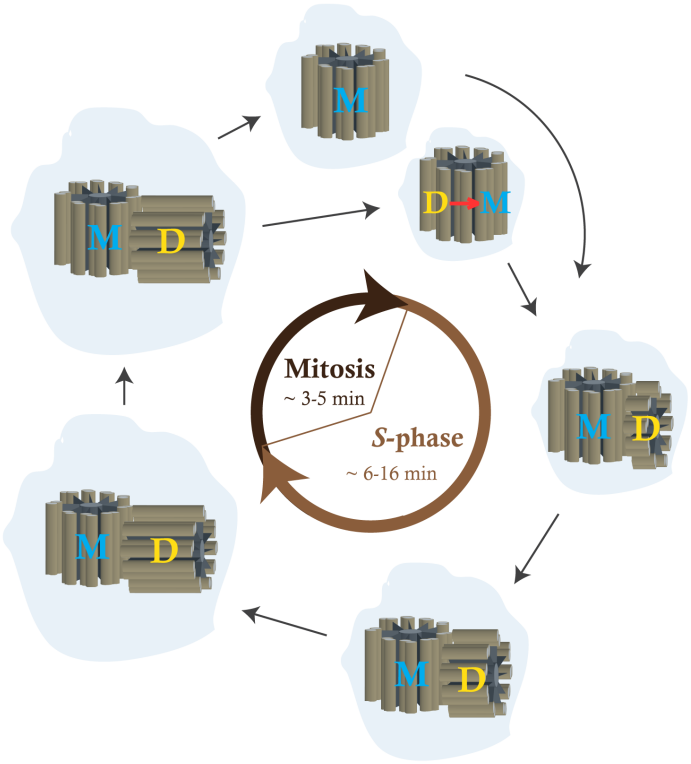


Figure 1.11 The centrosome cycle of the early *Drosophila* embryo.

Schematic illustrates the events of centriole duplication and PCM (*blue*) recruitment during the early mitotic cycles in *Drosophila*. This cycle is a compressed version of the canonical duplication cycle (shown in Figure 1.4). The events of centriole duplication alternate much more rapidly than normally, and lack detectable gap phases between them. In addition, PCM maturation is initiated at the very onset of interphase, thus embryonic centrosomes are constantly associated with high levels of PCM, not only during mitosis.

In most dividing cells duplicated centrosomes only separate in late interphase (Figure 1.4). In contrast, the centrosome pairs of the early fly embryo separate at the very beginning of the cycle, and immediately start their migration to opposite sides of the nucleus in preparation to form the future spindle poles (Callaini and Riparbelli 1990). Furthermore, early embryonic *Drosophila* centrosomes organize relatively large amounts of PCM and microtubules throughout their division cycle (Karr and Alberts 1986; Dix and Raff 2007); in other cell types this is primarily a mitotic feature (Khodjakov and Rieder 1999; Gomez-Ferreria and Sharp 2008).

In conclusion, the temporal aspects of centrosome maturation clearly differ between the early fly embryo and other systems, but the syncytial centriole duplication cycle appears to be a simply more compact, but similarly regulated, version of canonical centriole duplication (Figure 1.11).

1.4 LIVE IMAGING OF THE CENTROSOME CYCLE IN THE SYNCYTIAL BLASTODERM STAGE *DROSOPHILA* EMBRYO

The syncytial fly embryo represents an ideal model system for live imaging-based dynamic studies of centriole duplication. The rapid mitotic cycles are advantageous for live imaging experiments, as the entire duplication cycle can be imaged with high temporal resolution prior to the accumulation of detrimental levels of photodamage in the embryos. The highly synchronous divisions allow the parallel imaging of a large number of centrosomes at the same stage of the cell cycle, which is a great benefit for quantitative experiments. Finally, during the syncytial blastoderm stage the synchronously dividing somatic nuclei and their associated centrosomes are found <5μm beneath the plasma membrane (Warn et al. 1984) and are therefore easily accessible for epifluorescence imaging.

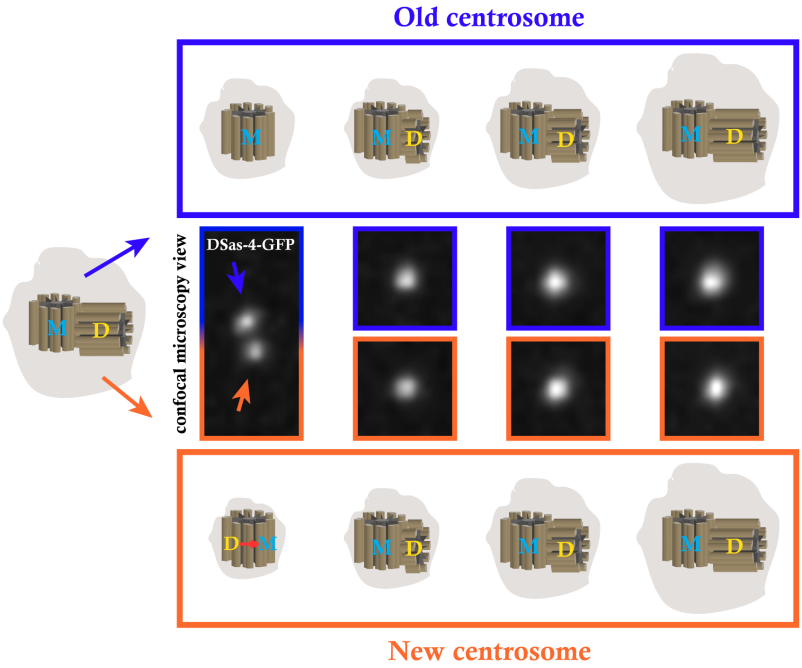


Figure 1.12 Studying centriole duplication using confocal microscopy in the *Drosophila* embryo: the use of centrosome lineage.

At the beginning of the mitotic cycle each embryonic nucleus is associated with two centrosomes, each of which contain a single centriole that will act as the parental centrioles for the upcoming duplication event. As these two parental centrioles derive from the same centrosome (that was inherited from the previous cycle), they differ in their age: one of them has acted as a mother at least once before, while the other was formed as a daughter in the previous mitotic cycle. Throughout this thesis I refer to the centrosome that inherited the original mother centriole as the 'old centrosome' (*dark blue*) while the other one – which inherited the former daughter centriole that is now to act as a mother for the first time – the 'new centrosome' (*orange*). While old and new centrosomes differ in the age of the parental centriole that they contain, the events of daughter centriole formation are the same. As exemplified by the fluorescence images in the middle, during conventional light microscopic analysis we cannot optically resolve parental and daughter centrioles in duplicating centrosomes. However, using the information that the parental centrioles within old and new centrosomes are different in their age while the daughter centrioles in the two centrosomes can be considered identical, it is possible to interpret which of the two centrioles might be responsible for the overall fluorescence changes of the whole centrosome. Thus, the comparative analysis of old and new centrosomes allows us to gather information about the behaviour of individual centrioles from the image data of whole centrosomes.

In this study I used confocal spinning disk microscopy for quantitative live imaging of the centriole duplication cycle in the early *Drosophila* embryo. Due to the diffraction limit of light, this method only allows the optical resolution of centrosomes, and not individual centrioles. I found a way, however, to retrieve information about single centrioles from the image data of whole centrosomes. I now describe this approach (Figure 1.12), as it forms the basis of several of the main conclusions of this study.

Based on the nature of the centriole duplication process, any pair of duplicating centrosomes will be different from one another: while the events of daughter centriole assembly will be the same in both centrosomes, these will differ in the age of the mother centriole that they contain. One centrosome of each pair will have inherited the mother centriole from the previous cycle — I refer to this centrosome as the "*old centrosome*" throughout this thesis (Figure 1.12, dark blue box) — whereas the other centrosome will have inherited the daughter centriole from the previous cycle, which now acts as a mother for the first time — I refer to this centrosome as the "*new centrosome"* throughout this thesis (Figure 1.12, orange box). This information can help interpret which centriole is responsible for the overall fluorescence changes of the whole centrosome: if a pair of centrosomes behave in a different way, that is most likely caused by the mother centrioles that they contain. If behave in an identical manner, that is most likely caused by changes in the growing daughter centrioles, or changes that affect both centrioles.

A great advantage of the syncytial *Drosophila* embryo is that, using microinjection techniques, we can interfere with protein function with extremely high temporal and spatial control *in vivo*. Usually small molecules or antibodies are used for this purpose (Brust-Mascher et al. 2014). Although using antibodies to inhibit protein function may seem fraught with potential problems, this technique seems to work very well in fly embryos, often recapitulating the phenotypic effect of removing a protein of interest by mutation (Gergely et al. 2000; Basto et al. 2006; Buttrick et al. 2008; Brust-Mascher et al. 2009; Conduit et al. 2010). If controlled properly, this technique provides a powerful way to rapidly inactivate a protein's function at any given stage of the cell

cycle. This approach is particularly useful for studying centriole duplication, as the genetic mutation or knockdown of key centriolar proteins prevents the formation of centrioles altogether. Inhibiting centriolar proteins with precise temporal control allows us to study their roles during specific events of centriole formation, which are potentially more downstream than their first crucial function in the assembly pathway.

1.5 THESIS OUTLINE

In this thesis I investigate the role and regulation of Asl during the centrosome cycle of the early *Drosophila* embryo. To address these questions, I first used quantitative live imaging of Asl-GFP (expressed at endogenous levels) to analyse its dynamic behaviour during the centrosome cycle. As a comparison, I also analysed the dynamic centrosomal behaviour of the core centriolar protein DSas-4-GFP. Using a combination of live imaging and immuno-inhibition, I next investigated the centriolar recruitment dependencies of Asl. I then addressed the functional roles of Asl during the centrosome duplication cycle through selectively blocking its initial incorporation or molecular turnover at centrioles by immuno-inhibition. Finally, I have started to address how the initial centriolar incorporation of Asl is regulated during the duplication process, and present my initial work on deciphering these mechanisms.

CHAPTER 2: MATERIALS AND METHODS

2.1 FLY HUSBANDRY

2.1.1 FLY HANDLING

Flies were maintained at 25 ºC or 18 ºC on *Drosophila* culture medium (5.5% glucose, 5% yeast extract, 3.5% wheat flour, 1% pen/strep, 0.75% agar, 0.4% propionic acid, 0.25% nipagen). Stocks were kept in 8cmx2.5cm plastic vials or 0.25 pint plastic bottles. Embryos were collected on apple juice plates (25% apple & raspberry juice, 2.5% sucrose, 2.25% agar) supplemented with fresh yeast suspension. Standard fly handling techniques were used (Roberts 1986).

2.1.2 *DROSOPHILA* STOCKS

Oregon R flies were used as the wild type stock in all experiments. Balancer chromosomes and markers used in this study have been described previously (Lindsley 1992). The GFP- or mCherry fusions of Asl or DSas-4 (wild type or mutant forms) were analyzed in the complete absence of the corresponding endogenous protein in all experiments of this study (*Asl-GFP/mCherry* were crossed into the asl^{B46} homozygous background, *DSas-4-GFP/mCherry* were crossed into the $DSas\text{-}4^{S2214}/Df(3R)BSC221$ background). There were only two experiments where Asl-GFP/mCherry was studied in a wild type background; these were the Asl self-interaction tests (where the interaction of Asl and Asl-GFP is assayed *in vivo*, Figures 5.2 and 5.5) and 3D SIM imaging of Asl-mCherry together with DSas-4-GFP (as attempts to generate an asl^{B46}, $DSas\text{-}4^{S2214}$ recombinant as the ideal genetic background failed due to the close linkage of the two genes; the $DSas\text{-}4^{S2214}/Df(3R)BSC221$ background was used to achieve sufficient centriolar DSas-4-GFP

fluorescence signal, Figures 3.5 and 3.12). All other GFP, RFP or mCherry fusion proteins were analysed in the presence of the corresponding endogenous protein.

In all experiments of this study the fly stocks expressed 2 copies of each transgene that they carried (homozygotes), with the exception of the *eDSas-4-GFP*,*DSas-4*^{S2214} line used for analysing the dynamic incorporation of DSas-4-GFP in embryos; this stock expressed 4 copies of *DSas-4-GFP* (homozygous for 2 different insertions) which produced endogenous levels of DSas-4-GFP protein in embryos. All mutant alleles, P-element lines and transgenic lines that were used, but not generated in this study, are described in Table 2.1 while all transgenic lines that were generated and used in this study are listed in Table 2.2.

Table 2.1. List of *Drosophila* lines that were obtained from other sources

Name	Description	Source
w^{118}*; P(EPg)HP37249*	Used for generating *asl*^{B46}	BDSC (#22014)
DSas-4^{S2214}	*dsas-4* null mutant allele used	(Basto et al. 2006)
Df(3R)BSC221	chromosomal deletion that removes *dsas-4*	(Cook et al. 2012)
(pUbq) Asl-GFP	Asl-GFP expressed from ubiquitin promoter; leads to moderate overexpression in embryos and slightly stronger overexpression in brains	(Stevens et al. 2010)
(pUbq) RFP-PACT	RFP-PACT (centriolar localization domain of D-PLP) expressed from ubiquitin promoter	(Lucas and Raff 2007)
(pUbq) RFP-DSpd-2	RFP-DSpd-2 expressed from ubiquitin promoter	(Novak et al. 2014)

2.1.2.1 GENERATION OF THE *ASL^{B46}* MUTANT LINE

The *asl^{B46}* mutant allele was generated through imprecise excision of the *P{EPg}HP37249* element located 473 upstream of the *asterless* (CG2919) start codon. To induce P-element excision, the *Δ2-3Sb* chromosome (which encodes the transposase) was crossed over the *P(EPg)HP37249* chromosome. Individual *w$^+$/Y;;Δ2-3Sb/P{EPg}HP37249* males were mated with *w$^-$/w$^-$;;PrDr/TM6B* females. The male progeny of these flies were screened for white eye colour (which indicated the loss of the *mini-white* gene encoded by the P-element, and therefore, excision of the P-element). Individual white eyed males were crossed to *w$^-$/w$^-$;;PrDr/TM6C* virgin females to generate stocks in which the excision events were balanced. Genomic DNA was then extracted from the founder males of each stock and imprecise excision events were screened by PCR as described in section 2.2.5. The *asl^{B46}* allele was the largest imprecise excision recovered in the screen of 250 individual excision events; the deletion removed the complete 5' UTR as well as the first 1775bp of the *asl* coding sequence.

2.1.2.2 TRANSGENIC LINES

Transgenic lines were generated through the injection of a P-element transformation vector containing the transgene into *w^{118}* embryos (generation of transformation vectors is described in section 2.2.1) The injection, selection of transgenic flies and generation of transgenic stocks (through mating of individual transgenic flies with *w^{118}* males or virgin females) was carried out at the Department of Genetics, University of Cambridge. I subsequently mapped the chromosome on which the transgene insertion happened using standard *Drosophila* crossing methods (Greenspan 2004) and established homozygous stocks of the transgenic lines. All transgenic lines generated and used in this study are described in Table 2.2.

Table 2.2. List of transgenic *Drosophila* lines that were generated and used in this study

Name	Description	Line used in this study (chr)
eDSas-4-GFP	DSas-4-GFP (C-terminal tag) expressed at endogenous levels * To match endogenous protein levels in embryos I used 4 copies of this transgene: (insertions #6 (ChrII) and #8 (ChrIII) both homozygous). In brains 2 copies (#8, homozygous) gave endogenous protein levels.	ZN1 #6 (II); ZN1 #8 (III)
eDSas-4-mCherry	DSas-4-mCherry (C-terminal tag) expressed at endogenous levels	ZN5 #11 (II)
eDSas-4 (SS299,300AA)-GFP	DSas-4-GFP S299A & S300A (C-terminal tag) expressed at endogenous levels	ZN2 #4 (III)
eDSas-4 (SS299,300AA)-mCherry	DSas-4-mCherry S299A & S300A (C-terminal tag) expressed at endogenous levels	ZN6 #10 (II)
eDSas-4 (S300D)-GFP	DSas-4-GFP S300D (C-terminal tag) expressed at endogenous levels	ZN3 #2-1 (III)
eDSas-4 (S300D)-mCherry	DSas-4-mCherry S300D (C-terminal tag) expressed at endogenous levels	ZN7 #2 (II)
eAsl-mCherry	Asl-mCherry (C-terminal tag) expressed at endogenous levels	ZN8 #11 (III)
eSak-GFP	Sak-GFP (C-terminal tag) expressed at endogenous levels	ZN4 #5 (II)

2.2 MOLECULAR BIOLOGY

2.2.1 CONSTRUCTION OF TRANSFORMATION VECTORS FOR THE GENERATION OF TRANSGENIC *DROSOPHILA* LINES

Gateway cloning (Life Technologies) was used to generate all vectors used for p-element mediated transformations. For all constructs generated in this study, the genetic region of each gene was cloned from 2kb upstream of the start codon up to the stop codon from w^{67} DNA (based on

Blachon et al. 2008). The constructs were cloned using Phusion High Fidelity PCR reactions (NEB, #M0531) through a nested PCR approach; the target sequences were cloned from the genomic template in the first reaction while flanking *attB* sites were introduced in the second PCR (Table 2.3). The resulting fragments were then introduced into the pDONR^{TM}/Zeo vector (Gateway) according to the Gateway BP reaction to generate *attL*-containing entry clones. To attach C-terminal GFP or mCherry fusions to the gene sequences, the entry clones were recombined with the appropriate *attR*-containing GFP (pUASt-GFP[CT]; source: DGRC, pTWG-1076) or mCherry (pZN10, see Table 2.4) destination vectors according to the Gateway LR reaction. PCR products and plasmids were purified using Qiagen reagents and protocols (gel extraction kit #28706 and plasmid mini- and midiprep kits, #12125 and #12145). MacVector software was used for the *in silico* construction and analysis of all constructs. The list of plasmids that were cloned and used in this study for the generation of transgenic lines is shown in Table 2.4.

Table 2.3. List of primers used for cloning the genetic regions of DSas-4, Asl or Sak

Gene/Sequence	Primer sequences (Forward & Reverse)
DSas-4	GCAGGCTTCCGGATGAATGTGCGCATCCGTG
	AGCTGGGTCATACTTGGCATAGTCTGTGTCCATTATGAGC
asl	GCAGGCTTCAGTGCTGGAACACTTCTCACAACATGTG
	AGCTGGGTCGCTGTGACCATTGCCTTTGGGCT
Sak	GCAGGCTTCAGACGACCTTTGGAGAACTGATTA
	AGCTGGGTCAAGAAGCATGCGATTATAATAAGG
attB	GGGGACAAGTTTGTACAAAAAAGCAGGCTTC
	GGGGACCACTTTGTACAAGAAAGCTGGGTC

Table 2.4. List of plasmids that were generated and used in this study for the generation of transgenic *Drosophila* lines

Plasmid ID	Description	Promoter	Resistance
pZN1	*eDSas-4* in pDONOR	*DSas4* endog.	Zeo
pZN2	*eAsl* in pDONOR	*asl* endog.	Zeo
pZN3	*(UASt) eDSas-4-GFP*	UASt, *DSas-4* endog.	Amp
pZN4	*eDSas-4 S299,300A* in pDONOR	*DSas-4* endog.	Zeo
pZN5	*eDSas-4 S300D* in pDONOR	*DSas-4* endog.	Zeo
pZN6	*eSak* in pDONOR	*Sak* endog.	Zeo
pZN7	*(UASt) eDSas-4-GFP S299,300A*	UASt, *DSas-4* endog.	Amp
pZN8	*(UASt) eDSas-4-GFP S300D*	UASt, *DSas-4* endog.	Amp
pZN9	*(UASt) eSak-GFP*	UASt, *Sak* endog.	Amp
pZN10	no promoter, -mCherry (CT)	none	Kan, Chlamph
pZN11	*eDSas-4-mCherry*	*DSas-4* endog.	Kan
pZN12	*eDSas-4-mCherry S299,300A*	*DSas-4* endog.	Kan
pZN13	*eDSas-4-mCherry S300D*	*DSas-4* endog.	Kan
pZN14	*eAsl-mCherry*	*asl* endog.	Kan
pZN36	*(UASt) eDSas-4-GFP 198-244 S/T>A*	UASt, *DSas-4* endog.	Amp
pZN37	*(UASt) eDSas-4-GFP 198-244 S/T>E*	UASt, *DSas-4* endog.	Amp
pZN38	*eDSas-4-mCherry 198-244 S/T>A*	*DSas-4* endog.	Kan
pZN39	*eDSas-4-mCherry 198-244 S/T>E*	*DSas-4* endog.	Kan

2.2.2 CONSTRUCTION OF VECTORS FOR *IN VITRO* RNA PRODUCTION (FOR RNA-MICROINJECTION EXPERIMENTS)

To generate the various *DSas-4* constructs for the purpose of *in vitro* RNA production the single intron within the *DSas-4* gene was first removed from the pZN1 *DSas-4* donor vector. The resulting construct was then used to introduce any deletions or base substitutions to generate

mutated constructs (as described in section 2.2.3). The *DSas-4* cDNA sequence (excluding the stop codon) was then amplified from each construct (using the primers shown in Table 2.5) and cloned into the pDONR^{TM}/Zeo (Gateway) according to the Gateway BP reaction to generate *attL*-containing entry clones. The entry clones were then recombined with the pRNA-GFP(CT) destination vector (gift from Dr. N. Muschalik and M. Cottee) according to the Gateway LR reaction. All plasmids were isolated using Qiagen reagents and protocols (plasmid mini- and midiprep kits, #12125 and #12145). MacVector software was used for the *in silico* construction and analysis of all constructs. The list of plasmids cloned and used in this study for *in vitro* RNA production is shown in Table 2.7.

Table 2.5. Primers used for amplifying the *DSas-4* cDNA sequence

cDNA	Primer sequences (Forward & Reverse)
DSas-4	GCAGGCTTCATGCAGGAGGCTGGCGAAAGTCC AGCTGGGTCATACTTGGCATAGTCTGTGTCCATTATGAGC

2.2.3 PLASMID MUTAGENESIS

Single or multiple base substitutions and smaller deletions (<100bp) were introduced into the appropriate entry clones using Quikchange II XL Site-Directed Mutagenesis Kit (Agilent Technologies, Inc. #200522) or Quikchange Multi Site-Directed Mutagenesis Kit (Agilent Technologies, Inc. #200515) according to the manual instructions. The primers used for site directed mutagenesis are listed in Table 2.6.

Table 2.6. List of primers used for site directed mutagenesis in this study. All codons affected are shown in red (not indicating the number of bases substituted), while sequences bordering the two sides of a deleted region are shown in blue and purple.

Primer sequence	Sites changed	Template
DSas-4 S299>A; S300>A	F: GGGAAACATTGATATGAACGCCGCCTGCATTCGAACCTTTATGGC R: GCCATAAAGGTTCGAATGCAGGCGGCGTTCATATCAATGTTTCCC	pZN1
DSas-4 S300>D	F: GGGAAACATTGATATGAACTCCGACTGCATTCGAACCTTTATGGC R: GCCATAAAGGTTCGAATGCAGTCGGAGTTCATATCAATGTTTCCC	pZN1
deletion of ubiquitin promoter from pUbq-mCherry(CT) destination vector	F: CCACACTGGACTAGTAGGTACCACTGATTGCAAGCGCACCGAAAGC R: GCTTTCGGTGCGCTTGCAATCAGTGGTACCTACTAGTCCAGTGTGG	pUbq-mCherry (CT) DEST (JR #80)
deletion of *DSas-4* intron	F: TAGCCCGGCTTGCCCCCAAAGTGTTACCTTCCGCGACAAT R: ATTGTCGCGGAAGGTAACACTTTGGGGGCAAGCCGGGCTA	pZN1
deletion of DSas-4 198-217	F: TTATCGGCAAGAACGCCTGCCCCAGAGTTCGTTTTGTAGAGC R: GCTCTACAAAACGAACTCTGGGGCAGGCGTTCTTGCCGATAA	pZN15
deletion of DSas-4 198-244	F: ATCGGCAAGAACGCCTGCCCCATGACAGGAGTTTGCTGGG R: CCCAGCAAACTCCTGTCATGGGGCAGGCGTTCTTGCCGAT	product of above
DSas-4 T257>A	F: GCTGGGCCAAGGTGCTGGACGCACAGAGTATAAAGCCAGCGC R: GCGCTGGCTTTATACTCTGTGCGTCCAGCACCTTGGCCCAGC	pZN15
DSas-4 S269>A	F: CGCAAATCCAAAGACGCGCTGCTCAAATCCGAGTGGAAGATGAC R: GTCATCTTCCACTCGGATTTGAGCAGCGCGTCTTTGGATTTGCG	product of above
DSas-4 S281>A	F: GAGTGGAAGATGACAGCAATGTAGCCATATTCGAGCTGCTCGAGC R: GCTCGAGCAGCTCGAATATGGCTACATTGCTGTCATCTTCCACTC	product of above
DSas-4 S299>A; S300>A; T304>A	F: CATTGATATGAACGCCGCCTGCATTCGAGCCTTTATGGCGCGCAAAG R: CTTTGCGCGCCATAAAGGCTCGAATGCAGGCGGCGTTCATATCAATG	product of above
DSas-4 T257>E	F: GCTGGGCCAAGGTGCTGGACGAACAGAGTATAAAGCCAGCGC R: GCGCTGGCTTTATACTCTGTTCGTCCAGCACCTTGGCCCAGC	pZN15
DSas-4 S269>E	F: CGCAAATCCAAAGACGCGAAGCTCAAATCCGAGTGGAAGATGAC R: GTCATCTTCCACTCGGATTTGAGCTTCGCGTCTTTGGATTTGCG	product of above
DSas-4 S281>E	F: GGAAGATGACAGCAATGTAGAGATATTCGAGCTGCTCGAGCAG R: CTGCTCGAGCAGCTCGAATATCTCTACATTGCTGTCATCTTCC	product of above
DSas-4 S300>E; T304>E	F: GATATGAACTCCGAGTGCATTCGAGAGTTTATGGCGCGCAAAGATC R: GATCTTTGCGCGCCATAAACTCTCGAATGCACTCGGAGTTCATATC	product of above
DSas-4 S198>A; S199>A; T200>A	F: CAAGAACGCCTGCGCTGCCGCTCCAGATCTAAAGTCTTCCTATGC R: GCATAGGAAGACTTTAGATCTGGAGCGGCAGCGCAGGCGTTCTTG	pZN15

DSas-4 S205>A; S206>A; S209>A; S210>A; T211>A	F: CCAGATCTAAAGGCTGCCTATGCGGCCGCCGCAACCGCCTCGAGC R: GCTCGAGGCGGTTGCGGCGGCCGCATAGGCAGCCTTTAGATCTGG	product of above
DSas-4 T212>A; S214>A; S215>A; T216>A; S217>A	F: CCTATGCGGCCGCCGCAGCCGCCGCGGCCGCCGCGCCCAGAGTTC R: GAACTCTGGGCGCGGCGGCCGCGGCGGCTGCGGCGGCCGCATAGG	product of above
DSas-4 S240>A; S241>A; S244>A	F: CGATGATGAAGCCGCCGCGGAAGCTGCTCCCATGACAGGAGTTTG R: CAAACTCCTGTCATGGGAGCAGCTTCCGCGGCGGCTTCATCATCG	product of above
DSas-4 T200>E	F: GCAAGAACGCCTGCAGTTCCGAGCCAGATCTAAAGTCTGAGTATGC R: GCATACTCAGACTTTAGATCTGGCTCGGAACTGCAGGCGTTCTTGC	pZN15
DSas-4 S206>E; S210>E	F: CAGATCTAAAGTCTGAGTATGCGTCCGAGACAACCGCCGAGAGC R: GCTCTCGGCGGTTGTCTCGGACGCATACTCAGACTTTAGATCTG	product of above
DSas-4 S214>E; S217>E	F: CGAGACAACCGCCGAGAGCACCGAGCCCAGAGTTCGTTTTGTAGAG R: CTCTACAAAACGAACTCTGGGCTCGGTGCTCTCGGCGGTTGTCTCG	product of above
DSas-4 S241>E; S244>E	F: CGATGATGAAGCCTCCGAGGAAGCTGAGCCCATGACAGGAGTTTGC R: GCAAACTCCTGTCATGGGCTCAGCTTCCTCGGAGGCTTCATCATCG	product of above

Table 2.7. List of plasmids that were generated and used in this study for *in vitro* RNA production

Plasmid ID	Description	Promoter	Resistance
pZN29	pRNA DSas4(-intron)-GFP	T3	Amp
pZN30	pRNA DSas4(-intron) Δ198-217 -GFP	T3	Amp
pZN31	pRNA DSas4(-intron) Δ198-244 -GFP	T3	Amp
pZN32	pRNA DSas4(-intron) 198-244 S/T>A -GFP	T3	Amp
pZN33	pRNA DSas4(-intron) 198-244 S/T>E -GFP	T3	Amp
pZN34	pRNA DSas4(-intron) 257-304 S/T>A -GFP	T3	Amp
pZN35	pRNA DSas4(-intron) 257-304 S/T>E-GFP	T3	Amp

2.2.4 PURIFICATION OF GENOMIC DNA FROM *DROSOPHILA*

To purify DNA for the purpose of cloning or sequencing, 30 anesthetized flies per sample were homogenized on ice in 400µl of Buffer A (100mM Tris-HCl (pH 7.5), 100mM EDTA, 100mM NaCl, 0.5% SDS) and incubated at 65 ºC for 30 minutes. 800µl of Buffer B (2:5 volume of 5M CH_3CO_2K and 6M LiCl respectively) was added followed by incubation on ice for 1 hour. Samples were then centrifuged at 12,000rpm at room temperature for 15 minutes. 1ml of the supernatant was transferred into a fresh tube, mixed with 600µl of isopropanol and centrifuged at 12,000rpm at room temperature for 15 minutes. The DNA pellet was then washed twice with 70% ethanol, air-dried and re-suspended in TE buffer.

To extract DNA for diagnostic PCRs, individual flies were homogenized in 50µl of buffer (10mM Tris- HCl (pH 8.0), 1mM EDTA, 25mM NaCl, 200µg/µl Proteinase K) and incubated at 55 ºC for 30 minutes, then at 95 ºC for 10 minutes. The resulting samples were then diluted three-fold in ddH_2O prior to use in PCR reactions.

2.2.5 DIAGNOSTIC PCR REACTIONS

Diagnostic PCR primers, reactions and programmes used for the screening of imprecise P-element excision or recombination events are described in Table 2.8.

2.2.6 DNA SEQUENCING

DNA sequencing was performed by Source BioScience and all sequence data was analyzed using MacVector.

Table 2.8 Diagnostic PCRs (': minutes; ": seconds)

Diagnostic PCR composition:

- 1µl DNA
- 0.5µl of each primer
- 5µl JumpStart REDTaq ReadyMix (Sigma #P0982) or OneTaq Quick-Load 2x MM (NEB, #M0486S)
- 3µl ddH_2O

PCR programme:

1. 94 ºC for 2'
2. 94 ºC for 30"
3. T_{ann} ºC for 30"
4. 72/68 ºC for t_{ext}
5. 72/68 ºC for t_{final}

Steps 2-4 repeated 35x

Diagnostic PCR primers used in this study:

Screen	Primers	T_{ann}	t_{ext}	t_{final}
P{EPg}HP37249 imprecise excision	TTCCTAAGTCTTAGCTGTGACCATTGCC CGGCACCTTCTACTACTTTGATGCG	58 ºC	5'	10'
asl^{B46} allele	CCCTCTCCTTAAGATCGCTAATGAG GTATGTGCAAATTCTGGTACAAATTGC	54 ºC	4'	10'
Df(3R)BSC221	CATATGGGATCATCGTTTCGAGAAGAC ACATATTTAATTAGCGCTTCCTGTCAGTG	52 ºC	2'	5'

2.2.7 *IN VITRO* RNA TRANSCRIPTION

To generate template DNA for *in vitro* transcription, 4µg of plasmid DNA was linearized using AscI in a total volume of 80µl (incubated for 8 hours at 37 ºC, followed by inactivation of the enzyme at 80 ºC for 20 minutes) and then precipitated using ethanol-precipitation (4µl 0.5M EDTA, 8µl 3M Na-acetate and 180µl 100% ethanol added to each reaction). The samples were incubated at -20 ºC overnight and the DNA was then pelleted by centrifugation at 14.8k rpm at 4 ºC for 1 hour. The pellet was washed twice with -20 ºC 70% ethanol, air-dried and re-suspended in 7 µl DEPC-treated ddH_2O.

Transcription reactions were performed using Ambion mMESSAGE mMACHINE T3 Kit (#AM1348) according to the manual instructions. A total of 2 μg linearized DNA template was used for each construct, in a final volume of 40 μl and the reactions were incubated for 1.5 hours at 37 ºC. The RNA generated in the reactions was then purified using Qiagen RNeasy MinElute kit (#74204) according to the manual instructions, and then diluted to 2μg/μl concentration for all embryo injection experiments.

2.3 BIOCHEMISTRY

2.3.1 IMMUNOPRECIPITATION OF PROTEINS FROM *DROSOPHILA* EMBRYO CYTOPLASM EXTRACTS

2.3.1.1 PREPARATION OF CYTOPLASM EXTRACTS

0-4 hour old embryos were washed 3 times in PBS+0.05% Triton X-100, dechorionated in 60% bleach solution for 2 minutes, washed again 3 times in PBS+0.05% Triton X-100 and stored at -80 ºC until further use. To prepare cytoplasm extracts, 200-400mg of frozen embryos were homogenized on ice in an equal volume of Homogenizing Buffer [50mM HEPES pH 7.6, 1mM $MgCl_2$, 1mM EGTA, 1/100V protease inhibitor cocktail (100mM benzamidine-HCl, 50mM phenanthroline, 1mg/ml aprotinin, 1mg/ml leupeptin, 0.3mg/ml pepstatin), 1/100V phosphatase inhibitor cocktail (Roche), 1/100V PMSF] using a hand pellet pestle and 1/1000V of 1mM DTT was added immediately. The lysate was centrifuged twice at 14.8k rpm in a tabletop microcentrifuge at 4 ºC. The clear cytoplasm fraction was saved and diluted 2-fold with Homogenizing Buffer prior to further use.

2.3.1.2 PREPARATION OF PULLDOWN BEADS

Protein-A Dynabeads (Life Technologies, #10002D) were used for immunoprecipitation experiments; these were freshly coupled with the pulldown antibody on the day of each pulldown experiment. 65µl bead slurry/rxn was first washed twice in PBS+0.1% Triton X-100. The beads were then incubated with 12.5µg/rxn anti-GFP (JR #118, rabbit polyclonal) or random rabbit antibody (JR #143) in 500µl/rxn PBS for 2.5 hours at 4 ºC followed by 1 hour at room temperature. The beads were washed twice with 250µl/rxn Conjugation Buffer (20mM fresh sodium phosphate buffer pH7.9, 0.15M NaCl) quickly and then resuspended in 541.66µl/rxn Conjugation Buffer+5mM BS3 (BS3: Thermo Fischer Scientific #21580) and incubated rotating at room temperature for 30 minutes. The crosslinking reaction was quenched by addition of 27µl 1M Tris-HCl pH7.5 followed by incubation at room temperature for 15 minutes with rotation. The beads were finally washed for 2x5 minutes with 500µl/rxn PBS+0.1% Triton X-100, then resuspended in 500µl/rxn Homogenizing Buffer and stored at 4 ºC until further use (up to a few hours).

2.3.1.3 IMMUNOPRECIPITATION

The buffer was removed from the antibody-coupled pulldown beads and replaced with 150µl/rxn of the freshly prepared, 2-fold diluted embryo extract and incubated rotation overnight at 4 ºC. The beads were then quickly washed twice at room temperature with 200µl PBS+0.1% Triton X-100, followed by 5x10 minute washes with 200µl PBS+0.1% Triton X-100 at 4 ºC. Finally the beads were resuspended in 50µl 2-fold concentrated SDS loading dye and boiled for 10 minutes. The eluted immunoprecipitation fraction as well as the input and unbound fractions were then analysed by SDS-PAGE followed by western blotting as described below.

2.3.2 PREPARATION OF DROSOPHILA EMBRYO AND BRAIN LYSATES FOR PROTEIN EXPRESSION ANALYSIS

To prepare embryos lysates, 0-3 hour old embryos were washed 3 times in PBS+0.05% Triton X-100, dechorionated in 60% bleach solution for 2 minutes, then washed again 3 times in PBS+0.05% Triton X-100. Using 2ml heptane, the embryos were washed into a glass vial containing methanol + 3% 0.5M EGTA, shaken for 30s, and left to fall into the lower, methanol+EGTA layer. All liquid was removed from the vial and the embryos were washed 3 times in methanol, then incubated minimum overnight and up to several weeks in methanol at 4 ºC. The methanol was then removed and the embryos were washed for 3x15 minutes in PBS+0.2% Triton X-100. The embryos were transferred into a watch glass containing fresh PBS+0.2% Triton X-100, 25 pre-cellularization staged embryos were selected and pipetted into a final volume of 10µl PBS+0.2% Triton X-100, mixed with 15µl 2-fold concentrated SDS loading dye and boiled for 10 minutes. The samples were stored at -20 ºC until analysis. 10µl of each sample was analyzed by SDS-PAGE followed by western blotting.

To prepare brain lysates for SDS-PAGE, 3rd instar larval brains were dissected in PBS and transferred immediately into 1-fold concentrated SDS loading dye. The samples were stored at -20 ºC until analysis, or loaded immediately onto a gel for SDS-PAGE followed by Western blotting. When Asl or Asl-GFP was analysed then 2 brains-equivalent of sample was analysed per lane, for DSas-4 or DSas-4-GFP 4 brains-equivalent of sample was used.

2.3.3 SDS-PAGE

Samples were run on 3-8% NuPAGE acrylamide gels (Life Technologies #EA03785BOX) using NuPAGE tris-acetate SDS running buffer (Life Technologies #LA0041) at 150V in a XCell SureLock Mini-Cell.

2.3.4 WESTERN BLOTTING

Samples were transferred from the acrylamide gel onto nitrocellulose membrane (BIO-RAD, 0.2μm, #162-0112) in a BIO-RAD Mini Trans-Blot system using transfer buffer (25% methanol, 1.13% glycine, 0.58% tris, 0.01% SDS). The membranes were blocked for 1 hour at room temperature in blocking solution (PBS+4% milk powder+0.1% Tween-20), incubated with the primary antibody for 1h at room temperature (antibodies were diluted to 1-5ng/ml in blocking solution), and washed for 1 minute in TBS+0.1% Tween-20 before incubation with the secondary antibody (diluted 3000-fold in blocking solution) for 45 minutes. For chemiluminescence analysis horseradish peroxidase–conjugated secondary antibodies were used (GE Healthcare, ECL anti-rabbit (#NA934V) or anti-mouse (#NA931V) IgG HRPO-linked whole antibody), while for quantitative analysis fluorophore-coupled antibodies were used (LI-COR IRDye 680LT anti-rabbit #926-68021; IRDye 800CW anti-mouse #926-32210). The membranes were washed for 3x15 minutes in TBS+0.1% Tween-20. For chemiluminescence analysis, the membranes were incubated for 1 minute in HRPO-substrate (Thermo Scientific SuperSignal West Femto Maximum Sensitivity Substrate, #34095; used this in 2 or 3-fold dilution compared to the manual instructions) and then exposed to X-ray film. For quantitative analysis, the membranes were scanned using a LI-COR Odyssey gel imager and scanner according to the manual instructions.

2.4 CELL BIOLOGY

2.4.1 PREPARATION OF EMBRYOS FOR LIVE IMAGING ANALYSIS

0-1.5 hour old embryos were dechorionated by hand on double-sided sticky tape and mounted onto a thin layer of glue (sticky tape dissolved in heptane) on a glass bottom microwell dish (MatTek, #P35G-1.5-14-C). The embryos were then desiccated for 1-2 minutes at 25 ºC, covered with Voltalef PCTFE oil and imaged immediately. For RNA injection experiments 0-30 minute old

embryos were used and the embryos were desiccated longer, for 5 minutes at 25 ºC, before RNA injection or antibody injection experiments.

2.4.2 MICROINJECTION OF ANTIBODIES OR RNA INTO LIVING EMBRYOS

The injection of TexasRed-coupled antibodies or *in vitro* transcribed RNA constructs into living embryos was performed on a Zeiss Axiovert microscope (the confocal microscope which was subsequently used to image these embryos, as described in detail below). The antibodies used for blocking the function of centrosomal proteins (described in Table 2.9) were injected into embryos during mitotic cycles 10-12, during the onset of mitosis (judged by centrosome positioning). These embryos were imaged immediately following the injection of the antibodies as described below in section 2.5.1, and photobleaching experiments were performed as described in section 2.5.2. *In vitro* transcribed RNA constructs were injected into 15-30 minute old embryos (*Asl-mCherry; asl*^{B4}) and these embryos were aged for 1-1.5 hour prior to imaging.

2.4.3 FIXATION AND STAINING OF EMBRYOS FOR IMMUNOFLUORESCENCE ANALYSIS

0-3 hour old embryos were washed 3 times in PBS+0.05% Triton X-100, dechorionated in 60% bleach solution for 2 minutes, then washed again 3 times in PBS+0.05% Triton X-100. Using 2ml heptane, the embryos were washed into a glass vial containing methanol + 3% 0.5M EGTA, shaken for 30s, and left to fall into the lower, methanol+EGTA layer. All liquid was removed from the vial and the embryos were washed 3 times in methanol, then incubated minimum overnight and up to several weeks in methanol at 4 ºC. Prior to staining, the methanol was removed and the embryos were washed for 3x20 minutes, then 2x30 minutes in in PBS+0.2% Triton X-100. The embryos were then incubated in the primary antibody solution (antibody diluted in in PBS+0.2% Triton X-100, see Table 2.9) at 4 ºC overnight, washed 3x20 minutes in in PBS+0.2% Triton X-100 and then

incubated in the secondary antibody solution (Alexa Fluor 488/568/647, Life Technologies ; diluted in PBS+0.2% Triton X-100) for 2 hours at room temperature. The embryos were washed in PBS+0.2% Triton X-100 2x15 minutes, incubated in in PBS+0.1% Triton X-100+1/5000 V 10mg/ml Hoescht for 15 minutes, washed again in in PBS+0.2% Triton X-100 for 15 minutes and then mounted onto glass slides using mounting medium (85% glycerol, 2.5% n-propylgallate).

2.4.4 FIXATION AND STAINING OF 3RD INSTAR LARVAL BRAINS FOR IMMUNO-FLUORESCENCE ANALYSIS

3rd instar larval brains were dissected in PBS, incubated in formaldehyde for 20 minutes, in 45% acetic acid for 15 seconds, and finally in 60% acetic acid for 3 minutes. The fixed brains were then immediately squashed onto a glass microscope slide using a coverslip and then flash frozen in liquid nitrogen. The coverslips were removed from the frozen samples and the slides were incubated in -20 ºC methanol for 5 minutes, then in PBS+0.1% Triton X-100 for 4x15 minutes. The slides were then dried and the samples were covered with 10 µl primary antibody solution (diluted in PBS+0.1% Triton X-100, see Table 2.9), sealed with a coverslip, and incubated overnight at 4 ºC in a humid chamber. Following 3x5 minute washes of the slides in PBS+0.1% Triton X-100, the samples were covered with 10 µl secondary antibody solution (Alexa Fluor 488/568/647, Life Technologies; diluted in PBS+0.1% Triton X-100), sealed with a coverslip, and incubated overnight at 4 ºC in a humid chamber. The slides were then washed 3x15 minutes in PBS+0.1% Triton X-100, incubated in PBS+0.1% Triton X-100+1/5000 V 10mg/ml Hoescht33258 (Life Technologies) for 10 minutes, and washed in PBS+0.1% Triton X-100 for 5 minutes. Finally the samples were covered with 10µl mounting medium (85% glycerol, 2.5% n-propylgallate), sealed with a coverslip, and stored at 4 ºC in dark till microscopic analysis.

Table 2.9 Primary antibodies used in this study (* AP: affinity purified; S: serum)

Antibody	ID	Species	Application	Specifics *
Anti-Asl (N-term)	JR #11	Rabbit	Injection into living embryos	AP, 5mg/ml
			Immunofluorescence - embryos	AP, 1:500
			Western blotting	AP, 1:500
	JR #199	Guinea Pig	Immunofluorescence - brains	S, 1:500
Anti-Asl (C-term)	JR #13	Rabbit	Injection into living embryos	AP, 5mg/ml
			Western blotting	AP, 1:500
Anti-DSas-4 (N-term)	JR #63	Rabbit	Injection into living embryos	AP, 5mg/ml
			Western blotting	AP, 1:500
Anti-actin	JR #221	Mouse	Western blotting	1:500
Anti-Cnn (N-term)	JR #37	Rabbit	Immunofluorescence - brains	AP, 1:500
Anti-PH3	JR #183	Goat	Immunofluorescence - brains	1:500
Anti- α-tubulin	JR #141	Mouse	Immunofluorescence - embryos	1:500
Anti- γ-tubulin	JR #142	Mouse	Immunofluorescence - brains	1:500

2.5 MICROSCOPY

2.5.1 LIVE CONFOCAL IMAGING OF *DROSOPHILA* EMBRYOS

Dechorionated living embryos were imaged at 21 ºC on a Perkin Elmer ERS Spinning Disc confocal system on a Zeiss Axiovert 200M microscope, using a Zeiss plan-apochromat 63x / 1.4NA, oil objective and a charge-coupled device camera (Orca ER, Hamamatsu Photonics). For imaging GFP alone the UltraVIEW ERS 'fast sequential' imaging mode was used (red/green dual

passband filter: 525nm pass band centre, 50nm half-power bandwidth and 640nm pass band centre, 120nm half-power bandwidth; for imaging 488nm and/or 568nm emission). For imaging GFP together with RFP, mCherry or TexasRed the UltraVIEW ERS 'emission discrimination' imaging mode was used (green emission filter: 527nm pass band centre, 55nm half-power bandwidth and blue/red emission filter: 445nm pass band centre, 60nm half-power bandwidth and 615nm pass band centre, 70nm half-power bandwidth). For all imaging experiments 15-19 confocal sections (0.5µm steps) were collected every 20 seconds. The number of confocal sections was selected as the minimal number required to capture the majority of the centrosomes in the imaging volume even in the time points (the period of mitosis anaphase) during which the centrosomes are most dispersed in the *z* direction (manual focusing was performed to follow the migration of centrosomes in the *z* direction between time points to minimize the number of confocal sections needed). 2x2 binning was used; this setting was selected in order to increase the fluorescence signal whilst limiting laser exposure time during imaging. (1x1 binning was insufficient to resolve the two centrioles of a centrosome, although allowed slightly earlier resolution of separating centrosomes during late mitosis/early *S*-phase. I also performed imaging of Asl-GFP using 1x1 binning and high temporal resolution, only focusing on this period of the cycle [data not shown in this thesis] – these data did not alter any of the conclusions presented in this thesis). The CCD camera gain was 200V, and images were recorded on the full area of the chip. The exposure times and laser power settings used for each experiment are shown in Table 2.10. These settings were determined for each fusion protein in a way to minimize laser power and exposure time whilst maintaining the fluorescence signal range on the linear range of the camera.

Table 2.10 Exposure and laser settings used for live confocal imaging

Protein/fluorophore	Laser λ (nm)	Exposure time (ms)	Power (%)	FS/ED*
DSas-4-GFP	488	400	100	either
Asl-GFP	488	400	100	either
RFP-PACT	568	400	100	ED
RFP-Spd-2	568	200	80	ED
Jupiter-mCherry	568	50	100	ED
Texas Red	568	200	50-60	ED

* FS: fast sequential capture mode; ED: emission discrimination capture mode

2.5.2 PHOTOBLEACHING

All photobleaching experiments shown in this thesis were carried out on the Perkin Elmer ERS spinning disc system. For photobleaching the GFP signal of individual centrosomes when imaging GFP alone, a focused 488nm laser was used. The photobleaching laser power was 80%, and 200 bleach cycles were performed for each photobleaching event. To photobleach GFP while also imaging RFP or Texas Red, a 440nm laser was used to preserve the red emission. The photobleaching laser power was 35-60% and 200 bleach cycles were performed.

In all photobleaching experiments up to 6-8 distantly spaced centrosomes were bleached in total per embryo – therefore in antibody injection experiments a maximum of 3-4 centrosomes in each the antibody-affected and control region. In order to maintain constant time gaps during time-lapse imaging, photobleaching was always performed 2 seconds prior to the start of imaging a z-stack (a photobleaching event with 200 bleach cycles takes 1.6 seconds).

2.5.3 SUPER-RESOLUTION IMAGING OF LIVING *DROSOPHILA* EMBRYOS

For super-resolution imaging dechorionated living embryos were imaged at 21 ºC on an OMX V3 system (GE Healthcare, USA), using an Olympus PlanApo N 60x / 1.42NA oil objective. To create each image, 20-23 optical sections were collected (0.125µm steps). All images shown in this study are single-timepoint images; no time lapse super-resolution images are shown as this resulted in the rapid bleaching of the fluorescence signal during imaging.

2.5.4 IMMUNOFLUORESCENCE IMAGING OF FIXED *DROSOPHILA* EMBRYOS AND BRAINS

Fixed *Drosophila* embryos were imaged at 21 ºC on the Olympus Fluoview FV1000 IX81 point scanning confocal system. Images were generated using 60x / 1.4NA oil objective and the FV1000 software. Fixed *Drosophila* brains were imaged also 21 ºC on a non-confocal epifluorescence microscope (Zeiss Axioskope II) equipped with a CoolSnapHQ (Photometrics) camera. Images were captured using a Zeiss plan-neoflour 60x / 1.25NA oil objective using MetaMorph software (Molecular Devices).

2.6 IMAGE ANALYSIS AND STATISTICS

2.6.1 ANALYSIS OF LIVE IMAGING DATA ACQUIRED ON THE PERKIN ELMER ERS SPINNING DISC CONFOCAL SYSTEM

All images and time-lapse movies acquired by live confocal imaging were analyzed using Volocity 3D image analysis software (Perkin Elmer, USA).

The changes of Asl-GFP or DSas-4-GFP fluorescence levels at centrosomes during the mitotic cycle were quantified the following way from time-lapse imaging data (protocol also described in detail in Table 2.11). Centrosomal fluorescence was calculated as the sum intensity of every

centrosomal voxel for each channel. A centrosomal voxel was defined as having an intensity >4.5 standard deviations (SDs) above the mean intensity of all voxels within the image; this setting was chosen because it selects centrosomal pixels most accurately as judged by eye while allowing consistent thresholding of centrosomal pixels above background fluorescence. Individual centrosomes were tracked along time based on distance of movement by the Volocity tracking protocol but correct tracking was always confirmed by eye for each centrosome that was analyzed. Once the fluorescence of individual centrosomes was obtained for each timepoint using Volocity, first the cytoplasmic background fluorescence was subtracted from these centrosomal fluorescence values (Microsoft Excel), then the resulting values were corrected for photobleaching during sampling (Microsoft Excel) as described in Table 2.11. The corrected centrosome tracks were then aligned in time using Microsoft Excel and analyzed using GraphPad Prism.

For comparing Asl-GFP, DSas-4-GFP or RFP-PACT levels of centrosomes in *S*-phase, centrosomal fluorescence was calculated as described in steps 1&2 of Table 2.11. Fluorescence values of old and young centrosome pairs were then compared using a paired *t*-test.

Table 2.11 Protocol used for measuring the changes in Asl-GFP or DSas-4-GFP along the mitotic cycle (tp=timepoint)

Step 1. Measuring centrosomal fluorescence & generation of centrosome tracks **(Volocity 5.2.1)**

1) **Find objects using SD intensity**: >4.5
2) **Exclude objects by size** (excl. <0.005µm)
3) **Exclude objects touching edge of image**
4) **Track objects** (if distance from object in previous time point is <4µm)

→ centrosomal fluorescence in tp 'n'

Step 2. Subtraction of cytoplasmic background fluorescence **(Microsoft Excel)**

Backgr-corr centrosomal fluorescence in tp 'n' =

centrosomal fluorescence in tp 'n' - backgr fluorescence within centrosome in tp 'n' *

* backgr fluoresc. in centrosome in tp 'n' = mean cytopl fluoresc. in tp 'n' * # of centrosomal voxels in tp 'n'

Step 3. Correction for photobleaching during sampling **(Microsoft Excel)**

Bleaching- corrected centrosomal fluoresc in tp 'n' =

$$\frac{\text{Backgr-corr centrosomal fluoresc in tp 'n'}}{\text{(total image fluoresc in tp 'n'/total image fluoresc in tp '1')}}$$

Step 4. Align multiple centrosome tracks in time **(Microsoft Excel, GraphPad Prism)**

A different method was used to quantify centrosomal Asl-GFP or DSas-4-GFP levels in all antibody-injection experiments or any FRAP experiments (in order to detect the small levels of Asl-GFP or DSas-4-GFP fluorescence that can be elicited in these experiments). In all antibody-injection or FRAP experiments the total GFP fluorescence was measured in a boxed region centered around the brightest centrosomal voxel using Volocity 6.1.1. The local cytoplasmic background fluorescence measured in an identically sized boxed region was then subtracted. In all antibody-injection experiments the fluorescence values of inhibited and control centrosomes were compared using a *t*-test (unpaired).

In all graphs that display data collected from individual embryos the error bars represent the standard deviation of the mean (s.d.), while in all graphs that display data pooled from multiple embryos the error bars represent the standard error of the mean (s.e.m.).

2.6.2 ANALYSIS OF LIVE IMAGING DATA ACQUIRED ON THE OMX V3 SUPER-RESOLUTION IMAGING SYSTEM

All super-resolution images acquired on the OMX V3 system were processed and reconstructed using SoftWorx software. For further analyses, Image J software was used for plotting the distribution of DSas-4-GFP and Asl-GFP within centrosomes the following way. Images were processed as maximum intensity projections and each pixel of the image was sub-divided into 10x10 pixels (in the case of DSas-4-GFP the maximum intensity projections were generated from images of centrosomes where one centriole was above the plane of the other to gain projections of individual centrioles, Figure 3.4D; in the case of Asl-GFP there was no need for such a selection as Asl-GFP only localizes to one centriole within each centrosome). The radial intensity profile was then calculated from the centre of each centrosome to a 1μm radius (0.05μm steps) in Image J. Using Microsoft Excel the local cytoplasmic background was subtracted from all values, and the resulting fluorescence values were then normalized (largest value=1). The normalized radial fluorescence intensity profiles of multiple centrosomes from multiple embryos were then averaged and plotted using GraphPad Prism.

2.6.3 IMAGE PROCESSING FOR PRESENTATION

All fluorescent images obtained on the Perkin Elmer ERS system or on the Olympus Fluoview system were processed using Volocity 6.1.1 and Adobe Photoshop software. All image data was first subjected to 3D rendering in Volocity, then the colour, contrast and brightness were adjusted for each channel (the contrast and brightness adjustments only alter the visual appearance of the images and do not adjust the voxel fluorescence intensity values, which are stored unaltered in the

program for quantification protocols). The Volocity 'smooth zoom filter' was applied to all images (this filter only affects the aesthetic appearance of images but does not alter quantification). Images were exported as TIFF files from Volocity and contrast was further adjusted using Adobe Photoshop (the γ value was always kept 1), while movies were exported as AVI files from Volocity.

All super-resolution images obtained on the OMX V3 system and shown in this study are maximum intensity projections generated with Image J software. No filter was applied to super-resolution data.

Images of fixed brains (obtained on the Zeiss non-confocal fluorescent microscope) were processed using Image J software. All images shown are maximum intensity projections, and the Image J 'smooth' protocol was applied.

CHAPTER 3:

THE DYNAMIC LOCALIZATION OF DSAS-4-GFP AND ASL-GFP AT CENTROSOMES IN THE *DROSOPHILA* EMBRYO

3.1 SUMMARY

At the time when I started this study it had been well documented that Asl has an important functional role in the earliest stages of procentriole assembly (Blachon et al. 2008; Dobbelaere et al. 2008). It had also recently been shown that Asl (and its human homologue Cep152) could bind to two other crucial centriole duplication proteins: Sak/Plk4 and DSas-4/CPAP (Cizmecioglu et al. 2010; Dzhindzhev et al. 2010; Hatch et al. 2010). This result was somewhat surprising, as Sak/Plk4 is widely believed to be the protein that initiates procentriole assembly, while DSas-4/CPAP is thought to act much later in the assembly pathway. Thus, Asl was assigned a rather imprecise function as a general "scaffold" upon which Sak/Plk4 and DSas-4/CPAP would assemble (Cizmecioglu et al. 2010; Dzhindzhev et al. 2010). The aim of my project was to characterize the dynamic incorporation and turnover of Asl in duplicating centrosomes in order to extend our understanding on how exactly Asl acts in the centriole duplication cycle. I chose to address these questions through quantitative live imaging of Asl-GFP at duplicating centrosomes of the syncytial blastoderm stage *Drosophila* embryo.

Prior to analysing the dynamic recruitment of Asl-GFP, my first aim was to validate this experimental approach by profiling the dynamic incorporation of another centriolar protein in this model system — a protein that's homologue has been well characterized in another organism. This was important, as neither the incorporation timing nor the dynamic properties of an Asl homologue had been characterized before. I chose to first analyse the dynamic behaviour of DSas-4, for three

reasons. First, the dynamic recruitment of *C. elegans* SAS-4 to duplicating centrosomes has been well characterized (Delattre et al. 2006; Dammermann et al. 2008). Second, the dynamic incorporation of DSas-4 would provide a baseline behavioural profile of a core centriolar protein in flies, a useful comparison for the behaviour of Asl. Finally, and most importantly, DSas-4/CPAP is known to biochemically and functionally interact with Asl/Cep152 so the dynamic incorporation profile of DSas-4 could help extend our understanding of the functional relationship between these proteins.

In this chapter I first describe the generation of fly lines that express physiological levels of DSas-4-GFP or Asl-GFP in the absence of the respective endogenous protein to allow accurate dynamic incorporation studies of these proteins. Next I present the dynamic incorporation and centrosomal turnover properties of DSas-4-GFP and Asl-GFP in syncytial *Drosophila* embryos. Interestingly, these results indicate that Asl behaves quite differently to DSas-4 as it is only incorporated into newly formed centrioles when they separate from their mothers at the end of mitosis. I support this conclusion with super-resolution image data from living embryos. Finally, I discuss how these results may provide important insight into the respective roles of these proteins in centriole assembly.

3.2 RESULTS

3.2.1 THE CENTROSOMAL INCORPORATION OF DSAS-4-GFP

3.2.1.1 GENERATION OF A DROSOPHILA LINE THAT EXPRESSES ENDOGENOUS LEVELS OF DSAS-4-GFP

To study the dynamic behaviour of DSas-4 in its most physiological context, I first generated fly lines that express DSas-4-GFP from the endogenous promoter, in the absence of endogenous DSas-4 protein. As this project was started well before the establishment of the CRISPR/Cas9 genome editing approach in *Drosophila* (Bassett et al. 2013), I used traditional p-element mediated transformation, which leads to transgene insertion at random genomic sites (O'Connor and Chia 1993). To achieve near-physiological expression levels of DSas-4-GFP, I cloned the entire *DSas-4* coding region together with ~2kb of upstream promoter sequence; this approach has been used previously to generate *Drosophila* lines expressing endogenous levels of centriolar fusion proteins (Blachon et al. 2008) (Figure 3.1A; see Chapter 2 for full details).

Western blotting revealed that the expression levels of DSas-4-GFP produced from this construct were nearly identical to the levels of wild type DSas-4 protein in *Drosophila* brains (Figure 3.1B) and embryos (Figure 3.1B'). Using confocal microscopy, DSas-4-GFP could be seen as a tight focus at embryonic centrosomes (Figure 3.1C). Crucially, the DSas-4-GFP construct successfully rescued the uncoordinated phenotype (Figure 3.1D) as well the sterility of a *DSas-4* mutant line, suggesting that this construct was fully functional.

3.2.1.2 DSAS-4-GFP IS INCORPORATED INTO DAUGHTER CENTRIOLES AS THEY ASSEMBLE

I first analysed the localization and levels of DSas-4-GFP at centrosomes in living embryos in *S*-phase. At the start of *S*-phase the parental centrioles in these embryos have disengaged and

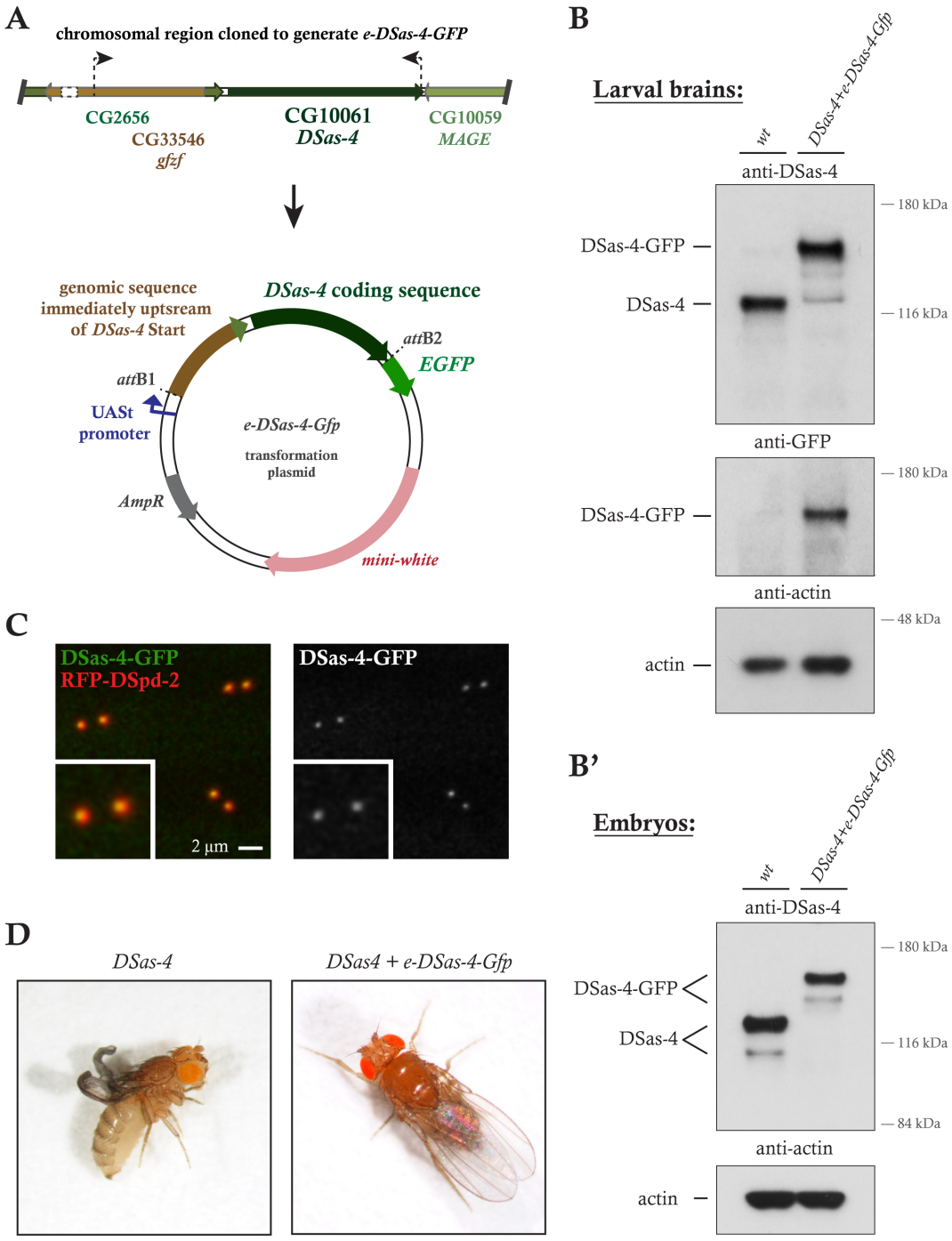


Figure 3.1 Generation of a *Drosophila* line expressing endogenous levels of DSas-4-GFP.

(A) Schematics show the genetic region of *DSas-4* that was cloned (top) and introduced into a P-element transformation vector (bottom) for the generation of transgenic lines. (B, B') Western blot analyses of 3rd instar larval brain lysates (B) and embryo lysates (B') confirm that DSas-4-GFP is expressed at similar levels to endogenous DSas-4. (C) Fluorescence images show that DSas-4-GFP localizes as a tight focus at centrosomes (co-labelled here with the centrosomal marker RFP-DSpd-2), suggesting that the new transgene produces functional protein. (D) The *e-DSas-4-Gfp* allele successfully rescues the uncoordinated phenotype of *DSas-4*, further confirming that the GFP-fusion protein is fully functional.

separated sufficiently to allow the analysis of individual centrosomes using conventional light microscopy; however we cannot resolve individual mother and daughter centrioles within an engaged centriole pair using this method (described in Chapter 1.4). DSas-4-GFP appeared to localize similarly at the older and younger centrosome of each pair (Figure 3.2A, see also Chapter 1.4 for definition of old and young centrosomes), although in a few of the centrosome pairs one member of the pair appeared to contain slightly more DSas-4-GFP than the other (arrow, Figure 3.2A). To test whether this was due to there being consistently slightly higher levels of DSas-4-GFP in either the old or new mother centriole, I measured the correlation of DSas-4-GFP levels with the levels of RFP-PACT, a marker that preferentially labels older centrioles (Conduit et al. 2010) (Figure 3.2B,C). I detected no reproducible correlation between the levels of DSas-4-GFP and RFP-PACT (Figure 3.2C) suggesting that centrosomes containing an old or new mother centriole generally contain similar levels of DSas-4-GFP. I believe that, in light of my full dataset, I now understand the reason behind the occasional asymmetry in DSas-4-GFP levels and I describe this later in this Chapter.

I next assessed how the levels of DSas-4-GFP change at centrosomes during the centriole duplication cycle (full method described in Chapter 2.6.1). I found that the amount of DSas-4-GFP at centrosomes continuously increased throughout *S*-phase (the time when daughter centrioles form and elongate, Figure 3.3A-C). Centrosomal DSas-4-GFP levels plateaued for a short period just around the onset of mitosis (as judged by the onset of nuclear envelope breakdown—NEB), reaching on average 3–fold the levels that were measured at the onset of *S*-phase (Figure 3.3A-C). After NEB, however, a continuous loss of centrosomal DSas-4-GFP could be seen up until the end of mitosis, by which point the centrosomal levels of DSas-4-GFP were reduced to approximately 2-fold the amount that was measured in early *S*-phase (Figure 3.3A-C). These data suggest that DSas-4-GFP is incorporated into forming daughter centrioles during their assembly; however an excess of DSas-4-GFP appears to be recruited during the assembly process, and this excess is then removed during mitosis. I think it is likely that the incomplete, still on-going loss of excessive

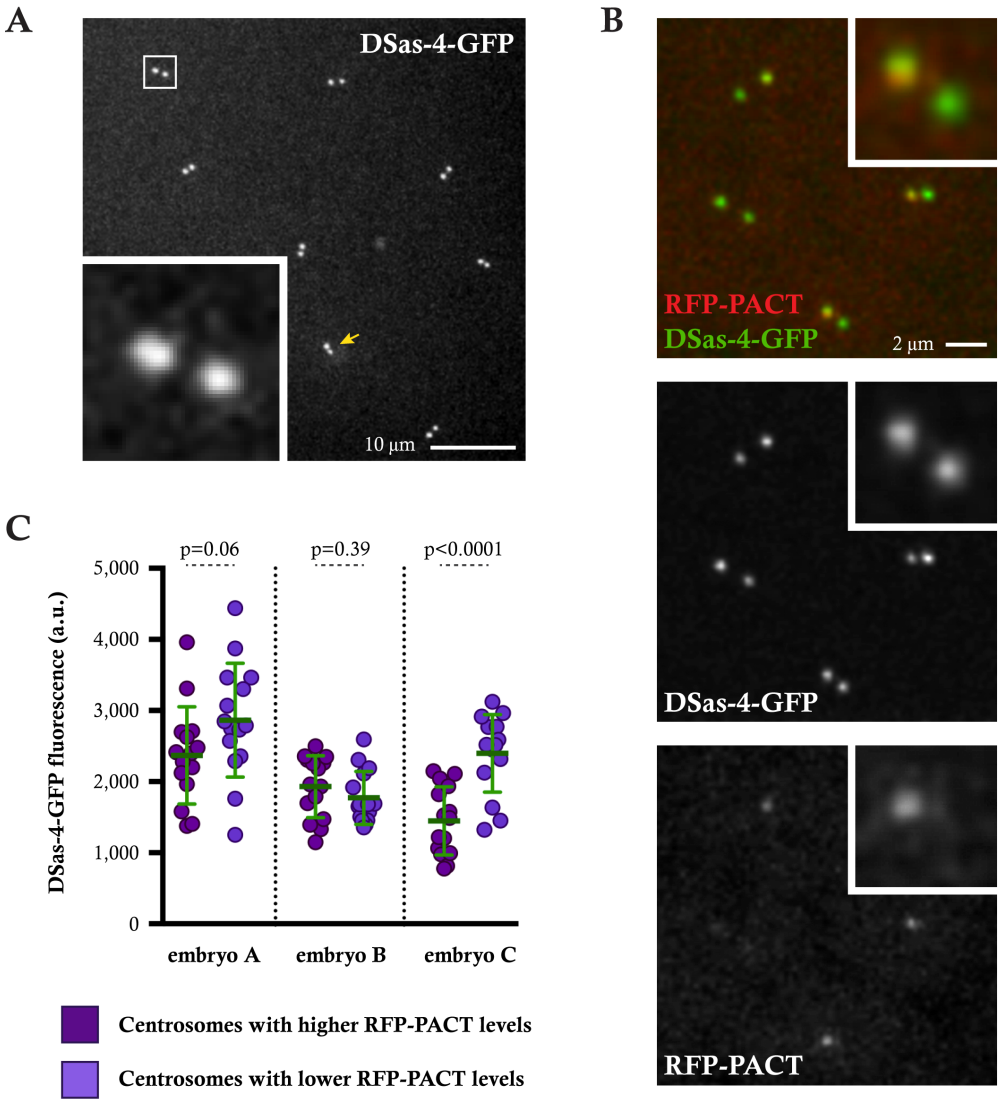


Figure 3.2 Live analyses of centrosomal DSas-4-GFP levels during *S*-phase of the cell cycle.

(A) Fluorescence image shows DSas-4-GFP levels at newly separated centrosomes (yellow arrow points to slightly asymmetric pair). (B) Fluorescence images show the correlation between the centrosomal levels of DSas-4-GFP (*green*) and a centriole age marker, RFP-PACT (*red*), during *S*-phase. (C) Graph shows the levels of DSas-4-GFP at old (*dark purple*) and new (*light purple*) centrosomes during early *S*-phase (see also Chapter 1.4 for the definition of old and new centrosomes). Statistical significance was calculated using paired *t*-tests. Error bars represent s.d. Note that in some embryos the new centrosomes contain more DSas-4-GFP than older ones (C), but this does not appear to be a consistent feature (C). A possible explanation for this observation is discussed in section 3.2.1.2.

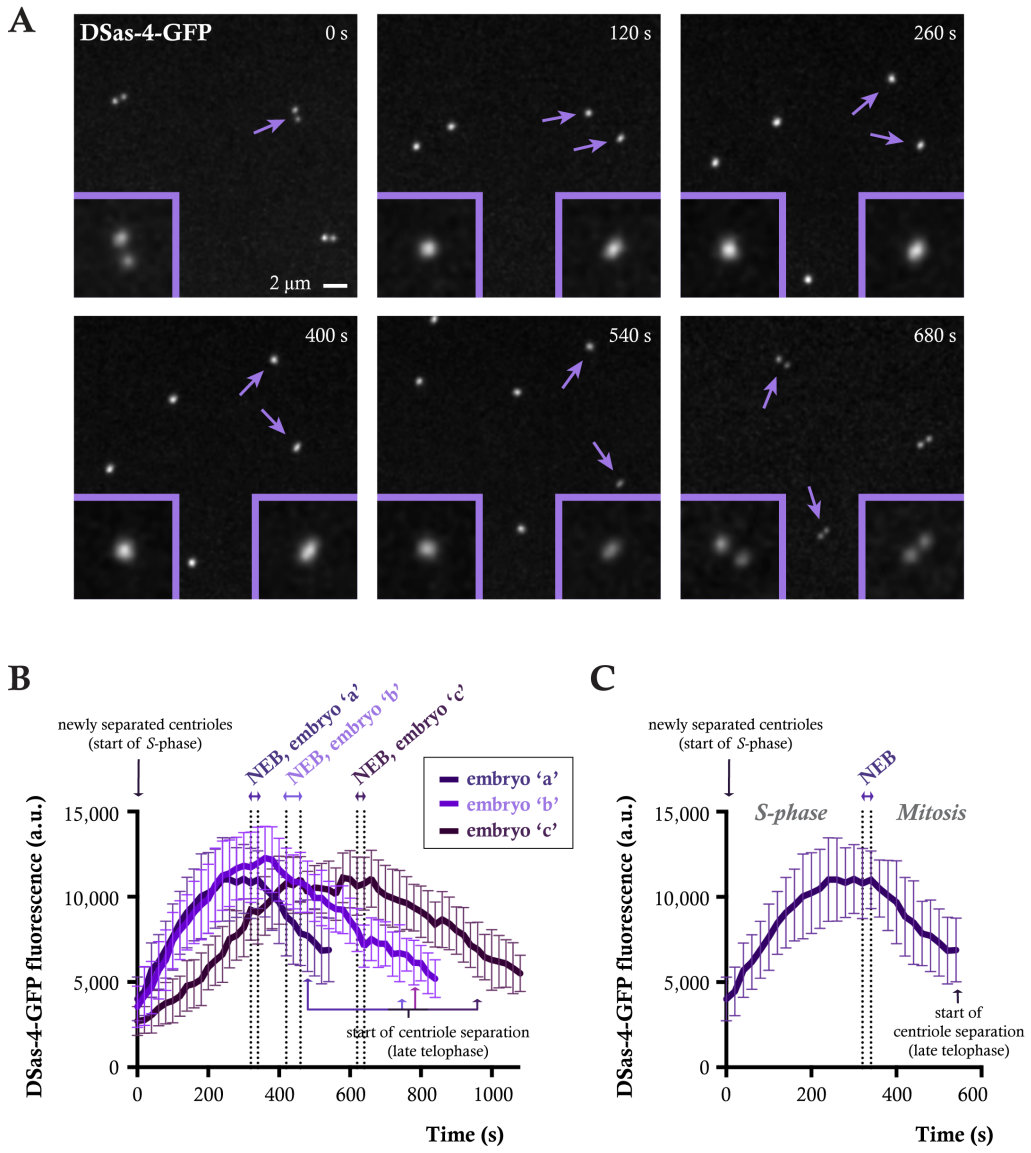


Figure 3.3 An analysis of DSas-4-GFP recruitment to centrosomes during the cell cycle.

(A) Fluorescence images from a time-lapse movie show the incorporation of DSas-4-GFP into duplicating centrosomes over a single cell cycle. (B) The graph shows averaged centrosomal DSas-4-GFP fluorescence (a.u.=arbitrary units) over a single cell cycle from three embryos (>25 centrosomes analysed in each embryo). (C) The graph shows averaged centrosomal DSas-4-GFP fluorescence along the cell cycle from a single embryo, for the ease of observation (embryo 'a' from graph B, n=26 centrosomes; this embryo is shown in the images in panel A). Time relative to centriole separation (t=0 s) is indicated in all images and graphs. The error bars in graphs (B,C) represent s.d.

DSas-4-GFP accounts for the occasional DSas-4-GFP asymmetry that I observed in some, but not all embryos in *S*-phase (Figure 3.2A arrow, see above).

DSas-4 is essential for centriole duplication (Basto et al. 2006), but it has also been implicated in PCM recruitment (Gopalakrishnan et al. 2011; Gopalakrishnan et al. 2012; Zheng et al. 2014). I wondered, therefore, whether the excess DSas-4 recruited to centrosomes during *S*-phase was being recruited to centrioles or to the PCM of the centrosomes. To address this, I carried out a detailed analysis of the sub-centrosomal localization of DSas-4-GFP using both conventional light microscopy and super-resolution imaging. As shown earlier, DSas-4-GFP forms a tight focus within centrosomes that appears narrower than the distribution of the PCM marker RFP-DSpd-2 (Figure 3.1C: shows *S*-phase; Figure 3.4A: shows mitosis onset). A radial profile analysis of the early mitotic centrosomal DSas-4-GFP signal revealed a profile that was indistinguishable from the profile of sub-resolution (170nm) fluorescent beads, demonstrating that the true distribution of DSas-4-GFP is below the resolution of our conventional microscope system (Figure 3.4B,C). Finally, and most convincingly, super-resolution imaging of live embryos confirmed that all detectable DSas-4-GFP signal is localized inside the ring of Asl-GFP (Figure 3.4D,E), which forms the border between centrioles and PCM (Fu and Glover 2012; Mennella et al. 2012). These results show that in *Drosophila* embryos all DSas-4-GFP that is detectably recruited during centriole duplication in *S*-phase is concentrated at centrioles.

This prompted me to test whether DSas-4-GFP was being recruited exclusively to the growing daughter centrioles or whether any protein was also being recruited to mother centrioles. This was important for two reasons. First, it would test a previously proposed model of centriole duplication; one which suggests that centriole components are initially concentrated around mother centrioles, from where they are gradually incorporated into the growing daughters (Dammermann et al. 2008). Any recruitment of DSas-4-GFP to mother centrioles during *S*-phase could support this model, while the exclusive recruitment of DSas-4-GFP to daughter centrioles would disagree with it. Second, it had been suggested that several PCM proteins are recruited to centrioles as part of

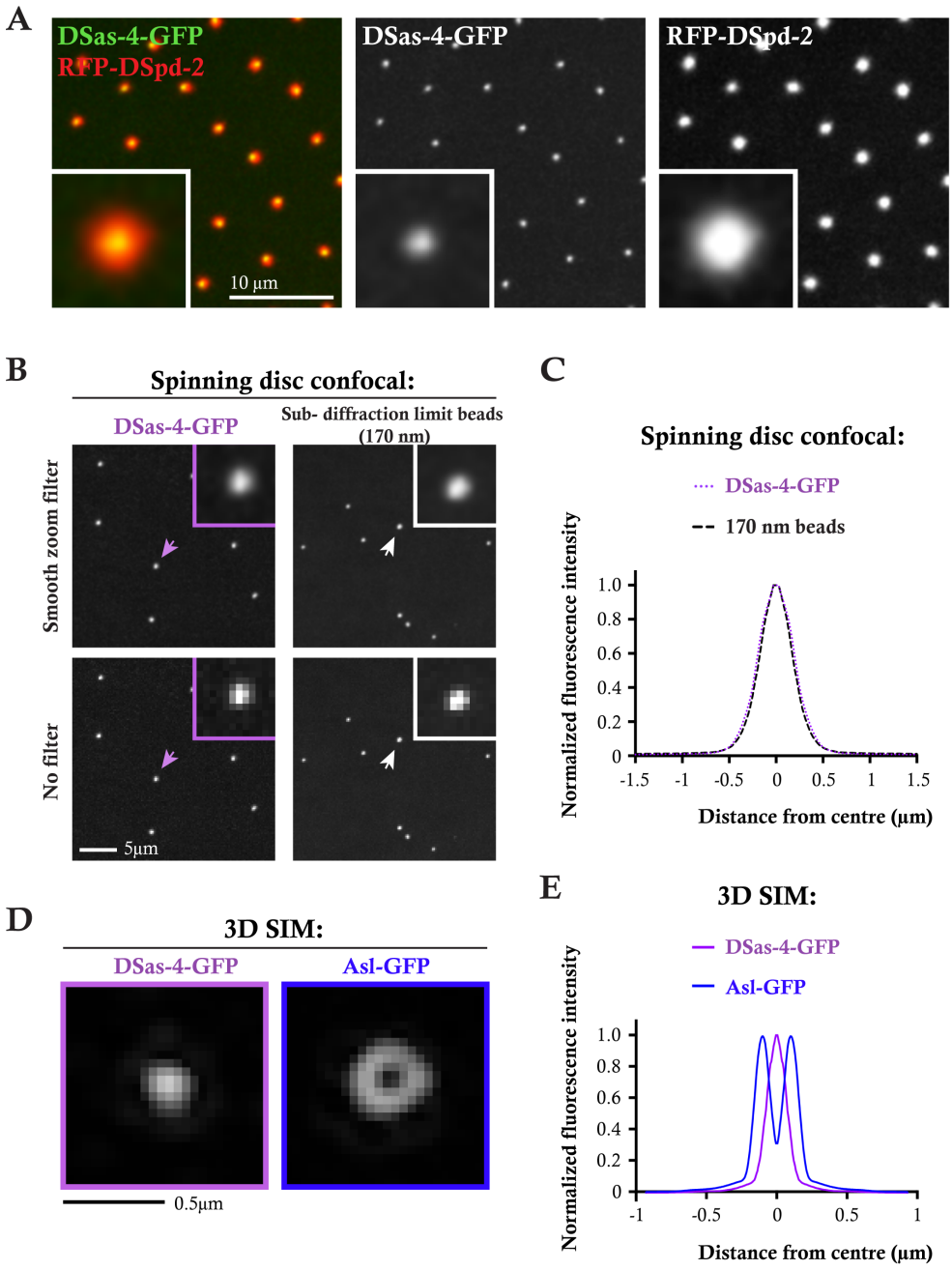


Figure 3.4 DSas-4-GFP is a *bona fide* centriolar protein that does not appear to localize to the PCM in *Drosophila* embryos.

(A) Fluorescent images taken in early mitosis (when DSas-4-GFP levels are at their peak) show that DSas-4-GFP (*green/white*) forms a tight focus at centrosomes and does not spread across the PCM, marked as the area occupied by RFP-Spd-2 (*red/white*). (B,C) Fluorescence images (B) and graph (C) show that on the conventional light microscope used for all quantitative live time-lapse imaging experiments the distribution of the DSas-4-GFP fluorescence signal at the centrosome (n=30 centrosomes in graph C) matches that of sub-resolution (170nm diameter) beads (n=30 beads in graph C). (D,E) 3D structured illumination microscopy images (D) and graph show the distribution of DSas-4-GFP fluorescence (n=8 centrioles in graph E) relative to Asl-GFP fluorescence (n=24 centrioles in graph E) in early mitosis, when DSas-4-GFP levels peak. See how the DSas-4-GFP focus occupies a narrower region than the ring of Asl-GFP (which localizes to the outer wall of the centriole) supporting that DSas-4-GFP is a *bona fide* centriolar protein. Further details are given in section 2.6.2.

cytoplasmic complexes that contain DSas-4 (Gopalakrishnan et al. 2011). It has recently been shown that the PCM is largely, if not exclusively, organised by the mother centrioles in several systems, including the early *Drosophila* embryo (Conduit et al. 2010; Wang et al. 2011). Thus, some DSas-4 would have to be recruited to mother centrioles if cytoplasmic DSas-4 complexes really play an essential role in recruiting the PCM.

To address these two questions, I observed the levels of DSas-4-GFP at the individual centrioles during *S*-phase using super-resolution imaging. Unfortunately I could not generate high quality time-lapse data with this technique as the DSas-4-GFP signal bleached too rapidly (unpublished data). Therefore, my analysis was restricted to individual images taken at various stages of the cell cycle.

Just after the parental centrioles separated at the telophase/*S*-phase transition, very low levels of DSas-4-GFP could already be seen at what I infer are the growing daughter centrioles (arrows, Figure 3.5A). In some, but not all, centrosome pairs, one of the parental centrioles appeared to contain more DSas-4-GFP than the other (arrowheads, Figure 3.5A). Upon progression into mid–*S*-phase, any difference between parental centrioles was no longer apparent, and the daughter centrioles had accumulated similar levels of DSas-4-GFP to their mothers (Figure 3.5B). Strikingly, by mitosis onset (when the centrosomal levels of DSas-4-GFP peak) every single centrosome showed a very clear asymmetry in the DSas-4-GFP levels of its two fully-grown centrioles (Figure 3.5C). Asl-mCherry – that localizes only around mother centrioles (described in section 3.2.2.2) – could always be seen surrounding the centriole with lower DSas-4-GFP levels within each pair (Figure 3.5D). This confirms that daughter centrioles contain more DSas-4-GFP than their mother centriole when its centrosomal levels peak around mitosis onset, therefore the excess of DSas-4-GFP is recruited to growing daughter centrioles during *S*-phase.

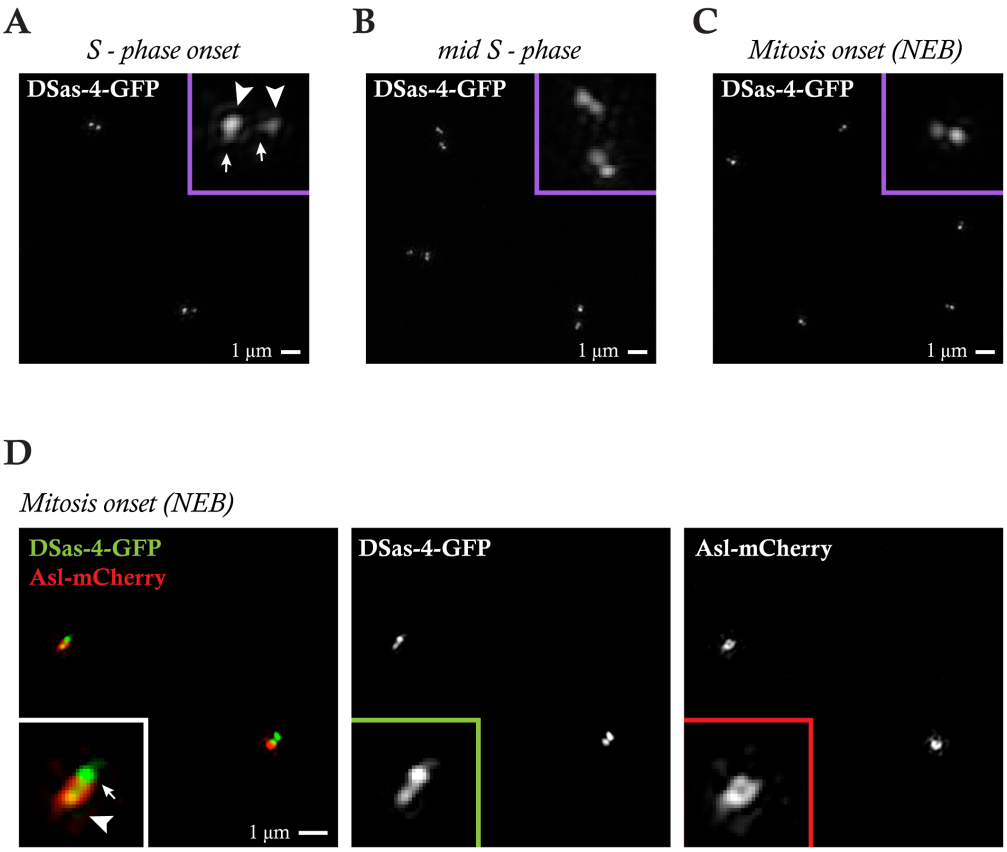


Figure 3.5 Growing daughter centrioles recruit excessive amounts of DSas-4-GFP during their assembly in *S*-phase.

(A-C) Super-resolution (3D SIM) fluorescent images show that DSas-4-GFP is incorporated into growing daughter centrioles from the beginning of their formation in *S*-phase until their assembly is completed around the onset of mitosis. Note the changes in DSas-4-GFP levels between different stages of the cycle; in early *S*-phase (A) the newly forming daughter centrioles (arrows) display only minimal amounts of DSas-4-GFP compared to the mother centrioles (arrowheads), by mid-*S*-phase the DSas-4-GFP levels of mother and daughter centrioles are nearly identical (B), however by the onset of mitosis one centriole from each pair accumulates significantly more DSas-4-GFP than the amount present in the other (C). (D) Super-resolution (3D-SIM) fluorescent images show the levels of DSas-4-GFP (*green/white*) and Asl-mCherry (*red/white*; marks the mother centrioles) at centrioles during the onset of mitosis. These images confirm that at the time of mitotic entry daughter centrioles contain more DSas-4-GFP than their mother. This suggests that the excess of DSas-4-GFP that is recruited to centrosomes during *S*-phase is concentrated at growing procentrioles instead of their mother.

3.2.1.3 CENTROSOMAL RECRUITMENT OF DSAS-4-GFP IS RESTRICTED TO *S*-PHASE OF THE EMBRYONIC CELL CYCLE, AND BY MITOSIS DSAS-4-GFP WITHIN DAUGHTER CENTRIOLES IS STABLY FIXED

To assay the dynamics of DSas-4-GFP incorporation, I carried out fluorescence recovery after photobleaching (FRAP) experiments. When centrosomes were bleached in early *S*-phase, DSas-4-GFP fluorescence recovered at approximately the same rate as DSas-4-GFP was being recruited to unbleached centrosomes (compare Figure 3.6A,B and the brown (bleached) recovery curve to the purple (unbleached) incorporation curve in Figure 3.6D). Importantly, this suggests that the DSas-4-GFP already incorporated into the mother centriole is not turning over, and all the fluorescence that "recovers" during *S*-phase is actually due to new incorporation of DSas-4-GFP into the daughter centriole (see cartoon in Figure 3.6B). In support of this interpretation, at the end of the subsequent mitosis, when mother and daughter centrioles had separated, almost no fluorescence was detectable in one of the centrioles (presumably the original mother centriole) (arrow, Figure 3.6B, t=1060s).

When centrosomes were bleached in early mitosis (after the accumulation of DSas-4-GFP at the centrosomes was complete) no fluorescence recovery could be detected at bleached centrosomes (Figure 3.6C,D), suggesting that by early mitosis DSas-4-GFP is also fixed in newly built daughter centrioles as well as mother centrioles (Figure 3.6A,E). This result also shows that during mitosis no molecular turnover is detectable even in the excessive fraction of DSas-4-GFP; during mitosis DSas-4-GFP recruitment has stopped and any "unfixed" molecules are gradually removed from the centrioles.

In conclusion, my results show that DSas-4-GFP is recruited in excess to growing daughter centrioles throughout *S*-phase. During mitosis the surplus DSas-4-GFP is gradually lost from new centrioles, and the DSas-4-GFP molecules that have been incorporated into new centrioles are permanently fixed by this stage (Figure 3.7). Thus, the dynamic behaviour of DSas-4-GFP strongly

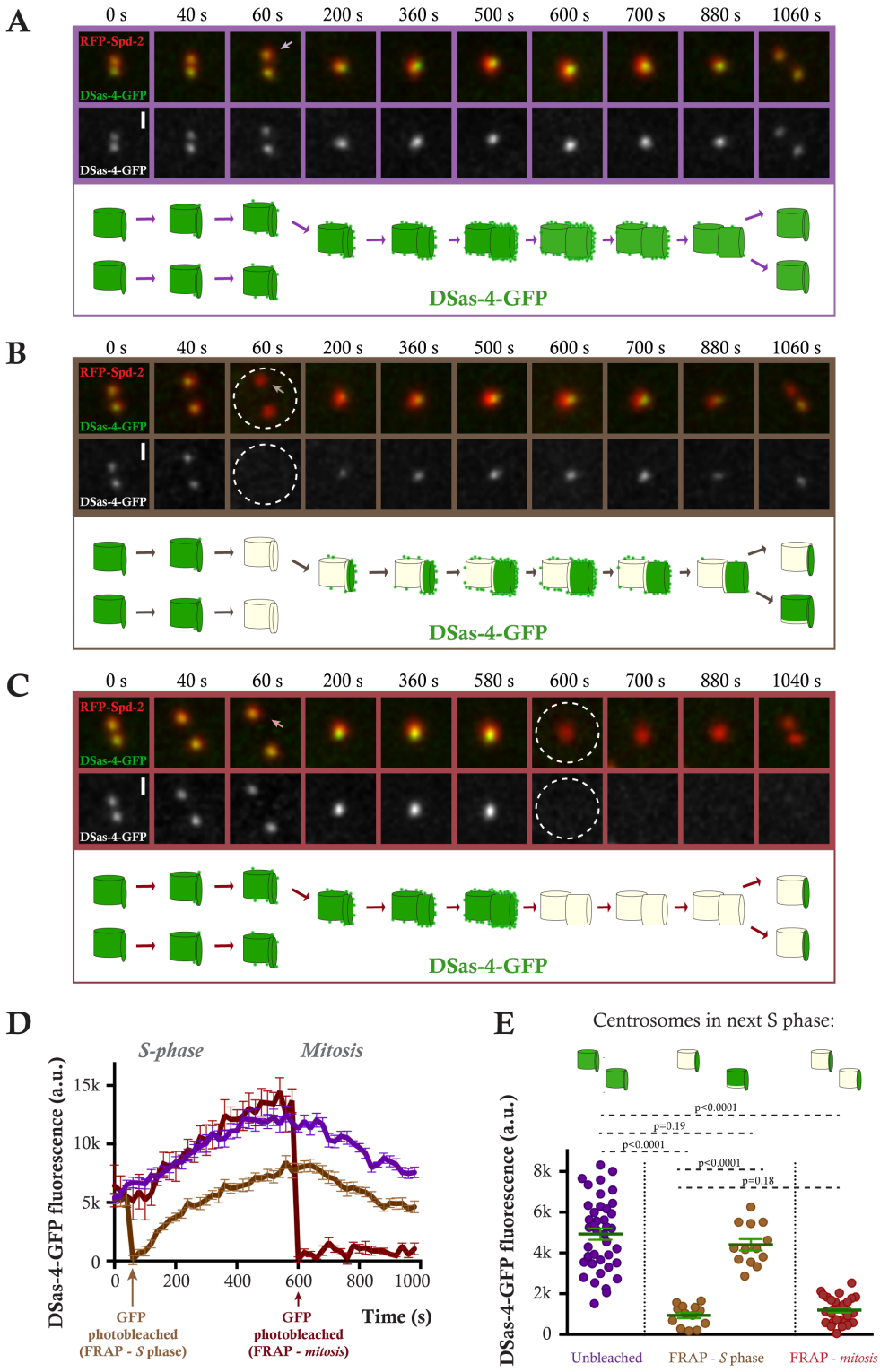


Figure 3.6 Figure legend on next page.

Figure 3.6 DSas-4-GFP is stably fixed in fully-grown centrioles.

(A-C) Fluorescence images from a time-lapse FRAP movie show the DSas-4-GFP (*green/white*) fluorescence levels of an unbleached control centrosome (A), a centrosome that was photobleached in early *S*-phase (B) and a centrosome the was photobleached in early mitosis (C); these embryos also expressed RFP-Spd-2 (*red*), so that the centrosomes could be followed even after photobleaching of DSas-4-GFP. Time relative to centriole separation (t=0s) is shown above each image. The arrows on the images at t=60s point to the centrosome that is followed in subsequent panels. The schematics under each fluorescence panel show the interpreted distribution of DSas-4-GFP fluorescence. (D) The graph shows the averaged centrosomal DSas-4-GFP fluorescence levels (a.u.=arbitrary units) of unbleached centrosomes (*purple*, n=8 centrosomes from 2 embryos), centrosomes that were bleached in early *S*-phase (*brown*, n=7 centrosomes from 2 embryos) and centrosomes that were bleached in early mitosis (*maroon*, n=4 centrosomes from 2 embryos). Time relative to centriole separation (t=0s) is shown. Error bars represent s.e.m. (E) The graph shows centrosomal DSas-4-GFP fluorescence at the start of the following *S*-phase for centrosomes that were unbleached (*purple*, n=40 centrosomes from 4 embryos), bleached in the previous *S*-phase (*brown*, n=26 centrosomes from 4 embryos) or bleached in the previous mitosis (*maroon*, n=28 centrosomes from 4 embryos). Error bars represent s.e.m. Note how centrosomes that were bleached in the previous *S*-phase are highly asymmetric in their DSas-4-GFP fluorescence, presumably because of the irreversible bleaching of the grandmother centriole in the previous *S*-phase — see cartoon in panel (B).

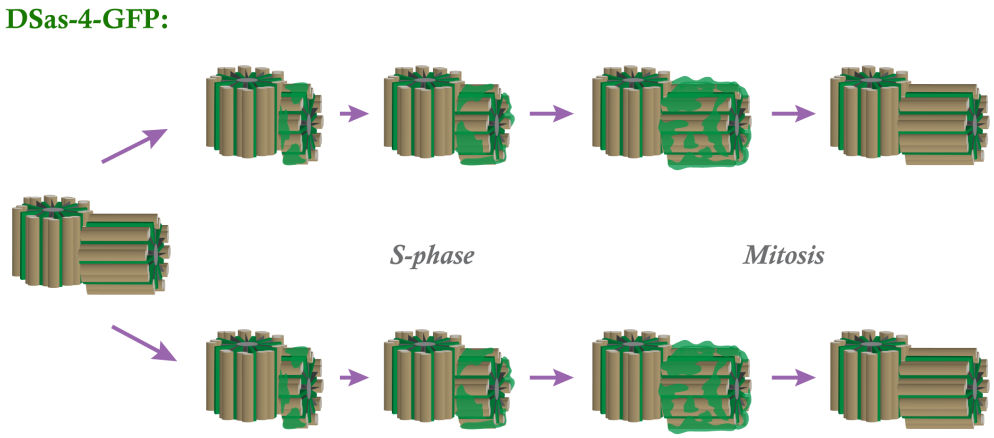


Figure 3.7 The model of DSas-4-GFP incorporation during centriole duplication in *Drosophila* embryos.

The schematics illustrate that DSas-4-GFP (*green*) is incorporated into forming daughter centrioles throughout their assembly during *S*-phase. Duplicating centrosomes recruit excessive levels of DSas-4-GFP; the surplus of DSas-4-GFP (shown here as tightly surrounding daughter centrioles) appears to be associated entirely with the growing daughter centriole, and cannot be detected within the PCM. By early mitosis DSas-4-GFP that has been incorporated into daughter centrioles is stably fixed, and the excessive fraction of DSas-4-GFP is gradually lost. No DSas-4-GFP recruitment (neither new incorporation nor turnover) can be detected during the mitotic phase of the cell cycle.

resembles that of SAS-4 in worms, although there are some minor differences, which I detail in the Discussion section.

3.2.2 THE CENTROSOMAL INCORPORATION OF ASL-GFP

3.2.2.1 GENERATION OF AN ASL NULL ALLELE

A *Drosophila* line that expresses Asl-GFP from its own endogenous promoter had been generated earlier (Blachon et al. 2008), and I used this for my studies of the dynamic behaviour of Asl-GFP at the centrosome. Similarly to DSas-4-GFP, however, I wanted to study this reporter construct in a null mutant background; first, to maintain physiological overall levels of Asl protein, and second, to get a complete readout of the behaviour of all Asl molecules within the embryo.

Two previously characterized mutations within *asl* (*asl*^{1} and *asl*^{mecD}) lead to early stop codons within the gene, resulting in the production of low levels of truncated Asl protein (Bonaccorsi et al. 1998; Varmark et al. 2007; Blachon et al. 2008). Two further mutations have also been mapped to the *asl* gene: *asl*^{2} and *asl*^{3} (Bonaccorsi et al. 1998). The phenotype of both these alleles is very similar to *asl*^{1} suggesting that they are also not null alleles. Taken together, none of the 4 previously existing *asl* mutations provided an ideal genetic background for my purposes, and I therefore decided to generate a new, functionally null allele of *asl*. Importantly, generation of such a mutant would also allow me to assess the *asl* null phenotype for the very first time and compare this to the previously reported phenotypes of mutants that still produce low levels of truncated Asl.

I summarise the generation of this new allele, *asl*^{B46}, through imprecise P-element excision in Figure 3.8 (see also Chapter 2.1.2.1). This new mutation is an approximately 2.1kb deletion that removes the 5' UTR of *asl*, as well as over half of the coding sequence, including the start codon: importantly, it does not affect the coding sequence of the neighbouring gene (Figure 3.8D).

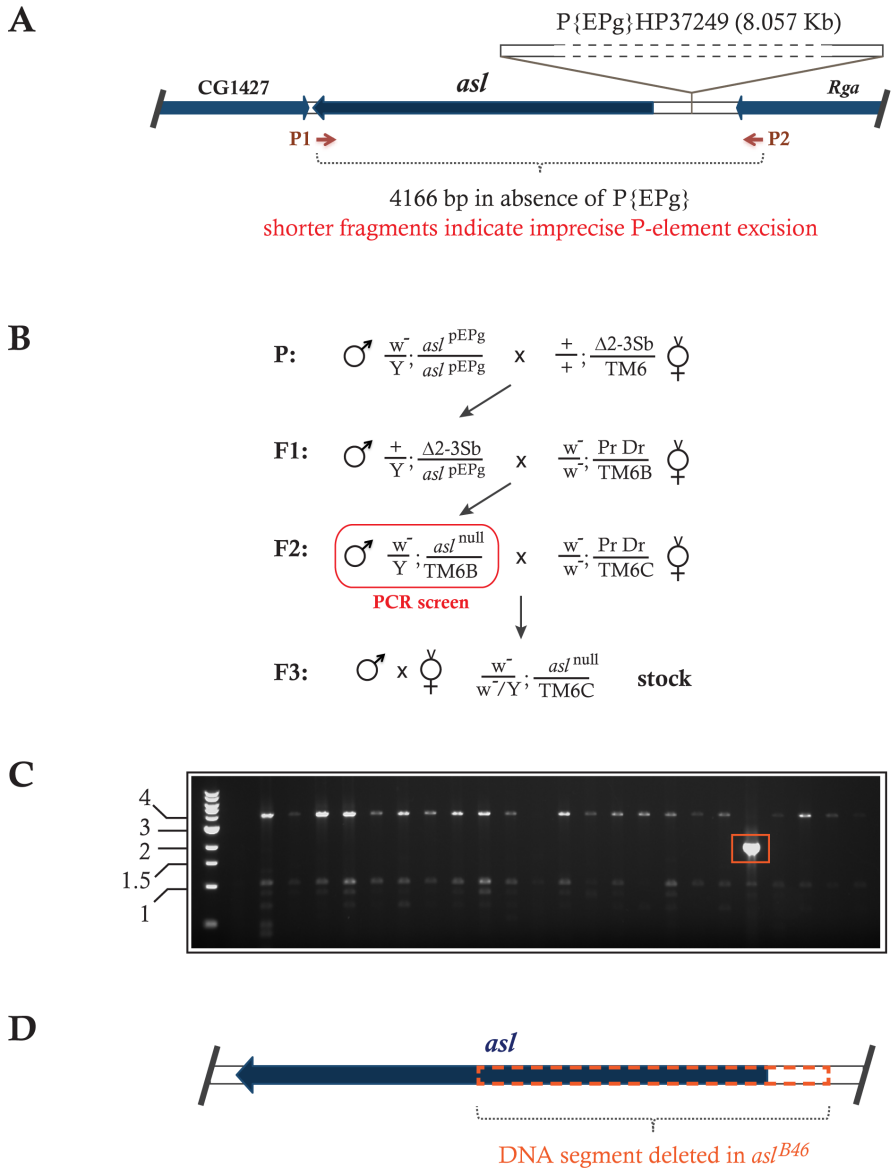


Figure 3.8 Generation of *asl*^{B46}, an *asl* null allele.

(A) The schematic shows the genetic region of the *asl* gene, indicating the binding sites of the PCR screen primers used for identifying imprecise excision of P{EPg}HP37249. (B) The crossing scheme used to induce P-element excision events (males were mated with virgin females in each cross). (C) Identification of the *asl*^{B46} allele in a screen for imprecise P-element excision events. The orange box highlights the PCR product that was amplified from the genomic DNA of the *asl*^{B46} founder male (~2kb). The larger, 4.1 kb main PCR product seen in the other lanes indicates that the excision of P{EPg}HP37249 has been precise in the case of these other males. Numbers on left indicate kilobases. (D) The schematic shows the genetic region that has been deleted in the *asl*^{B46} mutant.

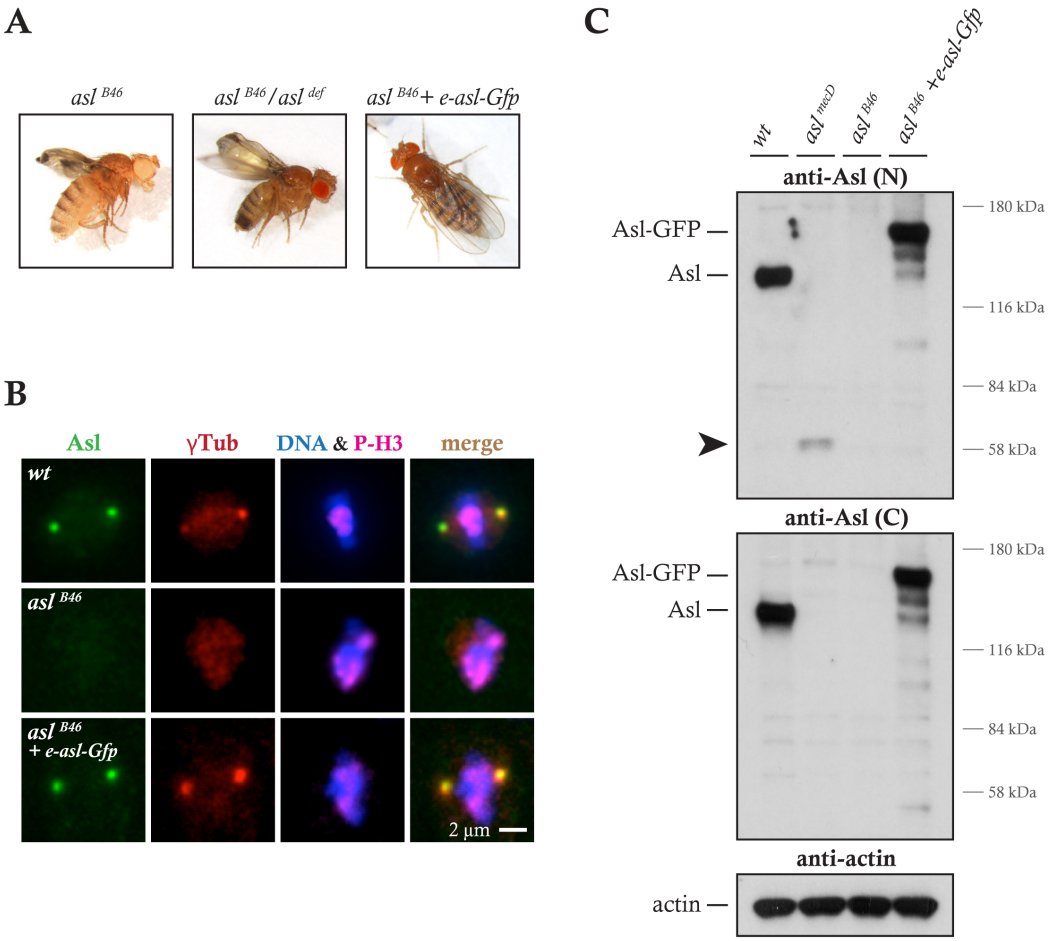


Figure 3.9 The *asl^{B46}* allele appears to be a functionally null allele that does not produce any detectable Asl protein.

(A) The images show that flies homozygous for the *asl^{B46}* allele are viable but display an uncoordinated phenotype, similar to that of *asl^{mecD}* flies. The uncoordinated phenotype is caused by a mutation in *asl* as *asl^{B46}/asl^{deficiency}* heterozygous flies show an identical phenotype, while the genetic combination of *asl^{B46}* with an *asl-Gfp* transgene fully rescues the phenotype. (B) Immunofluorescence images of mitotic cells in 3rd instar larval brains show that no Asl protein product can be detected in *asl^{B46}*, and these flies lack centrosomes (no γTub focus can be seen in these cells). (C) Western blot analysis of 3rd instar larval brain lysates confirms that no Asl protein product can be detected in *asl^{B46}* flies (using antibodies targeting either the N-terminal (upper panel) or C-terminal (lower panel) region of full length Asl. Note that the N-terminal antibody shows the low-level expression of a truncated N-terminal Asl fragment in *asl^{mecD}* flies (arrowhead).

I first assessed the phenotype of the newly generated asl^{B46} allele. Similarly to homozygous asl^{mecD} flies (Blachon et al. 2008), asl^{B46} flies were uncoordinated – this phenotype is characterized by proprioceptive deficit resulting from ciliary defects in mechanosensory neurons (Figure 3.9A). No Asl protein could be detected in asl^{B46} flies, either by immunofluorescence (Figure 3.9B) or by Western blotting (Figure 3.9C). Immunofluorescence analysis also confirmed the absence of centrosomes at the spindle poles of mitotic larval brain cells (Figure 3.9B). I did not perform electron microscopy analysis to verify the absence of centrioles in asl^{B46} flies, as I feel it is safe to conclude this already based on the absence of centrioles in asl^{mecD} (while asl^{B46} has a more severe effect on protein production than asl^{mecD}, it results in an identical uncoordinated phenotype). Taken together, these results show that the new asl^{B46} allele is likely a functionally null allele that does not produce any Asl protein product, but does not enhance the asl^{mecD} phenotype (Blachon et al. 2008) that has been described previously.

3.2.2.2 ASL-GFP IS FIRST RECRUITED TO DAUGHTER CENTRIOLES AT AROUND THE TIME THEY DISENGAGE FROM THEIR MOTHERS

I next assessed the localization of physiologically expressed Asl-GFP in the asl^{B46} background (Figure 3.10A). Surprisingly, in contrast to DSas-4-GFP, the levels of Asl-GFP at centrosome pairs in early *S*-phase, just following centriole disengagement, showed a strong and consistent asymmetry (Figure 3.10B). I wondered whether this asymmetry correlated with the centrosomes inheriting either the mother or daughter centriole from the previous cycle (see Chapter 1.4 for further explanation). To test this, I analysed Asl-GFP and RFP-PACT levels within the centrosome pairs (Figure 3.10C). In every case (97/97 centrosome pairs), the centrosome that inherited the mother centriole (old centrosome, higher RFP-PACT levels) from the previous cycle contained significantly higher levels of Asl-GFP than the centrosome that inherited the daughter centriole (new centrosome, lower RFP-PACT levels) (Figure 3.10D).

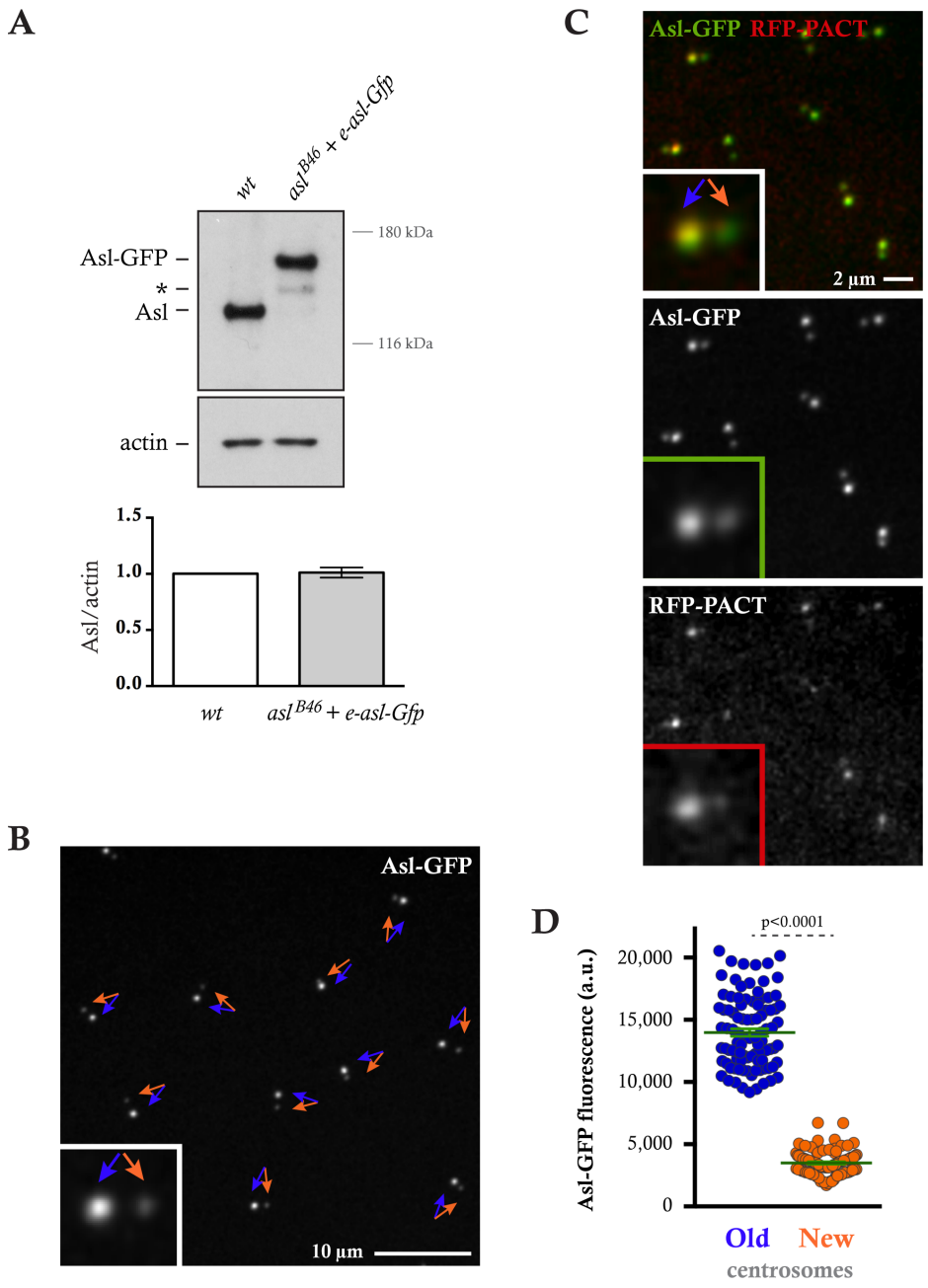


Figure 3.10 Live analysis of centrosomal Asl-GFP levels during *S*-phase of the cell cycle.

(A) Western blot analysis of embryo lysates shows that Asl-GFP is expressed at similar levels to endogenous Asl. A representative blot image is shown on top (chemiluminescence detection) while the quantification of Asl signal relative to actin is shown below (quantified using IR fluorescence detection, see Chapter 2.3.4). (B) Fluorescence image shows Asl-GFP levels at newly separated centrosome pairs in *S*-phase of the cell cycle. Note the strong asymmetry in Asl-GFP levels in every centrosome pair (*blue arrows*: centrosomes with higher Asl-GFP levels, *orange arrows*: centrosomes with lower Asl-GFP levels). (C) Fluorescence images show the correlation between the centrosomal levels of Asl-GFP (*green/white*) and a centriole age marker, RFP-PACT (*red/white*), during *S*-phase. (D) Graph shows the levels of Asl-GFP at old (*blue*) and new (*orange*) centrosomes during early *S*-phase; n=97 centrosome pairs from 4 embryos (see also Chapter 1.4 for the definition of old and new centrosomes). Statistical significance was calculated using a paired *t*-test. Error bars represent s.e.m.

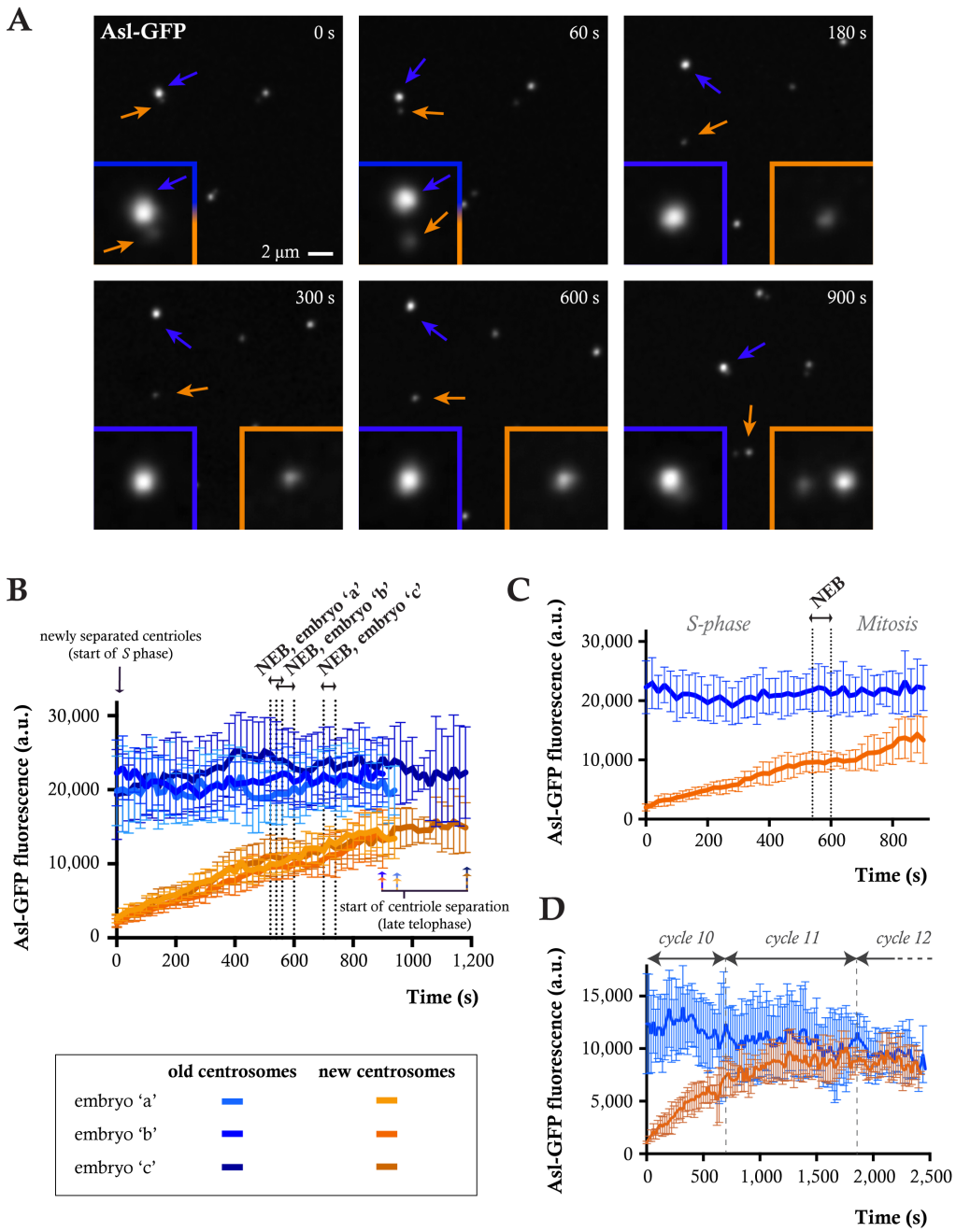


Figure 3.11 The recruitment of Asl-GFP to duplicating centrosomes during the cell cycle.

(A) Fluorescence images from a time-lapse movie show the incorporation of Asl-GFP into duplicating old (*blue*) and new (*orange*) centrosomes over a single cell cycle. (B) The graph shows averaged centrosomal Asl-GFP fluorescence (a.u.=arbitrary units) at old (*blue*) and new (*orange*) centrosomes over a single cell cycle, from three embryos (>15 centrosomes in each embryo). (C) The graph shows averaged centrosomal Asl-GFP fluorescence along the cell cycle from a single embryo, for the ease of observation (embryo 'b' from graph B, n=8 old & 10 new centrosomes; this embryo is shown in the images in panel A). (D) The graph shows averaged centrosomal Asl-GFP fluorescence over multiple cell cycles from a single embryo, n=7 for each old (*blue*) and new (*orange*) centrosomes. Note that new centrosomes formed in cycle 10 (*orange*) accumulate Asl-GFP over two cycles in order to reach their final Asl-GFP levels. (Young centrosomes formed in cycles 11 & 12 are not shown, for ease of presentation). Time relative to centriole separation (t=0 s) is indicated in all images and graphs. The error bars in graphs (B,C,D) represent s.d.

To understand how such asymmetric Asl-GFP levels arise, I followed the changes of Asl-GFP levels at both old and new centrosomes along the entire mitotic cycle by quantitative time-lapse imaging. Interestingly, I found that the behaviour of Asl-GFP at old and new centrosomes is very different. New centrosomes steadily accumulate Asl-GFP throughout *S*-phase and mitosis, and can continue to do so even in the following cycle (Figure 3.11A-D). However, surprisingly, Asl-GFP fluorescence in the oldest centrosomes does not appear to increase at all during the cell cycle, even though these old centrosomes assemble new daughters during this time (Figure 3.11A-C).

The constant levels of Asl-GFP at old centrosomes throughout the mitotic cycle strongly suggest that these centrosomes simply maintain the amount of Asl-GFP that is already present at the mother centriole in the beginning of the cycle. Therefore, even though Asl is essential for centriole duplication, it is not incorporated into daughter centrioles while they assemble. Thus, the continuous recruitment of Asl-GFP that we see at new centrosomes must be due to incorporation at the new mother centrioles. In conclusion, daughter centrioles interestingly only start to recruit Asl-GFP at about the time they disengage from their mother centriole and enter the duplication cycle for the first time as a new mother.

I verified these results using live super-resolution imaging. I imaged either Asl-mCherry in combination with DSas-4-GFP (as a centriole marker), or Asl-GFP alone (as the GFP signal allowed higher quality reconstruction of 3D SIM data). Single timepoint 3D SIM images revealed only a single ring of Asl-mCherry or Asl-GFP at each centrosome at any stage of the cell cycle (Figure 3.12A,B). Based on the relative position of DSas-4-GFP–labelled centrioles and the ring of Asl-mCherry, the latter always surrounded the mother centriole within each centrosome (Figure 3.12A). Asl-mCherry/GFP could be seen arriving at daughter centrioles around the time when they started separating from their mother centriole (Figure 3.12A-C). Already at this early stage of its recruitment, Asl-GFP appeared to form a ring around new centrioles (Figure 3.12C). In the rare cases where both separating centrioles were captured in a side view, it often appeared as the ring of Asl-GFP around new mother centrioles may cover a shorter surface than the Asl-GFP ring

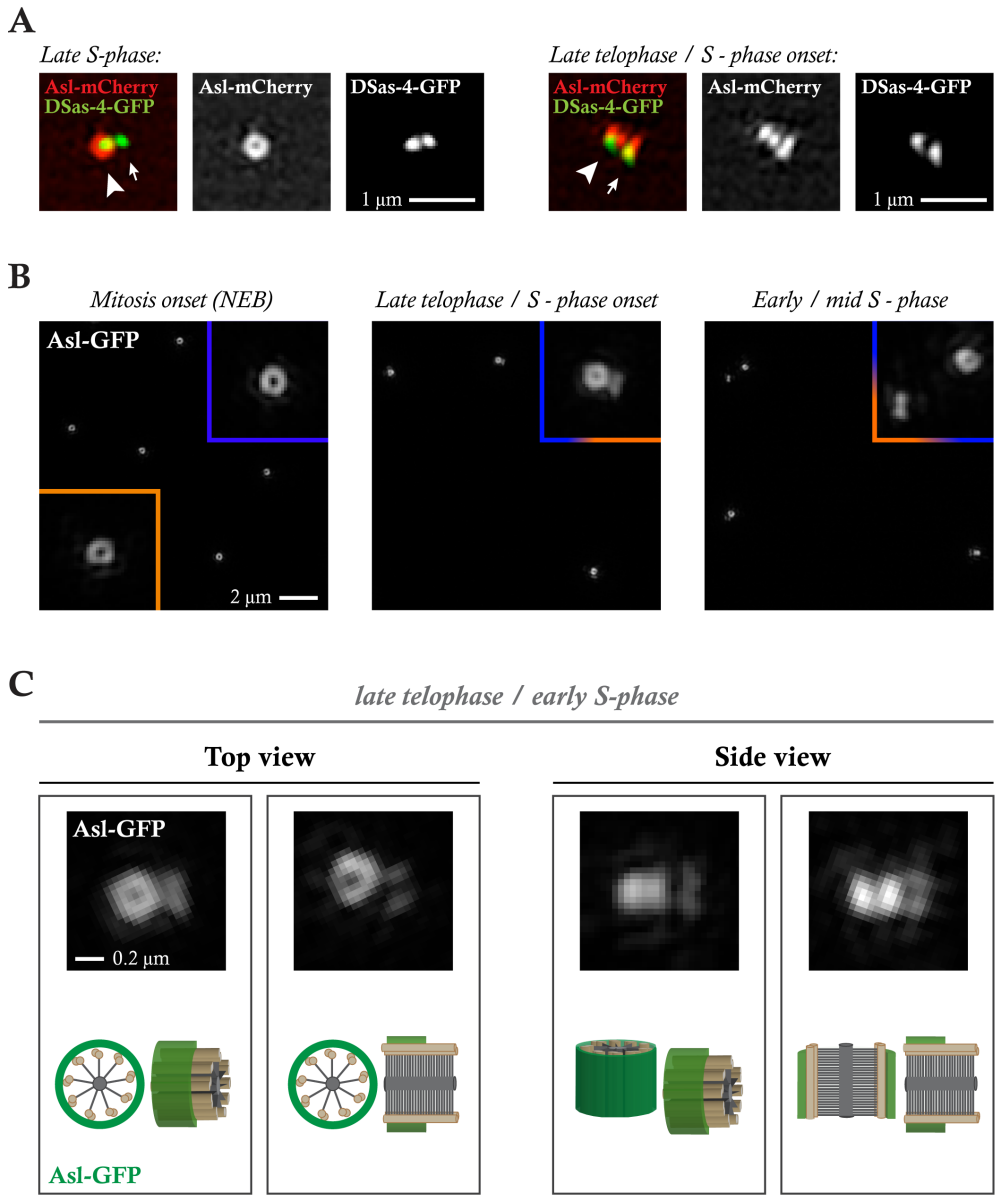


Figure 3.12 Asl-GFP forms a ring around parental centrioles in living *Drosophila* embryos.

(A, B) Super-resolution (3D SIM) fluorescent images show that Asl-mCherry (A) or Asl-GFP (B) can be detected as a ring surrounding only one centriole within each centrosome at any stage of the cell cycle. (A) Based on the relative position of the pair of centrioles (visualized by DSas-4-GFP) and the ring of Asl-mCherry, the centriole surrounded by Asl-mCherry is always the older, parental centriole (arrowheads) in each centrosome (representative examples shown) - this is in agreement with my interpretation of the quantitative confocal microscopy data. New centrioles (arrows) acquire their ring of Asl-mCherry once they separate from their mother centriole (late telophase/early *S*-phase). (B) Super-resolution (3D SIM) fluorescent images show Asl-GFP at centrosomes at different stages of the cell cycle (*blue*: old centrosomes; *orange*: new centrosomes). (C) Super-resolution (3D SIM) fluorescent images show that Asl-GFP already forms a ring around disengaged new centrioles at the earliest stages of its recruitment. The 'side view' images suggest that Asl-GFP is initially recruited to a shorter surface area of new centrioles than the surface it eventually binds on older centrioles (at the time of disengagement the actual length of a new centriole is equal to the length of its mother centriole in syncytial *Drosophila* embryos, according to Callaini & Riparbelli, JCS 1990). The schematics under the fluorescent panels show the interpretation of Asl-GFP localization (Asl-GFP shown in green).

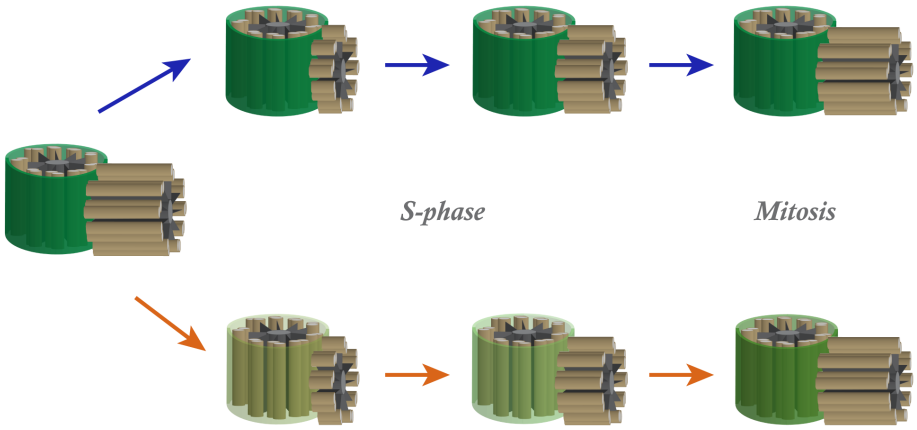


Figure 3.13 The model of Asl-GFP incorporation during centriole duplication in *Drosophila* embryos.

The schematics illustrate that Asl-GFP (*green*) is not incorporated into daughter centrioles during their assembly in *S*-phase or while they are still engaged with their mother centriole in mitosis (*blue* & *orange* arrows). Instead, fully-grown new centrioles initiate Asl-GFP recruitment around the time when they disengage from their mother centriole (left-side *orange* arrow). After the initiation of Asl-GFP recruitment, new mother centrioles continue to build up their Asl-GFP levels throughout the cell cycle (middle & right-side *orange* arrows). Older centrioles that have already accumulated high amounts of Asl-GFP do not alter their Asl-GFP levels at any stage of the centriole duplication process (*blue* arrows).

surrounding older centrioles (Figure 3.12C). This would suggest that Asl-GFP recruitment could be initiated at one end of the centriole. It is important to stress, however, that this latter observation is based on very limited, un-quantified data; this question requires further investigation.

3.2.2.3 HALF OF CENTROSOMAL ASL-GFP MOLECULES ARE IN DYNAMIC EXCHANGE WITH CYTOPLASMIC MOLECULES WHILE HALF ARE STABLY ASSOCIATED WITH THE MOTHER CENTRIOLE

I was surprised to find that old centrosomes do not change their Asl-GFP levels at all during centriole duplication; as described above, older mother centrioles contain constant levels of Asl-GFP while growing daughter centrioles do not recruit any before their disengagement. Thus, I wondered whether centriole duplication might be accompanied by a change in the dynamic properties of centrosomal Asl-GFP, instead of a change its centrosomal levels. To address this, I performed FRAP analysis of Asl-GFP at old centrosomes in both *S*-phase (start of centriole duplication) and early mitosis (completed centriole duplication).

Centrosomes that were photobleached in *S*-phase recovered Asl-GFP fluorescence, however, recovery plateaued at about 50% of the pre-bleach fluorescence signal (Figure 3.14A,B). The two most likely explanations for this behaviour are that either half of the centrosomal Asl-GFP pool is stably fixed while half is dynamic, or that centrosomal Asl-GFP is dynamic during *S*-phase but is not turning over during mitosis (and therefore recovery plateaus after *S*-phase). To discriminate between these two possibilities I tested whether Asl-GFP fluorescence also recovered immediately if centrosomes were photobleached during mitosis. As I show in Figure 3.14A, I found that it did. I did not quantify mitotic fluorescence recovery, as the qualitative result was sufficient to prove that the centrosomal turnover of Asl-GFP is not restricted to *S*-phase. Thus, the dynamic properties of Asl-GFP are not dramatically altered along the centrosome duplication cycle, but rather centrosomes have both a stably incorporated and a dynamic fraction of Asl-GFP, at an approximately equal ratio.

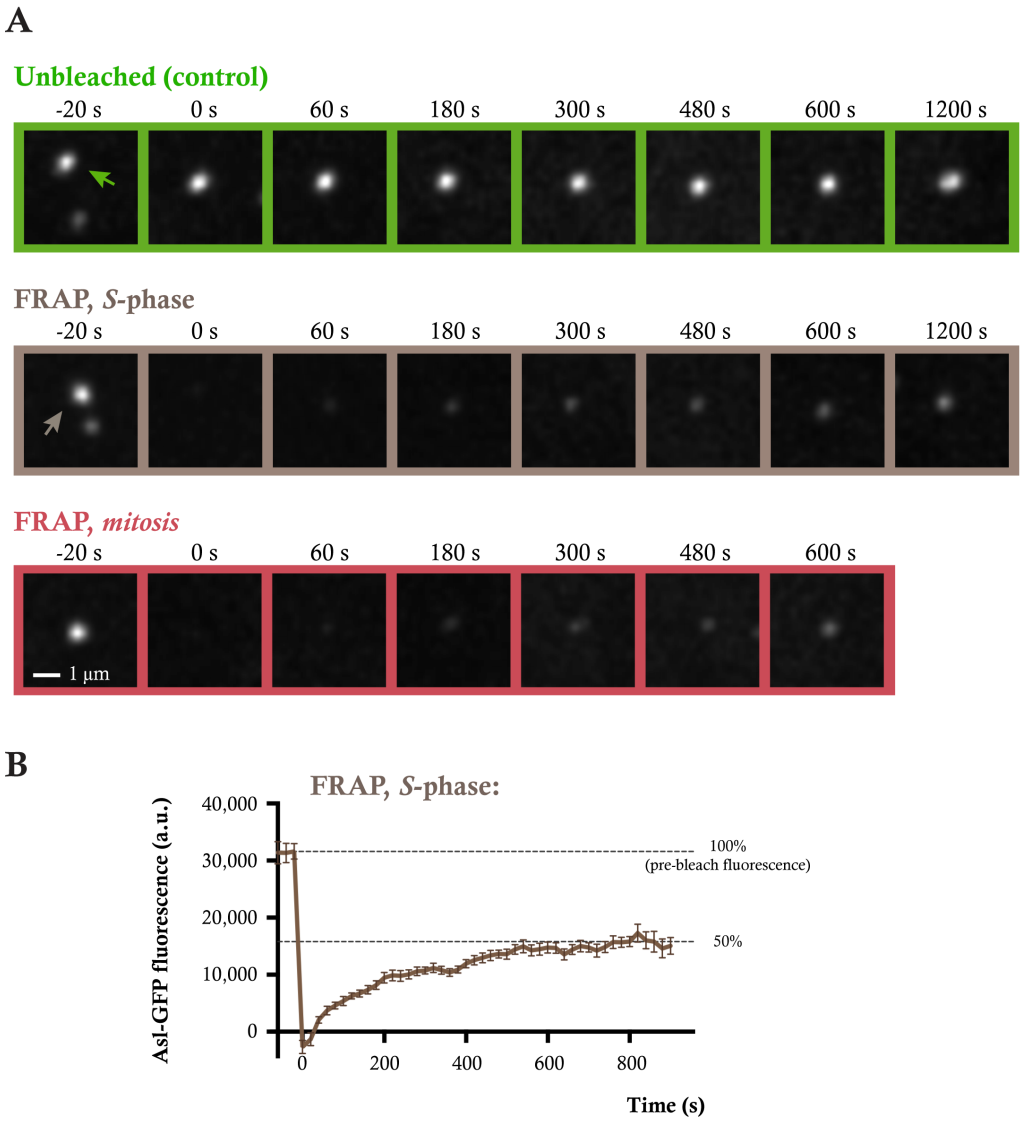


Figure 3.14 Approximately half of the total centrosomal Asl-GFP pool is immobile, while the other half remains in dynamic exchange with cytoplasmic molecules.

(A) Fluorescence images from a time-lapse FRAP movie show the Asl-GFP fluorescence levels of an unbleached control centrosome (top, *green* panel), a centrosome that was photobleached in early *S*-phase (middle, *brown* panel) and a centrosome the was photobleached in early mitosis (bottom, *maroon* panel). Time relative to photobleaching (t=0 s) is shown above each image. The arrows on the top two images (at t=-20s) point to the centrosome that was photobleached and followed in subsequent panels. Note how Asl-GFP fluorescence recovery occurs very similarly whether centrosomes were bleached in *S*-phase or in mitosis. (B) The graph shows the averaged centrosomal Asl-GFP fluorescence recovery (a.u.=arbitrary units) of centrosomes that were bleached in early *S*-phase (n=8 centrosomes from 3 embryos). Fluorescence recovery was not quantified for centrosomes that were bleached in mitosis; the reason behind this is explained in Chapter 3.2.2.3. Time relative to photobleaching (t=0 s) is shown. Error bars represent s.e.m.

In conclusion, although Asl is essential for centriole duplication, neither its centrosomal levels nor dynamic behaviour appear to be altered during the time of daughter centriole assembly. These surprising results propose that Asl acts in a fundamentally different manner than the four other essential centriole duplication proteins in flies which, in contrast to Asl, are all recruited to sites of daughter centriole assembly (Sak, DSas-6, Ana2: Raff lab unpublished data; DSas-4: this thesis).

3.3 DISCUSSION

3.3.1 PHYSIOLOGICAL EXPRESSION OF DSAS-4-GFP AND ASL-GFP IN LIVING *DROSOPHILA* EMBRYOS

In this chapter I have described the generation of fly lines that express physiological levels of DSas-4-GFP or Asl-GFP in the absence of the respective endogenous protein. The random insertion method used for generating the transformants, however, leaves room for the criticism that, while the levels of these fusion proteins appear physiological, the natural timing and regulation of their expression is most likely altered by the different genomic environment of the transgenes. As all the experiments that I describe in this study have been performed in the syncytial blastoderm stage embryo, prior to the maternal-to-zygotic transition (Tadros and Lipshitz 2009) and therefore in the near absence of transcription, I feel that it is valid to disregard such an effect as long as the total protein levels are normal. Therefore, I think it is safe to conclude that both DSas-4-GFP and Asl-GFP are physiologically expressed in the syncytial *Drosophila* embryo and thus can be used for accurate dynamic incorporation studies of these proteins.

3.3.2 THE DYNAMIC INCORPORATION OF DSAS-4-GFP PARTIALLY RESEMBLES THAT OF SAS-4, BUT ALSO SHOWS SEVERAL UNIQUE FEATURES

My results show that, in line with the behaviour of *C. elegans* SAS-4 (Dammermann et al. 2008), DSas-4 is incorporated into growing daughter centrioles throughout their formation during *S*-phase.

It remains to be further investigated whether newly incorporated DSas-4-GFP also switches from an initial dynamic state to permanently fixed around mitotic entry, as SAS-4 does (Dammermann et al. 2008).

In addition to the similarities, I also found some potentially interesting differences. DSas-4 appears to localize only to centrioles in contrast to SAS-4, which also displays a weak but obvious PCM localization (Dammermann et al. 2008). Furthermore, *Drosophila* centrioles recruit excessive amounts of DSas-4-GFP, which is lost during mitosis once daughter centriole formation is complete – this feature is not seen in *C. elegans* (Dammermann et al. 2008).

Interestingly, although *C. elegans* SAS-4 is not accumulated in excessive amounts during *S*-phase, another component of the central tube is: SAS-6. It is believed that SAS-6 is recruited during centriole duplication by ZYG-1, however once the central tube is assembled a negative feedback loop displaces ZYG-1 from centrioles, resulting in the loss of excess, unincorporated SAS-6 (Dammermann et al. 2004). It is an interesting question whether the behaviour of DSas-4-GFP might be analogous to that of SAS-6 instead of its homologue, SAS-4? Studies showing that the ZYG-1 –analogue kinase PLK4 acts on CPAP, the human homologue of SAS-4/DSas-4, (Chang et al. 2010) may provide ground for this speculation.

In *C. elegans*, the surplus levels of SAS-6 present at duplicating centrosomes have led to the proposal of two possible models to explain the recruitment of centriolar proteins to the sites of duplication. According to the first model, centriole duplication proteins are directly incorporated into the forming daughter centriole, while the second model suggests that they are first amorphously concentrated around the mother centriole, and are from there gradually incorporated into the growing daughter (Dammermann et al. 2008). According to my results, DSas-4-GFP is recruited according to the first model; the mother centriole does not appear to increase its DSas-4-GFP levels during the duplication cycle but instead excessive levels of DSas-4-GFP are recruited to

the growing centriole itself. This observation provides important information that may contribute to a more general discrimination between these two opposing models for daughter centriole assembly.

The dynamic behaviour of DSas-4-GFP reveals some interesting points that may be key for the future understanding of the molecular regulation of its incorporation. The centriolar incorporation of DSas-4-GFP clearly does not follow a model in which it gradually saturates its final binding sites on a growing procentriole – instead the excessive accumulation of DSas-4-GFP during *S*-phase suggest that its final binding sites do not limit its efficient centriolar recruitment. This is even more interesting considering the complete absence of mitotic DSas-4-GFP incorporation (or turnover within the non-fixed, eventually lost fraction) and the gradual loss of any non-fixed DSas-4-GFP molecules throughout mitosis (although successfully accumulated during *S*-phase, these unincorporated molecules can no longer associate with the daughter centriole in a mitotic environment). Taken together these data strongly suggest that the recruitment of DSas-4-GFP to daughter centrioles is regulated during the duplication cycle, but not through the availability of its final binding sites.

I envisage two main models that can explain my observations on DSas-4-GFP incorporation into centrioles. The first is a cell cycle–dependent change in the centriolar binding capacity of DSas-4-GFP between *S*-phase and mitosis. The second would be analogous to the mechanism that is believed to displace SAS-6 from centrosomes in *C.elegans* (Delattre et al. 2006; Dammermann et al. 2008); a centriolar intermediate initiating a negative feedback loop to block further DSas-4 recruitment and maintenance, independently of cell cycle progression. My data support the first model, as DSas-4-GFP loss appears to be consistently initiated at around the time of nuclear envelope breakdown, during the early stage of mitosis, regardless of the cell cycle length. In longer cycles DSas-4-GFP levels plateau for some time before the start of mitosis, while in earlier, shorter embryonic cycles DSas-4-GFP loss immediately follows a short peak (rather than plateau) of its high centriolar levels. Unless the time of daughter centriole assembly takes gradually longer in progressive embryonic cycles (which has not been described so far), it is most likely that entering

the mitotic phase of the cell cycle is responsible for the change seen in the recruitment and maintenance of DSas-4-GFP at centrosomes. This prediction, however, requires further investigation, in particular an analysis of the dynamic behaviour of DSas-4-GFP following an *S*-phase arrest. Nonetheless, my observations could be very important for the future understanding of both the mechanism of DSas-4 incorporation within the centriole as well as the recruitment of other centriolar proteins that bind to DSas-4.

3.3.3 ASL-GFP DISPLAYS A VERY SURPRISING DYNAMIC BEHAVIOUR AT CENTROSOMES

The localization or dynamic behaviour of Asl or any of its homologues had not been described at the time I started this project. By analysing the incorporation of Asl-GFP along the centriole duplication cycle, I found that, although Asl is essential for centriole duplication, Asl-GFP is not actually incorporated into forming daughter centrioles themselves; Asl is only incorporated into newly formed centrioles once they separate from their mothers at the end of mitosis. Thus, Asl is not in fact an integral component of centrioles. During the course of my PhD several other groups have also reported that Asl/Cep152 localizes only around the parental centriole within a pair of engaged centrioles, based on super-resolution immunofluorescence analyses of fixed cells (Sir et al. 2011; Fu and Glover 2012; Mennella et al. 2012; Sonnen et al. 2012; Lukinavicius et al. 2013) or immunoelectron microscopy (Sonnen et al. 2013). My results show that this is also the case in a living *Drosophila* embryo.

My quantitative analysis and qualitative super-resolution image data revealed that new fully formed centrioles initiate Asl-GFP recruitment at about the time they disengage from their mother centriole. In syncytial blastoderm stage *Drosophila* embryos centriole disengagement in late-anaphase/telophase is very rapidly followed by the initiation of centriole duplication in early *S*-phase, so I cannot be certain which of these events promotes the recruitment of Asl-GFP to new centrioles. Recently two different studies in fixed human cells – neither of which really focused on

the timing of Cep152 recruitment – showed that, albeit at low levels, Cep152 is present at new mother centrioles prior to the onset of *S*-phase (Sir et al. 2011; Sonnen et al. 2013). Thus, the data presented in these studies is consistent with initial Cep152 recruitment being linked to centriole disengagement and anaphase instead of the onset of centriole duplication in *S*-phase. Together, my results (in particular, the super-resolution image data which allows the optical resolution of separating centrioles earlier in time) and these two studies in human cells suggest that most likely Asl incorporation in *Drosophila* embryos is also elicited by a late mitotic environment rather than *S*-phase.

Although since the start of my project several recent reports have also shown that Asl/Cep152 is only associated with parental centrioles in fixed cells (Sir et al. 2011; Fu and Glover 2012; Mennella et al. 2012; Sonnen et al. 2012; Lukinavicius et al. 2013; Sonnen et al. 2013), none of these studies addressed how the absence of Asl/Cep152 at daughter centrioles could fit with its importance in centriole duplication, or whether Asl/Cep152 levels might change at the parental centriole during daughter centriole assembly. My data revealed that in old centrosomes, where the mother centriole had already accumulated Asl in a previous cycle, daughter centriole formation is not associated with a change in the centrosomal levels of Asl or an alteration of its molecular turnover. These results are extremely surprising as they suggest that daughter centriole assembly requires the mere presence of Asl around mother centrioles. In the following chapter I present data that supports this model.

Interestingly, my results show that new mother centrioles perform their first round of duplication successfully while containing significantly lower levels of Asl-GFP than older centrioles (Figure 3.11). This means that as centrioles age, they accumulate far more Asl than the amount required for supporting successful centriole duplication. It is likely that the higher levels of Asl accumulated by centrioles are linked to the role of Asl in PCM recruitment (Varmark et al. 2007; Conduit et al. 2010; Conduit et al. 2014b). The build-up of Asl-GFP at new centrioles occurs throughout the whole cycle, and usually continues in the following cycle, until the centrosomes reach their final

Asl-GFP levels. The rate of Asl-GFP recruitment appears constant throughout this accumulation process. Together these results suggest that once Asl incorporation is initiated its further accumulation is not subject to cell cycle –dependent regulation.

In this chapter I have identified Asl as the first core centriole duplication protein that is only associated with mother centrioles, and is not an integral component of newly assembling, or even fully-formed, daughter centrioles. This discovery reminded me of a very interesting and unexplained question in the centriole duplication field. It had been documented before in multiple studies based on various experiments that daughter centrioles do not appear to have the potential to duplicate during the cell cycle in which they are assembled (Kleylein-Sohn et al. 2007; Loncarek et al. 2008; Cunha-Ferreira et al. 2009; Wang et al. 2011). While mother centrioles have this potential throughout the cell cycle, albeit normally repressed due to the engagement with a daughter centriole (Kleylein-Sohn et al. 2007; Cunha-Ferreira et al. 2009), daughter centrioles only appear to acquire their ability to duplicate during or just after they have passed through their first mitosis, regardless of their engagement status (Loncarek et al. 2010; Wang et al. 2011). The exclusive presence of Asl at parental centrioles, the timing of its initial incorporation into new centrioles and its constant presence thereafter suggested that Asl incorporation dynamics could explain this fundamental difference between mother and daughter centrioles. If Asl is essential for centriole duplication, but not for centriole assembly, then its presence on mother centrioles might make them potentially competent to duplicate at any stage of the cell cycle, while its absence from daughter centrioles might make them incompetent to duplicate at any stage of the cell cycle. In the following chapter I investigate this possibility.

CHAPTER 4:

DSAS-4–DEPENDENT INCORPORATION OF ASL LICENSES NEW CENTRIOLES TO DUPLICATE FOR THE FIRST TIME

4.1 SUMMARY

After discovering the interesting incorporation pattern of Asl, my next aim was to understand which molecular pathways are responsible for its centrosomal recruitment. My goal was to identify the proteins that provide the centriolar binding sites for Asl, and to investigate how the complex, partially fixed, partially mobile Asl pools are established at centrosomes.

So far Cep63 is the only protein known to play an important role in the centrosomal localization of Cep152, the vertebrate homologue of Asl (Sir et al. 2011; Brown et al. 2013; Lukinavicius et al. 2013), and, as discussed in section *1.2.1.3*, Cep63 is more likely involved in the centrosomal maintenance of Cep152 rather than its initial recruitment to centrioles. Importantly, no homologue of Cep63 has been found in *Drosophila* to date, and no other protein has yet been identified to act in the centriolar localization of Asl. As Asl is indispensable for centriole duplication in flies, I reasoned that the protein responsible for its initial binding to centrioles must be essential for centriole duplication too. So far, two key centriolar proteins have been shown to interact with Asl in an evolutionarily conserved manner: DSas-4 and Sak (Dzhindzhev et al. 2010). However, it has been proposed that Asl scaffolds these two proteins to promote the onset of centriole duplication (Cizmecioglu et al. 2010; Dzhindzhev et al. 2010), which leaves unanswered how Asl itself arrives at centrioles.

A recent report has shown that centrosomal Asl has a strict molecular orientation: the C-terminus is located close to the centriole wall, while the N-terminus extends outwards, away from the centriole core (Mennella et al. 2012). This orientation suggested that the C-terminal, centriole-proximal, region of Asl is most likely involved in its initial anchoring at centrioles. This region of Asl can interact directly with DSas-4 (Dzhindzhev et al. 2010). I wondered, therefore, whether instead of Asl acting as a scaffolding platform for DSas-4 and Sak, Asl might be recruited by DSas-4 to newly formed daughter centrioles.

In the first half of this chapter I address the role of the DSas-4–Asl interaction in the centrosomal recruitment of Asl. Using immuno-inhibition coupled with a live imaging assay, I show that centriolar DSas-4 plays a functional role in the initial anchoring of Asl at newly disengaged daughter centrioles. Surprisingly, however, exchanging Asl molecules are recruited to mother centrioles through a different mechanism; most likely through an interaction with the initially incorporated, fixed Asl molecules. These results reveal that multiple molecular pathways act sequentially to establish the different Asl pools at centrosomes.

In the second half of this chapter I show that, while it is not an integral component of centrioles, Asl is essential for centriole duplication because its incorporation converts disengaged daughter centrioles into mother centrioles that can duplicate. Therefore, Asl fulfils an unexpected regulatory role in the centriole cycle: the presence of Asl at centrioles acts as a permanent 'license' for their subsequent duplication, while the absence of Asl prevents the duplication of disengaged centrioles in *S*-phase.

4.2 RESULTS

4.2.1 DSAS-4 PLAYS A KEY ROLE IN THE INITIAL RECRUITMENT OF ASL-GFP TO NEW CENTRIOLES

To block the interaction between centriolar DSas-4 molecules and cytoplasmic Asl, I injected living embryos with a DSas-4–specific antibody that targets a part of the mapped Asl–interacting region (Figure 4.1A). This antibody had been conjugated with Texas Red dye, allowing the visualization of the antibody and, thereby, the identification of inhibited centrosomes. To specifically study the initial step of Asl recruitment at newly disengaged daughter centrioles, I injected the DSas-4–inhibiting antibodies into syncytial embryos expressing Asl-GFP during early mitosis, when daughter centrioles were already fully formed but had not yet initiated Asl recruitment (Figure 4.1B, upper panels). I then followed the centrosomes through mitosis and into early *S*-phase: when the disengaged mother and daughter centrioles had sufficiently separated (Figure 4.1B, lower panels), I assayed the presence of Asl-GFP at the young centrosomes (Figure 4.2).

The injected anti-DSas-4 antibodies rapidly bound to centrosomes that were close to the site of injection (Figure 4.2A, DSas-4–blocked panels) but not to centrosomes that were further away from the injected area (Figure 4.2A, control panels). In early *S*-phase (following centriole separation) Asl-GFP localized at both old and new centrosomes in the control region (Figure 4.2B), in the same asymmetrical manner as described earlier in non-injected embryos (see Figure 3.10B). Asl-GFP also appeared to localize normally to anti-DSas-4–bound old centrosomes (Figure 4.2B). Strikingly, however, no Asl-GFP could be detected at anti-DSas-4–bound new centrosomes (Figure 4.2B,C). I conclude that the anti-DSas-4 antibodies disrupt the initial recruitment of Asl-GFP to newly assembled centrioles (most likely by interfering with the DSas-4–Asl interaction), but do not detectably interfere with the maintenance of Asl-GFP at the previously assembled old centrioles.

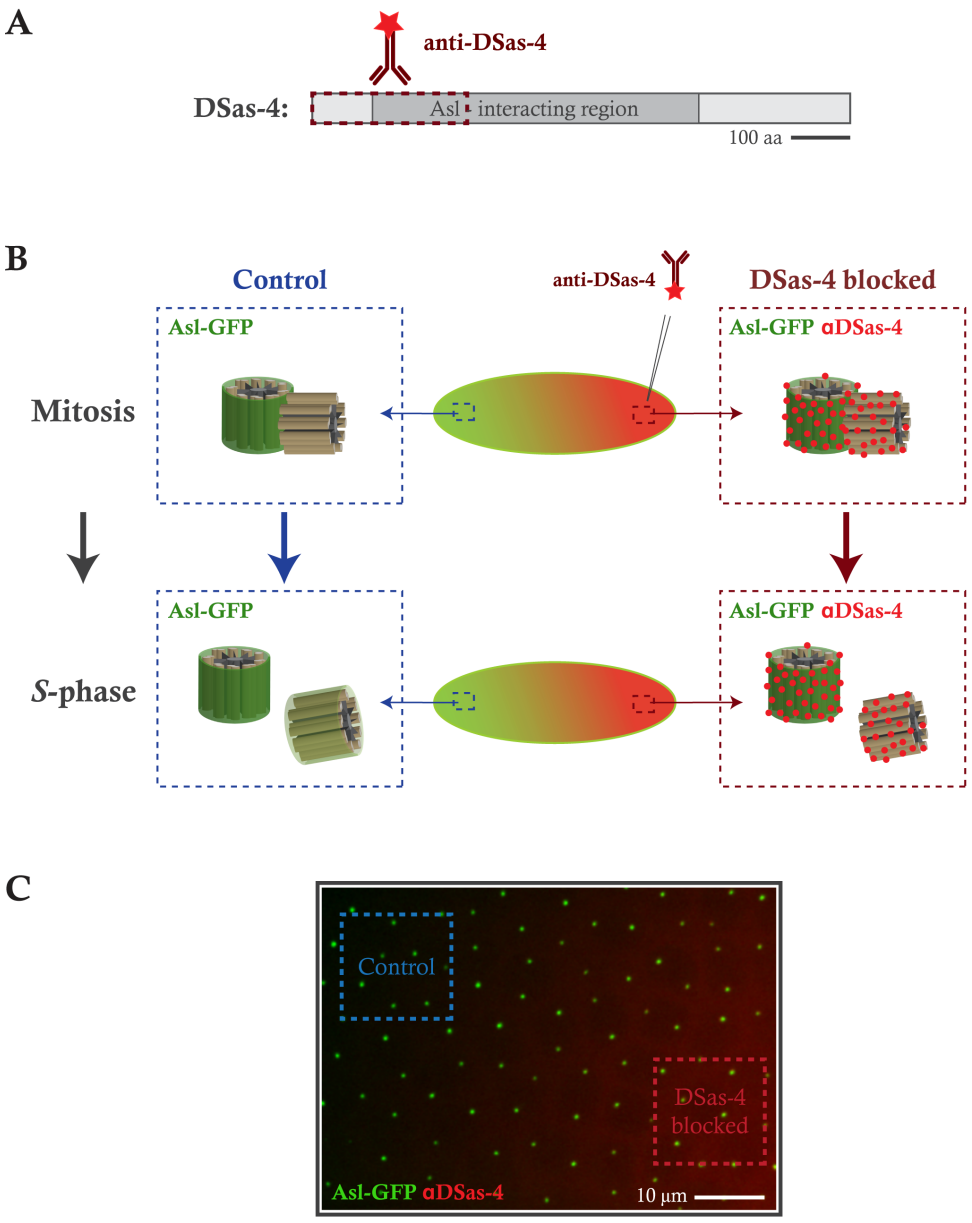


Figure 4.1 Testing the functional role of DSas-4 in the initial recruitment of Asl using immuno-inhibition.

(A) Schematic illustration of DSas-4, showing the region required for the interaction with Asl (Dzhindzhev et al. 2010). Red box indicates the region against which the inhibiting antibody used in my experiments was raised (Basto et al. 2006). (B) Schematic illustrates the immuno-inhibition approach I used for testing the role of DSas-4 in the initial recruitment of Asl. The DSas-4–specific antibody (*red*) was injected into one side of syncytial embryos during early mitosis (top panels), when daughter centrioles were fully grown but still engaged with their mother and therefore had not yet initiated Asl-GFP (*green*) recruitment. The localization of Asl at *DSas-4–blocked* (right panels) or *control* (left panels) new centrioles, was then assayed during the following *S*-phase, once they have disengaged from their mothers (bottom panels). (C) Fluorescent image shows an Asl-GFP–expressing embryo injected with Texas-Red–labelled anti-DSas-4 (injection site in the bottom right corner). Note that centrosomes close to the injection site are exposed to a high concentration of antibody, which bind to the centrosomes (*DSas-4 blocked* region); the centrosomes further away from the injection site show no detectable antibody signal and thus serve as internal controls (*control* region).

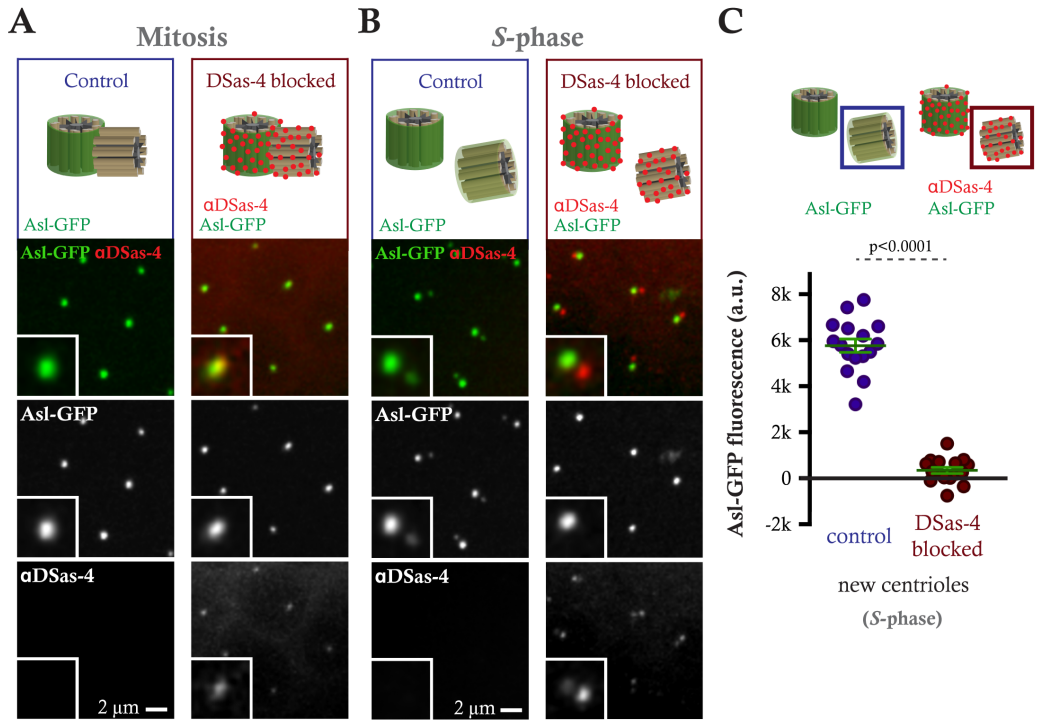


Figure 4.2 Immuno-inhibition of DSas-4 blocks the initial incorporation of Asl-GFP into newly assembled centrioles.

(A) Fluorescence images show the '*control*' and '*DSas-4 blocked*' regions (see Figure 4.1) of an embryo expressing Asl-GFP (*green*) that had been injected with Texas Red–labelled anti-DSas-4 antibodies (*red*) at the start of mitosis. (B) Fluorescence images show the same centrosomes as shown in (A) several minutes later, after the centrioles have separated at the start of *S*-phase. The schematics at the top of each panel in (A,B) illustrate how anti-DSas-4 antibodies bind to centrioles in mitosis and block the subsequent incorporation of Asl-GFP into new centrioles, however anti-DSas-4 antibodies do not interfere with Asl-GFP localization at old centrioles. (C) The graph quantifies Asl-GFP levels in new centrioles in early *S*-phase in the *'control'* region (*blue*) and in the '*DSas-4 –blocked'* region (*maroon*), as shown schematically above the graph (n=16 centrioles from 3 injected embryos for each region). Error bars indicate s.e.m.

To confirm that Asl-GFP recruitment was disrupted as a result of inhibiting the interaction between DSas-4 and Asl-GFP (and not because of a non-specific, steric inhibition by the centriole-bound antibodies) I tested whether blocking the DSas-4–interacting region of cytoplasmic Asl molecules would have a similar effect (Figure 4.3A,B). I used a Texas Red–coupled antibody that had been raised against the C-terminal, DSas-4–interacting region of Asl (Figure 4.3A). After injection, the anti-Asl antibodies bound to the centrosomes close to the site of injection but not to the more distant control centrosomes (Figure 4.4A). As mother and daughter centrioles separated after mitosis in the antibody-injected region, I found that anti-Asl often only decorated one centriole of these separating pairs (Figure 4.4B). The centrioles that were bound by anti-Asl were presumably the original mother centrioles, as only these would have incorporated Asl before the previous mitosis, when the antibody was injected. The absence of anti-Asl signal at disengaged new centrioles (arrowhead, Figure 4.4B) suggested that these centrioles could not accumulate Asl from the cytoplasm as a result of the immuno-inhibition event (Figure 4.4B schematic). Therefore, the binding of anti-Asl antibodies to the DSas-4–interacting region of cytoplasmic Asl molecules interferes with the initial recruitment of Asl to newly assembled centrioles.

Importantly, the newly separated mother and daughter centrioles in the Asl-blocked region contained similar levels of DSas-4-GFP as control centrioles. This suggests that anti-Asl antibodies do not affect the localization of DSas-4-GFP molecules that have been incorporated into centrioles before the inhibition event (Figure 4.4B,C).

In conclusion my results strongly suggest that DSas-4 plays a key role in the initial recruitment of Asl to newly assembled, disengaged daughter centrioles. Inhibition of centriolar Asl molecules does not, however, detectably affect the localization of DSas-4-GFP molecules within the same centriole; therefore DSas-4 appears to recruit Asl to centrioles in a non-reciprocal manner.

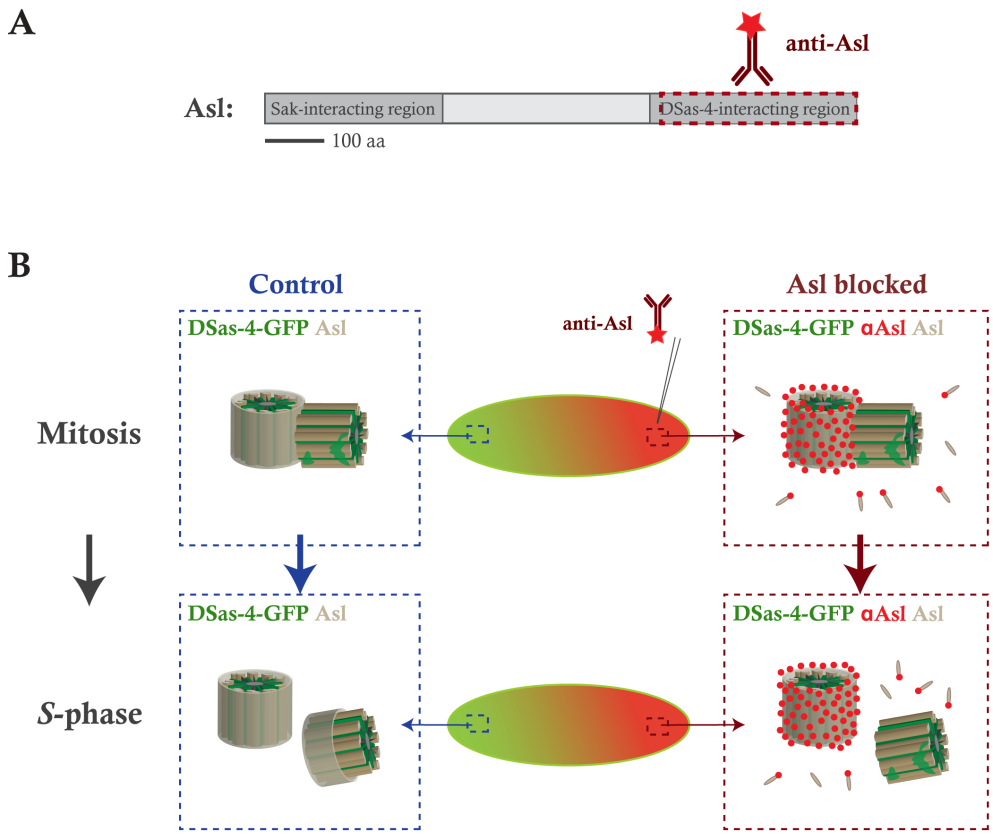


Figure 4.3. Immuno-inhibition of cytoplasmic Asl to prevent its centriolar recruitment: the generation of unmodified new centrioles that lack Asl.

(A) Schematic illustration of Asl, showing the regions required for the interaction with Sak and DSas-4 (Dzhindzhev et al. 2010). Red box indicates the region against which the inhibiting antibody (used in my experiments for blocking the interaction with DSas-4) was raised (Conduit et al. 2010). (B) Schematic illustrates the approach I used for generating unmodified new centrioles that lack Asl, by blocking the DSas-4–interacting region of cytoplasmic Asl molecules. Anti-Asl (*red*) was injected during early mitosis (top panels) into embryos expressing DSas-4-GFP (*green*) as a centriole marker. The anti-Asl antibodies bound not only to Asl molecules (*grey*) incorporated around the mother centrioles, but also to cytoplasmic Asl molecules; as a result, cytoplasmic Asl molecules could not bind to DSas-4, preventing the recruitment of Asl to newly disengaged centrioles (bottom panel).

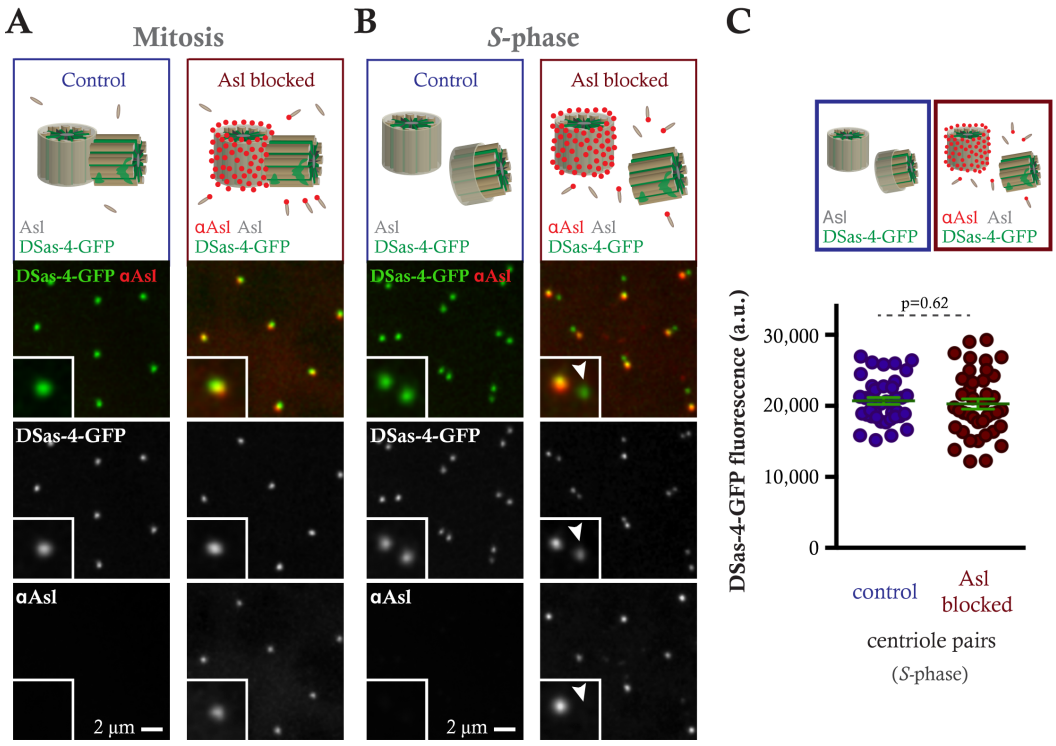


Figure 4.4 Immuno-inhibition of the DSas-4 –interacting region of cytoplasmic Asl prevents its incorporation into newly assembled, disengaged centrioles.

(A,B) Fluorescence images show the '*control*' and '*Asl blocked*' regions (see Figure 4.3) of an embryo expressing DSas-4-GFP (*green*) that had been injected with Texas Red–labelled anti-Asl antibodies (*red*) at the start of mitosis (A) and a few minutes later, after the centrioles have separated at the start of *S*-phase (B). The schematics at the top of each panel illustrate how anti-Asl antibodies bind not only to Asl incorporated around mother centrioles, but also to cytoplasmic Asl molecules and as a result block the subsequent incorporation of Asl-GFP into newly disengaged centrioles (arrowhead). (C) The graph quantifies DSas-4-GFP levels in disengaged centriole pairs in early *S*-phase in the *'control'* region (*blue*) and in the '*Asl blocked*' region (*maroon*), as shown schematically above the graph (n=40 centrioles from 4 injected embryos for each region). Error bars indicate s.e.m. Note that the DSas-4-GFP fluorescence levels of '*control*' and '*Asl blocked*' centriole pairs are very similar, suggesting that anti-Asl antibodies do not affect the localization of DSas-4-GFP molecules that have been incorporated into centrioles before antibody injection. Note that I compared centriole pairs instead of just new centrioles because I could not distinguish old and new centrioles in the '*control*' region of embryos based on DSas-4-GFP fluorescence alone.

4.2.2 MULTIPLE MOLECULAR MECHANISMS ARE RESPONSIBLE FOR ESTABLISHING THE COMPLETE ASL POOL AT CENTROSOMES

While anti-DSas-4 antibodies completely blocked the initial recruitment of Asl-GFP to new centrioles, the antibodies did not appear to affect the levels of Asl-GFP at older mother centrioles — that had accumulated Asl-GFP before inhibition (Figure 4.2A,B). This suggested that DSas-4–inhibiting antibodies do not affect the maintenance of stably incorporated Asl-GFP molecules, or the recruitment of the exchanging Asl molecules. To confirm this latter point, I compared Asl-GFP fluorescence recovery after photobleaching at anti-DSas-4–bound and control centrosomes (Figure 4.5). To accurately measure the effect of DSas-4 inhibition, I always compared centrosomes that were evenly matched in their total Asl-GFP levels (Figure 4.5C); this meant that the average size of the mobile Asl-GFP pool (which is about half of the total centrosomal Asl-GFP) would be approximately equal in all experimental groups.

Asl-GFP fluorescence recovered at DSas-4–blocked centrosomes, and the rate of fluorescence recovery was very similar to that of unbound centrosomes, or centrosomes in un-injected embryos (Figure 4.5B,B',B",D). Thus, although DSas-4 plays an essential role in the initial recruitment of Asl to centrioles, it does not appear to play a direct role in the centriolar recruitment of the exchanging Asl molecules.

The vertebrate homologue of Asl, Cep152, has been shown to self-interact in human cells (Hatch et al. 2010), while yeast two hybrid experiments and *in vitro* biophysical assays suggest that the same is true for *Drosophila* Asl (Conduit et al. 2014b and Zhe Feng personal communications). This raised the possibility that the immobile fraction of Asl may be responsible for recruiting the mobile fraction of Asl (so potentially explaining the 50:50 ratio of the immobile and mobile fractions). To test this possibility, I compared Asl-GFP recovery after photobleaching at anti-Asl–bound and control centrosomes (Figure 4.6). Strikingly, Asl-GFP recovery was abolished at anti-Asl–bound centrosomes (Figure 4.6B",D) in comparison to the normal fluorescence recovery of unbound control centrosomes (Figure 4.6B',D) or centrosomes of un-injected embryos (Figure 4.6B,D).

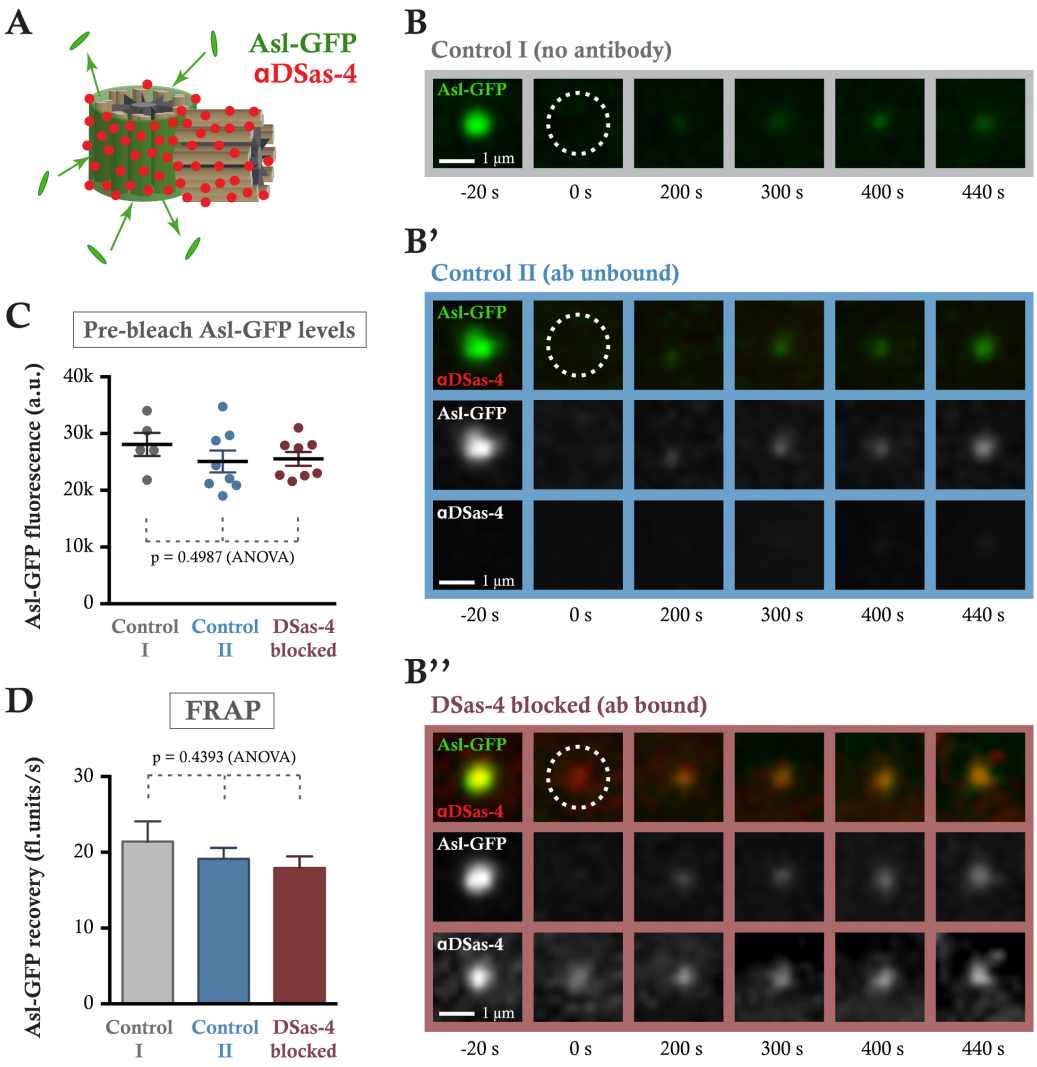


Figure 4.5 Immuno-inhibition of DSas-4 does not affect the turnover of Asl-GFP at older centrioles.

(A) Schematic illustrates the process that is addressed by the data presented in this Figure: the turnover of Asl-GFP (*green*) at older centrioles that are bound by anti-DSas-4 antibodies (*red*). (B-B'') Fluorescence images show Asl-GFP fluorescence recovery of centrosomes following photobleaching in *S*-phase. Time relative to photobleaching (t=0s) is indicated. (B) A centrosome in an un-injected embryo ('*control I'; boxed in grey*). (B') An unbound control centrosome in an embryo that had been injected with anti-DSas-4 ('*control II*'; boxed in *blue*). (B'') An anti-DSas-4–bound centrosome in an injected embryo (boxed in *pink*). (C) Graph quantifies the Asl-GFP fluorescence levels in the timepoint just prior to photobleaching for centrosomes that were used to measure FRAP rates. The categories match those described in panels B-B'' (n=5 centrosomes from 2 embryos for *'control I'*; n=8 centrosomes from 3 injected embryos for '*control II*'; n=8 centrosomes from 3 injected embryos for '*DSas-4 –blocked'*). Note that, on average, the pre-bleach levels of Asl-GFP match closely between all experimental groups, suggesting that the average mobile Asl-GFP pool is also closely matched between these categories (this is important as half of the total centrosomal Asl-GFP pool is mobile, see Figure 3.14) Error bars: s.e.m. (D) Graph quantifies Asl-GFP recovery (fluorescence units/s) following photobleaching of Asl-GFP at centrosomes in *S*-phase. These are the same centrosomes that are shown in panel C (therefore the sample sizes are exactly the same as described for panel C). Error bars: s.e.m.

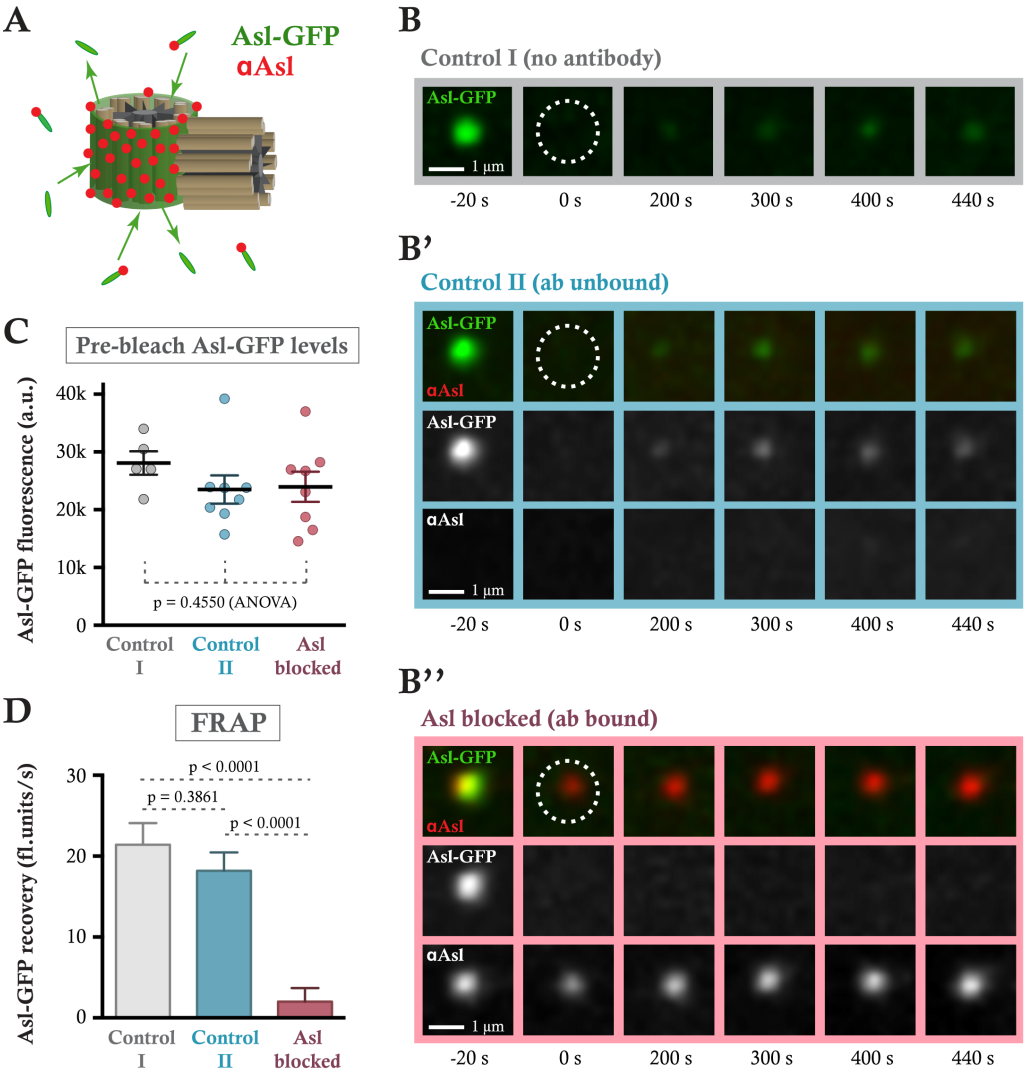


Figure 4.6. Immuno-inhibiting the Asl-GFP pool of older centrioles abolishes the turnover of Asl-GFP within centrosomes.

(A) Schematic illustrates the process that is addressed by the data presented in this Figure: the turnover of Asl-GFP (*green*) at older centrioles that are bound by anti-Asl (*red*). The data presented in panels B-D prove that Asl-GFP turnover is in fact abolished by the binding of anti-Asl antibodies. (B-B'') Fluorescence images show Asl-GFP fluorescence recovery of centrosomes following photobleaching in *S*-phase. Time relative to photobleaching (t=0s) is indicated. (B) A centrosome in an un-injected embryo ('*control I';* boxed in *grey*). (B') An unbound control centrosome in an embryo that had been injected with anti-Asl ('*control II*'; boxed in *blue*). (B'') An anti-Asl–bound centrosome in an injected embryo (boxed in *pink*). (C) Graph quantifies the Asl-GFP fluorescence levels in the timepoint just prior to photobleaching for centrosomes that were used to measure FRAP rates. The categories match those described in panels B-B'' (n=5 centrosomes from 2 embryos for *'control I'*; n=8 centrosomes from 3 injected embryos for '*control II*'; n=8 centrosomes from 3 injected embryos for '*Asl blocked'*). Note that, on average, the pre-bleach levels of Asl-GFP match closely between all experimental groups, suggesting that the average mobile Asl-GFP pool is also closely matched between these categories (this is important as half of the total centrosomal Asl-GFP pool is mobile, see Figure 3.14) Error bars: s.e.m. (D) Graph quantifies Asl-GFP recovery (fluorescence units/s) following photobleaching of Asl-GFP at centrosomes in *S*-phase. These are the same centrosomes that are shown in panel C (therefore the sample sizes are exactly the same as described for panel C). Error bars: s.e.m.

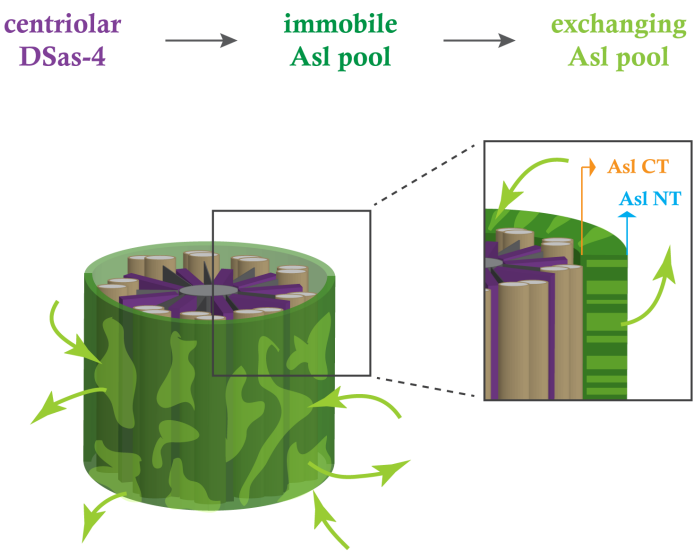


Figure 4.7 Model of the dynamic behaviour and recruitment of Asl-GFP at older centrioles.

Schematic illustrates how DSas-4 molecules present within the centriole are responsible for the recruitment of the immobile pool of Asl (Figures 4.2, 4.3 & 4.5), which then provides the binding sites that recruit the mobile pool (Figure 4.6). Immobile and mobile Asl molecules most likely do not occupy different layers (at a molecular resolution) around the centriole, based on my experiments together the well documented strict directionality of Asl molecules (Mennella et al. 2012) at centrioles. However, the dual dynamic behaviour of Asl at the centrosome also suggests that all Asl molecules are most likely not engaged in identical molecular interactions. Therefore a possible model would be that immobile Asl molecules directly interact with centriolar DSas-4, while mobile Asl molecules interact with the immobile ones in a parallel orientation (as they appear to interact in yeast two-hybrid studies; Dr. Jennifer Richens, personal communications), but do not form contact with centriolar DSas-4 (shown above in inset). This would explain the directional orientation of Asl at centrioles (Mennella et al. 2012).

Despite the absence of fresh Asl recruitment at anti-Asl–bound older centrosomes, the antibodies remained bound at these centrosomes throughout the timescale of my experiments (see, for example, Figures 4.4 and Figure 4.6B"). Thus, similarly to anti-DSas-4 antibodies, anti-Asl antibodies do not appear to interfere with the maintenance of Asl molecules that have been stably incorporated at centrosomes prior to the immuno-inhibition event.

In conclusion, these results suggest that Asl molecules are recruited to centrioles through a layered, multistep mechanism. Immobile Asl molecules are recruited to centrioles first in a DSas-4–dependent manner; this fixed pool of Asl appears to provide the binding sites for the mobile Asl pool at centrosomes (Figure 4.7).

4.2.3 DISENGAGED NEW CENTRIOLES THAT LACK ASL CAN NOT FORM A DAUGHTER

The interesting incorporation profile of Asl-GFP suggested that Asl might be responsible for converting disengaged daughter centrioles into mother centrioles that have the potential to duplicate. Understanding the molecular interactions required for Asl incorporation and having the ability to block these interactions at newly assembled, disengaged centrioles allowed me to test this hypothesis. Anti-DSas-4 antibodies successfully blocked the initial recruitment of Asl-GFP to new centrioles (Figure 4.2B,C). However, as DSas-4 itself is essential for centriole duplication, these DSas-4–blocked centrioles do not necessarily test the role of Asl in this process. In contrast, anti-Asl antibodies prevent the recruitment of Asl at new centrioles without actually binding to the centrioles (Figure 4.4B), providing a powerful system with which to study the role of Asl recruitment to physiologically formed daughter centrioles (Figure 4.3 and Figure 4.4B).

The simplest way to assay successful centriole duplication using confocal microscopy is to follow the separation of original mother centrioles and their newly formed daughters in late telophase/early S-phase. Asl-positive centrosomes (that were heavily decorated with anti-Asl

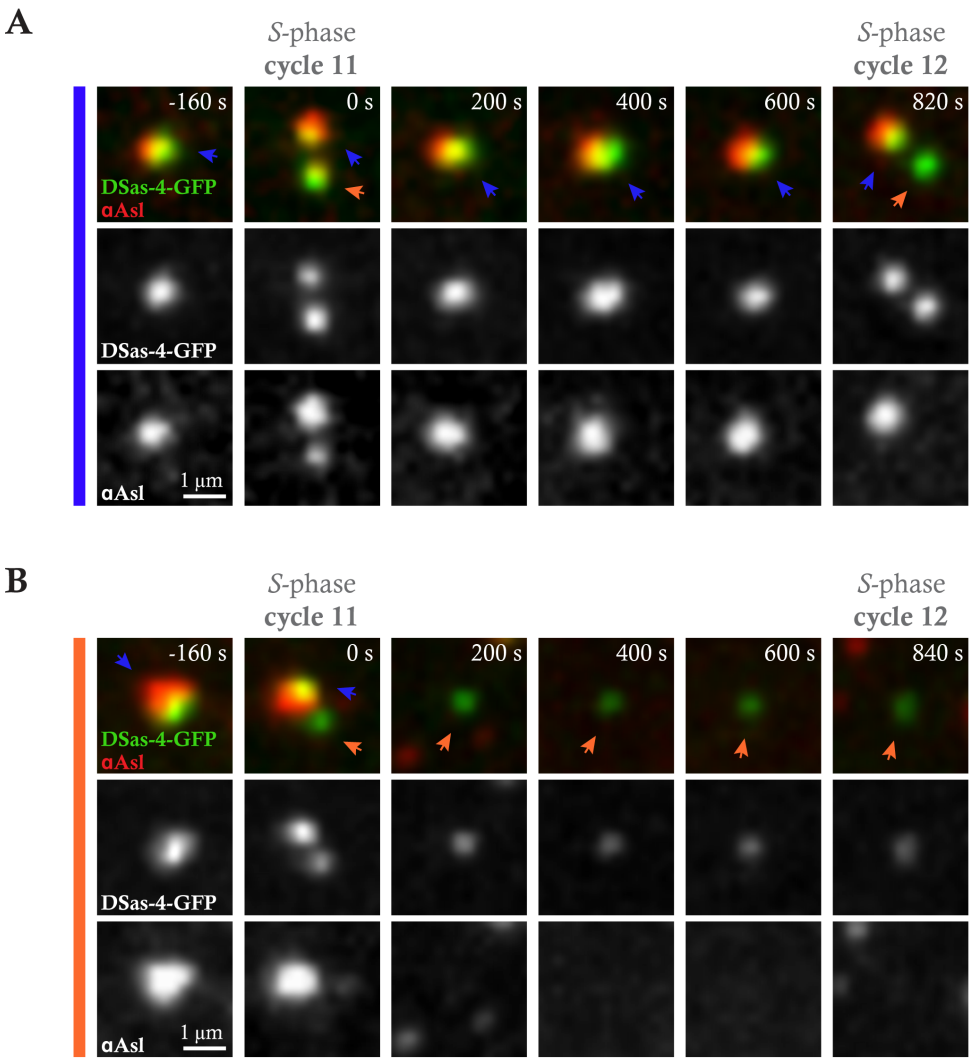


Figure 4.8 Asl-negative centrosomes fail to duplicate .

(A,B) Fluorescent images from a time-lapse movie of an embryo expressing DSas-4-GFP (*green*) that had been injected with anti-Asl antibodies (*red*). (A) The images show a representative example of an old centrosome successfully duplicating in consecutive cell cycles despite being strongly decorated with anti-Asl antibodies that interfere with the Asl-DSas-4 interaction. (B) The images show a representative example of a new Asl-negative centrosome, which fails to duplicate even though no antibodies can be detected at this centrosome. Time relative to centrosome separation (t=0s) in cycle 11 is indicated.

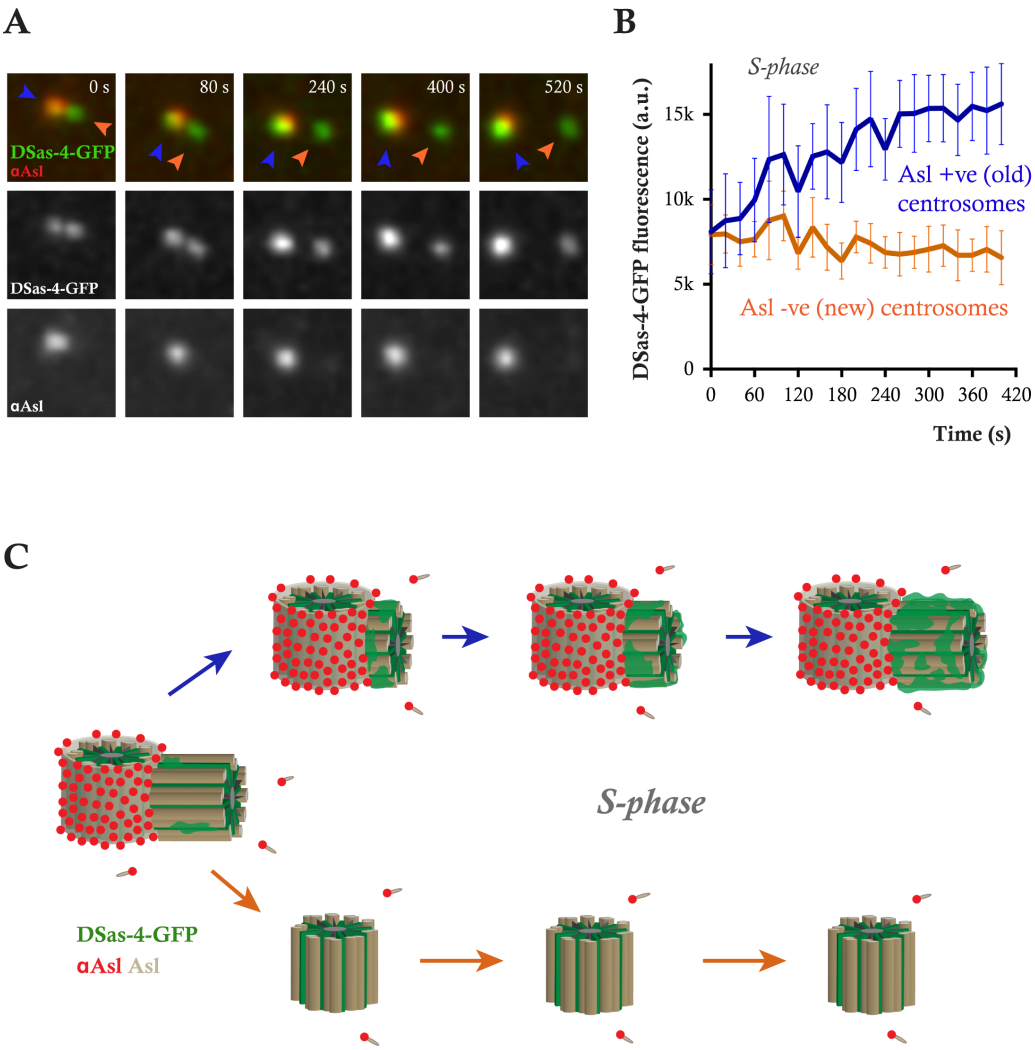


Figure 4.9 Disengaged new centrioles that lack Asl cannot template daughter centrioles.

(A) Fluorescent images from a time-lapse movie of an embryo expressing DSas-4-GFP (*green*) that had been injected with anti-Asl antibodies (*red*). Representative images show that DSas-4-GFP is incorporated into old centrosomes (*blue* arrowheads), even though the mother centriole is these centrosomes is strongly decorated with anti-Asl antibodies (*red*), however DSas-4-GFP is not recruited to the newly separated young centrosomes (*orange* arrowheads), even though no anti-Asl is detectable at these centrosomes. (B) Graph quantifies the incorporation of DSas-4-GFP into anti-Asl –bound old centrosomes (*blue* line, n=10 centrosomes from one embryo) during *S*-phase; there is no DSas-4-GFP incorporation at young Asl-negative centrosomes (*orange* line, n=10 centrosomes from one embryo), suggesting that these centrioles cannot form daughters. Error bars represent SD. Time relative to centrosome separation (t=0s) is indicated in both (A) and (B). (C) Schematic summarizes the conclusions of the results presented in Figure 4.8 & Figure 4.9 (this figure). Anti-Asl antibodies bind to Asl-positive old centrioles, but their binding does not block DSas-4-GFP recruitment and daughter centriole assembly. Anti-Asl antibodies do not bind to new centrioles in the injected region; this suggests that these centrioles fail to recruit Asl because the anti-Asl antibodies block the cytoplasmic Asl molecules in their vicinity. Although Asl-negative centrioles are not decorated with any antibody, they fail to recruit DSas-4-GFP and assemble a daughter centriole. This suggests that the presence of Asl around mother centrioles is essential for daughter centriole formation.

antibodies) duplicated successfully during consecutive cell cycles (Figure 4.8A). In contrast, Asl-negative centrosomes (that were not detectably bound by antibody) could not be seen splitting into two at the end of the cell cycle (Figure 4.8B), suggesting that these centrosomes are unable to duplicate. I noticed, however, that Asl-negative centrosomes appeared defective in their movement, presumably because they lacked PCM in the absence of Asl. I therefore decided to use an additional assay, one that is not affected by defective centrosome separation, to confirm that Asl-negative centrosomes cannot duplicate. For this reason I compared the recruitment of DSas-4-GFP, as a centriole marker that is incorporated into growing daughter centrioles, at Asl-positive and Asl-negative centrosomes during *S*-phase. Asl-positive centrosomes (that were heavily decorated by anti-Asl antibodies) recruited high levels of DSas-4-GFP during *S*-phase (Figure 4.9A,B), in line with the successful duplication of these centrosomes. In contrast, Asl-negative centrosomes (that were not detectably bound antibody) did not recruit DSas-4-GFP during *S*-phase at all (Figure 4.9A,B). As DSas-4-GFP is essential for centriole formation, that absence of its recruitment to Asl-negative centrosomes strongly suggests that the parental centrioles in these centrosomes are unable to assemble daughters (Figure 4.9C). These results strongly support that Asl incorporation is required to convert newly assembled, disengaged daughter centrioles into mother centrioles that can duplicate.

A previous study had shown that Asl is required for the recruitment of Sak/Plk4 to centrosomes (Dzhindzhev et al. 2010), which suggests that the most likely reason why Asl-negative centrosomes are unable to duplicate is because they fail to load Sak/Plk4 to catalyze procentriole assembly. To test this model, I decided to assess whether inhibiting the Sak-interacting region of centrosomal Asl molecules would abolish DSas-4-GFP recruitment to these centrosomes in a similar way as the complete absence of centrosomal Asl does. I used an antibody that had been raised against the N-terminal region of Asl that had been mapped to interact with Sak (based on Conduit et al. 2010 and Dzhindzhev et al. 2010) to immuno-inhibit the Asl-Sak interaction, and, similarly as in my earlier experiment, I aimed to compare DSas-4-GFP incorporation during *S*-phase at anti–Asl(N) bound (presumably no Sak recruitment) or unbound (control) centrosomes. Unfortunately, unlike the

previously used two antibodies, this Texas Red–coupled anti–Asl(N) antibody readily aggregated when injected into embryos (data not shown), making it impossible to accurately analyze this experiment. Therefore, so far, I could not confirm that DSas-4 is indeed recruited to forming centrioles as a consequence of Sak activity, rather than the mere presence of Asl at the mother centriole. Nonetheless, my previous results indicate that immobile Asl molecules surrounding mother centrioles recruit DSas-4 to daughter centrioles indirectly; therefore the intermediary role of Sak/Plk4 remains a very likely possibility.

4.3 DISCUSSION

4.3.1 THE MOLECULAR PATHWAYS OF ASL RECRUITMENT TO CENTROSOMES

In this chapter I have shown that the initial recruitment Asl to new centrioles is abolished when the DSas-4–Asl interaction region is blocked with antibodies raised against either of the two proteins. The anti-DSas-4 antibodies bound to centrosomes and prevented Asl recruitment, while the anti-Asl antibodies achieved the same effect without binding to centrosomes (presumably by binding to Asl in the cytoplasm). This strongly suggests that the inhibiting antibodies act by interfering with the DSas-4–Asl interaction, rather than through a general, steric effect at centrosomes. DSas-4 and Asl are known to interact directly *in vitro* (Dzhindzhev et al. 2010). I conclude, therefore, that Asl is initially recruited to new centrioles by DSas-4, possibly through a direct molecular interaction.

Interestingly, however, DSas-4 does not appear to play a direct role in recruiting the mobile fraction of Asl to centrioles, as anti-DSas-4 antibodies do not detectably interfere with the turnover of Asl at old centrioles (Figure 4.5). Instead, the recruitment of mobile Asl molecules appears to be driven through a self-interaction with the immobile Asl molecules that have already been incorporated into centrioles by DSas-4, as anti-Asl antibodies strongly block the turnover of Asl at

old centrioles (Figure 4.6). This "two step" recruitment mechanism provides a simple explanation for the 50:50 ratio of mobile and immobile Asl.

Although fixed and mobile Asl molecules appear to be anchored at centrosomes in a fundamentally different manner, their sub-centrosomal localization is indistinguishable by 3D-SIM super-resolution microscopy. A recent study has shown that Asl forms a monolayer around centrioles, in which its molecular orientation is strictly unidirectional (Mennella et al. 2012). This data can only be explained if the two behaviourally distinct pools of Asl occupy essentially the same space, instead of forming concentric rings, around centrioles (Figure 4.7). In addition, yeast two-hybrid data suggests that Asl molecules interact with each other in a parallel orientation (Dr. Jennifer Richens, personal communication), which supports the model that mobile Asl molecules might 'wedge between' DSas-4–bound immobile Asl molecules. These results reveal that the composition of the ring of Asl that surrounds mother centrioles is more complex than previously suspected: it is formed by two distinct pools of Asl molecules that are anchored at centrioles in a different way and have different dynamic behaviours.

Previous studies have suggested that there may be important differences in how DSas-4/CPAP and Asl/Cep152 proteins are recruited to centrioles in flies and in vertebrates (Cizmecioglu et al. 2010; Dzhindzhev et al. 2010). I think it possible, however, that my model of Asl recruitment to centrioles in flies may provide insight into the centriolar recruitment of vertebrate Cep152. I summarize below the current data on the centrosomal recruitment of Cep152 and discuss how my *Drosophila* data might alter the interpretation of previous results.

Several recent studies have demonstrated that, in vertebrates, the centrosomal localization of Cep152 is strongly dependent on Cep63 (Sir et al. 2011; Brown et al. 2013; Lukinavicius et al. 2013). Importantly, however, all of these studies only assessed the overall levels of Cep152 at centrosomes, without addressing its initial recruitment versus its maintenance. All three studies agreed that Cep63 and Cep152 were inter-dependent for their centrosomal localization; the two

proteins appear to interact in the cytoplasm and are recruited to centrosomes as a complex (Sir et al. 2011; Brown et al. 2013; Lukinavicius et al. 2013). This is supported by the direct molecular interaction of Cep63 and Cep152 (Brown et al. 2013; Lukinavicius et al. 2013), and by their identical incorporation timing and sub-centrosomal localization (Sir et al. 2011; Lukinavicius et al. 2013).

The C-terminal part of Cep152, which interacts with Cep63 (Brown et al. 2013), is sufficient for its centrosomal localization (Cizmecioglu et al. 2010; Hatch et al. 2010; Brown et al. 2013). In contrast, the centrosomal localization of Cep63 seems to depend on the opposite end of the protein than the region that binds Cep152, suggesting that the Cep63-Cep152 complex must be anchored through the binding of Cep63 at centrioles (Brown et al. 2013). Interestingly, however, the absence of Cep63 appears to disrupt Cep152 localization less severely in interphase (when new parental centrioles are acquiring their Cep152 pool) than during mitosis (when new parental centrioles have already acquired Cep152) (Sir et al. 2011). Furthermore, Cep63 knockout cells can amplify their centrioles during an *S*-phase arrest similarly to wild type cells (Sir et al. 2011), while Cep152 depletion significantly reduces centriole amplification (Cizmecioglu et al. 2010; Dzhindzhev et al. 2010). Even more puzzlingly, the requirement for Cep63 in normal centriole duplication shows a strong correlation with cell cycle length; rapidly cycling cells often fail to duplicate their centrioles in the absence of Cep63, while cell types that have longer doubling times do not appear to have such problems (Sir et al. 2011). Cep152, in contrast, is crucial for centriole duplication in every vertebrate cell type that has been analyzed to date (Blachon et al. 2008; Cizmecioglu et al. 2010; Dzhindzhev et al. 2010; Hatch et al. 2010; Kim et al. 2013; Sonnen et al. 2013). Collectively, these results suggest that Cep63 may not be essential for Cep152 recruitment to centrioles, but most likely enhances the efficiency of its recruitment and/or has an essential role in maintaining it there (Sir et al. 2011; Brown et al. 2013).

Is it possible that the key initial recruiter of Cep152 in vertebrates is actually CPAP (the DSas-4 homologue)? Importantly, the C-terminal region of Cep152 – that is responsible for its localization

to centrioles (Cizmecioglu et al. 2010; Hatch et al. 2010; Brown et al. 2013) – has been shown to interact with *both* CPAP and Cep63 (Cizmecioglu et al. 2010; Dzhindzhev et al. 2010; Brown et al. 2013). Perhaps then the attention on the Cep63–Cep152 interaction has distracted from a potential role of CPAP in Cep152 recruitment?

It is clear that in vertebrates the Cep152 molecules coating *mother* centrioles are important for the recruitment of CPAP to *forming procentrioles* (Cizmecioglu et al. 2010; Dzhindzhev et al. 2010) — leading to the idea that Cep152 recruits CPAP, although Cep152 may not necessarily have a direct role in this process (I will discuss this point in section 4.3.2). Importantly, however, the functional relationship between these two proteins has never been addressed within the *same centriole*. I think it possible, therefore, that, as in *Drosophila*, the CPAP-Cep152 interaction may initiate the recruitment of Cep152 at newly disengaged daughter centrioles. However, I suspect that a difference between fly and vertebrate centrioles may be making this harder to discern: while *Drosophila* centrioles permanently maintain their core cartwheel structure, vertebrate centrioles loose their cartwheel shortly after their assembly. As I discuss below, this difference may have influenced the current models that suggest that Asl/Cep152 recruitment has diverged through evolution between flies and humans.

Although the previous studies that addressed the functional relationship between CPAP and Cep152 focused on procentriole assembly, it can be clearly inferred from these data that it is not only CPAP recruitment to the procentriole that is affected upon Cep152 depletion; CPAP is also missing from the pre-existing mother centriole in these centrosomes (Cizmecioglu et al. 2010; Dzhindzhev et al. 2010). Strikingly, however, CPAP is also weak or absent from the centrosomes in a significant proportion of normal cells in asynchronous cultures (see, for example, Figure 4d in Dzhindzhev et al. 2010, or Figure 5A in Cizmecioglu et al. 2010)—although this was not commented on. While so far no study has precisely addressed the centriolar localization of CPAP during the cell cycle, I think that the data presented in Dzhindzhev et al. 2010 Figure 4d and Cizmecioglu et al. 2010 Figure 5A might suggest that, in contrast to *Drosophila* centrioles, human

parental centrioles may naturally lose CPAP. In line with this hypothesis, CPAP is degraded during late mitosis in an APC/C-Cdh1–dependent manner (Tang et al. 2009) – exactly as the centriolar cartwheel components HsSas-6 (Strnad et al. 2007) and STIL (Arquint and Nigg 2014), which are known to be removed from fully-grown daughter centrioles during mitosis, prior to their cytoplasmic degradation (Arquint and Nigg 2014). A natural loss of centriolar CPAP could have easily confounded our understanding of the recruitment dependencies of CPAP and Cep152, which is based entirely on experiments where protein recruitment and maintenance were assessed in combination, not individually. Perhaps CPAP initiates the centriolar recruitment of Cep152, but it is later removed from the centriole and the localization of Cep152 then becomes entirely dependent on Cep63. It remains to be addressed whether this potential model could be true; however I feel it cannot be ruled out based on currently available data.

4.3.2 ASL INCORPORATION LICENSES DISENGAGED DAUGHTER CENTRIOLES TO DUPLICATE FOR THE FIRST TIME

Although Asl is one of the few proteins that are essential for centriole duplication in flies (Blachon et al. 2008; Dzhindzhev et al. 2010), my results presented in Chapter 3 indicated that it is unlikely to be an integral component of centrioles, as it is not incorporated into these during their assembly. Here I have answered this puzzle by showing that the presence or absence of Asl at centrioles in fact plays a previously unexpected regulatory role in their duplication. But how can Asl, a protein possessing no known enzymatic activity, act in regulating centriole duplication? My data indicates that Asl acts as a duplication license: its presence is necessary, although in itself not sufficient, for the initiation of centriole duplication. I now explain how this discovery has changed the prevailing model of centriole duplication licensing.

Several earlier studies have shown that the engagement status of centrioles determines their duplicating ability (Tsou and Stearns 2006b; Loncarek et al. 2008). It was apparent in these and other studies, however, that the regulation of duplication was not identical at mother and daughter

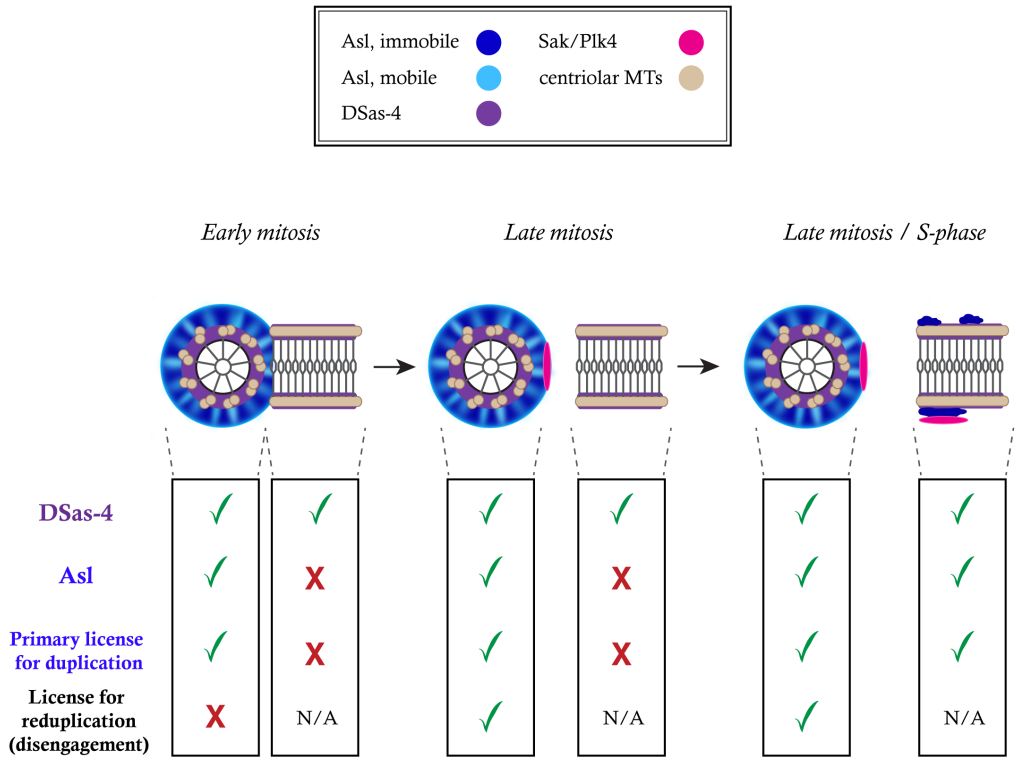


Figure 4.10. A dual licensing model for centriole duplication in *Drosophila*.

The schematic diagrams illustrate a centriole pair, with mother in end-on view (left) and daughter in side-on view (right), as they pass through mitosis. The table below illustrates the state of each centriole in terms of DSas-4 incorporation, Asl incorporation, and whether the centriole has a primary license for its first duplication or a reduplication licence for subsequent rounds of duplication. In early mitosis, the mother centriole has incorporated immobile Asl during a previous cell cycle, which irreversibly provided it with a primary license, but it is unable to duplicate again because it lacks a reduplication license, which it will acquire when it disengages from its daughter (Loncarek et al. 2008, Tsou et al. 2009, Wang et al. 2011). The daughter centriole has incorporated DSas-4 but not Asl, and so it lacks a primary license and cannot duplicate until it disengages and matures into a mother. In late mitosis, the centrioles disengage: the mother centriole thereby acquires a reduplication license (speculatively illustrated here by a free "patch" of Sak on its side); the separated daughter centriole cannot duplicate until it starts to incorporate Asl (shown here occurring in late mitosis/*S*-phase), which allows it to recruit Sak for the first time.

centrioles: experimental conditions that could over-ride the need for disengagement allowed mother centrioles to re-duplicate, but not daughters (Kleylein-Sohn et al. 2007; Loncarek et al. 2008; Cunha-Ferreira et al. 2009). It was recently suggested that new centrioles must acquire a permanent, Plk1-dependent 'modification' during their first mitosis to allow their subsequent duplication (Wang et al. 2011). However, the nature of this modification remained a mystery. The essential role of Asl in *Drosophila* centriole duplication, its surprising absence in fully-grown daughter centrioles and it permanent presence at parental centrioles suggested to me that, at least in *Drosophila*, Asl might be this proposed 'modification' that new centrioles must acquire for their subsequent duplication. The results I have presented in this chapter confirm that this is true: disengaged new centrioles that do not incorporate Asl fail to enter the centriole duplication cycle. The stable nature of initial Asl incorporation means that, once acquired, centrioles no longer require Asl recruitment prior to further duplication events.

In light of my results, I propose a "dual licensing" model (Figure 4.10) that explains how both old and new centrioles are licensed for subsequent duplication in *Drosophila*. Incorporation of the immobile Asl pool represents the primary license that allows new centrioles to duplicate for the first time, while centriole disengagement provides a re-duplication license that allows older centrioles to duplicate again (Figure 4.10). These two licenses in fact act together to form a layered regulation mechanism. The primary Asl license that is acquired before the first round of duplication is not lost and remains essential for later duplication events, but it is permanent and no longer subject to regulation. The regulation in subsequent rounds of duplication is taken over by re-duplication licensing, which depends on centriole disengagement. As the molecular role of Asl reveals, the primary license provides centrioles the ability to recruit Sak/Plk4 to the centriole wall (Dzhindzhev et al. 2010) to catalyze procentriole assembly. It will be crucial to determine how centriole disengagement allows subsequent rounds of Sak/Plk4 recruitment.

Could this model also apply to vertebrate cells? Although Asl is essential for centriole duplication in flies, in vertebrates Cep152 is important, but not essential (Blachon et al. 2008; Dzhindzhev et

al. 2010; Kim et al. 2013; Sonnen et al. 2013). Recently it has been shown that, unlike *Drosophila* DSpd-2, vertebrate Cep192 can also interact with Plk4, and so Cep152 and Cep192 seem to share the role of recruiting Plk4 (Kim et al. 2013; Sonnen et al. 2013). It is possible, therefore, that a similar mechanism as the one I described in flies could regulate the primary licensing of centrioles in higher animals too, with the difference that two proteins co-operate to fulfil the role of Asl in vertebrate cells.

How does Asl promote the duplication of mother centrioles? Previous studies have concluded that Asl/Cep152 somehow 'scaffolds' the association of Sak/Plk4 and DSas-4/CPAP to promote the onset of daughter centriole assembly. The evidence that Asl/Cep152 recruits Sak/Plk4 to centriole to promote centriole duplication is strong: it is clear that Sak/Plk4 and Asl/Cep152 interact directly *in vitro*, (Cizmecioglu et al. 2010; Dzhindzhev et al. 2010; Hatch et al. 2010), and multiple experiments solidly support that Asl/Cep152 recruits Sak/Plk4 through a direct molecular interaction to duplicating centrioles *in vivo* (Cizmecioglu et al. 2010; Dzhindzhev et al. 2010; Hatch et al. 2010; Kim et al. 2013; Sonnen et al. 2013). Asl/Cep152 also interacts with DSas-4/CPAP directly *in vitro* (Dzhindzhev et al. 2010), but the role of this interaction has been less well defined and seems to vary between flies and vertebrates (Dzhindzhev et al. 2010). Some studies have found that these proteins form cytoplasmic complexes (Cizmecioglu et al. 2010; Dzhindzhev et al. 2010; Gopalakrishnan et al. 2011), although my own data from fly embryo extracts do not support this latter point (see Chapter 5). It is also clear that Asl/Cep152 has a key role in the recruitment of DSas-4/CPAP to forming procentrioles. Unlike the case for Sak/Plk4, however, the *in vivo* recruitment assays performed so far have not addressed whether this recruitment is mediated by the direct interaction of the two proteins (Cizmecioglu et al. 2010; Dzhindzhev et al. 2010). My results show that blocking the DSas-4–interacting region of centrosomal Asl does not affect the recruitment of DSas-4 to the forming daughter centriole, and these blocked centrosomes duplicate normally. Crucially, inhibition of the very same region can prevent the incorporation of Asl at new mother centrioles. Together these data strongly suggest that the DSas-4–Asl interaction more likely mediates the recruitment of Asl to new mother centrioles, rather than the recruitment of

DSas-4 to the procentriole. Based on my results and recent studies by others (Cizmecioglu et al. 2010; Dzhindzhev et al. 2010; Hatch et al. 2010), I speculate that the role of Asl in centriole duplication is to recruit Sak/Plk4 to mother centrioles. The requirement for Asl for the recruitment of all the other duplication proteins is most likely an indirect effect through this role.

Interestingly, my results show that only the immobile pool of Asl is essential for centriole duplication, as abolishing Asl turnover at mother centrioles did not affect daughter centriole formation. It is currently unclear whether the mobile and immobile Asl pools have strictly separate functions at centrosomes: it is possible that immobile Asl molecules function in centriole duplication, while mobile Asl molecules are required for the dynamic regulation of PCM recruitment. Alternatively, the immobile Asl pool could be simply sufficient to promote duplication in the absence of the mobile Asl pool (as only a small fraction of the total Asl pool is sufficient to drive centriole duplication — see Chapter 3). Nonetheless, my data shows that once centrioles have incorporated immobile Asl, their future duplication no longer requires further Asl recruitment. Thus, the initial incorporation of Asl has a permanent effect on the duplication potential of a centriole.

Identification of Asl as the primary license required for the duplication of newly assembled centrioles raised some important further questions. First, do daughter centrioles also require disengagement in addition to Asl recruitment to allow their first round of duplication? Second, is the absence of Asl at engaged daughter centrioles important to avoid the formation of granddaughter centrioles, and therefore prevent centriole amplification? Finally, how is Asl incorporation regulated so that it only occurs around the time when fully-grown daughter centrioles separate from their mother? The first of these questions seems hard to address as the primary and re-duplication licensing steps appear to be regulated very similarly; in human cells both are dependent on Plk1 (Loncarek et al. 2010; Wang et al. 2011), suggesting that they are also likely to be co-regulated by Polo in flies. I address the second two questions in the following chapter to understand whether the specific timing of Asl incorporation has an important role in restraining the

over-duplication of centrioles, or whether it is simply a beneficial consequence of a different process that is unrelated to the regulation of centriole duplication.

CHAPTER 5:

INVESTIGATING THE MOLECULAR REGULATION OF ASL INCORPORATION AT NEWLY DISENGAGED CENTRIOLES

5.1 SUMMARY

I have shown that the recruitment of Asl to daughter centrioles as they disengage from their mothers is crucial for allowing the daughters to enter the duplication cycle for the first time. The initial incorporation of Asl is dependent on centriolar DSas-4, which I have shown is present within newly assembling centrioles nearly a whole cell cycle before it starts to recruit Asl. This suggests that the interaction of these two molecules must be carefully regulated during the cell cycle, and my next aim was to understand how.

The incorporation of Asl appears to be regulated in a switch-like manner (Figure 5.1B). Once initiated, Asl incorporation into the new mothers progresses steadily at all stages of the cell cycle, until the final centriolar levels of Asl are reached (Figure 3.11). Furthermore, the mobile Asl pool at old mother centrioles appears to continuously turn over throughout the cell cycle (Figure 3.14). Together these data suggest that the levels of cytoplasmic Asl are not limiting the incorporation into engaged daughter centrioles, as mother centrioles are constantly recruiting Asl while new procentrioles are not. Thus, it appears that cytoplasmic Asl and procentriolar DSas-4 cannot interact until the newly assembled centrioles progress in to a late mitotic environment (Figure 5.1B). These findings strongly suggested that the DSas-4–Asl interaction must be tightly regulated, possibly through the cell cycle–dependent post-translational modification of one or both proteins.

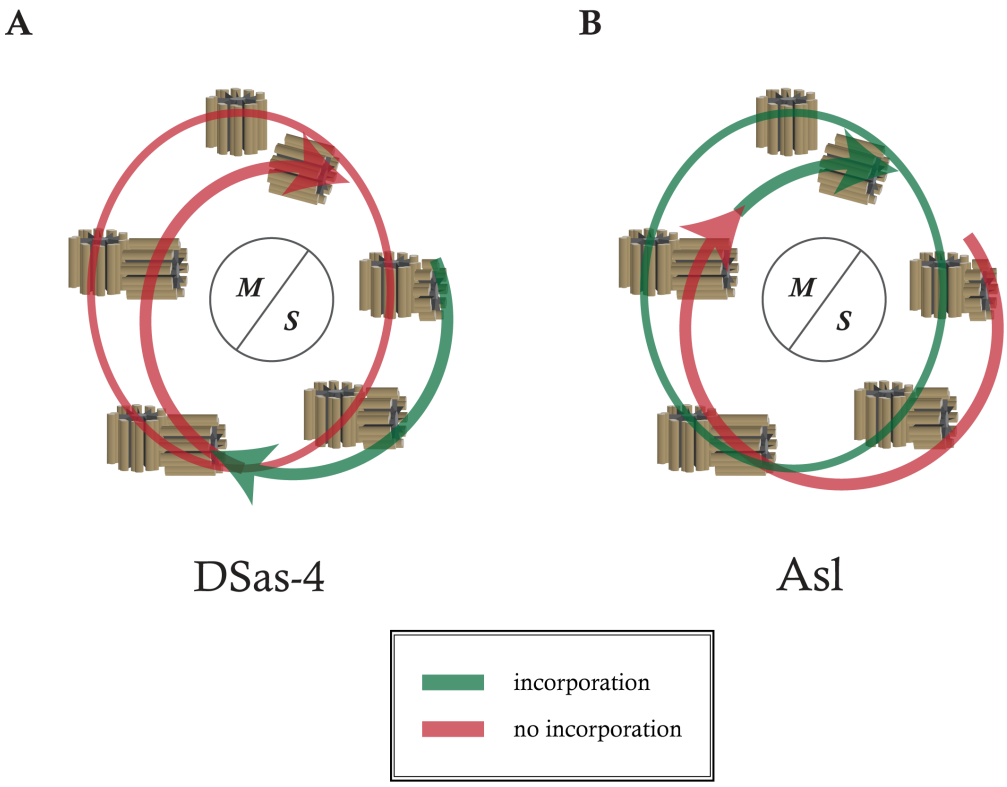


Figure 5.1 Comparison of the centriolar incorporation timings of DSas-4 and Asl during the cell cycle.

(A, B) Schematics illustrate the periods of the cell cycle when DSas-4 (A) or Asl (B) are recruited to duplicating centrioles (*green* arrows/ring) and the periods when they are not able to incorporate at centrioles (*red* arrows/ring). Arrows represent incorporation at daughter centrioles, while continuous rings represent mother centrioles. Note the reverse behaviour of DSas-4 and Asl during the centriole cycle; this suggests that the form of DSas-4 that is efficiently incorporated into growing daughter centrioles may not be able to interact with cytoplasmic Asl.

The centrosomal recruitment of DSas-4 also appears to be regulated during the cell cycle, but in a very different way to Asl. Excessive levels of DSas-4 are recruited to growing daughter centrioles during *S*-phase, while no recruitment takes place during mitosis, when the surplus DSas-4 recruited during *S*-phase is lost. This suggests that during *S*-phase cytoplasmic DSas-4 molecules are in a state that allows their efficient recruitment to the centrosomes, however, upon entry into mitosis, either DSas-4 is converted into a form that can no longer be recruited to centrioles, or the centriolar binding sites of DSas-4 are converted to a form that can no longer interact with the protein, or both (Figure 5.1A).

Interestingly, a cell cycle dependent modification that regulates CPAP behaviour has recently been described in human cells (Chang et al. 2010; summarized in Figure 1.8). According to this study, CPAP is phosphorylated by Plk2 prior to *S*-phase entry, and this modification is critical for procentriole assembly. Phosphorylated CPAP was found preferentially within the procentrioles, but not the parental centrioles, throughout the cell cycle until mid-mitosis. Intriguingly, CPAP within new centrioles was rapidly de-phosphorylated during the metaphase-anaphase transition, which was accompanied by a significant loss of CPAP from the centrosomes. I found these data very interesting and I wondered whether a similar mechanism might exist in flies. If so, perhaps DSas-4 can be incorporated into centrioles only when it is phosphorylated in *S*-phase, but can then only recruit Asl once it has been dephosphorylated towards the end of mitosis.

In this chapter I first investigate the cytoplasmic binding efficiency of DSas-4 and Asl and show that they do not appear to form cytoplasmic complexes efficiently *in vivo*. Next, I show that moderate overexpression of Asl-GFP can mis-regulate the control mechanism that governs the timing of its initial incorporation at centrioles to promote its early incorporation. Finally, I investigate the potential role of cell cycle –dependent phosphorylation in regulating the interaction between DSas-4 and Asl. I show that the phosphorylation mechanism that regulates CPAP behaviour in humans (Chang et al. 2010) does not appear to be conserved in flies; however, I

identify a small region of DSas-4 that may be regulated by phosphorylation and that appears to play a crucial part in promoting the initial incorporation of Asl at new centrioles.

5.2 RESULTS

5.2.1 DSAS-4 AND ASL DO NOT EFFICIENTLY FORM COMPLEXES IN THE CYTOPLASM

To understand how the molecular interaction between DSas-4 and Asl might be regulated, I first tested whether these proteins can form a complex with each other in the cytoplasm. I immuno-precipitated either Asl-GFP or DSas-4-GFP (each expressed from the endogenous promoter of the respective protein) from embryonic extracts and tested whether they co-precipitated with endogenous DSas-4 or Asl, respectively (Figure 5.2A,B). An anti-GFP antibody successfully captured both Asl-GFP (Figure 5.2C, top panels) and DSas-4-GFP (Figure 5.2D, top panels). I found that I could not co-precipitate significant levels of DSas-4 following the pulldown of Asl-GFP (Figure 5.2C, bottom panels). Although a weak DSas-4 band could be detected in the precipitate, a similar band was present in the control lane (Figure 5.2C, bottom panels). The reciprocal experiment gave a similar result as Asl was not detectably enriched in DSas-4-GFP immuno-precipitates (Figure 5.2D, bottom panels). Finally, I also attempted co-precipitation of DSas-4 with endogenous Asl, using an N-terminal Asl antibody (that targets a region far from the DSas-4–interacting domain). Again, I could not detect an interaction between the two proteins using this approach (data not shown). Thus, DSas-4 and Asl do not detectably interact in the cytoplasm *in vivo*; therefore their interaction appears to be not only temporally, but also spatially regulated, to ensure these molecules only efficiently interact at centrioles.

In contrast to my results, a previous study had reported that DSas-4 and Asl do form cytoplasmic complexes *in vivo* (Gopalakrishnan et al. 2011). A potential reason for this difference could be the extensive washing of the immuno-precipitated complexes in my experiments. I do not think this

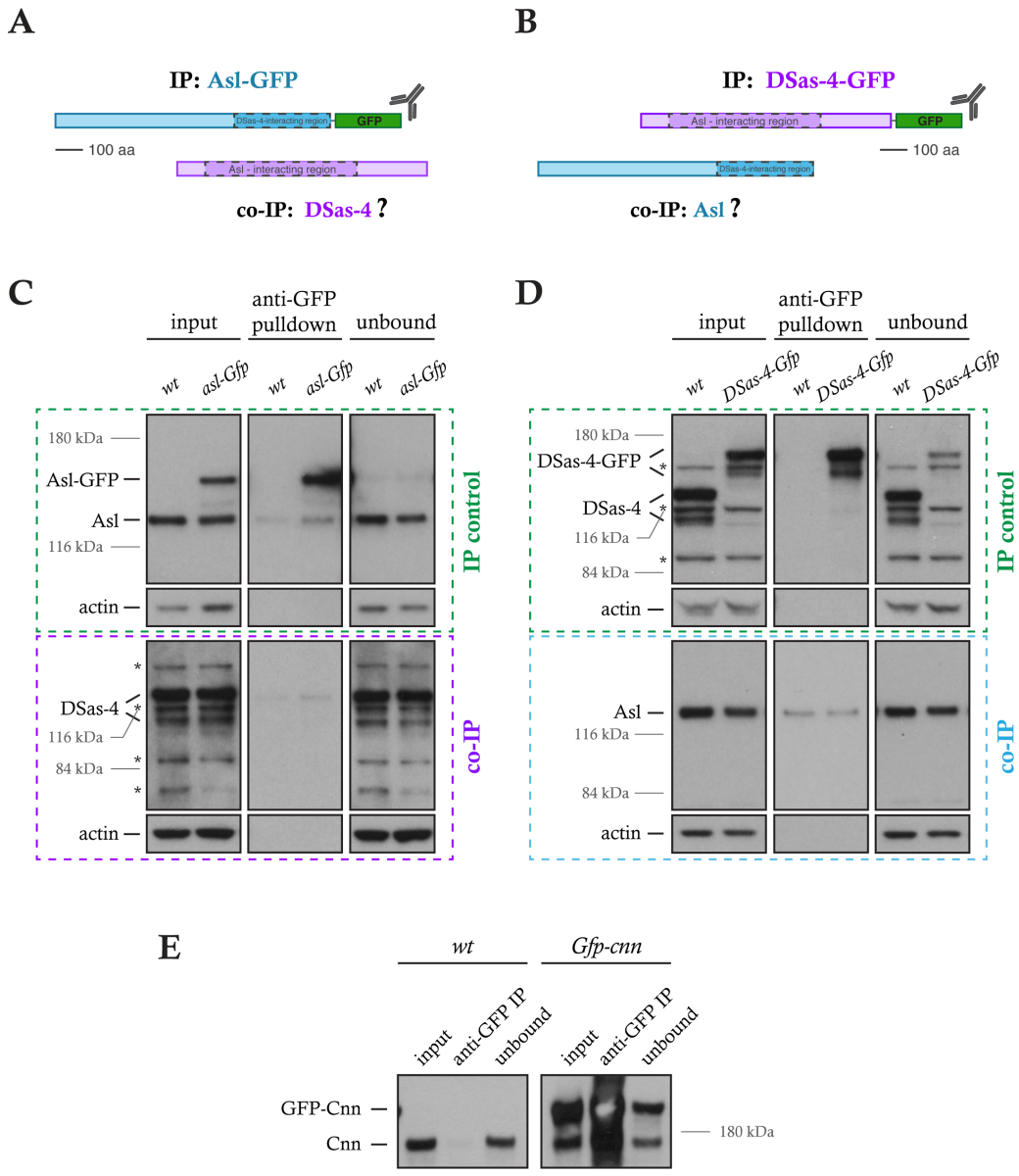


Figure 5.2 DSas-4 and Asl molecules do not interact readily in the cytoplasm, suggesting that their interaction is regulated at centrioles.

(A, B) Schematics illustrate the reciprocal co-immunoprecipitation approach used to assay the cytoplasmic interaction of DSas-4 and Asl. Asl-GFP (A) or DSas-4-GFP (B) were captured from embryonic cytoplasm extracts using anti-GFP antibodies. The co-precipitation of endogenous DSas-4 (A) or Asl (B) was then assayed. (C, D) Western blots of the reciprocal co-immuno precipitation experiments: the upper panels (*green* border; IP control) confirm the successful pulldown of Asl-GFP (C) or DSas-4-GFP (D); the lower panels (*purple/blue* border; co-IP) probe for the co-precipitation of DSas-4 (C) and Asl (D), respectively. Wild type embryos were used as a control. Note that neither DSas-4 (C) nor Asl (D) can be detected above the background signal from control embryos when these proteins are co-precipitated with Asl-GFP or DSas-4-GFP, respectively. (E) Western blots show the co-immunoprecipitation of endogenous Cnn with GFP-Cnn (positive control), in line with its recently suggested cytoplasmic dimerization (Conduit et al. 2014a).

likely, for two reasons. First, using the same immuno-precipitation protocol I could show co-precipitation of Cnn with GFP-Cnn (Figure 5.2E), in agreement with its recently suggested cytoplasmic dimerization (Conduit et al. 2014a). Second, my experiments show that while Asl-GFP and DSas-4-GFP are strongly depleted from the cytoplasm extracts as a result of their immunoprecipitation (Figure 5.2C,D top panels; compare input and unbound samples), the levels of DSas-4 (Figure 5.2C, bottom panels) and Asl (Figure 5.2D, bottom panels) are similar in input and unbound samples, supporting the conclusion that these endogenous proteins were not significantly co-precipitated with the GFP-fusion proteins.

Interestingly, I could weakly detect some co-precipitation of endogenous Asl with Asl-GFP (Figure 5.2C, top panels). Although the enrichment of endogenous Asl in these GFP pulldowns was weak, it was reproducible over several repeat experiments. Thus, Asl self-interaction, which appears to drive later steps of centrosomal Asl recruitment, does appear to occur, albeit weakly, in the cytoplasm. In conclusion, the combination of my live imaging and immuno-precipitation data suggest that the temporal and spatial control of the DSas-4–Asl interaction is the main mechanism that regulates the centriolar incorporation of Asl.

5.2.2 Moderate overexpression of Asl-GFP can drive its early incorporation at engaged daughter centrioles

During the early stages of my project I also tested the dynamic centrosomal incorporation of Asl-GFP when it was moderately overexpressed in embryos. For these experiments the expression of Asl-GFP was driven by the polyubiquitin promoter (Dobbelaere et al. 2008); this led to ~4-fold overexpression of Asl-GFP relative to endogenous Asl (Figure 5.3A). I noticed that this overexpression seemed to affect the centriole recruitment of Asl-GFP, which was now much less asymmetrically localized on newly separated old and new centrosomes (Figure 5.3B, 5.4A). In most centrosome pairs the older centrosome still contained more Asl-GFP than the new one, but in a small percentage of centrosome pairs this correlation was actually reversed (Figure 5.3B). The

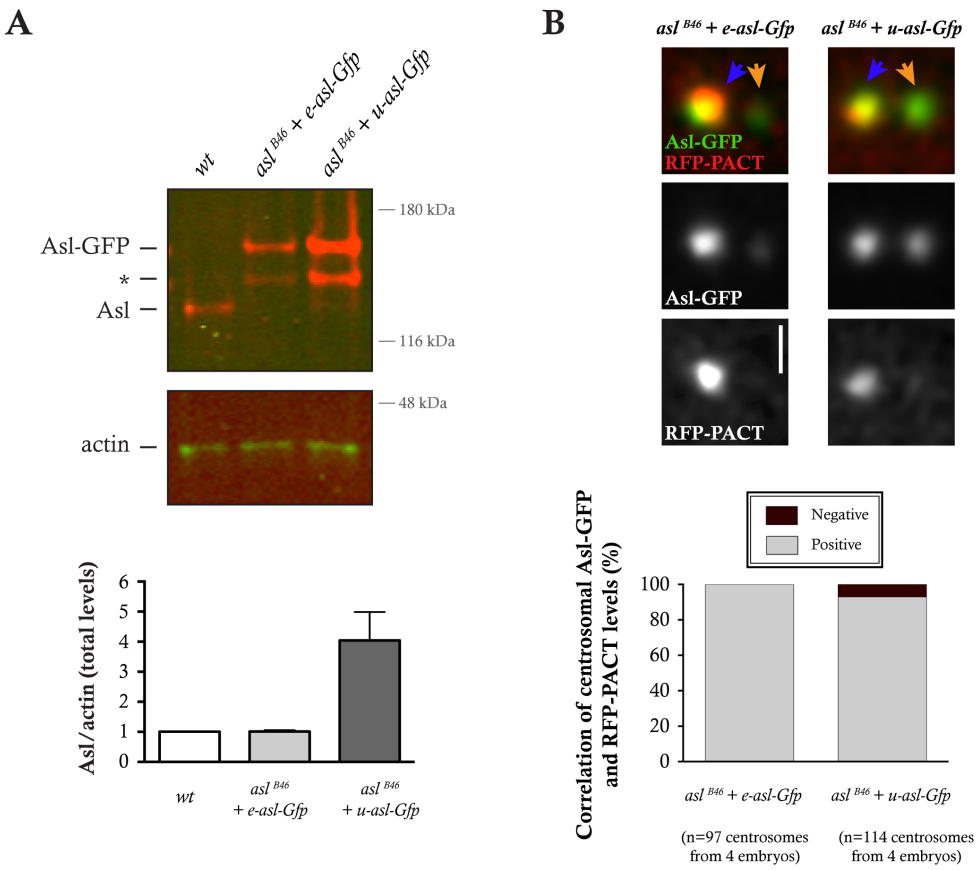


Figure 5.3 Overexpression of Asl-GFP leads to its more symmetric distribution at old and new centrosomes during early *S*-phase.

(A) Western blot shows the levels of endogenous Asl (lane 1), Asl-GFP expressed from its endogenous promoter in a mutant background (*asl^{B46}+e-asl-Gfp*, lane 2) and Asl-GFP expressed from the poly-ubiquitin promoter in a mutant background (*asl^{B46}+u-asl-Gfp*, lane 3). Note that these blots are analysed on a LICOR Odyssey system so that their intensity can be more accurately quantified. The quantification of the ratio of Asl to actin in each lane is shown below the actin loading control. Asl-GFP driven from the ubiquitin promoter is overexpressed by ~4-fold (3 technical repeats were performed). (B) Fluorescence images show the levels of Asl-GFP (*green*) and RFP-PACT (*red*) at old (*blue* arrows) and new (*orange* arrows) centrosomes during early *S*-phase in *asl^{B46}+e-asl-Gfp* (left) and *asl^{B46}+u-asl-Gfp* embryos (right). Note how the levels of Asl-GFP are much more symmetric between the two centrosomes when the fusion protein is overexpressed in the cytoplasm. Graph shows that when Asl-GFP is expressed at near-physiological levels (*asl^{B46}+e-asl-Gfp*) the older centrosome contains more Asl-GFP than the younger one during *S*-phase in 100% of centrosome pairs (positive correlation between centrosomal Asl-GFP and RFP-PACT levels). When Asl-GFP is overexpressed (*asl^{B46}+u-asl-Gfp*) the young centrosome contains more Asl-GFP than the older one in a small percentage of centrosome pairs (negative correlation between centrosomal Asl-GFP and RFP-PACT levels), illustrating how strongly the asymmetry of Asl-GFP at centrosome pairs is reduced.

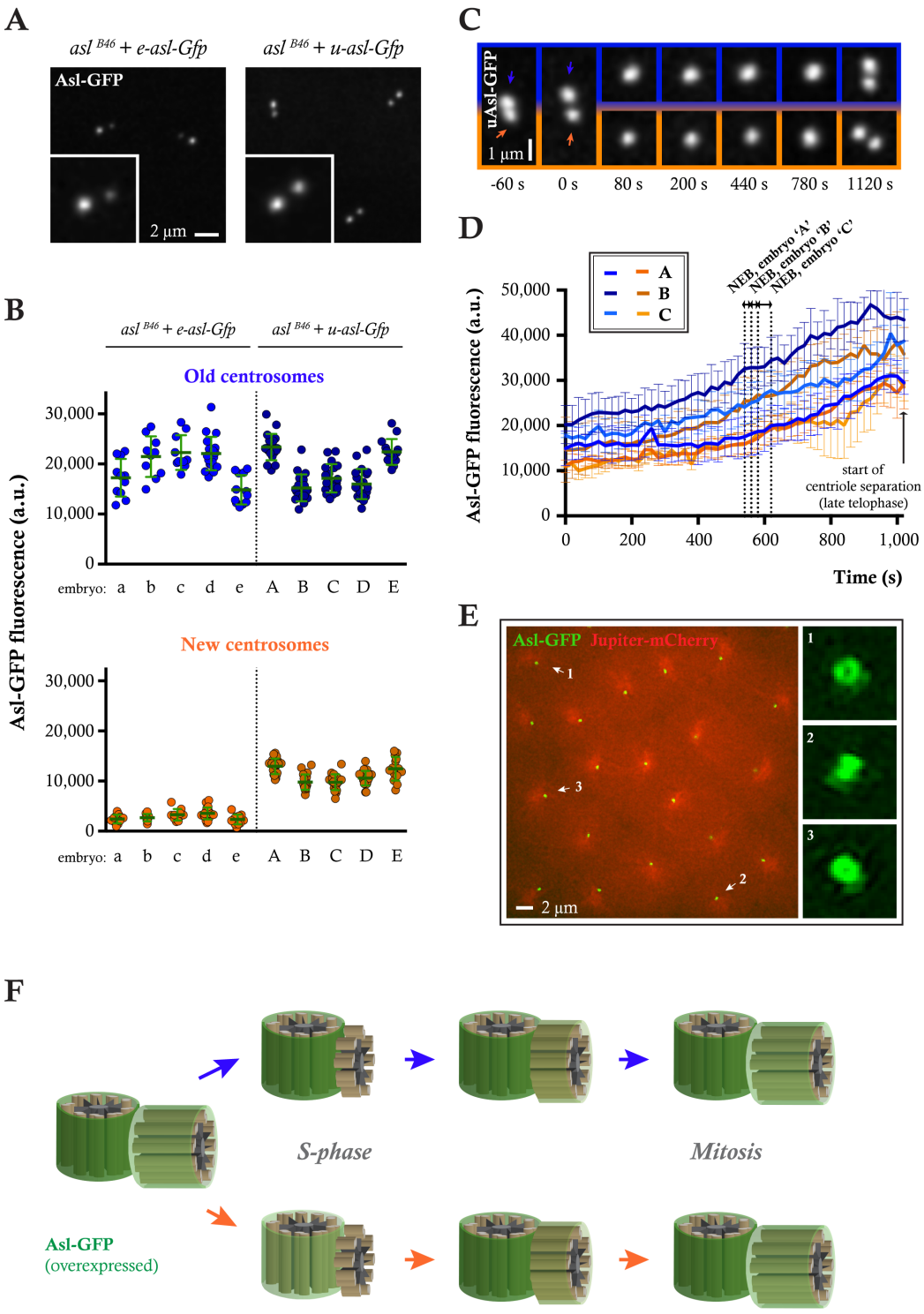


Figure 5.4 Figure legend on next page.

Figure 5.4 Overexpression of Asl-GFP can promote its early incorporation into engaged daughter centrioles.

(A) Fluorescence images show the levels of Asl-GFP (*white*) at centrosome pairs during *S*-phase in *asl^{B46}+e-asl-Gfp* (left) and *asl^{B46}+u-asl-Gfp* embryos (right). (B) Graphs show the quantification of Asl-GFP fluorescence levels in early *S*-phase at old (*blue*) or new (*orange*) centrosomes (each dot represents a single centrosome) in 5 different embryos that either express *e-asl-Gfp* (embryos a-e) or *u-asl-Gfp* (embryos A-E). Note that at old centrosomes (top panels) the centrosomal levels of Asl-GFP are approximately the same whether Asl-GFP is expressed at normal levels or is overexpressed; in new centrosomes (bottom panels) the overexpression of Asl-GFP leads to an increase in Asl-GFP levels. (C) Fluorescence images from a time-lapse movie show the incorporation of Asl-GFP into an old (*blue*) and new (*orange*) centrosome over a single cell cycle in an embryo expressing *u-asl-Gfp*. (D) The graph shows averaged centrosomal Asl-GFP fluorescence (a.u.=arbitrary units) at old (*blue*) and new (*orange*) centrosomes over a single cell cycle, from three embryos expressing *u-asl-Gfp* (>15 centrosomes in each embryo). Time relative to centriole separation (t=0 s) is indicated in both (C) and (D). Error bars: s.d. (E) Super-resolution (3D-SIM) fluorescent image shows the levels of Asl-GFP (*green*) at centrioles just before the onset of mitosis in a representative embryo expressing *u-asl-Gfp*. Jupiter-mCherry marks microtubules (and thus shows that this embryo is at the stage preceding NEB). Arrows and numbers point to centriole pairs that are shown enlarged on right. (F) A model of Asl-GFP incorporation in embryos overexpressing the fusion protein. Daughter centrioles initiate Asl-GFP incorporation while still engaged to their mother, which results in the growth of centrosomal Asl-GFP fluorescence along the cell cycle not only at new centrosomes (*orange* arrows) but also at old centrosomes (*blue* arrows). As a result of the early incorporation of Asl-GFP into engaged daughter centrioles, freshly separated old and new centrosomes contain similar levels of Asl-GFP during early *S*-phase.

decrease in Asl-GFP asymmetry was due to excessive amounts of Asl-GFP at new centrosomes as the levels of Asl-GFP at old centrosomes was not altered by Asl-GFP overexpression (Figure 5.4B).

Two possible scenarios could explain the elevated levels of overexpressed Asl-GFP at new centrosomes. First, Asl-GFP could be incorporated too early into engaged daughter centrioles; second, it could be incorporated at the correct time (when the new centrioles disengage), but too quickly. To discriminate between these possibilities, I examined the centrosomal incorporation profile of overexpressed Asl-GFP. In contrast to my observations with Asl-GFP expressed at endogenous levels (Figure 3.11), the centrosomal levels of overexpressed Asl-GFP increased gradually throughout the cycle at both new *and* old centrosomes (Figure 5.4C,D). As the overexpression of Asl-GFP did not affect its overall levels at newly separated old centrosomes (Figure 5.4B), I conclude that the surplus overexpressed Asl-GFP recruited to old centrosomes must be being incorporated too early into the engaged daughter centrioles.

To confirm this, I used live super-resolution imaging to directly visualize Asl-GFP at individual centrioles just prior to mitosis onset (when daughter centrioles are fully grown but normally have not yet initiated Asl-GFP recruitment). I found that Asl-GFP localized to daughter centrioles in several, but not all, embryos that overexpressed Asl-GFP (Figure 5.4E; compare to Figure 3.12B). In some embryos where Asl-GFP could not be detected at daughter centrioles prior to mitosis I found that it localized to these slightly later, but still before its normal time of incorporation (data not shown). These results are consistent with the quantitative incorporation data, where slight variations can be seen in the rate of Asl-GFP recruitment between different embryos (Figure 5.4D: old centrosomes in embryos B&C already recruit significant levels of Asl-GFP prior to mitotic entry, while the old centrosomes in embryo A only start to recruit Asl-GFP during mitosis). I think that the reason for this variation is that the degree of Asl-GFP overexpression appears to slightly differ between embryos (based on my quantitative Western blot analysis, Figure 5.3A). Nonetheless, the super-resolution data confirms that Asl-GFP overexpression can override the

regulation mechanism that normally ensures that Asl-GFP in only incorporated into daughter centrioles around the time when they disengage from their mothers (Figure 5.4F).

These results have important implications: if higher cytoplasmic concentrations of Asl-GFP are sufficient to drive early Asl incorporation into daughter centrioles, it is unlikely that the initial, DSas-4 dependent, incorporation of Asl is mediated by another protein that is only present at centrosomes during late mitosis. Instead, it suggests that the affinity of the DSas-4–Asl interaction that initiates Asl recruitment is likely to be regulated during the cell cycle. By increasing the likelihood of this low-efficiency interaction in *S*-phase, higher cytoplasmic levels of Asl-GFP could facilitate the early attainment of a certain "threshold" of centriolar Asl-GFP, which might then "kick start" further, more efficient, Asl incorporation (perhaps through the Asl-Asl interaction that appears to recruit the mobile fraction of Asl to centrioles).

I therefore wanted to test whether higher cytoplasmic concentrations of Asl-GFP could facilitate either of the two molecular interactions that appear to play a role in its centriolar recruitment: the Asl–DSas-4 interaction and the Asl self-interaction. I immuno-precipitated Asl-GFP from embryonic cytoplasm extracts and compared the co-precipitation of both DSas-4 and Asl between samples where Asl-GFP was expressed at endogenous or at elevated levels (Figure 5.5). The anti-GFP antibody used for immuno-precipitation captured Asl-GFP successfully (top panel, Figure 5.5B), but the overexpression of Asl-GFP did not detectably promote the formation of cytoplasmic DSas-4–Asl-GFP complexes (bottom panel, Figure 5.5B). Thus, this level of Asl-GFP overexpression cannot detectably drive the formation of DSas-4-Asl complexes in the cytoplasm; this does not rule out, however, the possibility that it could do so at the daughter centriole.

When expressed at endogenous levels, cytoplasmic Asl-GFP appeared to have a weak tendency to form complexes with endogenous Asl (Figure 5.5B top panel and Figure 5.5C). It was impossible, however, to tell conclusively whether overexpression of Asl-GFP increased this tendency. In terms of *total* levels, more endogenous Asl molecules co-precipitated with Asl-GFP when the latter was

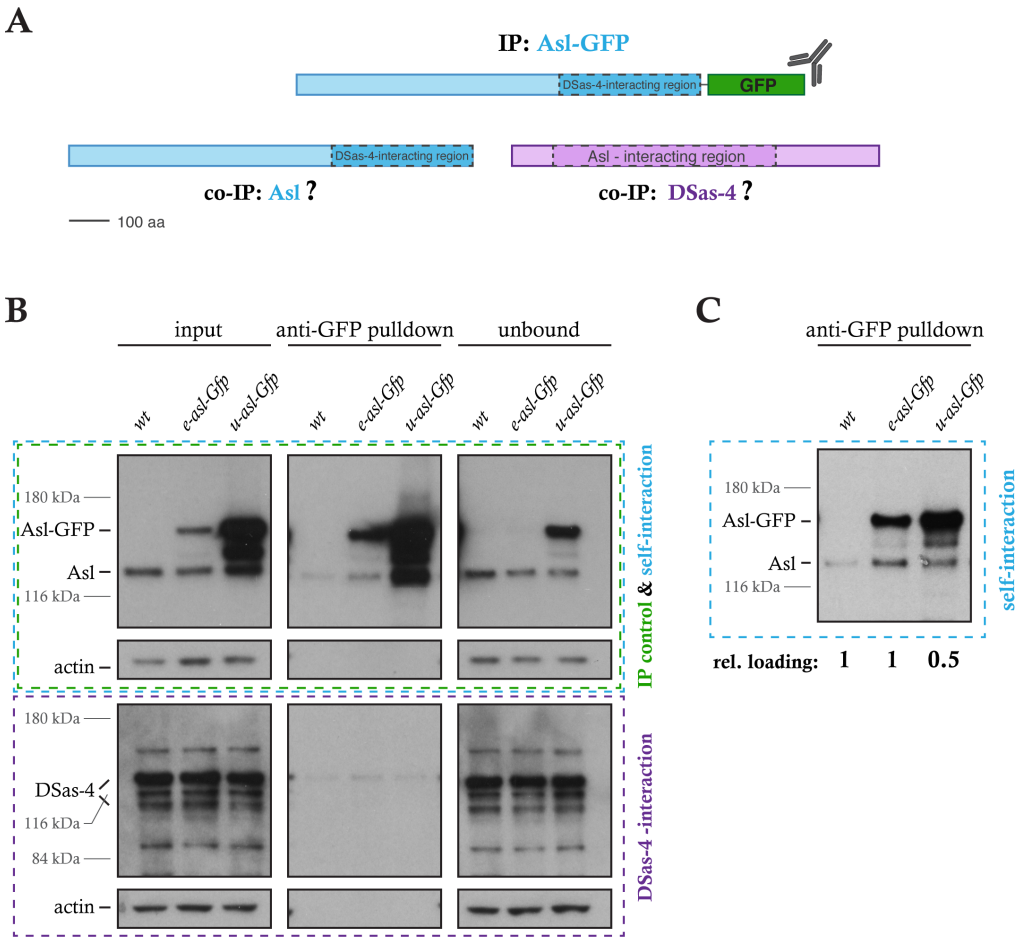


Figure 5.5 Overexpression of Asl-GFP does not promote the formation of cytoplasmic DSas-4 – Asl-GFP complexes, but appears to weakly enhance the self-interaction of Asl molecules.

(A) Schematic illustrates the immunoprecipitation approach used to assay the effect of Asl-GFP overexpression on its molecular interactions with DSas-4 and endogenous Asl (self-interaction) in the cytoplasm. Asl-GFP was immunoprecipitated from cytoplasm extracts of both *e-asl-Gfp* and *u-asl-Gfp* embryos using anti-GFP antibodies, and the co-precipitation of DSas-4 and endogenous Asl was then compared. (B) Western blot images show that anti-GFP antibodies captured Asl-GFP with high efficiency, although I could not completely deplete it from the *u-asl-Gfp* embryo extracts (top panels). Asl-GFP expressed at near-physiological levels co-precipitated with low levels of endogenous Asl, suggesting a weak self-interaction between cytoplasmic Asl molecules (top panel). Asl-GFP, when overexpressed, co-precipitated significantly more endogenous Asl, confirming that the total amount of cytoplasmic Asl complexes is elevated in these embryos (top panel – self-interaction). Overexpression of Asl-GFP did not, however, promote the co-precipitation of DSas-4 (bottom panel – DSas-4–interaction). (C) Western blot image compares the relative amount of endogenous Asl co-precipitated with Asl-GFP between *e-asl-Gfp* and *u-asl-Gfp* embryos (see text for details).

overexpressed (Figure 5.5B); in terms of *relative* levels, however, the overexpressed Asl-GFP actually precipitated less endogenous Asl (Figure 5.5C). I reasoned that this is because the overexpression of Asl-GFP will have resulted in a higher proportion of Asl-GFP-Asl-GFP complexes than Asl-GFP-Asl ones. Therefore, even if the proportion of Asl-GFP molecules engaged in self-interaction in the cytoplasm have increased as a result of overexpression, this cannot be accurately measured using this particular approach. In conclusion, overexpression of Asl-GFP did increase the total amount of cytoplasmic complexes containing multiple Asl molecules, and potentially their relative frequency as well. Thus it seems plausible that enhanced levels of self-interaction of Asl could contribute to the early incorporation of Asl-GFP into engaged daughter centrioles when its cytoplasmic concentrations are elevated.

5.2.3 Investigating the potential role of DSas-4 S300 phosphorylation in the initial recruitment of Asl to centrioles

A recent study had described a phosphorylation pattern of CPAP at human centrioles (Chang et al. 2010; summarized in Figure 1.8). According to my data, this pattern of phosphorylation has a perfect negative correlation with the centriolar presence of *Drosophila* Asterless. Chang et al. (2010) showed that Plk2 phosphorylates CPAP molecules that are incorporated into growing procentrioles at two serine residues, S589 and S595, and this modification is crucial for procentriole assembly. Interestingly, towards the end of the cell cycle, at the metaphase-anaphase transition, the phosphate groups are removed from the fully-grown procentrioles, and as a result phosphorylated CPAP is only found in engaged daughter centrioles, not parental centrioles (Chang et al. 2010).

My bioinformatic analysis showed that CPAP S589 is only conserved in vertebrate species, but S595 is widely conserved across evolution, and an equivalent serine appears to be present in all *Drosophila* species that I analysed (Figure 5.6A). Interestingly, Chang et al. (2010) showed that

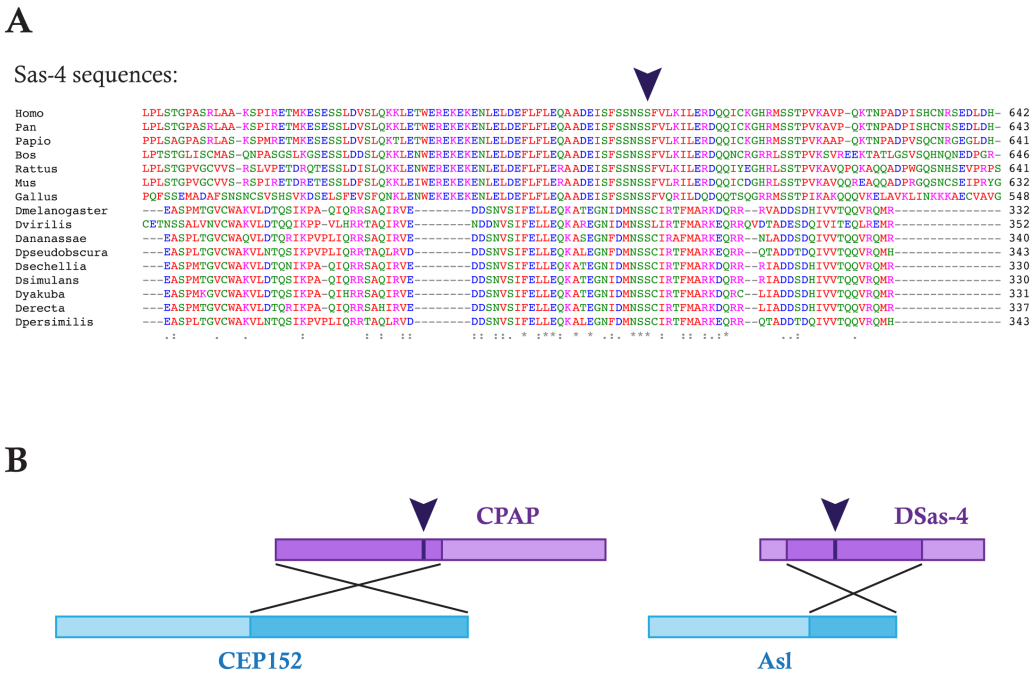


Figure 5.6 CPAP S595 is conserved across evolution and is positioned within the Cep152-interacting region.

(A) A short region of the protein sequence alignment of DSas-4/CPAP homologues in different species across evolution (from insects to mammals). Numbers on the right indicate the position of the last residue shown within the full protein sequence of the given species. Arrow points to S595 within human CPAP; this residue is completely conserved across evolution, while its neighbouring region is highly conserved. (B) Schematics illustrate the interacting regions of CPAP/DSas-4 (*purple*) and Cep152/Asl (*blue*). Darker boxes indicate the interaction regions within each protein that have been mapped in Dzhindzhev et al. 2010. Arrows point to the relative position of CPAP S595 and its equivalent residue in *Drosophila melanogaster*, DSas-4 S300. Note that both in humans and flies this residue is found within the region of CPAP/DSas-4 that interacts with Cep152 or Asl, respectively.

CPAP S595, but not S589, can also be phosphorylated by human Plk4, in addition to Plk2 (which does not have a homologue in flies).

According to my protein sequence alignments, the equivalent site of CPAP S595 in *Drosophila melanogaster* DSas-4 is S300 (Figure 5.6A). The amino acid sequence surrounding this residue is well conserved amongst *Drosophila* species, and a number of other conserved serine and threonine residues are located close by. Both DSas-4 S300 and CPAP S595 are positioned within the region that has been mapped to interact with Asl and Cep152, respectively (Figure 5.6B).

I generated transgenic fly lines expressing GFP fusions of DSas-4 S300D (hereafter DSas-4 S>D–GFP) or DSas-4 S299A & S300A (DSas-4 S>A–GFP) from the endogenous *DSas-4* promoter sequence, and confirmed that these constructs were indeed expressed at physiological levels (Figure 5.7A). I first assessed whether interference with potential phosphorylation at DSas-4 S300 had any affect on centriole duplication, as was shown for CPAP S595. I found that both DSas-4 S>A–GFP and DSas-4 S>D–GFP localize at centrioles normally (Figure 5.7C) and rescued the uncoordinated phenotype as well as the sterility of a *DSas-4* mutant line, although the rescue of uncoordination did not appear as efficient with either mutated construct as with DSas-4-GFP (Figure 5.7B). Moreover, centriole duplication appears to proceed normally in embryos where endogenous DSas-4 had been replaced with either of the two mutated GFP-fusions (Figure 5.7C). These results suggest that, in contrast to CPAP S595, the potential alteration of DSas-4 S300 by cell cycle–dependent phosphorylation does not appear to be essential for *Drosophila* centriole duplication *in vivo*.

I wondered, however, whether either DSas-4 S>A–GFP or DSas-4 S>D–GFP might affect the efficiency of Asl recruitment to centrioles in a subtle way. I assessed whether the cytoplasmic form of either construct showed an enhanced interaction with Asl by immuno-precipitating the different DSas-4-GFP constructs from embryonic cytoplasm extracts and testing the co-precipitation of Asl (Figure 5.8A). Similarly to WT DSas-4-GFP, neither of the mutated versions co-precipitated with

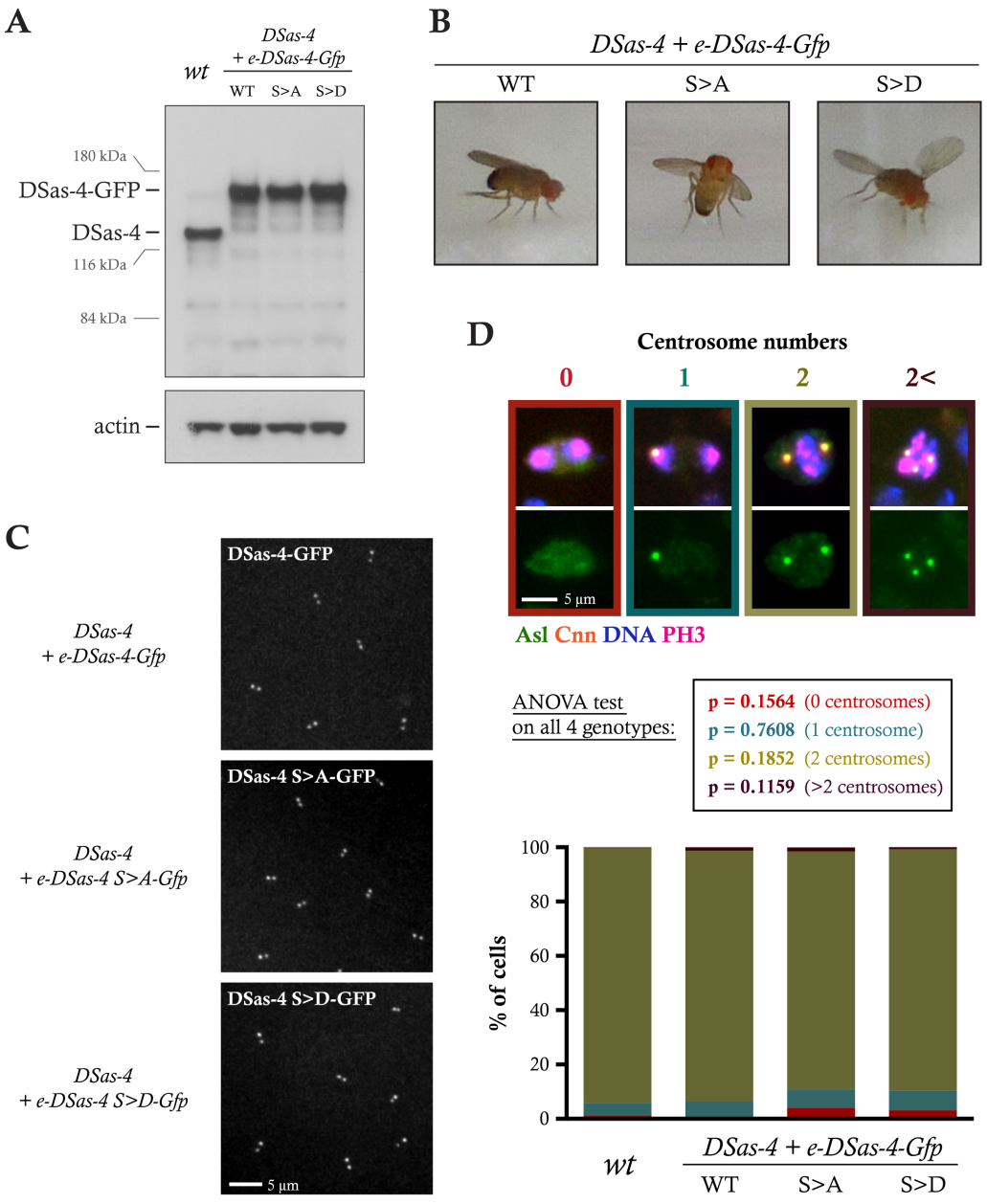


Figure 5.7 Neither mimicking nor abolishing potential phosphorylation at DSas-4 S300 affects the incorporation of DSas-4-GFP into procentrioles, or interferes with efficient centriole duplication.

(A) Western blot shows that *e-DSas-4 S>A–Gfp* and *e-DSas-4 S>D–Gfp* constructs are each expressed at near-physiological levels in 3rd instar larval brains. (B) Images show that *e-DSas-4 S>A–Gfp* and *e-DSas-4 S>D–Gfp* constructs rescue the uncoordinated phenotype of a *DSas-4* mutant. However, neither construct rescues the mutant phenotype as efficiently as *e-DSas-4–Gfp*, based on the wing positioning of flies (these images are representative). (C) Fluorescence images show that both DSas-4 S>A–GFP and DSas-4 S>D–GFP localize at centrosomes similarly as DSas-4–GFP during *S*-phase in syncytial embryos. (D) The expression of *e-DSas-4 S>A–Gfp* or *e-DSas-4 S>D–Gfp* in a *DSas-4* mutant background does not result in a significant change in centrosome numbers in 3rd instar larval brain cells (n=5 brains for *wt* and *DSas-4+eDSas-4-Gfp* each; 6 brains for *DSas-4+eDSas-4 S>A–Gfp* and *DSas-4+eDSas-4 S>D–Gfp* each. Statistical significance was calculated using one-way ANOVA test for each category.

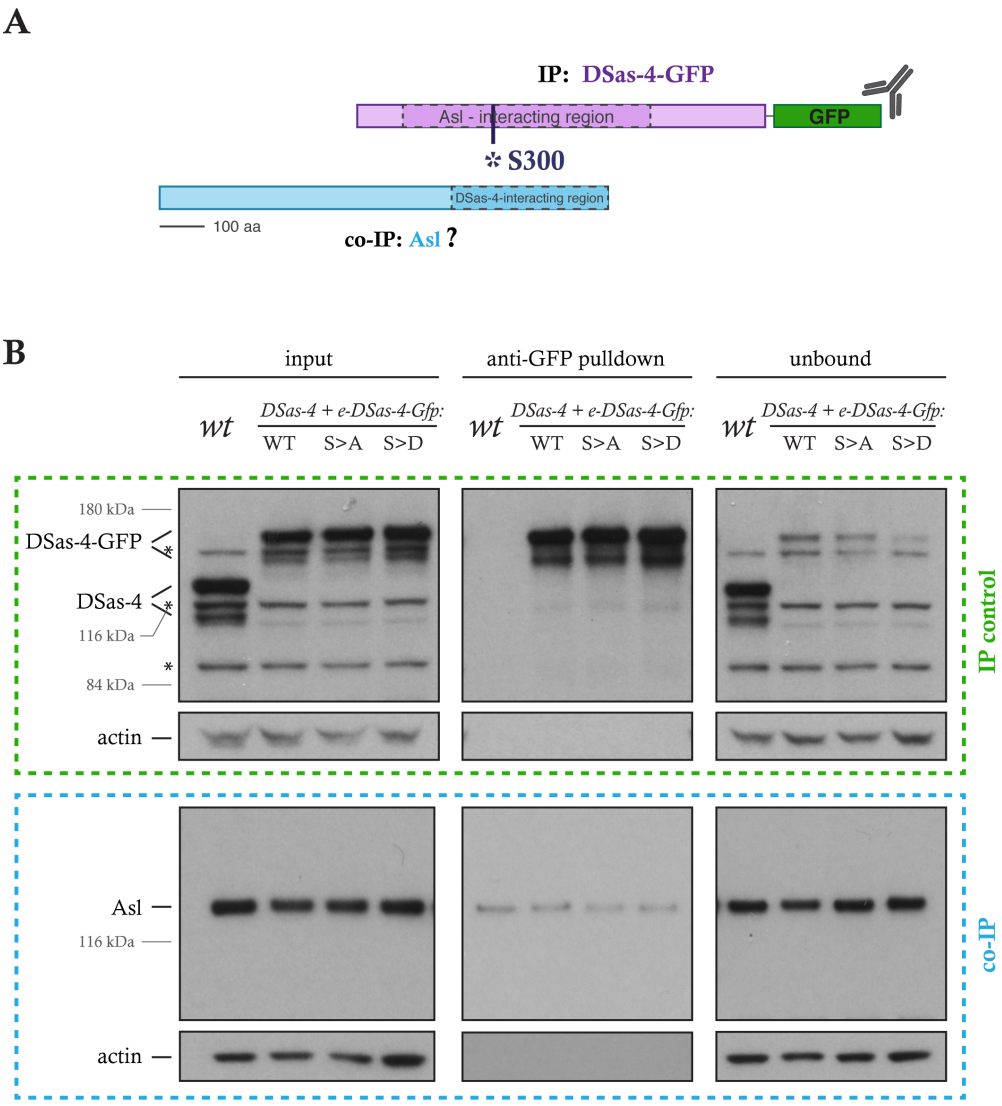


Figure 5.8 Neither mimicking nor abolishing potential phosphorylation at DSas-4 S300 promotes the interaction between cytoplasmic DSas-4 and Asl.

(A) Schematic illustrates the immunoprecipitation approach used to assay the effect of potential phosphorylation at DSas-4 S300 on its interaction with Asl in the cytoplasm. DSas-4–GFP, DSas-4 S>A–GFP or DSas-4 S>D–GFP were immunoprecipitated from embryonic cytoplasm extracts using anti-GFP antibodies and the co-precipitation of Asl-GFP with the different constructs was compared. (B) Western blot images show that anti-GFP antibodies captured each of the three different DSas-4–GFP constructs with high efficiency (top panels – IP control) however Asl did not co-precipitate at detectable levels with either construct (bottom panels; Asl signal similar to the *wt* control for each anti-GFP pulldown).

Asl from the cytoplasm (Figure 5.8B). To more directly test whether centriolar DSas-4 S>A and DSas-4 S>D had any difference in their ability to recruit Asl, I generated fly lines co-expressing Asl-GFP together with the mCherry fusion of either of the two mutated DSas-4 constructs. Unfortunately, during the last 2 months of my studies, the laboratory confocal microscope was broken, so I was unable to complete these studies thus far.

Although the phosphorylation of DSas-4 S300 is clearly not essential for centriole formation in flies, I wondered whether it might contribute to its efficiency – especially as neither mutated construct appeared to completely rescue the uncoordinated phenotype of a *DSas-4* mutant line (Figure 5.7B). To address this, I tested whether the replacement of endogenous DSas-4 with either DSas-4 S>A–GFP or DSas-4 S>D–GFP might have a moderate affect on the average number of centrosomes in 3rd instar larval brain cells. My analysis suggested that both mutant constructs supported centriole duplication with similar efficiency as the wild type protein (Figure 5.7D). In conclusion, unlike CPAP S595, any potential post-translational modification of DSas-4 S300 is dispensable for efficient formation of procentrioles in flies *in vivo*. Taken together, my studies suggest that cell cycle–dependent phosphorylation of DSas-4 S300 is very unlikely to be crucial for the efficient incorporation of DSas-4 into growing centrioles, or a key regulator of Asl recruitment to new centrioles.

Multisite phosphorylation of proteins is known to regulate various switch-like responses – interactions, enzymatic activity, degradation or inactivation of proteins (Nash et al. 2001; Thomson and Gunawardena 2009; Varedi et al. 2010; Koivomagi et al. 2011; Conduit et al. 2014a). As the initial loading of Asl also appears to be a switch-like process, I wondered whether DSas-4 S300 might play a role in this as part of a co-regulated cluster of sites, and thus its mutation alone might just lead to a very subtle affect. Indeed, in the region surrounding S300 I noticed a number of conserved serine and threonine residues (T257; S269; S281; S299; T304) that I thought might potentially act together with S300 (Figure 5.9A). To test this I performed a preliminary phenotypic assessment of DSas-4 that is mutated at these residues using an RNA-injection assay (Figure 5.9B).



Figure 5.9 Investigating whether multisite phosphorylation within DSas-4 257-304 might play a role in regulating the initial incorporation of Asl at new centrioles.

(A) A short region of the protein sequence alignment of DSas-4 homologues in different *Drosophila* species. Numbers on the right indicate the position of the last residue shown within the full protein sequence of the given species. Arrows point to other serine and threonine residues that are found within the well-conserved region surrounding DSas-4 S300 (DSas-4 257-304). (B) Sequences indicate the amino acid substitutions that I introduced into full length DSas-4-GFP to test whether potential phosphorylation at several of these sites affects the incorporation of DSas-4 or Asl at daughter centrioles (apart from S300 I did not test any other individual site, only the combinations shown in this panel). (C) Schematic illustrates the RNA injection assay that I used for preliminary assessment of DSas-4 257-304 S/T>A–GFP and DSas-4 257-304 S/T>E–GFP. I generated mRNA constructs encoding the different transgenes using *in vitro* transcription. I injected this mRNA into young embryos that expressed Asl-mCherry (*red*) and waited for these embryos to develop while expressing the injected mRNA. Once the embryos reached the syncytial blastoderm stage (minimum 1 hour later) I imaged both the injected constructs (*green*) and Asl-mCherry, allowing me to simultaneously assess the incorporation efficiency of the transgenic constructs and their effect on Asl-mCherry recruitment.

I cloned full length DSas-4-GFP constructs that were mutated at these 6 highly conserved S/T residues in region aa257-304 (Figure 5.9B) and transcribed mRNA from these constructs *in vitro* (Figure 5.9C). I then injected the mRNA constructs into freshly laid embryos that expressed Asl-mCherry (Figure 5.9C). I left the embryos to develop and translate the foreign mRNA for at least 60 minutes, and then imaged both Asl-mCherry and DSas-4-GFP at duplicating centrosomes during the syncytial blastoderm stage (Figure 5.9C).

The combined mutation of DSas-4 T257, S269, S281, S300 and T304 to glutamic acid did not detectably interfere with the localization of this GFP fusion construct to centrioles (Figure 5.10A,B). Moreover, the expression of this mutated form of DSas-4-GFP had no detectable effect on the efficiency of Asl-mCherry recruitment (Figure 5.10A,B). These results are qualitative, as it was impossible to control the exact amount of RNA injected into individual embryos (even though all the RNA constructs were used at equal concentrations). Moreover, these negative results could potentially have been affected by the presence of wild type DSas-4 protein in the injected embryos (*DSas-4* mutant background could not be used for these experiments as *DSas-4* mutant females are unable to mate or lay eggs).

I also mutated T257, S269, S281, S299, S300 and T304 to alanine within DSas-4–GFP, to compare with the phospho-mimicking construct. Unfortunately I could not yet complete this comparative analysis, as our laboratory confocal microscope was broken during the final period of my studies.

In summary, my thorough analysis of S300, and my initial analysis of its neighbouring region, strongly suggest that this region of DSas-4 does not play an important part in regulating the centriolar loading of Asl, or in centriole assembly.

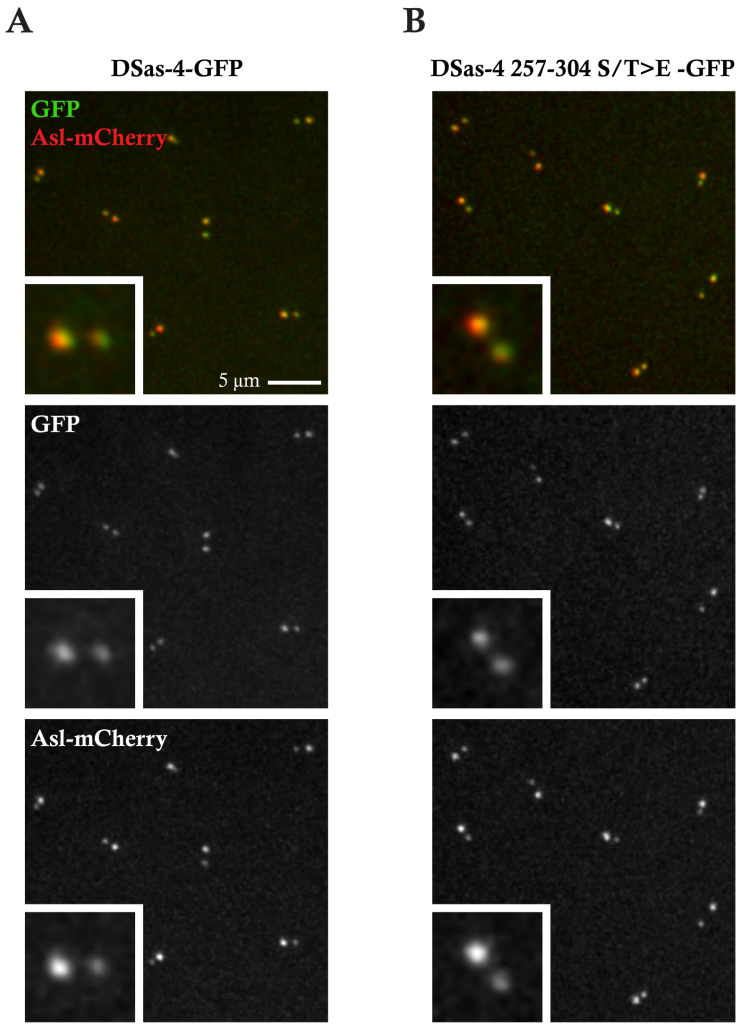


Figure 5.10 Potential multisite phosphorylation within DSas-4 257-304 does not appear to play a critical role in its efficient centriolar incorporation or the regulation of Asl recruitment.

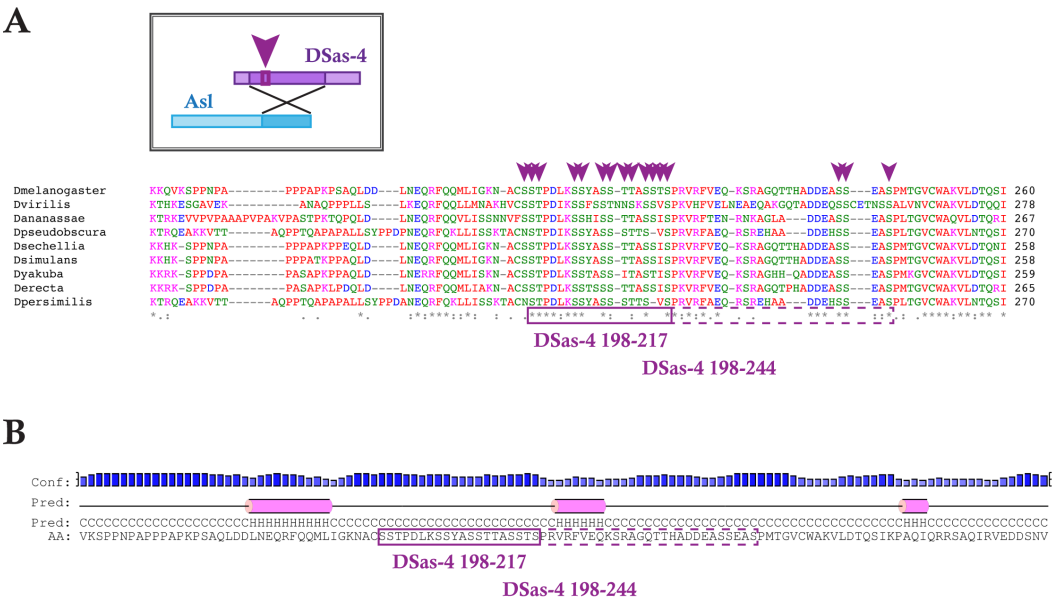
(A,B) Fluorescence images show that DSas-4-GFP (A) or DSas-4 257-304 S/T>E–GFP (B) (each in *green*) — both expressed from injected *in vitro* transcribed RNA — localize similarly at centrosomes during *S*-phase in syncytial embryos. The phospho-mimetic construct does not appear to affect the centrosomal localization of Asl-mCherry (*red*) at newly separated centrosomes, suggesting that potential phosphorylation within this region does not interfere with the regulation of Asl-mCherry recruitment to newly assembled centrioles. Note that endogenous WT DSas-4 was present in these injected embryos.

5.2.4 INVESTIGATING THE ROLE OF REGION 198-244 WITHIN DSAS-4 IN THE INITIAL RECRUITMENT OF ASL TO CENTRIOLES

When analysing sequence alignments of DSas-4 proteins, I noticed a conserved stretch of residues within the Asl-interacting region that had a very high (65%) serine/threonine content (Figure 5.11A; DSas-4 198-217). Two of these perfectly conserved residues were followed by a proline, suggesting they might be Cdk1 target sites. In the neighbouring region, I identified another highly conserved, but smaller patch of serines (Figure 5.11A; DSas-4 240-244), one of which also appeared to be a potential Cdk1 target site. Secondary structure predictions suggested that this extended region is mostly unstructured, with a short helix separating the first and second patch of conserved serines (Figure 5.11B). I decided to test the importance of DSas-4 198-244 in both the centrosomal incorporation of DSas-4 itself and in Asl recruitment. As a preliminary analysis, I deleted both the shorter region (DSas-4Δ198-217) and the extended region (DSas-4Δ198-244) from full length DSas-4 (Figure 5.11C), and assessed the phenotype of these deletion constructs using the previously described RNA injection assay (Figure 5.9C).

Both DSas-4Δ198-217–GFP and DSas-4Δ198-244–GFP localized at centrosomes similarly to WT DSas-4–GFP at all stages of the embryonic cell cycle (Figure 5.12A-C). Although I did not quantitatively compare the centrosomal levels of DSas-4-GFP for these different constructs (as the amount of mRNA injected into individual embryos varied) these qualitative results show that aa198-244 are not crucial for DSas-4 incorporation into centrioles.

I next tested whether either DSas-4 deletion affected the recruitment of Asl-mCherry to freshly disengaged new centrioles. Strikingly, the expression of DSas-4Δ198-217–GFP strongly interfered with the initial loading of Asl-mCherry onto new centrioles (Figure 5.12B); barely any Asl-mCherry could be detected at young centrosomes in early *S*-phase. This phenotype was more pronounced during the later syncytial cycles rather than the earlier ones. I speculate that this is because centrioles that were formed in earlier cycles incorporated a higher proportion of


A
DSas-4
Asl
Dmelanogaster KKQVKSPPNPA---------PPPAPKPSAQLDD---LNEQRFQQMLIGKN-ACSSTPDLKSSYASS-TTASSTSPRVRFVEQ-KSRAGQTTHADDEASS---EASPMTGVCWAKVLDTQSI 260
Dvirilis KTHKESGAVEK----------ANAQPPPLLS----LKEQRFQQLLMNAKHVCSSTPDIKSSFSSTNNSKSSVSPKVHFVELNEAEQAKGQTADDEQSSCETNSSALVNVCWAKVLDTQQI 278
Dananassae KTRKEVVPVPAAAPVPAKVPASTPKTQPQLD----LNEQRFQQVLISSNNVFSSTPDLKSSHISS-TTASSISPKVRFTEN-RNKAGLA---DDEASS---EASPLTGVCWAQVLDTQRI 267
Dpseudobscura KTRQEAKKVTT------AQPPTQAPAPALLSYPPDPNEQRFQKLLISSKTACNSTPDIKSSYASS-STTS-VSPRVRFAEQ-RSREHAA---DDEHSS---EASPLTGVCWAKVLNTQSI 270
Dsechellia KKHK-SPPNPA---------PPPAPKPPEQLD----LNEQRFQQMLIGKN-ACSSTPDLKSSYASS-TTASSISPRVRFVEQ-KSRAGQTTHADDEASS---EASPMTGVCWAKVLDTQNI 258
Dsimulans KKHK-SPPNPA---------PPPATKPPAQLD----LNEQRFQQMLIGKN-ACSSTPDLKSSYASS-TTASSISPRVRFVEQ-KSRAGQTTHADDEASS---EASPMTGVCWAKVLDTQSI 258
Dyakuba KKRK-SPPDPA---------PASAPKPPAQLD----LNERRFQQMLISKN-ACSSTPDLKSSTASS-ITASTISPKVRFVEQ-KSRAGHH-QADDEASS---EASPMKGVCWAKVLDTQSI 259
Derecta KKRK-SPPDPA---------PASAPKLPDQLD----LNEQRFQQMLIAKN-ACSSTPDLKSSTSSS-TTASSISPKVRFVEQ-KSRAGQTPHADDEASS---EASPMTGVCWAKVLDTQRI 265
Dpersimilis KTRQEAKKVTT------AQPPTQAPAPALLSYPPDANEQRFQKLLISSKTACNSTPDLKSSYASS-STTS-VSPRVRFAEQ-RSREHAA---DDEHSS---EASPLTGVCWAKVLNTQSI 270
DSas-4 198-217
DSas-4 198-244
B
Conf:
Pred:
Pred: CCCCCCCCCCCCCCCCCCCCCHHHHHHHHHHCCCCCCCCCCCCCCCCCCCCCCCCCCHHHHHCCCCCCCCCCCCCCCCCCC

endogenous WT DSas-4 molecules; the mutated protein is synthetized from injected mRNA and so takes some time to build up in the cytoplasm. Interestingly, the Asl-mCherry levels at older centrosomes did not appear to be affected by the expression of DSas-4Δ198-217–GFP (Figure 5.12). This was most likely because the initial recruitment of Asl-mCherry to the parental centrioles was less affected during the earlier cycles (as the mutant protein was still at low levels), and the subsequent continuous turnover of the mobile fraction of Asl-mCherry molecules does not depend on DSas-4.

The larger deletion, DSas-4Δ198-244–GFP, had an even more severe effect on the initial centriolar recruitment of Asl-mCherry. Often this protein could not be detected at newly separated young centrosomes at all (Figure 5.12C). Strikingly, the effect of DSas-4Δ198-244–GFP was so strong (even in the presence of endogenous WT DSas-4) that it closely resembled the outcome of inhibiting the DSas-4–Asl interaction though immuno-inhibition, which I described in the previous chapter. The Asl-negative centrioles that were formed as a result of DSas-4Δ198-244–GFP expression showed the same characteristics as those of Asl-negative centrioles that were generated by immuno-inhibition. They failed to accumulate further DSas-4Δ198-244–GFP, which is a sign of their inability to duplicate (Figure 5.13A). Their separation from the older centrosome was often strongly impaired, most likely due to PCM recruitment defects in the absence of Asl (Figure 5.13B). Importantly, just like DSas-4Δ198-217–GFP, this larger deletion also appeared to exclusively affect the initial step of Asl-mCherry recruitment to new centrioles; the levels of Asl-mCherry at older centrosomes appeared to be very similar to that of control centrosomes (Figure 5.12A,C).

These results strongly suggest that the region between aa198-244 plays a crucial role in the initial DSas-4–dependent recruitment of Asl to new centrioles, with the majority of this role being mediated by only a short stretch of 20 residues, aa198-217. The question remains whether the importance of this region lies in the regulated phosphorylation of its many S/T residues, or whether

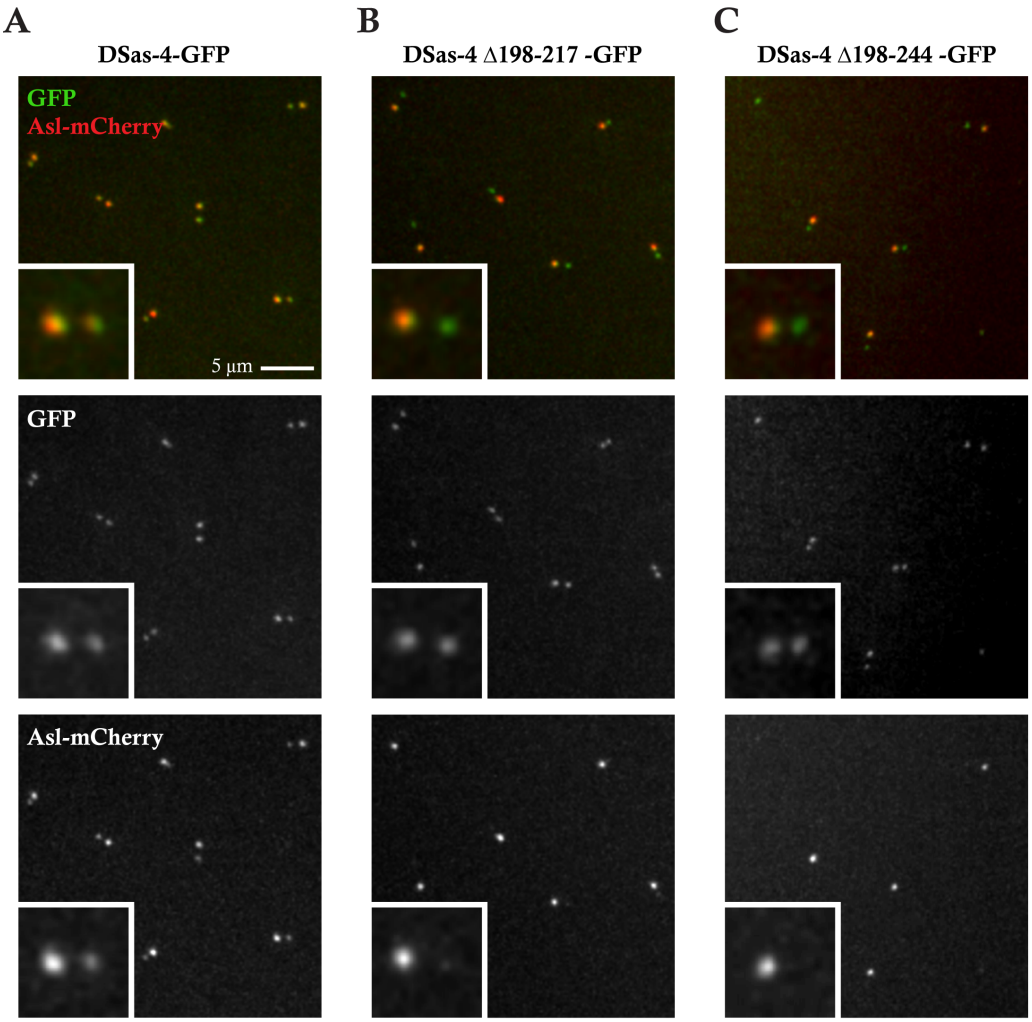


Figure 5.12 DSas-4 198-244 is not essential for its own centriolar incorporation, but plays a crucial role in the initial recruitment of Asl to newly assembled centrioles.

(A-C) Fluorescence images show that DSas-4-GFP (A), DSas-4 Δ198-217–GFP (B) or DSas-4Δ198-244–GFP (C) (each in *green)* — all expressed from injected *in vitro* transcribed RNA — all localize similarly at centrosomes during *S*-phase in syncytial embryos. The expression of DSas-4 Δ198-217–GFP strongly interferes with, while the expression of DSas-4Δ198-244–GFP can completely prevent the recruitment of Asl-mCherry (*red*) to disengaged new centrioles. The levels of Asl-mCherry at old centrosomes do not appear to be affected by the expression of these mutated forms of DSas-4-GFP. Note that endogenous WT DSas-4 was present in these injected embryos.

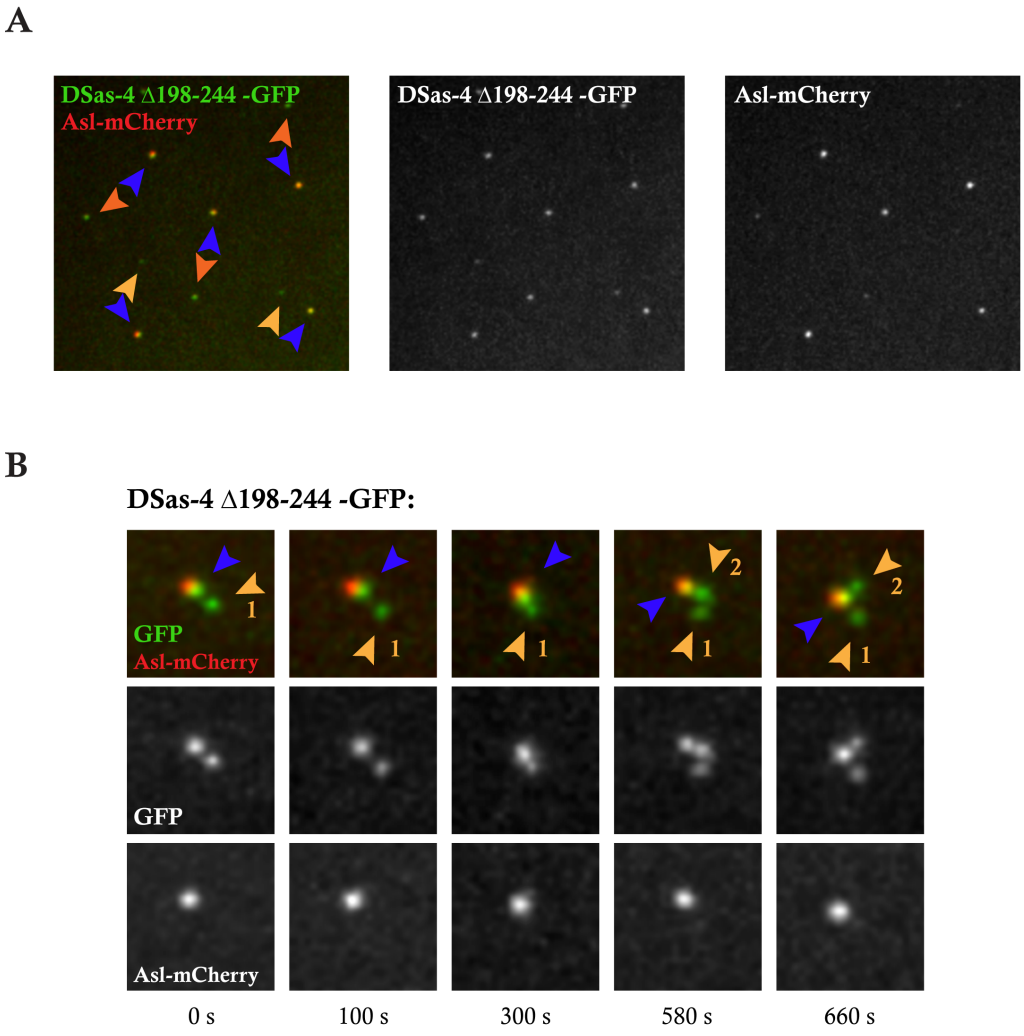


Figure 5.13 DSas-4Δ198-244–GFP expression has an equally severe effect on centriolar Asl recruitment and Asl-dependent processes as immuno-inhibiting of the interaction between DSas-4 and Asl.

(A) Fluorescence images taken from an embryo during mitosis show that Asl-negative centrosomes (*light orange* arrows) formed as a result of DSas-4Δ198-244–GFP (*green*) expression failed to recruit DSas-4-GFP during the preceding *S*-phase suggesting that they are unable to duplicate. Note that, as shown in Figure 5.14, in early *S*-phase the levels of DSas-4Δ198-244–GFP appear symmetrical between Asl–positive old centrosomes and the Asl-negative new centrosomes, and similar to the levels of DSas-4–GFP. Therefore the difference in centrosomal DSas-4Δ198-244–GFP levels seen here must be primarily due to the absence of daughter centriole assembly within Asl-negative centrosomes; however, a loss a parental DSas-4Δ198-244–GFP from Asl-negative centrosomes cannot be ruled out. (B) Fluorescence images from a time-lapse movie show that Asl-negative centrosomes (*light orange* arrows) formed as a result of DSas-4Δ198-244–GFP expression are often defective in their separation from the old centrosome, similarly to the Asl-negative centrosomes that I generated by immuno-inhibiting the DSas-4–interacting region of Asl (Figure 4.9). Time relative to centriole separation at the beginning of the first cycle (t=0 s) is shown. The images show that the first young centrosome (*light orange arrow 1*) fails to move away from the old centrosome (*blue* arrow) during the entire cell cycle, therefore at the start of the next cycle (580s) there are two young centrosomes (*light orange arrows 1&2*) next to the old centrosome, and neither of these move away as the following cycle progresses (660s). I observed this behaviour regularly in the case of Asl-negative centrosomes.

this short stretch of amino acids itself is in some way crucial for the interaction between DSas-4 and Asl. To test this, I have generated constructs in which I have mutated all of the serine and threonine residues within aa198-217 or aa198-244 to alanine, and ones in which the majority of these residues are changed to glutamic acid (Figure 5.11D). The preliminary phenotypic assessment of these constructs using the mRNA injection assay will be important work I plan to carry out in the near future. I have also cloned GFP and mCherry fusions of both DSas-4 198-244 S>A and DSas-4 198-244 S>E into P-element transformation vectors to allow the generation of transgenic fly lines, which will allow precise quantitative studies of the function of this region.

5.3 DISCUSSION

5.3.1 ATTEMPTS TO IDENTIFY THE MECHANISMS THAT REGULATE THE INITIAL, DSAS-4–DEPENDENT, INCORPORATION OF ASL AT CENTRIOLES

My earlier work had revealed that DSas-4 plays a crucial role in the initial step of Asl recruitment to newly disengaged centrioles. The very different incorporation timing of these two proteins within the same centriole suggested that their molecular interaction at centrioles must be tightly regulated. Of the various possible control mechanisms, posttranslational alteration of one or both proteins during the cell cycle seemed to best explain this regulation, in light of my current data. In this chapter I have described my initial attempts to identify the molecular mechanisms that regulate the interaction between these two proteins, and thereby govern the timing of Asl incorporation.

My analysis suggested that DSas-4 S300 and its neighbouring region do not play a part in regulating the initial loading of Asl onto new centrioles. Moreover, I could not find any functional importance of potential phosphorylation in this region. Thus, it appears that although DSas-4 S300 is conserved across evolution, the regulation mechanism that acts on the equivalent residue of human CPAP must have evolved later and is not present in flies.

Apart from CPAP S595, no other post-translational modification has been found in any homologue of DSas-4 or Asl that correlates with the centriolar presence of Asl. In fact, apart from the two Plk2 target sites within CPAP described above (Chang et al. 2010), barely any sites of phosphorylation have been reported in DSas-4, Asl or their vertebrate homologues at all (Dr. Janina Baumbach identified just 1 site of centrosome-specific phosphorylation in DSas-4 and 1 site in Asl using mass spectrometry during her PhD work in the Raff lab). The minimal number of phosphorylation sites identified so far in these proteins is surprising, considering that both CPAP and Cep152 are known substrates of Plk4 *in vitro* (Chang et al. 2010; Hatch et al. 2010) as well as other kinases (CPAP: Plk2 – based on Chang et al. 2010; Cep152: Plk1 – based on Sonnen et al. 2013), and ever increasing evidence supports that many aspects of their molecular behaviour appear to be strongly regulated during the cell cycle. The relatively low abundance of DSas-4 and Asl within centrosomes compared to several other phosphorylated PCM proteins (Habermann et al. 2012; Conduit et al. 2014a) probably hinders the efficient identification of their post-translational modifications during proteomic analysis of the partially purified centrosomes. Although analysing of the centrosomal form of each of these two protein in isolation seems a much better route, it could still be problematic because at most half of the centrosomal pool of either protein is expected to adopt the form that allows the DSas-4-Asl interaction (DSas-4: because only one centriole per centrosome recruits Asl; Asl: because the mobile Asl pool at centrosomes is incorporated independently of DSas-4).

For the reasons above, I used bioinformatics and primary sequence analysis to identify candidate molecular regions within DSas-4 and Asl that might be required for their regulated interaction. Multisite phosphorylation of proteins has been described as a common regulator of switch-like responses (Nash et al. 2001; Thomson and Gunawardena 2009; Varedi et al. 2010; Koivomagi et al. 2011; Conduit et al. 2014a), such as the initiation of centriolar Asl incorporation. I therefore concentrated my analysis on regions within the previously mapped interacting domains of the two proteins that were highly conserved amongst *Drosophila* species and contained an unusually high percentage of serine or threonine residues. I first focused on DSas-4, as the temporal and sub-

centrosomal recruitment pattern of Asl suggested to me that a regulation mechanism governing its initial incorporation timing must target its centriolar anchor protein, rather than cytoplasmic Asl alone. This led to the identification of DSas-4 198-244 as a region that could potentially be a target of multisite phosphorylation. My results show that DSas-4 198-244 is not required for the centriolar incorporation of DSas-4 itself, but has a critical importance in the initial centriolar loading of Asl. My next aim is to determine whether multisite phosphorylation within this region might be responsible for the regulation of Asl recruitment. For this purpose I have generated mutated forms of DSas-4 that are either non-phosphorylatable between aa198-244, or constitutively mimic phosphorylation in this region. My immediate future aim is to test how these mutations affect the centriolar recruitment of Asl using the RNA injection assay as a preliminary screen, followed by the precise phenotypic assessment of transgenic flies. As any potential effects of these mutations will be provoked by artificially designed DSas-4 constructs, I also aim to investigate whether multisite phosphorylation can actually be detected in this region *in vivo*, to complement my functional assays.

Perhaps the most interesting question related to the regulation of Asl incorporation is whether its absence at engaged daughter centrioles is functionally significant. Is this an important component of the control mechanisms that restrain centriole amplification, or is it simply a by-product of a regulation mechanism that really targets something else? As an example, I think it is possible that a similar, though not identical, mechanism might regulate the efficient incorporation of DSas-4 into growing centrioles as has been described for CPAP in human cells (Chang et al. 2010), which could have a secondary effect on the DSas-4–Asl interaction. Interestingly, the constant presence of Asl at mother centrioles throughout the cell cycle does not result in their overduplication as long as other centriole duplication factors are not overexpressed or while their first daughter centriole remains engaged normally – so why might it be important to avoid the presence of Asl altogether at daughter centrioles? Importantly, unlike mother centrioles, the entire circumference of engaged daughter centrioles is free (in other words, they are not engaged with their own daughter), so the presence of Asl around them could potentially allow the formation of a single granddaughter

centriole within centrosomes (and this granddaughter might then nucleate a great-granddaughter, and so on). It will be interesting to test this question in the future by experimentally inducing the early incorporation of Asl into engaged daughter centrioles. I have shown that moderate overexpression of Asl-GFP from the polyubiquitin promoter can drive such early incorporation, but this Asl-GFP construct does not appear to drive centriole amplification (Franz et al. 2013). However, it is important to note that, when overexpressed in this manner, the timing and efficiency of Asl-GFP incorporation appears to vary between individual embryos, therefore this approach is not ideal for studying the importance of the natural timing of Asl incorporation. Instead, I hope that deciphering the molecular regulation of Asl recruitment will eventually allow one to efficiently drive Asl onto engaged daughter centrioles for the purpose of studying this question.

Future investigations of how the induced presence of Asl at daughter centrioles might affect centriole duplication can also contribute to our understanding of one of the biggest mysteries of the field: why a single daughter centriole is formed in each centrosome in each cell cycle. Currently, we do not understand why only a single daughter centriole is formed, or how the engagement of this daughter to the mother centriole represses the formation of further daughters around the same mother (Tsou and Stearns 2006b; Loncarek et al. 2008; Wang et al. 2011). A possible explanation for both of these questions could be that although Sak/Plk4 is recruited by a ring of Asl that coats the mother centriole, it somehow ends up being concentrated at a single focus on the mother centriole surface. Sak/Plk4 is known to dimerize (Holland et al. 2010), and its potential further self-association (Slevin et al. 2012) at centrioles could result in such a behavior. Earlier studies showing that Sak/Plk4 overexpression can force the formation multiple daughter centrioles surrounding the same mother centriole (Kleylein-Sohn et al. 2007; Cunha-Ferreira et al. 2009) strongly support that the kinase is capable of binding along the entire circumference of mother centrioles, but in wild type cells it somehow avoids doing so. Efficient concentration of Sak/Plk4 to one focus could explain why only a single daughter would be assembled per mother centriole, and, as only mother centrioles have the ability to recruit Sak/Plk4, only a single daughter would be assembled per centrosome. If such a mechanism does indeed regulate centriole numbers, it is possible that the

presence of Asl on growing daughter centrioles would not lead to granddaughter centriole formation, as Sak/Plk4 would preferentially localize to the first focus, at the side of the mother centriole. In conclusion, it will be interesting to test how the induced presence of Asl at engaged daughter centrioles might affect centriole amplification, and therefore, whether the specific timing of Asl incorporation at new centrioles is an important aspect of avoiding this.

5.3.2 MODERATE OVEREXPRESSION OF ASL-GFP LEADS TO ITS EARLY INCORPORATION INTO ENGAGED DAUGHTER CENTRIOLES

Driving Asl-GFP expression from the polyubiquitin promoter leads to approximately 4-fold overexpression compared to endogenous Asl levels, and I have shown that this relatively mild increase is sufficient to alter the natural timing of Asl-GFP recruitment, albeit with variable efficiency between individual embryos. Interestingly, however, the early incorporation of Asl-GFP into engaged daughter centrioles does not detectably effect centriole duplication (Franz et al. 2013) or PCM recruitment (my preliminary studies suggest that centrosomal Cnn levels during early *S*-phase are very similar when Asl-GFP is overexpressed or expressed at near-physiological levels, data not shown). Therefore, at first sight, it appears that overexpression of Asl-GFP does not have any significant physiological consequences, given that its two key roles, centriole duplication (Blachon et al. 2008) and initiation of PCM recruitment (Conduit et al. 2014b), appear unaltered.

I noticed, however, that flies overexpressing Asl-GFP are in fact not normal: they show signs of uncoordination (their wings are continuously held in an upright position), frequent nuclear fallouts occur during their early embryonic cycles, and my preliminary observations suggest that they develop slower than flies expressing Asl-GFP at physiological levels (data not shown). I also noticed that flies overexpressing Asl-GFP in the presence of endogenous Asl appear even unhealthier than flies that overexpress Asl-GFP in the asl^{B46} null mutant background. These suggest that elevated cellular levels of Asl affect the physiology of flies in a way that is not directly linked to centriole numbers or centrosome function; instead, it appears to be linked to cilia function (uncoordination) and perhaps cell cycle control (nuclear fallouts, developmental delays).

Importantly, these results are preliminary and the different genetic background of the independent fly lines could potentially affect the phenotypes that I have mentioned. Nonetheless, I do find the phenotypes of Asl-GFP overexpression very interesting and aim to investigate these more closely in the future, following backcrossing all lines with wild type flies to achieve an isogenised genetic background. In particular, I aim to address whether Asl has a role in accurate cell cycle progression that is not directly linked to centrosome function. I find this possibility very interesting as mutations within Cep152 have been linked to Seckel syndrome (Kalay et al. 2011), a genetic condition that is mostly caused by mutations in a variety of genes that function in the ATR–dependent DNA damage signalling (Verloes et al. 1993). It is an interesting question whether Asl might also play a role in DNA damage checkpoint mechanisms (either be allowing their efficient activation at centrosomes or in a centrosome-independent manner) and if so, does Asl-GFP overexpression possibly interfere with the correct function of these pathways.

In summary, I have described my initial work on deciphering the molecular regulation of Asl incorporation at centrioles. I have identified a short, conserved region within DSas-4 (aa198-244) that is unusually rich in serine and threonine residues, and my preliminary data show that this region is crucial for Asl recruitment. My next aim is to test whether multisite phosphorylation within this region might be responsible for altering the DSas-4–Asl interaction, and thereby regulates the timing of initial Asl recruitment at centrioles. I have also shown that moderate overexpression of Asl-GFP can mis-regulate the mechanisms that control the timing of initial Asl incorporation and thus promote its early centriolar recruitment. Interestingly, this does not appear to alter centriole duplication or PCM recruitment, but somehow has a marked affect on the physiology of flies. In the future I aim to investigate why the mild overexpression of Asl-GFP appears unfavourable for cells, and whether this could potentially be linked to a novel role of Asl that is not directly linked to centrosome function.

CHAPTER 6: DISCUSSION

6.1 SUMMARY

Asl was originally described as a protein that plays a key role in PCM recruitment (Bonaccorsi et al. 1998; Varmark et al. 2007); recently, however, it was discovered to be essential for centriole duplication as well in both flies and vertebrates (Blachon et al. 2008). At the time I started this study Asl, and its vertebrate homologue Cep152, were shown to interact with two key centriolar proteins, Sak/Plk4 and DSas-4/CPAP, in an evolutionarily conserved manner (Cizmecioglu et al. 2010; Dzhindzhev et al. 2010; Hatch et al. 2010). These results were somewhat surprising; Sak/Plk4 has been known to act most upstream in the procentriole assembly process, while DSas-4/CPAP has a later role, and has been described to act most downstream of all the essential centriole duplication proteins. Based on these studies Asl/Cep152 were assigned the role of a 'scaffold' that in some way promotes the early stages of procentriole assembly (Cizmecioglu et al. 2010; Dzhindzhev et al. 2010).

Although the molecular interactions and functions of Asl/Cep152 had been extensively characterized in recent years, little was known about how it really acts in centriole duplication. It had remained unclear how Asl/Cep152 is initially recruited to new centrioles; in vertebrate cells Cep63 was identified to have an important role in the efficient localization of Cep152, but does not appear essential for its initial recruitment (Sir et al. 2011), furthermore Cep63 does not appear to have a homologue in flies. During the same time as I carried out these studies, several other groups had also reported that, as I also observed, Asl/Cep152 only appears to be present around parental centrioles, and can not be detected at daughter centrioles while those are engaged with their mother (Sir et al. 2011; Fu and Glover 2012; Lawo et al. 2012; Mennella et al. 2012; Sonnen et al. 2012; Lukinavicius et al. 2013). These observations reveal an obvious paradox in the proposed early role

of Asl/Cep152 in procentriole assembly and its extremely delayed incorporation into daughter centrioles that I have characterised extensively in this work; it has not been addressed how Asl can promote centriole duplication if it is not present in forming centrioles.

In this thesis I have shown that in flies the initial recruitment of Asl to centrioles is dependent on DSas-4, and results in stable incorporation of Asl at newly disengaged daughter centrioles. A subsequent, DSas-4–independent mechanism then drives the accumulation of a mobile Asl pool at centrosomes; my data suggest that this recruitment step may be driven by a self-interaction with stably incorporated Asl molecules. My data reveal that the initial, DSas-4–dependent, incorporation of Asl is a switch-like process: new, fully grown centrioles are unable to recruit Asl until they pass through their first mitosis – although they contain DSas-4 for nearly a whole cell cycle before this time – however, once Asl recruitment is initiated, it progresses with a similar rate at any stage of the cell cycle. This behaviour of Asl strongly suggests that its interaction with centriolar DSas-4 is tightly regulated during the cell cycle, and the focus of my current studies is to decipher the molecular mechanisms responsible for controlling the interaction of these proteins.

My studies have also revealed that centriole duplication requires the mere presence of Asl around mother centrioles. Daughter centrioles do not incorporate Asl while they grow and remain engaged with their mother, but rely on Asl recruitment for their conversion into mother centrioles, to enter the centriole duplication for the first time. As a fraction of centrosomal Asl molecules are stably incorporated at centrioles, the very first event of Asl recruitment converts daughter centrioles into mother centrioles in a permanent manner: once a centriole has acquired Asl, it no longer relies on any further Asl recruitment prior to starting subsequent duplication events. I also discovered that, at least in *Drosophila* embryos, mother centrioles accumulate significantly higher levels of Asl than the amount required for their successful duplication; it is possible that these excessive levels of Asl are linked to its additional role in PCM recruitment (Varmark et al. 2007; Conduit et al. 2010; Conduit et al. 2014b).

As I have discussed the results of this thesis project in the context of other studies within the concluding sections of the relevant chapters, here I aim to present the implications of my work in a wider context, and I describe how my studies have extended our understanding of the overall control of centriole duplication. I also introduce a few key questions that my results have raised, and outline how I aim to investigate some of these in the near future.

6.2 ASTERLESS: A PRIMARY LICENSE OF CENTRIOLE DUPLICATION

My studies have revealed Asl as the first essential centriole duplication protein that is required to identify mother centrioles – thus, to generate the functional templates of duplication – instead of being needed for the physical assembly of new centrioles. The absence of Asl in engaged daughter centrioles can explain why these are unable to template granddaughter centrioles under various experimental conditions that allow re-duplication or overduplication of mother centrioles (Kleylein-Sohn et al. 2007; Loncarek et al. 2008; Cunha-Ferreira et al. 2009; Wang et al. 2011). My findings have extended our understanding of how centrioles are permitted to enter the duplication cycle: while the previously proposed licensing model explained how older centrioles – that have duplicated before – can re-enter the cycle (Tsou and Stearns 2006b; Tsou and Stearns 2006a), my results reveal how newly assembled centrioles can duplicate for the first time. Accordingly, we have termed Asl a '*primary license*', as it gives new centrioles the permission for their first round of duplication in flies.

I have shown that Asl recruitment is crucial to allow the first duplication event of centrioles, however, due to the stable nature of initial Asl incorporation, this primary license is not lost (and undoubtedly remains crucial during later cycles). Instead, further regulation appears to be taken over by the re-duplication licensing mechanism: disengagement (Tsou and Stearns 2006b; Tsou and Stearns 2006a). The molecular role of Asl as a primary license is most likely the recruitment of Sak to the mother centriole wall to catalyses procentriole assembly (Dzhindzhev et al. 2010). Plk4

recruitment in vertebrates is dependent on both Cep152 and Cep192; thus, it is possible that a similar primary licensing mechanism as the one I have described in flies also operates in higher animals, however two molecules are likely to share this role in these species. It is an interesting question how disengagement allows new duplication events to take place.

A key question is whether Asl acts as a *bona fide* license of centriole duplication, considering that its recruitment is required only before the first duplication event? In the popular analogy to DNA replication (which is signified in the name of the licensing model of centriole duplication), licenses are defined as factors (proteins) that are necessary, but not sufficient, to promote replication, as they provide a 'platform' for a certain activity (Cdk) to catalyse replication. I think that Asl perfectly matches these criteria, being the platform for Sak recruitment. However, the association of *bona fide* DNA replication licenses with the physical strands of DNA is conventionally believed to be mutually exclusive with on-going replication. As I've described above, this is not true for Asl: once incorporated, Asl remains stably associated with duplicating mother centrioles at all stages of the cell cycle. Importantly, however, the DNA replication process shows that the most basal layer of origin licensing, the components of the ORC complex, *can* act exactly as Asl does – they just don't do so in a universal manner.

The multi-subunit ORC complex (which defines the sites of replication initiation) is formed by 6 proteins that are highly conserved across eukaryotes (Bell and Stillman 1992; Diffley et al. 1994; Gavin et al. 1995). Despite their high functional conservation, the behaviour of these proteins shows strong differences between species. In yeast, all the ORC subunits remain bound to DNA throughout the cell cycle, but are phosphorylated by Cdk to prevent DNA re-replication (Vas et al. 2001). In contrast, Cdk-dependent phosphorylation dissociates the mammalian ORC subunits from chromatin as cells enter *S*-phase (Lee et al. 2012), moreover the largest subunit, Orc1, is not only displaced, but degraded between *S* and *G1* phases (Tatsumi et al. 2003). As a result, homologous proteins – the ORC subunits – appear to act as *bona fide* licenses in some species, but not others –

yet they are generally all classed as licensing factors of DNA replication (as, for example, defined in Siddiqui 2013).

I think that the way Asl acts in licensing centriole duplication is highly analogous to the function of ORC proteins in yeast replication, and thus Asl can be classed as a true license of centriole duplication. This analogy, however, immediately points to the question: is Asl also modified upon the initiation of centriole duplication to render it harmless in terms of centriole amplification? If so, is the presence of the second layer of licensing, centriole disengagement, functionally linked to 'exposing' the primary license, or could Asl possibly alternate between different states during the licensing and duplication phases of the centriole cycle? I believe that these are extremely interesting questions that will no doubt be answered in the future. I hope that learning from how the highly analogous process of DNA replication is controlled will provide help in deciphering the regulation of the centriole cycle.

It is clear that the centriolar presence of Asl and centriole disengagement somehow act together and form a layered control mechanism that ensures the formation of a single daughter per mother centriole at any one time. It is so far a mystery, however, how a protein coating the entire circumference of mother centrioles and the physical separation of daughter centrioles could achieve such precise regulation. It appears that the role of centriole disengagement is not the physical exposure of a 'special site' on the mother centriole where another daughter can form, as laser ablation experiments show that daughter centrioles are not always assembled at the same site on a mother centriole (Loncarek et al. 2008). Instead, I think it is more likely that the regulation mechanism that restricts centriole numbers is somehow more intrinsic to the interaction properties of the key duplication proteins, and is controlled through a combination of positive and negative feedback loops during their accumulation at mother centrioles.

My results reveal that the initial incorporation of Asl at newly formed centrioles is subject to strong cell cycle–dependent regulation. Considering that Asl acts as a license for centriole duplication, it

is tempting to speculate that the regulated timing of its initial recruitment to centrioles is a crucial element of the control mechanisms that restrain centriole amplification. However, I am not certain this will turn out to be the case: first, the permanent presence of Asl at mother centrioles during the cell cycle does not result in their overduplication; second, forcing Asl-GFP onto engaged daughters does not seem to result in centriole amplification (this study; Franz 2013). Instead, I think that stringent regulation of Asl incorporation is in itself not critical for the efficient control of centriole duplication, but most likely makes this control more robust. To better explain this argument, I again use the example of the regulation of Orc proteins during DNA replication. The behaviour of these in yeast shows that re-replication can be efficiently avoided whilst these licensing proteins are continuously associated with DNA (provided that they are efficiently regulated post-translationally) nonetheless they have evolved to become removed/degraded during replication, as is the case for the other *bona fide* licensing proteins, in mammals. As evolution shows, this removal was not necessary *per se*, but most likely provided an additional layer of security to the regulation of DNA replication. I think that the absence of Asl in daughter centrioles is a similar beneficial, though probably not crucial, safeguard in the centriole licensing system. However, further studies will be necessary to thoroughly investigate this question.

6.3 FUTURE WORK

The next step towards understanding how Asl acts in regulating centriole duplication will be to unravel how its centriolar presence and, once incorporated, its function are regulated during the cell cycle. In this thesis I have presented my initial attempts at answering the first of these questions. The dynamic behaviour of Asl suggests that its initial incorporation is most likely regulated through posttranslational modification of its centriolar binding sites – most likely being DSas-4 – and/or Asl itself. I have so far identified a short region within DSas-4 that is crucial for Asl recruitment and, according to its sequence, is potentially a target of multisite phosphorylation. I am currently investigating whether the initial loading of Asl is indeed controlled through potential

phosphorylation within this region of DSas-4, or whether this short sequence is in itself important for the localization of Asl. In parallel, I also aim to address whether phosphorylation within this region of DSas-4 can be detected *in vivo*, through the combination of mass spectrometry, western blot and immuno-fluorescence approaches.

Alternative regulation mechanisms that might control the timing of Asl incorporation include the regulated stability of cytoplasmic Asl, or the centrosomal binding of another protein that facilitates the interaction between DSas-4 and Asl. I have ruled out the first of these options, because young mother centrioles successfully accumulate cytoplasmic Asl at all stages of the embryonic cell cycle whilst there is no detectable incorporation at engaged daughters. I cannot rule out the second possibility at this stage; however, my results showing that Asl overexpression can drive its early incorporation into daughter centrioles suggests that any protein that might mediate the interaction between DSas-4 and Asl would also have to be present in new centrioles well before late mitosis. Thus, my data suggest that such a control mechanism is overall less likely than the post-translational regulation of the DSas-4-Asl interaction. Importantly, however, such a mechanism could still contribute towards the initial incorporation of Asl, so I aim to also explore this possibility.

It will be interesting to explore whether the function of Asl at mother centrioles is subject to any potential cell cycle–dependent posttranslational regulation that might contribute to efficient control of centriole duplication. I believe that deciphering any such regulation will be very complicated because Asl is also involved in the initiation of PCM recruitment, and is very likely to be regulated in a cell cycle–dependent manner for the purposes of that process. However, establishing whether the function of Asl in centriole duplication is in any way altered at mother centrioles during the cell cycle will be very important to complete our understanding of how this protein really acts in this process.

Finally, I aim address whether Asl might have any molecular roles that are not directly linked to centrosome numbers or function. This hypothesis had emerged as I noticed that flies overexpressing Asl-GFP appear to show physiological defects, even though neither centriole duplication nor PCM recruitment appear to be mis-regulated in these embryos. Furthermore, according to my preliminary observations, the development of these flies appears slower than that of flies that completely lack Asl. To investigate this more closely, I first aim to compare the developmental timing of *asl* null mutant flies with that of isogenic flies that lack centrioles due to the null mutation a different gene, such as *DSas-4* or *Sak*. In parallel, I aim to test whether overexpression of Asl-GFP in a *DSas-4* or *Sak* null mutant background aggravates the phenotypes of these lines. If these studies suggest any potential centriole-independent developmental delays that may be linked to Asl levels, I will address these using the power of *in vivo* imaging assays; using the Fucci system to compare the cell cycle profiles of different genotypes, and twin spot analysis to address their relative cellular fitness.

6.4 CONCLUSIONS

I have shown that the essential centriole duplication protein, Asl, is not incorporated into daughter centrioles during their assembly but is recruited to these around the time when they disengage from their mother, and are about to enter the duplication cycle for the first time as a new mother centriole. Once they have accumulated Asl, mother centrioles do not alter their total Asl levels during their duplication events. The initial recruitment of Asl is dependent on centriolar DSas-4, while a subsequent, DSas-4–independent recruitment step results in the accumulation of a mobile Asl pool at the centrosome. The initial, DSas-4 dependent incorporation of Asl is required to convert disengaged daughter centrioles into mother centrioles that can duplicate for the first time; thus, we have named Asl a primary license of centriole duplication. As the initially acquired Asl molecules are stably incorporated at centrioles, their centriolar loading has a permanent effect; old mother centrioles do not rely on further Asl recruitment to allow their subsequent rounds of duplication. Thus, I have identified a previously unsuspected regulatory role of Asl in the centriole duplication cycle. In the future I aim to develop this study further by investigating how the centriolar presence and function of Asl are regulated in conjunction with cell cycle progression.

REFERENCES

Andersen JS, Wilkinson CJ, Mayor T, Mortensen P, Nigg EA, Mann M. 2003. Proteomic characterization of the human centrosome by protein correlation profiling. *Nature* **426**: 570-574.

Arquint C, Gabryjonczyk AM, Nigg EA. 2014. Centrosomes as signalling centres. *Philosophical transactions of the Royal Society of London Series B, Biological sciences* **369**.

Arquint C, Nigg EA. 2014. STIL microcephaly mutations interfere with APC/C-mediated degradation and cause centriole amplification. *Current biology : CB* **24**: 351-360.

Arquint C, Sonnen KF, Stierhof YD, Nigg EA. 2012. Cell-cycle-regulated expression of STIL controls centriole number in human cells. *Journal of cell science* **125**: 1342-1352.

Azimzadeh J. 2014. Exploring the evolutionary history of centrosomes. *Philosophical transactions of the Royal Society of London Series B, Biological sciences* **369**.

Azimzadeh J, Marshall WF. 2010. Building the centriole. *Current biology : CB* **20**: R816-825.

Barr FA, Sillje HH, Nigg EA. 2004. Polo-like kinases and the orchestration of cell division. *Nature reviews Molecular cell biology* **5**: 429-440.

Barros TP, Kinoshita K, Hyman AA, Raff JW. 2005. Aurora A activates D-TACC-Msps complexes exclusively at centrosomes to stabilize centrosomal microtubules. *The Journal of cell biology* **170**: 1039-1046.

Bassett AR, Tibbit C, Ponting CP, Liu JL. 2013. Highly efficient targeted mutagenesis of Drosophila with the CRISPR/Cas9 system. *Cell reports* **4**: 220-228.

Basto R, Lau J, Vinogradova T, Gardiol A, Woods CG, Khodjakov A, Raff JW. 2006. Flies without centrioles. *Cell* **125**: 1375-1386.

Bell SP, Stillman B. 1992. ATP-dependent recognition of eukaryotic origins of DNA replication by a multiprotein complex. *Nature* **357**: 128-134.

Berdnik D, Knoblich JA. 2002. Drosophila Aurora-A is required for centrosome maturation and actin-dependent asymmetric protein localization during mitosis. *Current biology : CB* **12**: 640-647.

Betschinger J, Knoblich JA. 2004. Dare to be different: asymmetric cell division in Drosophila, C. elegans and vertebrates. *Current biology : CB* **14**: R674-685.

Bettencourt-Dias M, Giet R, Sinka R, Mazumdar A, Lock WG, Balloux F, Zafiropoulos PJ, Yamaguchi S, Winter S, Carthew RW et al. 2004. Genome-wide survey of protein kinases required for cell cycle progression. *Nature* **432**: 980-987.

Bettencourt-Dias M, Hildebrandt F, Pellman D, Woods G, Godinho SA. 2011. Centrosomes and cilia in human disease. *Trends in genetics : TIG* **27**: 307-315.

Bettencourt-Dias M, Rodrigues-Martins A, Carpenter L, Riparbelli M, Lehmann L, Gatt MK, Carmo N, Balloux F, Callaini G, Glover DM. 2005. SAK/PLK4 is required for centriole duplication and flagella development. *Current biology : CB* **15**: 2199-2207.

Bienkowska D, Cowan CR. 2012. Centrosomes can initiate a polarity axis from any position within one-cell C. elegans embryos. *Current biology : CB* **22**: 583-589.

Blachon S, Gopalakrishnan J, Omori Y, Polyanovsky A, Church A, Nicastro D, Malicki J, Avidor-Reiss T. 2008. Drosophila asterless and vertebrate Cep152 Are orthologs essential for centriole duplication. *Genetics* **180**: 2081-2094.

Bloodgood RA. 2010. Sensory reception is an attribute of both primary cilia and motile cilia. *Journal of cell science* **123**: 505-509.

Bonaccorsi S, Giansanti MG, Gatti M. 1998. Spindle self-organization and cytokinesis during male meiosis in asterless mutants of Drosophila melanogaster. *The Journal of cell biology* **142**: 751-761.

Bornens M. 2012. The centrosome in cells and organisms. *Science* **335**: 422-426.

Brown NJ, Marjanovic M, Luders J, Stracker TH, Costanzo V. 2013. Cep63 and cep152 cooperate to ensure centriole duplication. *PloS one* **8**: e69986.

Brownlee CW, Klebba JE, Buster DW, Rogers GC. 2011. The Protein Phosphatase 2A regulatory subunit Twins stabilizes Plk4 to induce centriole amplification. *The Journal of cell biology* **195**: 231-243.

Brust-Mascher I, Civelekoglu-Scholey G, Scholey JM. 2014. Analysis of mitotic protein dynamics and function in Drosophila embryos by live cell imaging and quantitative modeling. *Methods Mol Biol* **1136**: 3-30.

Brust-Mascher I, Sommi P, Cheerambathur DK, Scholey JM. 2009. Kinesin-5-dependent poleward flux and spindle length control in Drosophila embryo mitosis. *Molecular biology of the cell* **20**: 1749-1762.

Budde PP, Kumagai A, Dunphy WG, Heald R. 2001. Regulation of Op18 during spindle assembly in Xenopus egg extracts. *The Journal of cell biology* **153**: 149-158.

Buttrick GJ, Beaumont LM, Leitch J, Yau C, Hughes JR, Wakefield JG. 2008. Akt regulates centrosome migration and spindle orientation in the early Drosophila melanogaster embryo. *The Journal of cell biology* **180**: 537-548.

Callaini G, Riparbelli MG. 1990. Centriole and centrosome cycle in the early Drosophila embryo. *Journal of cell science* **97 (Pt 3)**: 539-543.

Callaini G, Whitfield WG, Riparbelli MG. 1997. Centriole and centrosome dynamics during the embryonic cell cycles that follow the formation of the cellular blastoderm in Drosophila. *Experimental cell research* **234**: 183-190.

Carvalho-Santos Z, Azimzadeh J, Pereira-Leal JB, Bettencourt-Dias M. 2011. Evolution: Tracing the origins of centrioles, cilia, and flagella. *The Journal of cell biology* **194**: 165-175.

Carvalho-Santos Z, Machado P, Branco P, Tavares-Cadete F, Rodrigues-Martins A, Pereira-Leal JB, Bettencourt-Dias M. 2010. Stepwise evolution of the centriole-assembly pathway. *Journal of cell science* **123**: 1414-1426.

Chan JY. 2011. A clinical overview of centrosome amplification in human cancers. *International journal of biological sciences* **7**: 1122-1144.

Chang J, Cizmecioglu O, Hoffmann I, Rhee K. 2010. PLK2 phosphorylation is critical for CPAP function in procentriole formation during the centrosome cycle. *The EMBO journal* **29**: 2395-2406.

Chavali PL, Putz M, Gergely F. 2014. Small organelle, big responsibility: the role of centrosomes in development and disease. *Philosophical transactions of the Royal Society of London Series B, Biological sciences* **369**.

Cizmecioglu O, Arnold M, Bahtz R, Settele F, Ehret L, Haselmann-Weiss U, Antony C, Hoffmann I. 2010. Cep152 acts as a scaffold for recruitment of Plk4 and CPAP to the centrosome. *The Journal of cell biology* **191**: 731-739.

Conde C, Caceres A. 2009. Microtubule assembly, organization and dynamics in axons and dendrites. *Nature reviews Neuroscience* **10**: 319-332.

Conduit PT, Brunk K, Dobbelaere J, Dix CI, Lucas EP, Raff JW. 2010. Centrioles regulate centrosome size by controlling the rate of Cnn incorporation into the PCM. *Current biology : CB* **20**: 2178-2186.

Conduit PT, Feng Z, Richens JH, Baumbach J, Wainman A, Bakshi SD, Dobbelaere J, Johnson S, Lea SM, Raff JW. 2014a. The centrosome-specific phosphorylation of Cnn by Polo/Plk1 drives Cnn scaffold assembly and centrosome maturation. *Developmental cell* **28**: 659-669.

Conduit PT, Richens JH, Wainman A, Holder J, Vicente CC, Pratt MB, Dix CI, Novak ZA, Dobbie IM, Schermelleh L et al. 2014b. A molecular mechanism of mitotic centrosome assembly in Drosophila. *eLife*: e03399.

Cook RK, Christensen SJ, Deal JA, Coburn RA, Deal ME, Gresens JM, Kaufman TC, Cook KR. 2012. The generation of chromosomal deletions to provide extensive coverage and subdivision of the Drosophila melanogaster genome. *Genome biology* **13**: R21.

Corbit KC, Shyer AE, Dowdle WE, Gaulden J, Singla V, Chen MH, Chuang PT, Reiter JF. 2008. Kif3a constrains beta-catenin-dependent Wnt signalling through dual ciliary and non-ciliary mechanisms. *Nature cell biology* **10**: 70-76.

Cottee MA, Muschalik N, Wong YL, Johnson CM, Johnson S, Andreeva A, Oegema K, Lea SM, Raff JW, van Breugel M. 2013. Crystal structures of the CPAP/STIL complex reveal its role in centriole assembly and human microcephaly. *eLife* **2**: e01071.

Cottee MA, Raff JW, Lea SM, Roque H. 2011. SAS-6 oligomerization: the key to the centriole? *Nature chemical biology* **7**: 650-653.

Cowan CR, Hyman AA. 2004. Centrosomes direct cell polarity independently of microtubule assembly in C. elegans embryos. *Nature* **431**: 92-96.

Cunha-Ferreira I, Bento I, Pimenta-Marques A, Jana SC, Lince-Faria M, Duarte P, Borrego-Pinto J, Gilberto S, Amado T, Brito D et al. 2013. Regulation of autophosphorylation controls PLK4 self-destruction and centriole number. *Current biology : CB* **23**: 2245-2254.

Cunha-Ferreira I, Rodrigues-Martins A, Bento I, Riparbelli M, Zhang W, Laue E, Callaini G, Glover DM, Bettencourt-Dias M. 2009. The SCF/Slimb ubiquitin ligase limits centrosome amplification through degradation of SAK/PLK4. *Current biology : CB* **19**: 43-49.

Dammermann A, Maddox PS, Desai A, Oegema K. 2008. SAS-4 is recruited to a dynamic structure in newly forming centrioles that is stabilized by the gamma-tubulin-mediated addition of centriolar microtubules. *The Journal of cell biology* **180**: 771-785.

Dammermann A, Muller-Reichert T, Pelletier L, Habermann B, Desai A, Oegema K. 2004. Centriole assembly requires both centriolar and pericentriolar material proteins. *Developmental cell* **7**: 815-829.

Debec A, Sullivan W, Bettencourt-Dias M. 2010. Centrioles: active players or passengers during mitosis? *Cellular and molecular life sciences : CMLS* **67**: 2173-2194.

Delattre M, Canard C, Gonczy P. 2006. Sequential protein recruitment in C. elegans centriole formation. *Current biology : CB* **16**: 1844-1849.

Delattre M, Leidel S, Wani K, Baumer K, Bamat J, Schnabel H, Feichtinger R, Schnabel R, Gonczy P. 2004. Centriolar SAS-5 is required for centrosome duplication in C. elegans. *Nature cell biology* **6**: 656-664.

Diffley JF, Cocker JH, Dowell SJ, Rowley A. 1994. Two steps in the assembly of complexes at yeast replication origins in vivo. *Cell* **78**: 303-316.

Dix CI, Raff JW. 2007. Drosophila Spd-2 recruits PCM to the sperm centriole, but is dispensable for centriole duplication. *Current biology : CB* **17**: 1759-1764.

Dobbelaere J, Josue F, Suijkerbuijk S, Baum B, Tapon N, Raff J. 2008. A genome-wide RNAi screen to dissect centriole duplication and centrosome maturation in Drosophila. *PLoS biology* **6**: e224.

Doxsey S, McCollum D, Theurkauf W. 2005a. Centrosomes in cellular regulation. *Annual review of cell and developmental biology* **21**: 411-434.

Doxsey S, Zimmerman W, Mikule K. 2005b. Centrosome control of the cell cycle. *Trends in cell biology* **15**: 303-311.

Dzhindzhev NS, Tzolovsky G, Lipinszki Z, Schneider S, Lattao R, Fu J, Debski J, Dadlez M, Glover DM. 2014. Plk4 Phosphorylates Ana2 to Trigger Sas6 Recruitment and Procentriole Formation. *Current biology : CB*.

Dzhindzhev NS, Yu QD, Weiskopf K, Tzolovsky G, Cunha-Ferreira I, Riparbelli M, Rodrigues-Martins A, Bettencourt-Dias M, Callaini G, Glover DM. 2010. Asterless is a scaffold for the onset of centriole assembly. *Nature* **467**: 714-718.

Edgar BA, Sprenger F, Duronio RJ, Leopold P, O'Farrell PH. 1994. Distinct molecular mechanism regulate cell cycle timing at successive stages of Drosophila embryogenesis. *Genes & development* **8**: 440-452.

Foe VE, Alberts BM. 1983. Studies of nuclear and cytoplasmic behaviour during the five mitotic cycles that precede gastrulation in Drosophila embryogenesis. *Journal of cell science* **61**: 31-70.

Foe VE, O'Dell, G.M., Edgar, B.A., ed. 1993. *The development of Drosophila melanogaster.* Cold Spring Harbor Laboratory Press.

Fong KW, Choi YK, Rattner JB, Qi RZ. 2008. CDK5RAP2 is a pericentriolar protein that functions in centrosomal attachment of the gamma-tubulin ring complex. *Molecular biology of the cell* **19**: 115-125.

Franz A, Roque H, Saurya S, Dobbelaere J, Raff JW. 2013. CP110 exhibits novel regulatory activities during centriole assembly in Drosophila. *The Journal of cell biology* **203**: 785-799.

Friedlander M, Wahrman J. 1970. The spindle as a basal body distributor. A study in the meiosis of the male silkworm moth, Bombyx mori. *Journal of cell science* **7**: 65-89.

Fry AM, Leaper MJ, Bayliss R. 2014. The primary cilium: guardian of organ development and homeostasis. *Organogenesis* **10**: 62-68.

Fu J, Glover DM. 2012. Structured illumination of the interface between centriole and peri-centriolar material. *Open biology* **2**: 120104.

Ganem NJ, Godinho SA, Pellman D. 2009. A mechanism linking extra centrosomes to chromosomal instability. *Nature* **460**: 278-282.

Gavin KA, Hidaka M, Stillman B. 1995. Conserved initiator proteins in eukaryotes. *Science* **270**: 1667-1671.

Gerdes JM, Davis EE, Katsanis N. 2009. The vertebrate primary cilium in development, homeostasis, and disease. *Cell* **137**: 32-45.

Gerdes JM, Liu Y, Zaghloul NA, Leitch CC, Lawson SS, Kato M, Beachy PA, Beales PL, DeMartino GN, Fisher S et al. 2007. Disruption of the basal body compromises proteasomal function and perturbs intracellular Wnt response. *Nature genetics* **39**: 1350-1360.

Gergely F, Kidd D, Jeffers K, Wakefield JG, Raff JW. 2000. D-TACC: a novel centrosomal protein required for normal spindle function in the early Drosophila embryo. *The EMBO journal* **19**: 241-252.

Giet R, McLean D, Descamps S, Lee MJ, Raff JW, Prigent C, Glover DM. 2002. Drosophila Aurora A kinase is required to localize D-TACC to centrosomes and to regulate astral microtubules. *The Journal of cell biology* **156**: 437-451.

Gilbert SF, ed. 2000. *Developmental Biology, 6th edition*.

Godinho SA, Pellman D. 2014. Causes and consequences of centrosome abnormalities in cancer. *Philosophical transactions of the Royal Society of London Series B, Biological sciences* **369**.

Godinho SA, Picone R, Burute M, Dagher R, Su Y, Leung CT, Polyak K, Brugge JS, Thery M, Pellman D. 2014. Oncogene-like induction of cellular invasion from centrosome amplification. *Nature* **510**: 167-171.

Goetz SC, Anderson KV. 2010. The primary cilium: a signalling centre during vertebrate development. *Nature reviews Genetics* **11**: 331-344.

Gomez-Ferreria MA, Rath U, Buster DW, Chanda SK, Caldwell JS, Rines DR, Sharp DJ. 2007. Human Cep192 is required for mitotic centrosome and spindle assembly. *Current biology : CB* **17**: 1960-1966.

Gomez-Ferreria MA, Sharp DJ. 2008. Cep192 and the generation of the mitotic spindle. *Cell Cycle* **7**: 1507-1510.

Gonczy P. 2012. Towards a molecular architecture of centriole assembly. *Nature reviews Molecular cell biology* **13**: 425-435.

Gonczy P, Rose LS. 2005. Asymmetric cell division and axis formation in the embryo. *WormBook : the online review of C elegans biology*: 1-20.

Gonzalez C, Tavosanis G, Mollinari C. 1998. Centrosomes and microtubule organisation during Drosophila development. *Journal of cell science* **111 (Pt 18)**: 2697-2706.

Gopalakrishnan J, Chim YC, Ha A, Basiri ML, Lerit DA, Rusan NM, Avidor-Reiss T. 2012. Tubulin nucleotide status controls Sas-4-dependent pericentriolar material recruitment. *Nature cell biology* **14**: 865-873.

Gopalakrishnan J, Mennella V, Blachon S, Zhai B, Smith AH, Megraw TL, Nicastro D, Gygi SP, Agard DA, Avidor-Reiss T. 2011. Sas-4 provides a scaffold for cytoplasmic complexes and tethers them in a centrosome. *Nature communications* **2**: 359.

Goulas S, Conder R, Knoblich JA. 2012. The Par complex and integrins direct asymmetric cell division in adult intestinal stem cells. *Cell stem cell* **11**: 529-540.

Graser S, Stierhof YD, Lavoie SB, Gassner OS, Lamla S, Le Clech M, Nigg EA. 2007. Cep164, a novel centriole appendage protein required for primary cilium formation. *The Journal of cell biology* **179**: 321-330.

Greenspan RJ. 2004. *Fly pushing: The theory and practice of Drosophila genetics.* Cold Spring Harbour Laboratory Press, New York.

Guderian G, Westendorf J, Uldschmid A, Nigg EA. 2010. Plk4 trans-autophosphorylation regulates centriole number by controlling betaTrCP-mediated degradation. *Journal of cell science* **123**: 2163-2169.

Guichard P, Desfosses A, Maheshwari A, Hachet V, Dietrich C, Brune A, Ishikawa T, Sachse C, Gonczy P. 2012. Cartwheel architecture of Trichonympha basal body. *Science* **337**: 553.

Habedanck R, Stierhof YD, Wilkinson CJ, Nigg EA. 2005. The Polo kinase Plk4 functions in centriole duplication. *Nature cell biology* **7**: 1140-1146.

Habermann K, Mirgorodskaya E, Gobom J, Lehmann V, Muller H, Blumlein K, Deery MJ, Czogiel I, Erdmann C, Ralser M et al. 2012. Functional analysis of centrosomal kinase

substrates in Drosophila melanogaster reveals a new function of the nuclear envelope component otefin in cell cycle progression. *Molecular and cellular biology* **32**: 3554-3569.

Han YG, Kim HJ, Dlugosz AA, Ellison DW, Gilbertson RJ, Alvarez-Buylla A. 2009. Dual and opposing roles of primary cilia in medulloblastoma development. *Nature medicine* **15**: 1062-1065.

Hannak E, Kirkham M, Hyman AA, Oegema K. 2001. Aurora-A kinase is required for centrosome maturation in Caenorhabditis elegans. *The Journal of cell biology* **155**: 1109-1116.

Haren L, Stearns T, Luders J. 2009. Plk1-dependent recruitment of gamma-tubulin complexes to mitotic centrosomes involves multiple PCM components. *PloS one* **4**: e5976.

Hassounah NB, Bunch TA, McDermott KM. 2012. Molecular pathways: the role of primary cilia in cancer progression and therapeutics with a focus on Hedgehog signaling. *Clinical cancer research : an official journal of the American Association for Cancer Research* **18**: 2429-2435.

Hatch EM, Kulukian A, Holland AJ, Cleveland DW, Stearns T. 2010. Cep152 interacts with Plk4 and is required for centriole duplication. *The Journal of cell biology* **191**: 721-729.

Hilbert M, Erat MC, Hachet V, Guichard P, Blank ID, Fluckiger I, Slater L, Lowe ED, Hatzopoulos GN, Steinmetz MO et al. 2013. Caenorhabditis elegans centriolar protein SAS-6 forms a spiral that is consistent with imparting a ninefold symmetry. *Proceedings of the National Academy of Sciences of the United States of America* **110**: 11373-11378.

Hinchcliffe EH, Li C, Thompson EA, Maller JL, Sluder G. 1999. Requirement of Cdk2-cyclin E activity for repeated centrosome reproduction in Xenopus egg extracts. *Science* **283**: 851-854.

Hirono M. 2014. Cartwheel assembly. *Philosophical transactions of the Royal Society of London Series B, Biological sciences* **369**.

Hirota T, Kunitoku N, Sasayama T, Marumoto T, Zhang D, Nitta M, Hatakeyama K, Saya H. 2003. Aurora-A and an interacting activator, the LIM protein Ajuba, are required for mitotic commitment in human cells. *Cell* **114**: 585-598.

Hodges ME, Scheumann N, Wickstead B, Langdale JA, Gull K. 2010. Reconstructing the evolutionary history of the centriole from protein components. *Journal of cell science* **123**: 1407-1413.

Holland AJ, Lan W, Niessen S, Hoover H, Cleveland DW. 2010. Polo-like kinase 4 kinase activity limits centrosome overduplication by autoregulating its own stability. *The Journal of cell biology* **188**: 191-198.

Hoyer-Fender S. 2010. Centriole maturation and transformation to basal body. *Seminars in cell & developmental biology* **21**: 142-147.

Huang J, Raff JW. 1999. The disappearance of cyclin B at the end of mitosis is regulated spatially in Drosophila cells. *The EMBO journal* **18**: 2184-2195.

Huang JY, Raff JW. 2002. The dynamic localisation of the Drosophila APC/C: evidence for the existence of multiple complexes that perform distinct functions and are differentially localised. *Journal of cell science* **115**: 2847-2856.

Huangfu D, Liu A, Rakeman AS, Murcia NS, Niswander L, Anderson KV. 2003. Hedgehog signalling in the mouse requires intraflagellar transport proteins. *Nature* **426**: 83-87.

Hung LY, Tang CJ, Tang TK. 2000. Protein 4.1 R-135 interacts with a novel centrosomal protein (CPAP) which is associated with the gamma-tubulin complex. *Molecular and cellular biology* **20**: 7813-7825.

Ibanez-Tallon I, Heintz N, Omran H. 2003. To beat or not to beat: roles of cilia in development and disease. *Human molecular genetics* **12 Spec No 1**: R27-35.

Ibanez-Tallon I, Pagenstecher A, Fliegauf M, Olbrich H, Kispert A, Ketelsen UP, North A, Heintz N, Omran H. 2004. Dysfunction of axonemal dynein heavy chain Mdnah5 inhibits ependymal flow and reveals a novel mechanism for hydrocephalus formation. *Human molecular genetics* **13**: 2133-2141.

Ishikawa H, Kubo A, Tsukita S, Tsukita S. 2005. Odf2-deficient mother centrioles lack distal/subdistal appendages and the ability to generate primary cilia. *Nature cell biology* **7**: 517-524.

Jackman M, Lindon C, Nigg EA, Pines J. 2003. Active cyclin B1-Cdk1 first appears on centrosomes in prophase. *Nature cell biology* **5**: 143-148.

Kalay E, Yigit G, Aslan Y, Brown KE, Pohl E, Bicknell LS, Kayserili H, Li Y, Tuysuz B, Nurnberg G et al. 2011. CEP152 is a genome maintenance protein disrupted in Seckel syndrome. *Nature genetics* **43**: 23-26.

Karr TL, Alberts BM. 1986. Organization of the cytoskeleton in early Drosophila embryos. *The Journal of cell biology* **102**: 1494-1509.

Keil TA. 2012. Sensory cilia in arthropods. *Arthropod structure & development* **41**: 515-534.

Kemp CA, Kopish KR, Zipperlen P, Ahringer J, O'Connell KF. 2004. Centrosome maturation and duplication in C. elegans require the coiled-coil protein SPD-2. *Developmental cell* **6**: 511-523.

Khodjakov A, Rieder CL. 1999. The sudden recruitment of gamma-tubulin to the centrosome at the onset of mitosis and its dynamic exchange throughout the cell cycle, do not require microtubules. *The Journal of cell biology* **146**: 585-596.

Kim TS, Park JE, Shukla A, Choi S, Murugan RN, Lee JH, Ahn M, Rhee K, Bang JK, Kim BY et al. 2013. Hierarchical recruitment of Plk4 and regulation of centriole biogenesis by two centrosomal scaffolds, Cep192 and Cep152. *Proceedings of the National Academy of Sciences of the United States of America* **110**: E4849-4857.

Kirkham M, Muller-Reichert T, Oegema K, Grill S, Hyman AA. 2003. SAS-4 is a C. elegans centriolar protein that controls centrosome size. *Cell* **112**: 575-587.

Kitagawa D, Vakonakis I, Olieric N, Hilbert M, Keller D, Olieric V, Bortfeld M, Erat MC, Fluckiger I, Gonczy P et al. 2011. Structural basis of the 9-fold symmetry of centrioles. *Cell* **144**: 364-375.

Kleylein-Sohn J, Westendorf J, Le Clech M, Habedanck R, Stierhof YD, Nigg EA. 2007. Plk4-induced centriole biogenesis in human cells. *Developmental cell* **13**: 190-202.

Knoblich JA. 2008. Mechanisms of asymmetric stem cell division. *Cell* **132**: 583-597.

Kobayashi T, Dynlacht BD. 2011. Regulating the transition from centriole to basal body. *The Journal of cell biology* **193**: 435-444.

Kohlmaier G, Loncarek J, Meng X, McEwen BF, Mogensen MM, Spektor A, Dynlacht BD, Khodjakov A, Gonczy P. 2009. Overly long centrioles and defective cell division upon excess of the SAS-4-related protein CPAP. *Current biology : CB* **19**: 1012-1018.

Koivomagi M, Valk E, Venta R, Iofik A, Lepiku M, Balog ER, Rubin SM, Morgan DO, Loog M. 2011. Cascades of multisite phosphorylation control Sic1 destruction at the onset of S phase. *Nature* **480**: 128-131.

Kollman JM, Merdes A, Mourey L, Agard DA. 2011. Microtubule nucleation by gamma-tubulin complexes. *Nature reviews Molecular cell biology* **12**: 709-721.

Kotak S, Gonczy P. 2013. Mechanisms of spindle positioning: cortical force generators in the limelight. *Current opinion in cell biology* **25**: 741-748.

Kuriyama R, Borisy GG. 1981. Microtubule-nucleating activity of centrosomes in Chinese hamster ovary cells is independent of the centriole cycle but coupled to the mitotic cycle. *The Journal of cell biology* **91**: 822-826.

Lacey KR, Jackson PK, Stearns T. 1999. Cyclin-dependent kinase control of centrosome duplication. *Proceedings of the National Academy of Sciences of the United States of America* **96**: 2817-2822.

Lawo S, Hasegan M, Gupta GD, Pelletier L. 2012. Subdiffraction imaging of centrosomes reveals higher-order organizational features of pericentriolar material. *Nature cell biology* **14**: 1148-1158.

Lee KY, Bang SW, Yoon SW, Lee SH, Yoon JB, Hwang DS. 2012. Phosphorylation of ORC2 protein dissociates origin recognition complex from chromatin and replication origins. *The Journal of biological chemistry* **287**: 11891-11898.

Lee MJ, Gergely F, Jeffers K, Peak-Chew SY, Raff JW. 2001. Msps/XMAP215 interacts with the centrosomal protein D-TACC to regulate microtubule behaviour. *Nature cell biology* **3**: 643-649.

Leidel S, Delattre M, Cerutti L, Baumer K, Gonczy P. 2005. SAS-6 defines a protein family required for centrosome duplication in C. elegans and in human cells. *Nature cell biology* **7**: 115-125.

Leidel S, Gonczy P. 2003. SAS-4 is essential for centrosome duplication in C elegans and is recruited to daughter centrioles once per cell cycle. *Developmental cell* **4**: 431-439.

Lettman MM, Wong YL, Viscardi V, Niessen S, Chen SH, Shiau AK, Zhou H, Desai A, Oegema K. 2013. Direct binding of SAS-6 to ZYG-1 recruits SAS-6 to the mother centriole for cartwheel assembly. *Developmental cell* **25**: 284-298.

Leung GC, Hudson JW, Kozarova A, Davidson A, Dennis JW, Sicheri F. 2002. The Sak polo-box comprises a structural domain sufficient for mitotic subcellular localization. *Nature structural biology* **9**: 719-724.

Lindsley DZ, G. 1992. *The genome of Drosophila melanogaster.* . Academic Press.

Loncarek J, Hergert P, Khodjakov A. 2010. Centriole reduplication during prolonged interphase requires procentriole maturation governed by Plk1. *Current biology : CB* **20**: 1277-1282.

Loncarek J, Hergert P, Magidson V, Khodjakov A. 2008. Control of daughter centriole formation by the pericentriolar material. *Nature cell biology* **10**: 322-328.

Lucas EP, Raff JW. 2007. Maintaining the proper connection between the centrioles and the pericentriolar matrix requires Drosophila centrosomin. *The Journal of cell biology* **178**: 725-732.

Lukinavicius G, Lavogina D, Orpinell M, Umezawa K, Reymond L, Garin N, Gonczy P, Johnsson K. 2013. Selective chemical crosslinking reveals a Cep57-Cep63-Cep152 centrosomal complex. *Current biology : CB* **23**: 265-270.

Mahjoub MR. 2013. The importance of a single primary cilium. *Organogenesis* **9**: 61-69.

Mahmood S, Ahmad W, Hassan MJ. 2011. Autosomal Recessive Primary Microcephaly (MCPH): clinical manifestations, genetic heterogeneity and mutation continuum. *Orphanet journal of rare diseases* **6**: 39.

Marshall WF. 2009. Centriole evolution. *Current opinion in cell biology* **21**: 14-19.

Matsumoto Y, Hayashi K, Nishida E. 1999. Cyclin-dependent kinase 2 (Cdk2) is required for centrosome duplication in mammalian cells. *Current biology : CB* **9**: 429-432.

Mennella V, Agard DA, Huang B, Pelletier L. 2014. Amorphous no more: subdiffraction view of the pericentriolar material architecture. *Trends in cell biology* **24**: 188-197.

Mennella V, Keszthelyi B, McDonald KL, Chhun B, Kan F, Rogers GC, Huang B, Agard DA. 2012. Subdiffraction-resolution fluorescence microscopy reveals a domain of the centrosome critical for pericentriolar material organization. *Nature cell biology* **14**: 1159-1168.

Meraldi P, Lukas J, Fry AM, Bartek J, Nigg EA. 1999. Centrosome duplication in mammalian somatic cells requires E2F and Cdk2-cyclin A. *Nature cell biology* **1**: 88-93.

Mitchell DR. 2007. The evolution of eukaryotic cilia and flagella as motile and sensory organelles. *Advances in experimental medicine and biology* **607**: 130-140.

Moritz M, Braunfeld MB, Fung JC, Sedat JW, Alberts BM, Agard DA. 1995a. Three-dimensional structural characterization of centrosomes from early Drosophila embryos. *The Journal of cell biology* **130**: 1149-1159.

Moritz M, Braunfeld MB, Sedat JW, Alberts B, Agard DA. 1995b. Microtubule nucleation by gamma-tubulin-containing rings in the centrosome. *Nature* **378**: 638-640.

Nakazawa Y, Hiraki M, Kamiya R, Hirono M. 2007. SAS-6 is a cartwheel protein that establishes the 9-fold symmetry of the centriole. *Current biology : CB* **17**: 2169-2174.

Nash P, Tang X, Orlicky S, Chen Q, Gertler FB, Mendenhall MD, Sicheri F, Pawson T, Tyers M. 2001. Multisite phosphorylation of a CDK inhibitor sets a threshold for the onset of DNA replication. *Nature* **414**: 514-521.

Nigg EA. 2002. Centrosome aberrations: cause or consequence of cancer progression? *Nature reviews Cancer* **2**: 815-825.

-. 2007. Centrosome duplication: of rules and licenses. *Trends in cell biology* **17**: 215-221.

Nigg EA, Raff JW. 2009. Centrioles, centrosomes, and cilia in health and disease. *Cell* **139**: 663-678.

Novak ZA, Conduit PT, Wainman A, Raff JW. 2014. Asterless licenses daughter centrioles to duplicate for the first time in Drosophila embryos. *Current biology : CB* **24**: 1276-1282.

Novorol C, Burkhardt J, Wood KJ, Iqbal A, Roque C, Coutts N, Almeida AD, He J, Wilkinson CJ, Harris WA. 2013. Microcephaly models in the developing zebrafish retinal neuroepithelium point to an underlying defect in metaphase progression. *Open biology* **3**: 130065.

O'Connell KF, Caron C, Kopish KR, Hurd DD, Kemphues KJ, Li Y, White JG. 2001. The C. elegans zyg-1 gene encodes a regulator of centrosome duplication with distinct maternal and paternal roles in the embryo. *Cell* **105**: 547-558.

O'Connor M, Chia W. 1993. P element-mediated germ-line transformation of Drosophila. *Methods Mol Biol* **18**: 75-85.

Paintrand M, Moudjou M, Delacroix H, Bornens M. 1992. Centrosome organization and centriole architecture: their sensitivity to divalent cations. *Journal of structural biology* **108**: 107-128.

Peel N, Stevens NR, Basto R, Raff JW. 2007. Overexpressing centriole-replication proteins in vivo induces centriole overduplication and de novo formation. *Current biology : CB* **17**: 834-843.

Pelletier L, O'Toole E, Schwager A, Hyman AA, Muller-Reichert T. 2006. Centriole assembly in Caenorhabditis elegans. *Nature* **444**: 619-623.

Pelletier L, Ozlu N, Hannak E, Cowan C, Habermann B, Ruer M, Muller-Reichert T, Hyman AA. 2004. The Caenorhabditis elegans centrosomal protein SPD-2 is required for both pericentriolar material recruitment and centriole duplication. *Current biology : CB* **14**: 863-873.

Peters JM. 2002. The anaphase-promoting complex: proteolysis in mitosis and beyond. *Molecular cell* **9**: 931-943.

Piel M, Meyer P, Khodjakov A, Rieder CL, Bornens M. 2000. The respective contributions of the mother and daughter centrioles to centrosome activity and behavior in vertebrate cells. *The Journal of cell biology* **149**: 317-330.

Pihan GA. 2013. Centrosome dysfunction contributes to chromosome instability, chromoanagenesis, and genome reprograming in cancer. *Frontiers in oncology* **3**: 277.

Qiao R, Cabral G, Lettman MM, Dammermann A, Dong G. 2012. SAS-6 coiled-coil structure and interaction with SAS-5 suggest a regulatory mechanism in C. elegans centriole assembly. *The EMBO journal* **31**: 4334-4347.

Raff JW, Glover DM. 1988. Nuclear and cytoplasmic mitotic cycles continue in Drosophila embryos in which DNA synthesis is inhibited with aphidicolin. *The Journal of cell biology* **107**: 2009-2019.

-. 1989. Centrosomes, and not nuclei, initiate pole cell formation in Drosophila embryos. *Cell* **57**: 611-619.

Raff JW, Jeffers K, Huang JY. 2002. The roles of Fzy/Cdc20 and Fzr/Cdh1 in regulating the destruction of cyclin B in space and time. *The Journal of cell biology* **157**: 1139-1149.

Rebollo E, Sampaio P, Januschke J, Llamazares S, Varmark H, Gonzalez C. 2007. Functionally unequal centrosomes drive spindle orientation in asymmetrically dividing Drosophila neural stem cells. *Developmental cell* **12**: 467-474.

Reiter JF, Blacque OE, Leroux MR. 2012. The base of the cilium: roles for transition fibres and the transition zone in ciliary formation, maintenance and compartmentalization. *EMBO reports* **13**: 608-618.

Rieder CL, Faruki S, Khodjakov A. 2001. The centrosome in vertebrates: more than a microtubule-organizing center. *Trends in cell biology* **11**: 413-419.

Roberts D. 1986. *Drosophila, a practical approach*. IRL Press, Oxford.

Rodrigues-Martins A, Bettencourt-Dias M, Riparbelli M, Ferreira C, Ferreira I, Callaini G, Glover DM. 2007a. DSAS-6 organizes a tube-like centriole precursor, and its absence suggests modularity in centriole assembly. *Current biology : CB* **17**: 1465-1472.

Rodrigues-Martins A, Riparbelli M, Callaini G, Glover DM, Bettencourt-Dias M. 2007b. Revisiting the role of the mother centriole in centriole biogenesis. *Science* **316**: 1046-1050.

Rogers GC, Rusan NM, Roberts DM, Peifer M, Rogers SL. 2009. The SCF Slimb ubiquitin ligase regulates Plk4/Sak levels to block centriole reduplication. *The Journal of cell biology* **184**: 225-239.

Rohatgi R, Snell WJ. 2010. The ciliary membrane. *Current opinion in cell biology* **22**: 541-546.

Satir P, Pedersen LB, Christensen ST. 2010. The primary cilium at a glance. *Journal of cell science* **123**: 499-503.

Schmidt TI, Kleylein-Sohn J, Westendorf J, Le Clech M, Lavoie SB, Stierhof YD, Nigg EA. 2009. Control of centriole length by CPAP and CP110. *Current biology : CB* **19**: 1005-1011.

Seeger-Nukpezah T, Little JL, Serzhanova V, Golemis EA. 2013. Cilia and cilia-associated proteins in cancer. *Drug discovery today Disease mechanisms* **10**: e135-e142.

Shimanovskaya E, Viscardi V, Lesigang J, Lettman MM, Qiao R, Svergun DI, Round A, Oegema K, Dong G. 2014. Structure of the C. elegans ZYG-1 cryptic polo box suggests a conserved mechanism for centriolar docking of Plk4 kinases. *Structure* **22**: 1090-1104.

Siddiqui K, On KF, Diffley JF. 2013. Regulating DNA replication in eukarya. *Cold Spring Harbor perspectives in biology* **5**.

Siegrist SE, Doe CQ. 2007. Microtubule-induced cortical cell polarity. *Genes & development* **21**: 483-496.

Singla V, Reiter JF. 2006. The primary cilium as the cell's antenna: signaling at a sensory organelle. *Science* **313**: 629-633.

Singla V, Romaguera-Ros M, Garcia-Verdugo JM, Reiter JF. 2010. Ofd1, a human disease gene, regulates the length and distal structure of centrioles. *Developmental cell* **18**: 410-424.

Sir JH, Barr AR, Nicholas AK, Carvalho OP, Khurshid M, Sossick A, Reichelt S, D'Santos C, Woods CG, Gergely F. 2011. A primary microcephaly protein complex forms a ring around parental centrioles. *Nature genetics* **43**: 1147-1153.

Slevin LK, Nye J, Pinkerton DC, Buster DW, Rogers GC, Slep KC. 2012. The structure of the plk4 cryptic polo box reveals two tandem polo boxes required for centriole duplication. *Structure* **20**: 1905-1917.

Sluder G, Nordberg JJ. 2004. The good, the bad and the ugly: the practical consequences of centrosome amplification. *Current opinion in cell biology* **16**: 49-54.

Sonnen KF, Gabryjonczyk AM, Anselm E, Stierhof YD, Nigg EA. 2013. Human Cep192 and Cep152 cooperate in Plk4 recruitment and centriole duplication. *Journal of cell science* **126**: 3223-3233.

Sonnen KF, Schermelleh L, Leonhardt H, Nigg EA. 2012. 3D-structured illumination microscopy provides novel insight into architecture of human centrosomes. *Biology open* **1**: 965-976.

Stevens NR, Dobbelaere J, Brunk K, Franz A, Raff JW. 2010. Drosophila Ana2 is a conserved centriole duplication factor. *The Journal of cell biology* **188**: 313-323.

Stevens NR, Raposo AA, Basto R, St Johnston D, Raff JW. 2007. From stem cell to embryo without centrioles. *Current biology : CB* **17**: 1498-1503.

Strnad P, Leidel S, Vinogradova T, Euteneuer U, Khodjakov A, Gonczy P. 2007. Regulated HsSAS-6 levels ensure formation of a single procentriole per centriole during the centrosome duplication cycle. *Developmental cell* **13**: 203-213.

Su TT, Sprenger F, DiGregorio PJ, Campbell SD, O'Farrell PH. 1998. Exit from mitosis in Drosophila syncytial embryos requires proteolysis and cyclin degradation, and is associated with localized dephosphorylation. *Genes & development* **12**: 1495-1503.

Sullivan W, Theurkauf WE. 1995. The cytoskeleton and morphogenesis of the early Drosophila embryo. *Current opinion in cell biology* **7**: 18-22.

Sun T, Hevner RF. 2014. Growth and folding of the mammalian cerebral cortex: from molecules to malformations. *Nature reviews Neuroscience* **15**: 217-232.

Tadros W, Lipshitz HD. 2009. The maternal-to-zygotic transition: a play in two acts. *Development* **136**: 3033-3042.

Takada S, Kelkar A, Theurkauf WE. 2003. Drosophila checkpoint kinase 2 couples centrosome function and spindle assembly to genomic integrity. *Cell* **113**: 87-99.

Tang CJ, Fu RH, Wu KS, Hsu WB, Tang TK. 2009. CPAP is a cell-cycle regulated protein that controls centriole length. *Nature cell biology* **11**: 825-831.

Tang CJ, Lin SY, Hsu WB, Lin YN, Wu CT, Lin YC, Chang CW, Wu KS, Tang TK. 2011. The human microcephaly protein STIL interacts with CPAP and is required for procentriole formation. *The EMBO journal* **30**: 4790-4804.

Tang N, Marshall WF. 2012. Centrosome positioning in vertebrate development. *Journal of cell science* **125**: 4951-4961.

Tatsumi Y, Ohta S, Kimura H, Tsurimoto T, Obuse C. 2003. The ORC1 cycle in human cells: I. cell cycle-regulated oscillation of human ORC1. *The Journal of biological chemistry* **278**: 41528-41534.

Terada Y, Uetake Y, Kuriyama R. 2003. Interaction of Aurora-A and centrosomin at the microtubule-nucleating site in Drosophila and mammalian cells. *The Journal of cell biology* **162**: 757-763.

Thomson M, Gunawardena J. 2009. Unlimited multistability in multisite phosphorylation systems. *Nature* **460**: 274-277.

Tobin JL, Beales PL. 2009. The nonmotile ciliopathies. *Genetics in medicine : official journal of the American College of Medical Genetics* **11**: 386-402.

Tsou MF, Stearns T. 2006a. Controlling centrosome number: licenses and blocks. *Current opinion in cell biology* **18**: 74-78.

-. 2006b. Mechanism limiting centrosome duplication to once per cell cycle. *Nature* **442**: 947-951.

Tsou MF, Wang WJ, George KA, Uryu K, Stearns T, Jallepalli PV. 2009. Polo kinase and separase regulate the mitotic licensing of centriole duplication in human cells. *Developmental cell* **17**: 344-354.

Vaizel-Ohayon D, Schejter ED. 1999. Mutations in centrosomin reveal requirements for centrosomal function during early Drosophila embryogenesis. *Current biology : CB* **9**: 889-898.

van Breugel M, Hirono M, Andreeva A, Yanagisawa HA, Yamaguchi S, Nakazawa Y, Morgner N, Petrovich M, Ebong IO, Robinson CV et al. 2011. Structures of SAS-6 suggest its organization in centrioles. *Science* **331**: 1196-1199.

van Breugel M, Wilcken R, McLaughlin SH, Rutherford TJ, Johnson CM. 2014. Structure of the SAS-6 cartwheel hub from Leishmania major. *eLife* **3**: e01812.

Varedi KS, Ventura AC, Merajver SD, Lin XN. 2010. Multisite phosphorylation provides an effective and flexible mechanism for switch-like protein degradation. *PloS one* **5**: e14029.

Varmark H, Llamazares S, Rebollo E, Lange B, Reina J, Schwarz H, Gonzalez C. 2007. Asterless is a centriolar protein required for centrosome function and embryo development in Drosophila. *Current biology : CB* **17**: 1735-1745.

Vas A, Mok W, Leatherwood J. 2001. Control of DNA rereplication via Cdc2 phosphorylation sites in the origin recognition complex. *Molecular and cellular biology* **21**: 5767-5777.

Verloes A, Drunat S, Gressens P, Passemard S. 1993. Primary Autosomal Recessive Microcephalies and Seckel Syndrome Spectrum Disorders. in *GeneReviews(R)* (eds. RA Pagon, MP Adam, HH Ardinger, TD Bird, CR Dolan, CT Fong, RJH Smith, K Stephens), Seattle (WA).

Vidwans SJ, Wong ML, O'Farrell PH. 1999. Mitotic regulators govern progress through steps in the centrosome duplication cycle. *The Journal of cell biology* **147**: 1371-1378.

Wakefield JG, Huang JY, Raff JW. 2000. Centrosomes have a role in regulating the destruction of cyclin B in early Drosophila embryos. *Current biology : CB* **10**: 1367-1370.

Wang WJ, Soni RK, Uryu K, Tsou MF. 2011. The conversion of centrioles to centrosomes: essential coupling of duplication with segregation. *The Journal of cell biology* **193**: 727-739.

Warn RM, Magrath R, Webb S. 1984. Distribution of F-actin during cleavage of the Drosophila syncytial blastoderm. *The Journal of cell biology* **98**: 156-162.

Warnke S, Kemmler S, Hames RS, Tsai HL, Hoffmann-Rohrer U, Fry AM, Hoffmann I. 2004. Polo-like kinase-2 is required for centriole duplication in mammalian cells. *Current biology : CB* **14**: 1200-1207.

Winey M, O'Toole E. 2014. Centriole structure. *Philosophical transactions of the Royal Society of London Series B, Biological sciences* **369**.

Wloga D, Gaertig J. 2010. Post-translational modifications of microtubules. *Journal of cell science* **123**: 3447-3455.

Wong C, Stearns T. 2003. Centrosome number is controlled by a centrosome-intrinsic block to reduplication. *Nature cell biology* **5**: 539-544.

Wong SY, Seol AD, So PL, Ermilov AN, Bichakjian CK, Epstein EH, Jr., Dlugosz AA, Reiter JF. 2009. Primary cilia can both mediate and suppress Hedgehog pathway-dependent tumorigenesis. *Nature medicine* **15**: 1055-1061.

Zheng X, Gooi LM, Wason A, Gabriel E, Mehrjardi NZ, Yang Q, Zhang X, Debec A, Basiri ML, Avidor-Reiss T et al. 2014. Conserved TCP domain of Sas-4/CPAP is essential for pericentriolar material tethering during centrosome biogenesis. *Proceedings of the National Academy of Sciences of the United States of America* **111**: E354-363.

Zitouni S, Nabais C, Jana SC, Guerrero A, Bettencourt-Dias M. 2014. Polo-like kinases: structural variations lead to multiple functions. *Nature reviews Molecular cell biology* **15**: 433-452.

Zyss D, Gergely F. 2009. Centrosome function in cancer: guilty or innocent? *Trends in cell biology* **19**: 334-346.

APPENDIX

Novak ZA, Conduit PT, Wainman A, Raff JW.:

Asterless licenses daughter centrioles to duplicate for the first time in *Drosophila* embryos.

Current Biology **24** (2014): 1276-1282.

Please cite this article in press as: Novak et al., Asterless Licenses Daughter Centrioles to Duplicate for the First Time in *Drosophila* Embryos, Current Biology (2014), http://dx.doi.org/10.1016/j.cub.2014.04.023

Current Biology *24*, 1–7, June 2, 2014 ©2014 The Authors http://dx.doi.org/10.1016/j.cub.2014.04.023

Report

Asterless Licenses Daughter Centrioles to Duplicate for the First Time in *Drosophila* Embryos

Zsofia A. Novak,[1] Paul T. Conduit,[1] Alan Wainman,[1,2] and Jordan W. Raff[1,*]

[1]Sir William Dunn School of Pathology, University of Oxford, South Parks Road, Oxford OX1 3RE, UK

[2]Oxford Micron Advanced Bioimaging Unit, Department of Biochemistry, University of Oxford, South Parks Road, Oxford OX1 3QU, UK

Summary

Centrioles form centrosomes and cilia, and defects in any of these three organelles are associated with human disease [1]. Centrioles duplicate once per cell cycle, when a mother centriole assembles an adjacent daughter during S phase. Daughter centrioles cannot support the assembly of another daughter until they mature into mothers during the next cell cycle [2–5]. The molecular nature of this daughter-to-mother transition remains mysterious. Pioneering studies in *C. elegans* identified a set of core proteins essential for centriole duplication [6–12], and a similar set have now been identified in other species [10, 13–18]. The protein kinase ZYG-1/Sak/Plk4 recruits the inner centriole cartwheel components SAS-6 and SAS-5/Ana2/STIL, which then recruit SAS-4/CPAP, which in turn helps assemble the outer centriole microtubules [19, 20]. In flies and humans, the Asterless/Cep152 protein interacts with Sak/Plk4 and Sas-4/CPAP and is required for centriole duplication, although its precise role in the assembly pathway is unclear [21–24]. Here, we show that Asl is not incorporated into daughter centrioles as they assemble during S phase but is only incorporated once mother and daughter separate at the end of mitosis. The initial incorporation of Asterless (Asl) is irreversible, requires DSas-4, and, crucially, is essential for daughter centrioles to mature into mothers that can support centriole duplication. We therefore propose a "dual-licensing" model of centriole duplication, in which Asl incorporation provides a permanent primary license to allow new centrioles to duplicate for the first time, while centriole disengagement provides a reduplication license to allow mother centrioles to duplicate again.

Results

Daughter Centrioles Incorporate DSas-4, but Not Asl, during Their Assembly

To better understand how Asl and DSas-4 might function together in fly centriole duplication, we followed the behavior of GFP-fusions of these proteins in centrosomes during the rapid, early, mitotic cycles in living syncytial blastoderm *Drosophila* embryos. For all experiments, we expressed near-endogenous levels of either DSas-4-GFP or Asl-GFP [21] in the absence of the corresponding endogenous protein (Figures S1A and S1B available online).

In early S phase, just after the centrosomes have separated (Figure 1A, t = 0 s), the level of DSas-4-GFP fluorescence was similar at the two centrosomes and gradually increased during S phase, as new daughter centrioles assembled (Figures 1A and 1B). DSas-4-GFP levels plateaued shortly before the start of mitosis (nuclear envelope breakdown [NEB]; Figures 1A and 1B), when new daughter centrioles have reached their full size [25]; the fluorescence then steadily declined as mitosis proceeded. This behavior suggests that a pool of DSas-4 is stably incorporated into daughter centrioles as they form but that some "excess" DSas-4 is recruited during S phase and then lost during mitosis (Figure 1E). Fluorescence recovery after photobleaching (FRAP) experiments strongly supported this interpretation (Figures S1C–S1G).

Previous superresolution microscopy studies have shown that DSas-4 is tightly concentrated at centrioles in fly cells and does not spread into the pericentriolar paterial (PCM); it localizes within an outer ring of Asl that lies at the outer edge of the centrioles [26, 27]. We confirmed that this was also the case for the DSas-4-GFP and Asl-GFP fusion proteins in living embryos using 3D-structured illumination superresolution microscopy (Figures 1G–1I). Note that our superresolution images of DSas-4-GFP and Asl-GFP reveal the localization of the C terminus of both proteins, which are not predicted to colocalize: the C terminus of DSas-4 interacts with the N terminus of the centriole cartwheel protein Ana2 [28] and so would be predicted to lie internally to the C terminus of Asl, which is what we observe. Thus, we are confident that DSas-4-GFP is a bona fide marker of centrioles in these embryos.

In contrast to DSas-4, we observed dramatically different levels of Asl-GFP at the two separating centrioles in early S phase (Figure 1C, t = 0 s). An analysis with the centriole-age marker RFP-PACT [29] revealed that the centrosome that inherited the original mother centriole (hereafter the "old" centrosome) always exhibited more Asl-GFP than the centrosome that inherited the original daughter centriole (hereafter the "new" centrosome) (Figures S2A and S2B). Asl-GFP fluorescence in new centrosomes (Figures 1C and 1D, orange labels) steadily increased throughout S phase and into mitosis. Surprisingly, Asl-GFP fluorescence in the oldest centrosomes (Figures 1C and 1D, blue labels) did not appear to increase at all, even though these old centrosomes formed new daughters during this time. This strongly suggests that new daughter centrioles do not incorporate Asl-GFP while they assemble and that the incorporation of Asl-GFP we observe at new centrosomes (orange labels, Figures 1C and 1D) must be due to incorporation at the new mother centrioles (Figure 1F). We conclude that although Asl is essential for centriole duplication [21], Asl-GFP is surprisingly not incorporated into daughter centrioles as they assemble during S phase but only starts to be incorporated at about the time they separate from their mothers at the end of mitosis.

FRAP analysis of Asl-GFP at old centrosomes (where total GFP fluorescence levels are constant; Figures 1C and 1D) revealed that Asl-GFP fluorescence recovered after bleaching but plateaued at ~50% recovery (Figures S2C and S2D).

*Correspondence: jordan.raff@path.ox.ac.uk

This is an open access article under the CC BY license (http://creativecommons.org/licenses/by/3.0/).

Please cite this article in press as: Novak et al., Asterless Licenses Daughter Centrioles to Duplicate for the First Time in *Drosophila* Embryos, Current Biology (2014), http://dx.doi.org/10.1016/j.cub.2014.04.023

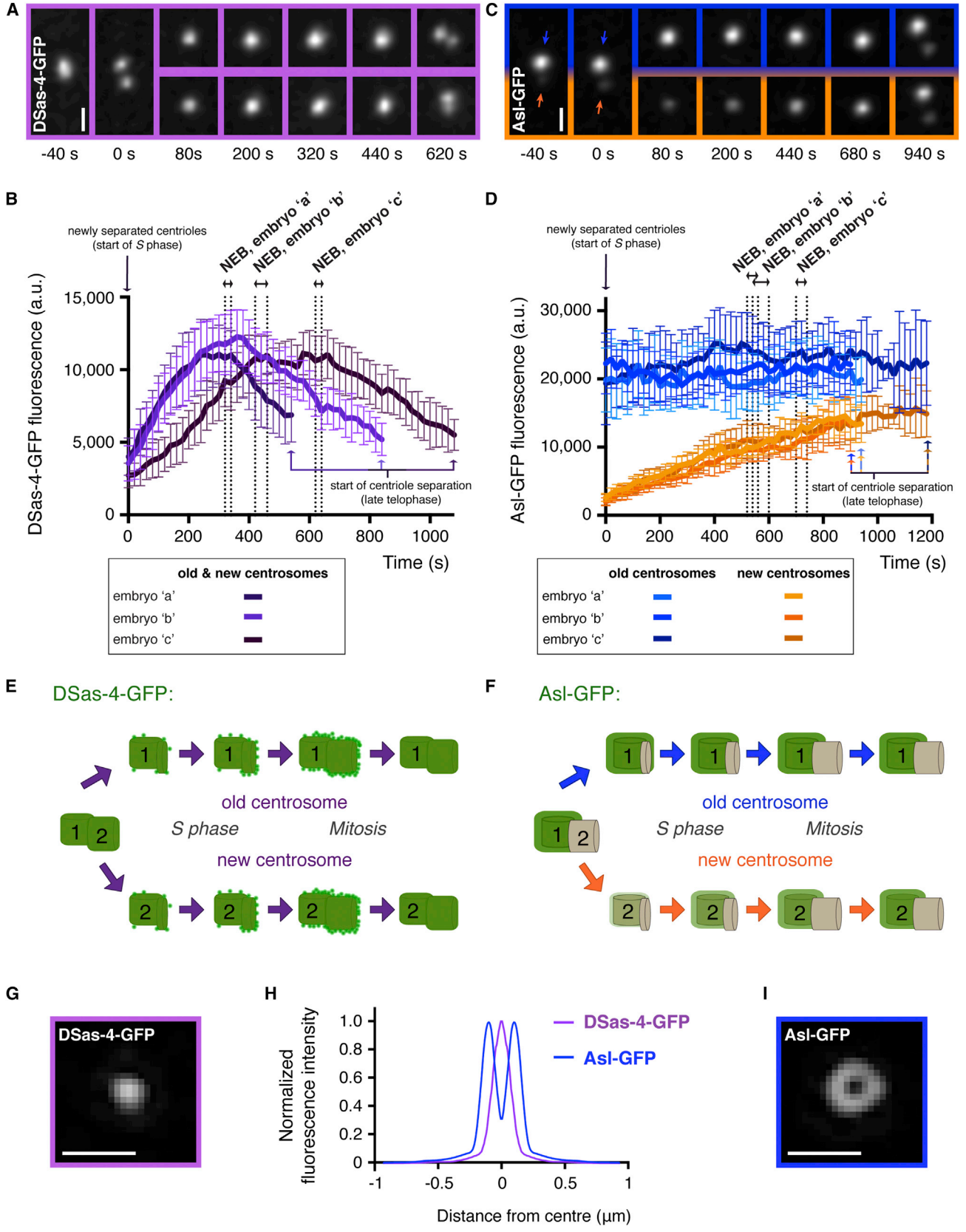


Figure 1. Daughter Centrioles Incorporate DSas-4, but Not Asl, during Their Assembly

(A) Fluorescence images from a time-lapse movie show DSas-4-GFP incorporation into newly separated centrosomes over a single cell cycle; time (s) relative to centriole separation at t = 0 s is indicated. Scale bar, 1 μm.

(legend continued on next page)

Thus, there are two fractions of Asl-GFP at mother centrosomes: ~50% appears to be irreversibly incorporated (hereafter the "immobile" fraction), while ~50% can still exchange with the cytosolic pool (hereafter the "mobile" fraction). Similar results were obtained for new centrosomes, but this analysis was complicated because new centrosomes also incorporate additional Asl-GFP protein during the cell cycle (Figures 1C and 1D and data not shown).

The Initial Incorporation of Asl into Newly Formed Centrioles Depends on DSas-4

The C-terminal region of Asl can interact with the N-terminal region of DSas-4 [22], and superresolution microscopy has revealed that these interacting domains precisely colocalize at the centriole wall [26]. We therefore tested whether DSas-4 might be required to recruit Asl to new centrioles at the end of mitosis.

We injected Texas-red-labeled, affinity-purified antibodies raised against the N-terminal region of DSas-4 (that should interfere with the binding of DSas-4 to Asl; Figure S3A) into embryos expressing Asl-GFP. This was done just as the embryos entered mitosis, when daughter centrioles had fully formed [25] (and so had incorporated DSas-4) but had not yet separated from their mothers (and so had not yet incorporated Asl). The antibodies bound to the centrioles that were close to the injection site (Figure 2A, DSas-4 blocked; Figure S3B), but not to centrioles that were further away from the injection site (Figure 2A, "control"; Figure S3B). By the time the centrioles had separated at the start of S phase (Figures 2B and S3C), Asl-GFP localized to both old and new centrosomes in the control region but failed to localize to the new centrosomes in the DSas-4-antibody-blocked region (Figures 2B and 2C); importantly, new centrosomes were decorated with anti-DSas-4 antibodies, indicating that new centrosomes were present and the new mother centrioles in these centrosomes had successfully incorporated DSas-4. We conclude that DSas-4 is incorporated into new centrioles before Asl and that the anti-DSas-4 antibodies block the interaction between DSas-4 and Asl, and so block the subsequent incorporation of Asl into new centrioles at the end of mitosis (see schematic illustration, Figure 2B). We cannot formally exclude the unlikely possibility, however, that the anti-DSas-4 antibodies block the incorporation of Asl into new centrioles by a mechanism that does not depend on their blocking the interaction of DSas-4 with Asl.

We noticed that the anti-DSas-4 antibodies did not detectably perturb the localization of Asl-GFP in old centrosomes, even though their centrioles were decorated with the antibodies (Figure 2B). FRAP experiments indicated that the mobile fraction of Asl-GFP in old centrosomes continued to turn over with near-normal kinetics, despite the presence of the antibodies (Figure S3D). Thus, although anti-DSas-4 antibodies successfully block the initial recruitment of Asl to new centrioles, they do not block either the recruitment of the mobile Asl fraction to old centrioles or the maintenance of the immobile Asl fraction there.

Asl Incorporation Allows Newly Assembled, Disengaged Centrioles To Duplicate for the First Time

Asl is essential for centriole duplication in flies [21, 30], so we reasoned that its incorporation into newly assembled centrioles might be required to allow them to mature into mothers competent for duplication in the next cell cycle. To investigate this possibility, we needed to specifically block the incorporation of Asl into newly disengaged daughter centrioles. As just described, injections of anti-DSas-4 antibodies did block this incorporation (Figures 2A–2C), and we showed previously that these antibodies also block centriole duplication [17]. Because DSas-4 itself is essential for centriole duplication, however, we could not be sure that it was the lack of Asl incorporation into new centrioles that was blocking their subsequent duplication. We needed to block Asl incorporation without directly interfering with DSas-4 function.

We therefore used Texas-red-labeled, affinity-purified antibodies raised against the C-terminal region of Asl, which should interfere with its binding to DSas-4 (Figure S3A). We injected the antibodies into DSas-4-GFP-expressing embryos that were entering mitosis. The antibodies bound to centrosomes close to the injection site (Figure 2D), and, as the centrosomes separated at the end of mitosis, DSas-4-GFP fluorescence was localized to both old and new centrosomes, indicating that the antibodies did not interfere with the localization of DSas-4-GFP molecules that had already been incorporated into the centrioles at the time of the antibody injection (Figures 2E and 2F). We noticed, however, that the anti-Asl antibodies often decorated only one centrosome of the separating pair (Figure 2E)—presumably the old centrosome, because it contains the original mother centriole that would have already incorporated Asl at the time of the antibody injection. This finding suggests that the antibodies bind to Asl molecules in the mother centrioles but also to Asl molecules in the cytoplasm, thereby blocking their incorporation into the newly assembled centrioles (see schematic illustration, Figure 2E).

To test whether these newly separated centrioles that lacked Asl could support centriole duplication, we compared the incorporation of the centriole marker DSas-4-GFP at old centrosomes (that have inherited an old mother centriole containing both DSas-4 and Asl) and at new centrosomes (that have inherited a new mother centriole containing DSas-4, but not Asl [arrowhead, Figure 2E]). Despite being heavily decorated with anti-Asl antibodies, old centrosomes incorporated additional DSas-4-GFP, indicating that mother centrioles were assembling new daughters (Figures 3 and S3F, blue

(B) Graph shows averaged centrosomal DSas-4-GFP fluorescence (a.u. = arbitrary units) over time from three embryos (>25 centrosomes analyzed in each). Error bars indicate the SD.

(C and D) Images (C) and graph (D) show Asl-GFP incorporation into newly separated centrosomes, presented as in (A) and (B), respectively. Note that new centrosomes (orange box and graph) have not reached as high a level of fluorescence as the old centrosomes (blue box and graph) by the end of the cycle; this is because new centrosomes continue to incorporate some Asl-GFP in the following cell cycle (Figure S2E). For this reason, the analysis of old centrosomes shown here focuses on older (i.e., brighter) centrosomes that had already reached their full brightness (see Figure S2E legend for more detail).

(E and F) Schematic interpretation of how DSas-4-GFP (E) and Asl-GFP (F) incorporate into centrioles.

(G–I) Three-dimensional structured illumination microscopy (3D-SIM) superresolution images of centriolar DSas-4-GFP (G) or Asl-GFP (I) in living embryos (see the Supplemental Experimental Procedures for a full explanation of how these data were obtained and analyzed). Scale bars, 0.5 μm. (H) Graph shows the average centriolar fluorescence intensity profiles of DSas-4-GFP (purple, n = 8) and Asl-GFP (blue, n = 24) in 3D-SIM images. Note that in (E), the immobile fraction of DSas-4-GFP is shown associated with the centrioles, while, for simplicity, the mobile fraction (that subsequently dissociates during mitosis) is shown tightly surrounding the centrioles based on our localization data (G and H).

See also Figures S1 and S2 and the Supplemental Experimental Procedures.

Please cite this article in press as: Novak et al., Asterless Licenses Daughter Centrioles to Duplicate for the First Time in *Drosophila* Embryos, Current Biology (2014), http://dx.doi.org/10.1016/j.cub.2014.04.023

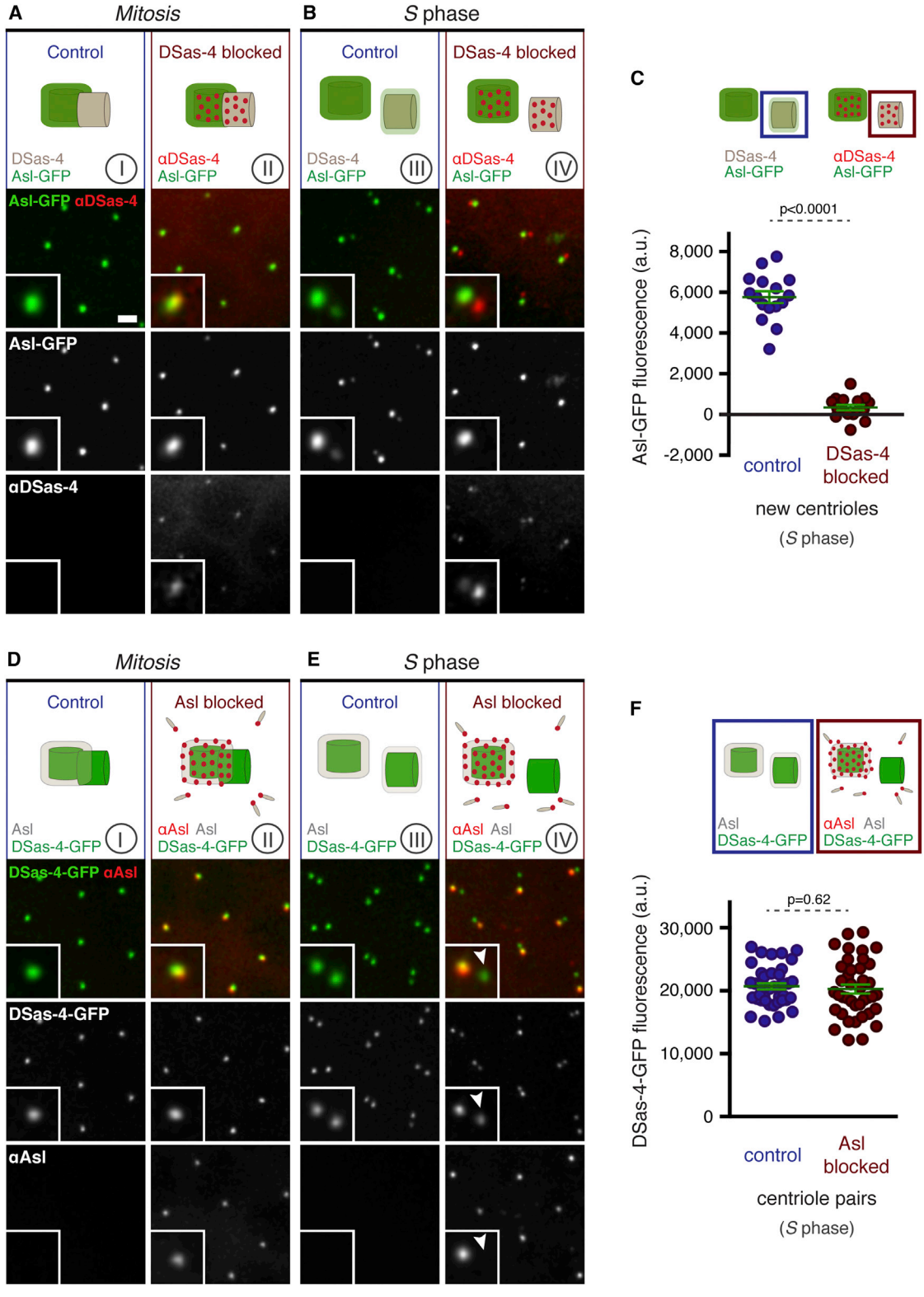


Figure 2. The Initial Incorporation of Asl-GFP into Newly Assembled Centrioles Can Be Inhibited with Anti-DSas-4 or Anti-Asl Antibodies

(A and B) Fluorescence images show two regions ("control" and "DSas-4-blocked") of an embryo expressing Asl-GFP (green) that has been injected with Texas-red-labeled anti-DSas-4 antibodies (red) at the start of mitosis (columns I and II) and several minutes later after the centrioles have separated at the start of S phase (columns III and IV). The control region (columns I and III) is far from the injection site (see Figures S3B and S3C), so no antibodies are detectable; the DSas-4-blocked region (columns II and IV) is close to the injection site, and the antibodies bind to the centrioles. The schematic at the top of each panel illustrates how the DSas-4 antibodies bind to centrioles in mitosis (II) and block the subsequent incorporation of Asl-GFP into the new centriole at the start of S phase, but they do not interfere with Asl-GFP localization at the old centriole (IV).

(legend continued on next page)

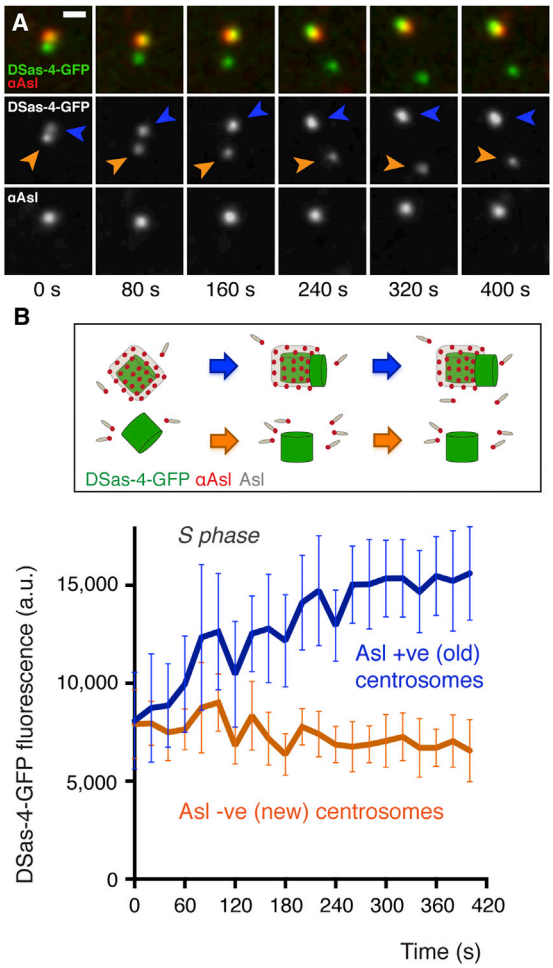


Figure 3. Asl Recruitment to New Centrioles Is Required for Their Duplication

(A) Fluorescence images from a time-lapse movie of an embryo expressing DSas-4-GFP (green) that has been injected with Texas-red-labeled anti-Asl antibodies (red); time (s) relative to centriole separation at t = 0 s is indicated. DSas-4-GFP is incorporated into newly separated old centrosomes (blue arrowheads), even though these centrioles are strongly decorated with anti-Asl antibodies. DSas-4-GFP is not, however, incorporated into newly separated young centrosomes (orange arrowheads), even though no anti-Asl antibodies are detectably binding to these centrosomes. Scale bar, 1 μm.

(B) Graph (with explanatory schematic) quantifies the incorporation of DSas-4-GFP into old anti-Asl-decorated centrosomes (blue line); there is no incorporation into young Asl-negative centrosomes (orange line). Error bars indicate the SEM.

See also Figure S3 and the Supplemental Experimental Procedures.

labels). In contrast, even though new centrosomes were not detectably decorated with anti-Asl antibodies, they did not incorporate any additional DSas-4-GFP, indicating that these new mother centrioles could not assemble daughters (Figures 3 and S3F, orange labels). Thus, new centrioles that lack Asl appear unable to initiate centriole duplication, even though they have disengaged from their mothers and have passed through mitosis.

Discussion

Our observations demonstrate that Asl recruitment to disengaged new centrioles has a critical role in allowing these centrioles to mature into mothers that can duplicate for the first time. During all subsequent duplication cycles, however, mother centrioles already contain a pool of immobile Asl, and this appears to be sufficient to allow subsequent rounds of duplication, because anti-Asl antibodies block the recruitment of the mobile fraction of Asl to mother centrioles (Figure S3E) but do not block their duplication (Figure 3). For an old centriole to duplicate again, therefore, disengagement of the daughter centriole appears to be the crucial licensing event that allows reduplication [4, 5, 31], because immobile Asl incorporation has already occurred. Taken together, our findings suggest a dual-licensing model in which the recruitment of the immobile fraction of Asl by DSas-4 provides an irreversible primary license to allow newly formed centrioles to duplicate for the first time, while centriole disengagement provides a reduplication license [5] to allow older centrioles to duplicate again (Figure 4).

How might Asl perform this primary licensing function? In flies, Asl localizes Sak to centrioles [22], probably explaining why Asl incorporation is a crucial step in converting a disengaged daughter centriole into a mother centriole that can duplicate. Cep152 (human Asl) is also required for the efficient loading of Plk4 (human Sak) onto centrioles in vertebrate cells [22–24], although it appears to share this function with Cep192 (human SPD-2) [32, 33]. Our model is consistent with superresolution microscopy studies on fixed cells, which show that Asl/Cep152 is associated with the mother centriole in an engaged centriole pair [27, 32, 34, 35], suggesting that a similar model may operate in vertebrates. Although the primary and reduplication licensing steps are mechanistically different, we suspect that they share a common purpose: to provide an Asl platform that is competent to recruit Sak to initiate daughter centriole assembly (Figure 4).

Our model can explain why only mother centrioles can support certain types of experimentally induced centriole reduplication, including that induced by Sak overexpression [2, 3] or by ablation of one of the engaged centrioles during an arrested S phase [4]. It can also explain why daughter centrioles appear to have to be "modified" before they can support any duplication [5]; our results strongly suggest that this modification, at least in flies, is Asl incorporation.

How is Asl recruited to centrioles? We speculate that DSas-4 initially recruits the immobile fraction of Asl, which

(C) The graph quantifies Asl-GFP levels in new centrioles in early S phase in the control region and in the DSas-4-blocked region (n = 16 centrioles from three injected embryos), as shown schematically above the graph. Error bars indicate the SEM.

(D and E) Fluorescence images show two regions of an embryo expressing DSas-4-GFP (green) injected with Texas-red-labeled anti-Asl antibodies (red), presented as in (A) and (B) above. The schematics illustrate how the anti-Asl antibodies do not perturb the localization of DSas-4-GFP that is already incorporated into the centrioles at the time of antibody injection but bind the endogenous (nonfluorescent) Asl molecules (gray) in the cytoplasm and so block their incorporation into the new centriole.

(F) The graph quantifies DSas-4-GFP levels in centriole pairs in early S phase in either control or Asl-blocked regions (n = 40 centriole pairs from four embryos), as illustrated schematically above the graph. Note that we compare centriole pairs instead of individual centrioles in this experiment because we cannot distinguish old and young control centrioles based on DSas-4-GFP levels alone. Scale bars, 2 μm. Error bars indicate the SEM.

See also Figure S3 and the Supplemental Experimental Procedures.

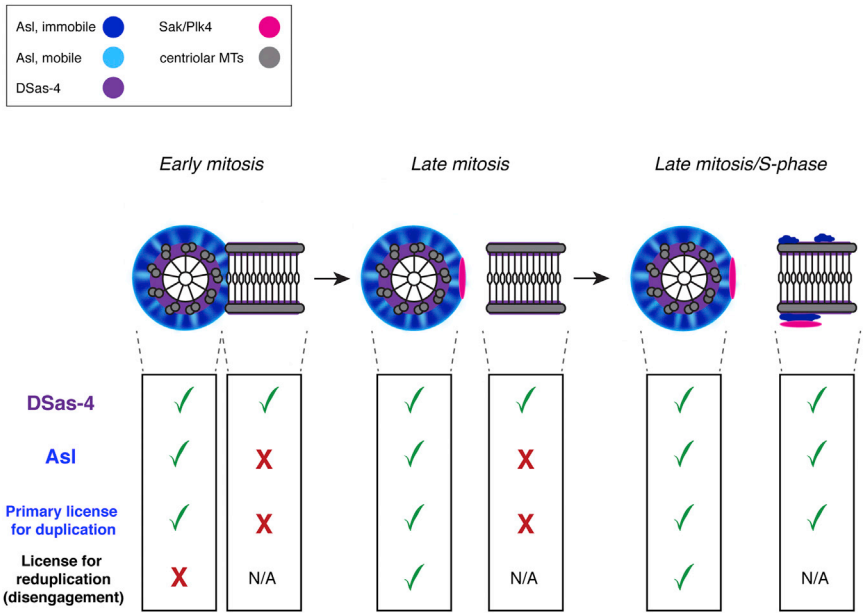


Figure 4. A Dual Licensing Model of Centriole Duplication

The schematic diagrams illustrate a centriole pair, with mother in end-on view (left) and daughter in side-on view (right), as they pass through mitosis. The table below illustrates the state of each centriole in terms of DSas-4 incorporation, Asl incorporation, and whether the centriole has a primary license for its first duplication or a reduplication license for subsequent rounds of duplication. In early mitosis, the mother centriole has incorporated immobile Asl during a previous cell cycle, which irreversibly provided it with a primary license, but it is unable to duplicate again because it lacks a reduplication license, which it will acquire when it disengages from its daughter [4, 5, 37]. The daughter centriole has incorporated DSas-4, but not Asl, and so it lacks a primary license and cannot duplicate until it disengages and matures into a mother. In late mitosis, the centrioles disengage: the mother centriole thereby acquires a reduplication license (speculatively illustrated here by a free "patch" of Sak on its side); the separated daughter centriole cannot duplicate until it starts to incorporate Asl (shown here occurring in late mitosis/S phase), which allows it to recruit Sak for the first time. In *Drosophila* blastoderm embryos, Asl incorporation starts around the time centrioles disengage at the end of mitosis; because centriole disengagement is also closely linked to S phase initiation, we cannot tell whether Asl incorporation is triggered by centriole disengagement or by S phase initiation.

then recruits the mobile fraction. This would explain the 50:50 ratio of immobile to mobile Asl (Figures S2C, S2D, S3D, and S3E). Our finding that anti-Asl antibodies strongly block the recruitment of the mobile fraction of Asl to mother centrosomes (Figure S3E) also supports this possibility. It is tempting to speculate that the mobile fraction of Asl may be important for the previously described role of Asl in mitotic PCM recruitment [22, 29, 36]. It is also interesting to note that only very low levels of Asl seem to be required at new mother centrioles to allow duplication (Figures 1C and 1D).

It remains to be determined what regulates the interaction between DSas-4 and Asl such that Asl is only recruited to daughter centrioles at about the time they separate from their mothers. We speculate that the phosphorylation state of either or both proteins could be altered at the end of mitosis, perhaps increasing the affinity of their interaction. Polo/Plk1 seems to play a crucial part in resetting the reduplication license at old centrioles through the regulation of centriole disengagement [37]; perhaps it also has an important role in the primary licensing of new centrioles by regulating the interaction between DSas-4 and Asl.

Supplemental Information

Supplemental Information includes three figures and Supplemental Experimental Procedures and can be found with this article online at http://dx.doi.org/10.1016/j.cub.2014.04.023.

Acknowledgments

We thank Ian Dobbie, Lothar Schermelleh, and Justin Demmerle from Micron Oxford for help and advice on live 3D structured illumination microscopy imaging. We also thank members of the J.W.R. laboratory and Francis Barr for advice and comments on the manuscript, Saroj Saurya for technical assistance, and Tomer Avidor-Reiss for the Asl-GFP *Drosophila* line. The research was funded by a Wellcome Trust PhD studentship (to Z.A.N.), a Cancer Research UK program grant (C5395/A10530) (to P.T.C., A.W., and J.W.R.), and a Wellcome Trust strategic award (091911) to the Micron Oxford Advanced Bioimaging Unit (for A.W.).

Received: December 22, 2013
Revised: March 11, 2014
Accepted: April 11, 2014
Published: May 15, 2014

References

1. Nigg, E.A., and Raff, J.W. (2009). Centrioles, centrosomes, and cilia in health and disease. Cell *139*, 663–678.
2. Kleylein-Sohn, J., Westendorf, J., Le Clech, M., Habedanck, R., Stierhof, Y.D., and Nigg, E.A. (2007). Plk4-induced centriole biogenesis in human cells. Dev. Cell *13*, 190–202.
3. Cunha-Ferreira, I., Rodrigues-Martins, A., Bento, I., Riparbelli, M., Zhang, W., Laue, E., Callaini, G., Glover, D.M., and Bettencourt-Dias, M. (2009). The SCF/Slimb ubiquitin ligase limits centrosome amplification through degradation of SAK/PLK4. Curr. Biol. *19*, 43–49.
4. Loncarek, J., Hergert, P., Magidson, V., and Khodjakov, A. (2008). Control of daughter centriole formation by the pericentriolar material. Nat. Cell Biol. *10*, 322–328.
5. Wang, W.J., Soni, R.K., Uryu, K., and Tsou, M.F. (2011). The conversion of centrioles to centrosomes: essential coupling of duplication with segregation. J. Cell Biol. *193*, 727–739.
6. Pelletier, L., Ozlü, N., Hannak, E., Cowan, C., Habermann, B., Ruer, M., Müller-Reichert, T., and Hyman, A.A. (2004). The Caenorhabditis elegans centrosomal protein SPD-2 is required for both pericentriolar material recruitment and centriole duplication. Curr. Biol. *14*, 863–873.
7. Kemp, C.A., Kopish, K.R., Zipperlen, P., Ahringer, J., and O'Connell, K.F. (2004). Centrosome maturation and duplication in C. elegans require the coiled-coil protein SPD-2. Dev. Cell *6*, 511–523.
8. O'Connell, K.F., Caron, C., Kopish, K.R., Hurd, D.D., Kemphues, K.J., Li, Y., and White, J.G. (2001). The C. elegans zyg-1 gene encodes a regulator of centrosome duplication with distinct maternal and paternal roles in the embryo. Cell *105*, 547–558.
9. Dammermann, A., Müller-Reichert, T., Pelletier, L., Habermann, B., Desai, A., and Oegema, K. (2004). Centriole assembly requires both centriolar and pericentriolar material proteins. Dev. Cell *7*, 815–829.
10. Leidel, S., Delattre, M., Cerutti, L., Baumer, K., and Gönczy, P. (2005). SAS-6 defines a protein family required for centrosome duplication in C. elegans and in human cells. Nat. Cell Biol. *7*, 115–125.
11. Delattre, M., Leidel, S., Wani, K., Baumer, K., Bamat, J., Schnabel, H., Feichtinger, R., Schnabel, R., and Gönczy, P. (2004). Centriolar SAS-5

is required for centrosome duplication in C. elegans. Nat. Cell Biol. *6*, 656–664.

12. Leidel, S., and Gönczy, P. (2003). SAS-4 is essential for centrosome duplication in C elegans and is recruited to daughter centrioles once per cell cycle. Dev. Cell *4*, 431–439.
13. Bettencourt-Dias, M., Rodrigues-Martins, A., Carpenter, L., Riparbelli, M., Lehmann, L., Gatt, M.K., Carmo, N., Balloux, F., Callaini, G., and Glover, D.M. (2005). SAK/PLK4 is required for centriole duplication and flagella development. Curr. Biol. *15*, 2199–2207.
14. Habedanck, R., Stierhof, Y.D., Wilkinson, C.J., and Nigg, E.A. (2005). The Polo kinase Plk4 functions in centriole duplication. Nat. Cell Biol. *7*, 1140–1146.
15. Stevens, N.R., Dobbelaere, J., Brunk, K., Franz, A., and Raff, J.W. (2010). Drosophila Ana2 is a conserved centriole duplication factor. J. Cell Biol. *188*, 313–323.
16. Arquint, C., Sonnen, K.F., Stierhof, Y.D., and Nigg, E.A. (2012). Cell-cycle-regulated expression of STIL controls centriole number in human cells. J. Cell Sci. *125*, 1342–1352.
17. Basto, R., Lau, J., Vinogradova, T., Gardiol, A., Woods, C.G., Khodjakov, A., and Raff, J.W. (2006). Flies without centrioles. Cell *125*, 1375–1386.
18. Hung, L.Y., Tang, C.J., and Tang, T.K. (2000). Protein 4.1 R-135 interacts with a novel centrosomal protein (CPAP) which is associated with the gamma-tubulin complex. Mol. Cell. Biol. *20*, 7813–7825.
19. Pelletier, L., O'Toole, E., Schwager, A., Hyman, A.A., and Müller-Reichert, T. (2006). Centriole assembly in Caenorhabditis elegans. Nature *444*, 619–623.
20. Delattre, M., Canard, C., and Gönczy, P. (2006). Sequential protein recruitment in C. elegans centriole formation. Curr. Biol. *16*, 1844–1849.
21. Blachon, S., Gopalakrishnan, J., Omori, Y., Polyanovsky, A., Church, A., Nicastro, D., Malicki, J., and Avidor-Reiss, T. (2008). Drosophila asterless and vertebrate Cep152 Are orthologs essential for centriole duplication. Genetics *180*, 2081–2094.
22. Dzhindzhev, N.S., Yu, Q.D., Weiskopf, K., Tzolovsky, G., Cunha-Ferreira, I., Riparbelli, M., Rodrigues-Martins, A., Bettencourt-Dias, M., Callaini, G., and Glover, D.M. (2010). Asterless is a scaffold for the onset of centriole assembly. Nature *467*, 714–718.
23. Cizmecioglu, O., Arnold, M., Bahtz, R., Settele, F., Ehret, L., Haselmann-Weiss, U., Antony, C., and Hoffmann, I. (2010). Cep152 acts as a scaffold for recruitment of Plk4 and CPAP to the centrosome. J. Cell Biol. *191*, 731–739.
24. Hatch, E.M., Kulukian, A., Holland, A.J., Cleveland, D.W., and Stearns, T. (2010). Cep152 interacts with Plk4 and is required for centriole duplication. J. Cell Biol. *191*, 721–729.
25. Callaini, G., and Riparbelli, M.G. (1990). Centriole and centrosome cycle in the early Drosophila embryo. J. Cell Sci. *97*, 539–543.
26. Mennella, V., Keszthelyi, B., McDonald, K.L., Chhun, B., Kan, F., Rogers, G.C., Huang, B., and Agard, D.A. (2012). Subdiffraction-resolution fluorescence microscopy reveals a domain of the centrosome critical for pericentriolar material organization. Nat. Cell Biol. *14*, 1159–1168.
27. Fu, J., and Glover, D.M. (2012). Structured illumination of the interface between centriole and peri-centriolar material. Open Biol. *2*, 120104.
28. Cottee, M.A., Muschalik, N., Wong, Y.L., Johnson, C.M., Johnson, S., Andreeva, A., Oegema, K., Lea, S.M., Raff, J.W., and van Breugel, M. (2013). Crystal structures of the CPAP/STIL complex reveal its role in centriole assembly and human microcephaly. Elife *2*, e01071.
29. Conduit, P.T., Brunk, K., Dobbelaere, J., Dix, C.I., Lucas, E.P., and Raff, J.W. (2010). Centrioles regulate centrosome size by controlling the rate of Cnn incorporation into the PCM. Curr. Biol. *20*, 2178–2186.
30. Dobbelaere, J., Josué, F., Suijkerbuijk, S., Baum, B., Tapon, N., and Raff, J. (2008). A genome-wide RNAi screen to dissect centriole duplication and centrosome maturation in Drosophila. PLoS Biol. *6*, e224.
31. Tsou, M.F., and Stearns, T. (2006). Mechanism limiting centrosome duplication to once per cell cycle. Nature *442*, 947–951.
32. Sonnen, K.F., Gabryjonczyk, A.M., Anselm, E., Stierhof, Y.D., and Nigg, E.A. (2013). Human Cep192 and Cep152 cooperate in Plk4 recruitment and centriole duplication. J. Cell Sci. *126*, 3223–3233.
33. Kim, T.S., Park, J.E., Shukla, A., Choi, S., Murugan, R.N., Lee, J.H., Ahn, M., Rhee, K., Bang, J.K., Kim, B.Y., et al. (2013). Hierarchical recruitment of Plk4 and regulation of centriole biogenesis by two centrosomal scaffolds, Cep192 and Cep152. Proc. Natl. Acad. Sci. USA *110*, E4849–E4857.
34. Sir, J.H., Barr, A.R., Nicholas, A.K., Carvalho, O.P., Khurshid, M., Sossick, A., Reichelt, S., D'Santos, C., Woods, C.G., and Gergely, F. (2011). A primary microcephaly protein complex forms a ring around parental centrioles. Nat. Genet. *43*, 1147–1153.
35. Lukinavičius, G., Lavogina, D., Orpinell, M., Umezawa, K., Reymond, L., Garin, N., Gönczy, P., and Johnsson, K. (2013). Selective chemical crosslinking reveals a Cep57-Cep63-Cep152 centrosomal complex. Curr. Biol. *23*, 265–270.
36. Varmark, H., Llamazares, S., Rebollo, E., Lange, B., Reina, J., Schwarz, H., and Gonzalez, C. (2007). Asterless is a centriolar protein required for centrosome function and embryo development in Drosophila. Curr. Biol. *17*, 1735–1745.
37. Tsou, M.F., Wang, W.J., George, K.A., Uryu, K., Stearns, T., and Jallepalli, P.V. (2009). Polo kinase and separase regulate the mitotic licensing of centriole duplication in human cells. Dev. Cell *17*, 344–354.

Current Biology, Volume *24*

Supplemental Information

Asterless Licenses Daughter Centrioles to Duplicate for the First Time in *Drosophila* Embryos

Zsofia A. Novak, Paul T. Conduit, Alan Wainman, and Jordan W. Raff

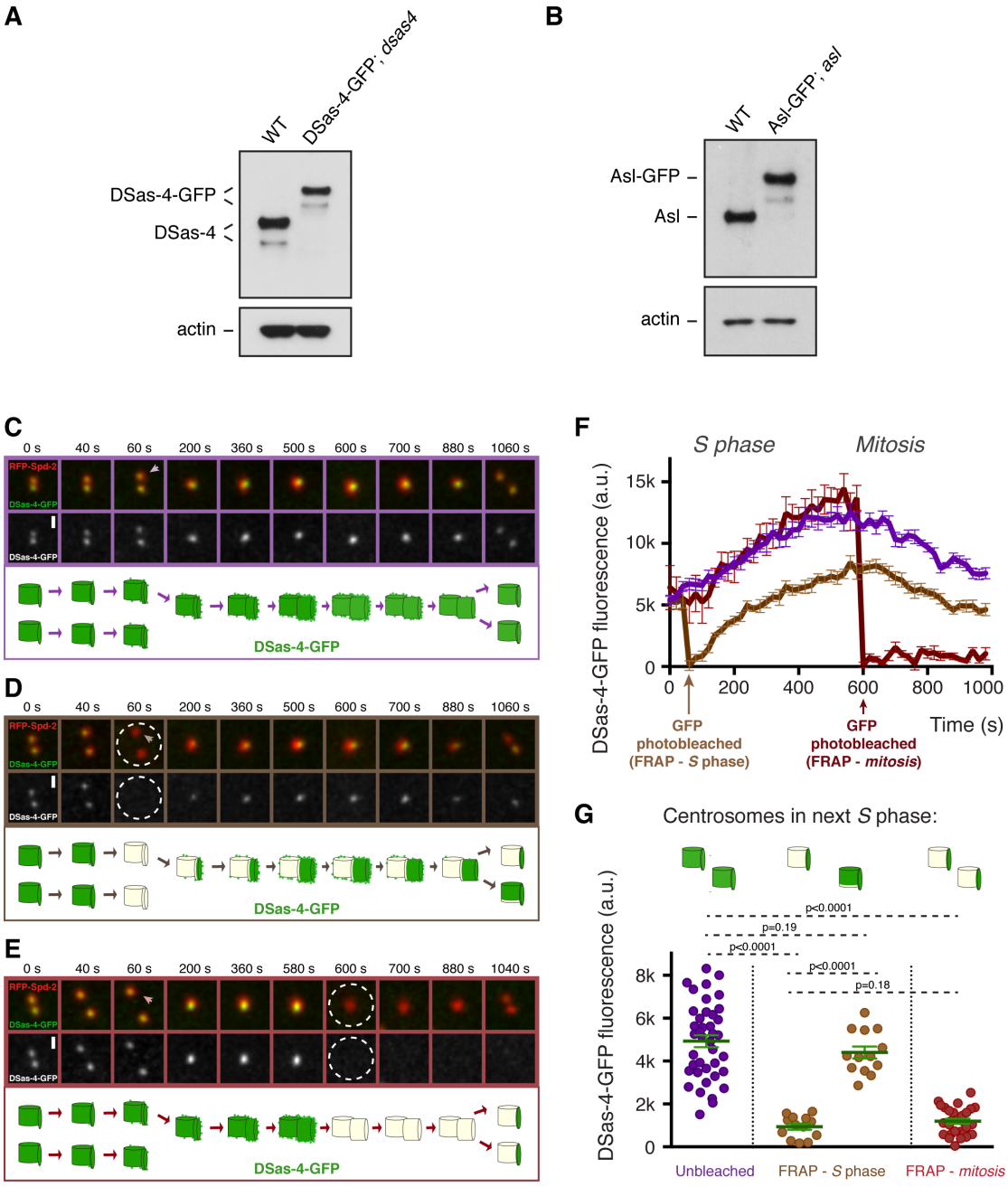


Figure S1. DSas-4-GFP is stably incorporated into growing centrioles during *S*-phase and excess DSas-4-GFP is lost from centrioles during mitosis (related to Figure 1). (A,B) Western blot analyses of embryo extracts shows that, in the embryos used for our analyses, DSas-4-GFP (A) and Asl-GFP (B) are expressed at similar levels to the corresponding endogenous protein in wild-type embryos. Representative blots from 3 independent repeats of each experiment are shown. (C-E) Fluorescence images from time-lapse FRAP movies show DSas-4-GFP (*green* in merged panels)

incorporation into newly separated (t=0s) control (non-bleached) centrosomes (C), centrosomes that were bleached in early *S*-phase (t=60s) (D), or centrosomes that were bleached in mitosis (t=600s) (E). The arrows at t=60s identify the centrosome from the separating pair that was followed in the subsequent panels. These embryos also expressed the centrosome marker RFP-DSpd-2 (*red*) so that centrioles could be followed even after photobleaching. A schematic interpretation of the distribution of DSas-4-GFP at each time point is shown below each set of fluorescence panels. Scale bars: 1μm. (F) Graph shows the quantification through time of DSas-4-GFP fluorescence levels at non-bleached centrosomes (*purple*, n=8 centrosomes from 2 embryos), centrosomes bleached in *S*-phase (*brown*, n=7 centrosomes from 2 embryos) and centrosomes bleached in mitosis (*red*, n=4 centrosomes from 2 embryos). The colours of the lines match the colours of the boxes surrounding the images shown in (C-E). Error bars represent s.e.m. Note how the centrosomes bleached in *S*-phase (*brown* line) show a very similar pattern of incorporation as the control centrosomes (*purple* line), although they are less bright, presumably because the DSas-4-GFP incorporated into the mother centriole does not turn over, and so its fluorescence has been irreversibly bleached (as depicted in the cartoon in (D)). This interpretation is supported by the observation that the centrosomes bleached in mitosis do not detectably incorporate DSas-4-GFP during mitosis. (G) Quantification of centrosomal DSas-4-GFP fluorescence at the start of the next *S*-phase for centrosomes that were unbleached (*purple*, n = 40 centrosomes from 4 embryos), bleached in the previous *S*-phase (*brown*, n = 26 centrosomes from 4 embryos), or bleached in the previous mitosis (red, n = 28 centrosomes from 4 embryos). Error bars represent s.e.m. Note how centrosomes bleached in the previous *S*-phase are highly asymmetric in fluorescence, presumably due to the irreversible bleaching of the mother centriole in *S*-phase.

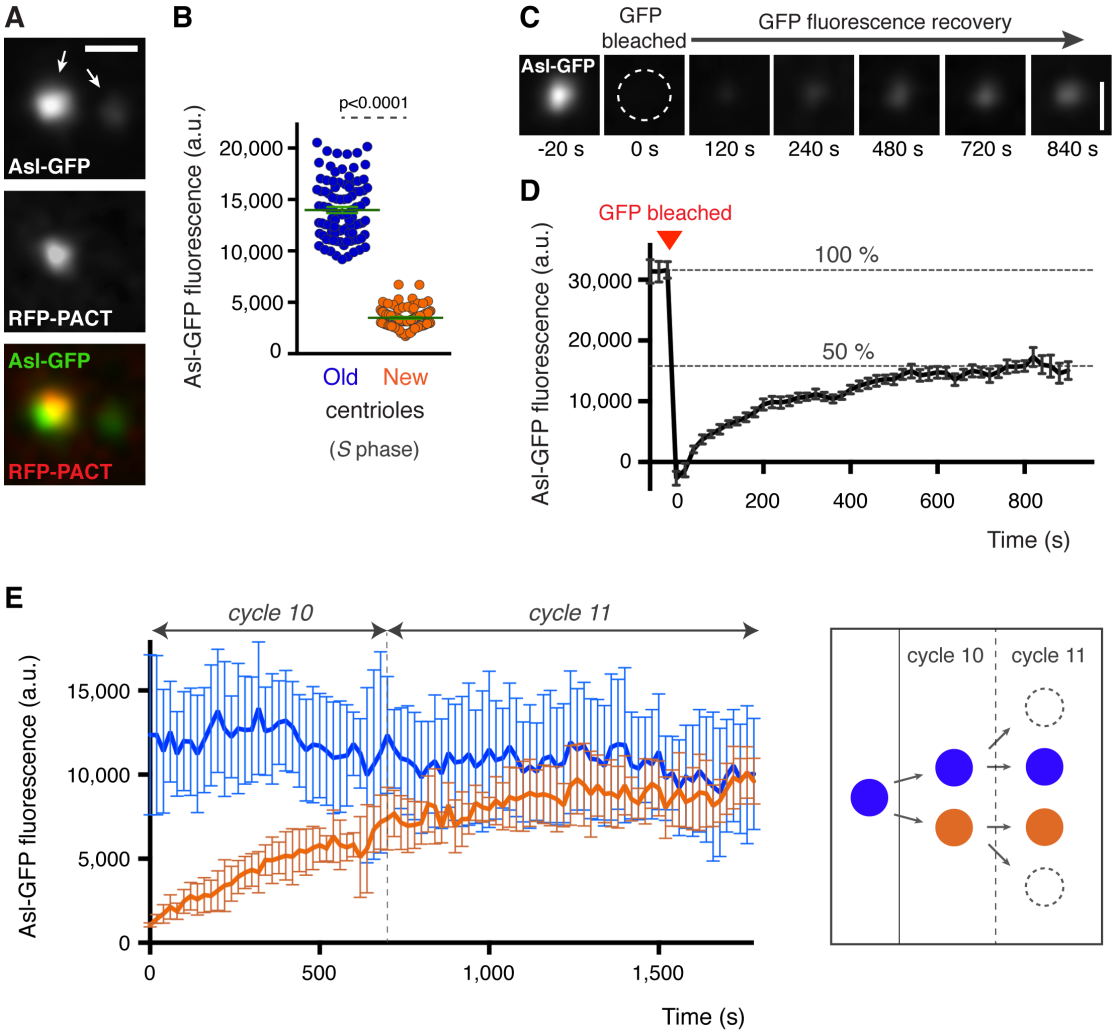


Figure S2. Further characterization of Asl-GFP behavior in living embryos (related to Figure 1).

(A) Images show the levels of Asl-GFP and RFP-PACT in two newly separated centrosomes in early *S*-phase. RFP-PACT fluorescence preferentially marks the older centriole [1], confirming that the centrosome with the older centriole contains more Asl-GFP. Scale bar: 1μm. (B) Graph quantifying Asl-GFP fluorescence levels at old and new centrioles (n=95 centriole pairs from 4 embryos). The old and new centrioles were distinguished based on RFP-PACT fluorescence. Statistical significance was calculated using a paired two-tailed t-test. Error bars represent s.e.m. (C,D) Images (C) and graph (D) show Asl-GFP fluorescence recovery following photobleaching of the Asl-GFP signal at old centrosomes at the start of *S*-phase. Time relative to photobleaching at t=0s is shown under each image. Scale bar: 1μm. Note how Asl-

GFP fluorescence recovers to only ~50% of the original pre-bleached levels; as total Asl-GFP fluorescence levels are not increasing at these centrosomes (Figure 1D, *blue* line), this indicates that ~50% of the Asl-GFP is turning over, while ~50% is immobile. In (D), the averaged fluorescence of 17 centrosomes from 3 embryos is shown. Error bars represent s.e.m. (E) Graph shows the averaged centrosomal Asl-GFP fluorescence (a.u.) over two complete nuclear cycles in a representative embryo (n=7 centrosomes each for old and new centrosomes). Error bars represent s.d. Multiple embryos were analyzed and they each showed the same qualitative result, a single embryo is shown for clarity. The graph illustrates how the old centrosomes (*blue*) maintain a relatively constant level of fluorescence over time, while the new centrosomes (*orange*), gradually accumulate fluorescence over two cycles; fluorescence levels at these new centrosomes plateau at approximately the same level as the old centrosomes towards the end of the second cycle. Because new centrosomes incorporate Asl-GFP over two cycles, if we simply compare the incorporation of Asl at *all* old and new centrosomes (in an unbiased manner), then the old centrosomes, on average, slightly increase in fluorescence due to the incorporation of Asl-GFP into the old centrosomes that are only one cycle old. For this reason, we only compare Asl-GFP levels in new centrosomes and the brightest (i.e., oldest) old centrosomes in Figure 1D (and here in Figure S2E), as these oldest centrosomes have stopped incorporating Asl-GFP. This analysis most clearly reveals that no Asl-GFP is being incorporated into the newly forming daughter centrioles, as the analysis is not complicated by the low level of incorporation into mother centrioles that are only one cell cycle old. Note that, although photobleaching is corrected for in these analyses, the centrosomes get slightly dimmer during the extended time course of these experiments (most easily visualized by the slow decline in fluorescence of the oldest centrosomes (*blue*) in (E)). This is a consistent feature that we see in extended time course experiments with many GFP-fusion proteins, and we suspect it occurs because the autofluorescence of the embryo bleaches more slowly than the GFP fluorescence; thus, our correction for photobleaching (which is based on photobleaching of the whole embryo) slightly under-corrects for the photobleaching of GFP.

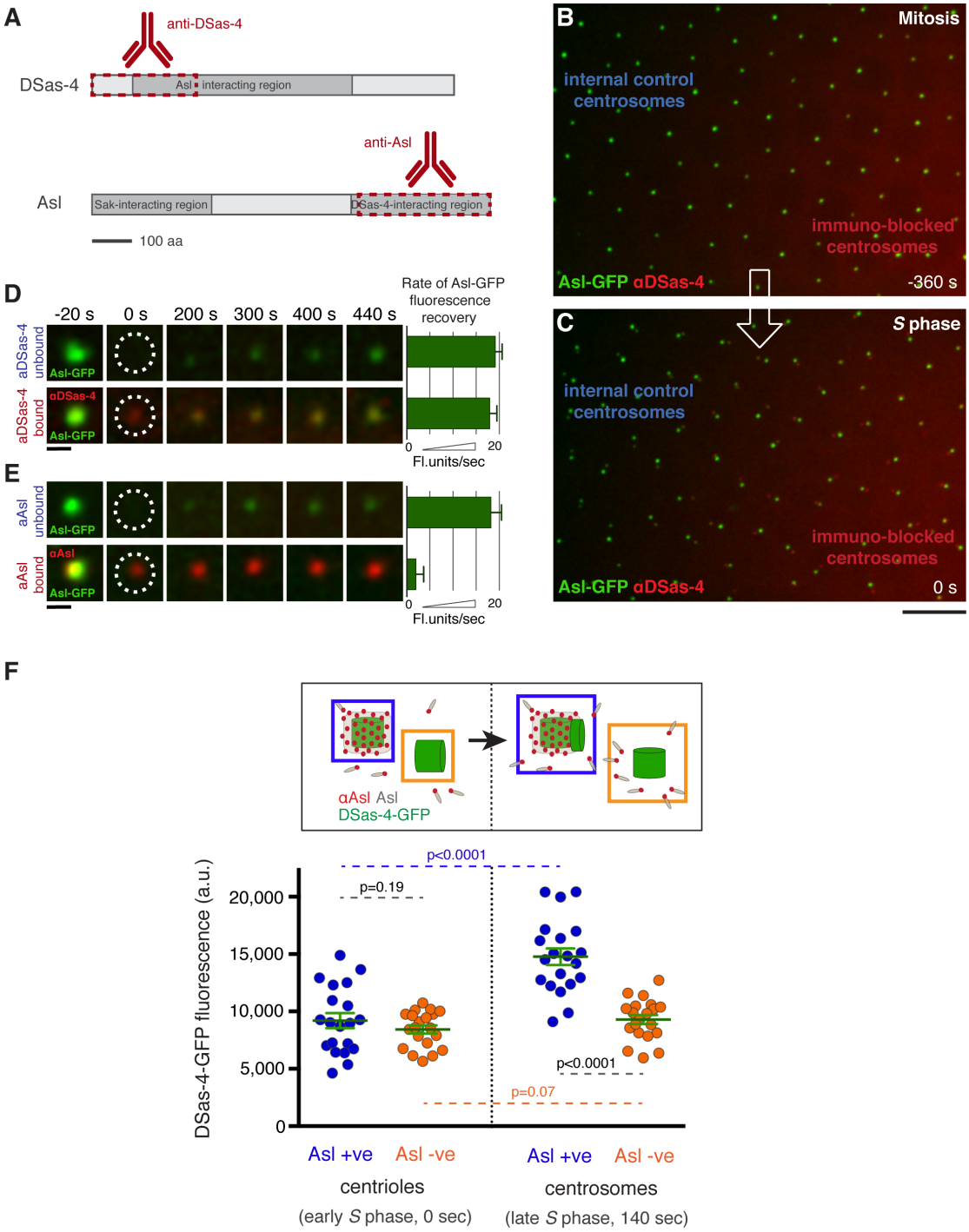


Figure S3. Multiple molecular mechanisms contribute to the recruitment of Asl to centrosomes (related to Figure 2 and Figure 3). (A) Schematic illustration of the regions of DSas-4 and Asl required for their interaction with each other and for the interaction of Asl with Sak/Plk4 [2]. Red boxes indicate the regions of DSas-4 and Asl, respectively, against which the inhibiting antibodies used in our experiments were raised. (B,C) Images show an example of an embryo antibody injection

experiment. The embryo shown here expressed Asl-GFP (*green*) and was injected during mitosis (B) with Texas-Red-labelled anti-DSas-4 antibodies (*red*) in the bottom right corner. The centrosomes close to the injection site are exposed to a high concentration of the antibodies, which binds to the centrosomes; the centrosomes further away show no detectable antibody signal and serve as internal controls. As the centrosomes separate in *S*-phase (C), Asl-GFP is detectable on the new centrosomes in the control area but not near the injection site, where the anti-DSas-4 antibodies decorate the new centrosomes—this is more easily seen in the high magnification images shown in Figure 2A. Scale bar: 10μm. (D,E) Images and graphs show Asl-GFP fluorescence (green) recovery rates following photobleaching of Asl-GFP at old centrosomes, either in a control area or an area near to the injection site following an injection of Texas-Red-labelled antibodies against either DSas-4 (D) or Asl (E); near the injection site, the old centrosomes are decorated with the injected antibodies (red). The initial recovery rates (fluorescence units/sec, during the first 180s after photobleaching) are shown in the graphs to the right of the images. The anti-DSas-4 antibodies (D) do not significantly perturb the turnover of mobile fraction of Asl (n=8 centrosomes from 3 embryos; p=0.58), while the anti-Asl antibodies (E) strongly perturb the turnover of the mobile fraction of Asl (n=8 centrosomes from 3 embryos; p=< 0.0001). Scale bars: 1μm. Error bars represent s.e.m. (F) Graph (with explanatory schematic) showing that old centrioles (that contain Asl—*blue*) and new centrioles (that lack Asl—*orange*) contain similar levels of DSas-4-GFP fluorescence at the time when they first separate and start duplication in early *S*-phase. Later in *S*-phase, the old centrosomes (*blue*) have incorporated additional DSas-4-GFP, indicating that new daughter centrioles have started to assemble, despite the presence of the anti-Asl antibodies; in contrast, the new centrioles (orange) have not incorporated any additional DSas-4, indicating that they are not assembling new daughter centrioles (n=20 centrosomes from 2 embryos for each category). Time relative to centriole separation at t=0 is shown in brackets under the graph. Statistical significance was calculated using a paired two-tailed *t*-test for each comparison. Error bars represent s.e.m.

SUPPLEMENTAL EXPERIMENTAL PROCEDURES

Fly strains and genetics. The Asl-GFP [3] and RFP-PACT [4] constructs used in this study have been described previously. The DSas-4-GFP construct was made by cloning the genetic region of *dsas-4*, from 2kb upstream of the start codon up to the stop codon, into the pUAST-GFPCT vector (Drosophila Genomics Resource Centre, pTWG-1076). The RFP-DSpd-2 construct was generated by cloning the *dspd-2* coding sequence into the pWUbq-RFP(NT) [4] Gateway vector. Transgenic lines were generated at the Department of Genetics, University of Cambridge. For all experiments, Asl-GFP was expressed in an asl^{B46} genetic null mutant background (in which the 5' UTR as well as the first 1775 bp of the *asl* coding region have been deleted — Janina Baumbach, A. W., Z.A.N. and J. W. R., manuscript in preparation), while DSas-4-GFP was expressed in a $sas4^{S2214}$ mutant [5] background.

Microscopy. 1-2h old living embryos were dechorionated by hand on sticky tape, mounted on a thin film of glue (sticky tape dissolved in heptane) on a glass bottom dish, covered with Voltalef oil and imaged immediately at 22^0C. For all imaging experiments shown in this study, with the exception of the super resolultion analysis, embryos were imaged on a Perkin Elmer ERS Spinning Disc confocal system on a Zeiss Axiovert microscope (using a 63x, 1.4NA, oil objective and a charge-coupled device camera: Orca ER, Hamamatsu Photonics). 15-17 confocal sections (0.5µm steps) were collected every 20 seconds. For photobleaching the GFP signal of individual centrosomes, a focused 488nm (when imaging GFP alone) or 440nm laser (when imaging Texas Red or RFP together with GFP) was used. For super resolution analyses (Figure 1 G-I) living embryos were imaged on OMX V3 (GE Healthcare, USA) system (60x, 1.35NA oil objective). 20-23 optical sections were collected to create each image (0.125µm steps).

Image analysis. All images acquired on the Perkin Elmer ERS Spinning Disc confocal system were analysed using Volocity software (Perkin Elmer, USA). To evaluate the changes in Asl-GFP or DSas-4-GFP fluorescence levels during the mitotic cycle, centrosomal fluorescence was calculated as a sum intensity of every centrosomal voxel for each channel (a centrosomal voxel was defined as having an intensity >4.5 standard deviations (SDs) above the mean intensity of all voxels within

the image; this setting was chosen because it selects centrosomal pixels most accurately as judged by eye while allowing consistent thresholding of centrosomal pixels above background fluorescence). Cytoplasmic background fluorescence was then subtracted from centrosomal fluorescence values (background fluorescence within centrosome at timepoint n = mean cytoplasmic fluorescence in timepoint n * number of centrosomal voxels in timepoint n). At each time point centrosomal fluorescence values were corrected for bleaching during sampling using the following method: corrected centrosomal fluorescence at timepoint n = centrosomal fluorescence at timepoint n / (total fluorescence of image at timepoint n/total fluorescence of image at timepoint 1). For DSas-4-GFP, >20 centrosomes were analysed in each of 12 embryos in total (3 embryos (>25 centrosomes each) shown in Figure 1B). For Asl-GFP, 15-25 centrosomes were analysed from each of 10 embryos in total (3 embryos (>15 centrosomes each) shown in Figure 1D).

For comparing Asl-GFP or RFP-PACT levels of centrosomes in *S*-phase (Figure S2B), centrosomal fluorescence was calculated as described above and then local cytoplasmic background fluorescence was subtracted from these values. Fluorescence values of old and young centrosome pairs were compared using a paired *t*-test.

To measure centrosomal Asl-GFP or DSas-4-GFP levels in all antibody-injection experiments (Figures 2C,F; 3B; S3F) or any FRAP experiments (Figures S1F,G; S2D; S3D,E), centrosomal fluorescence was calculated using a different method: we measured the total GFP fluorescence in a boxed region centered around the brightest centrosomal voxel and subtracted the local cytoplasmic background fluorescence. Fluorescence values of inhibited and control centrosomes (Figure 2C,F) were compared using a *t*-test (unpaired). To compare Asl-GFP fluorescence recovery in all antibody-injection experiments (Figure S3D,E) the initial rate of Asl-GFP recovery was calculated by linear regression analysis on fluorescence values measured during the first 180 seconds after photobleaching (10 measurements). A total of 8 centrosomes were analysed from 3 embryos for each group, and recovery rates were compared using a *t*-test (unpaired). To assess DSas-4-GFP recruitment to centrosomes following Asl inhibition, >25 centrosome pairs were analysed from 3 embryos in total. All 3 embryos showed the same qualitative result; in Figure 3B, data from a single embryo (10 Asl-positive and 10 Asl-negative centrosomes) is shown, as the

continuous tracking of Asl-negative centrosomes in the other embryos was more affected by the defective separation and movement of these centrosomes (most likely due to the recruitment of only minimal amounts of PCM in the absence of Asl), in Figure S3F 20 Asl-positive and 20 Asl-negative centrosomes are shown in early (0 sec) and late *S*-phase (140 sec later), from 2 embryos. Fluorescence values were compared using a paired *t*-test.

In all graphs that display data collected from individual embryos (Figure 1B,D; Figure 3B, Figure S2E) the error bars represent s.d., while in all graphs that display data pooled from multiple embryos (Figure 2C,F; Figure S1F,G; S2B,D; Figure S3D,E,F) the error bars represent s.e.m.

All super-resolution images acquired on the OMX V3 system were processed and reconstructed using SoftWorx software. For further analyses, Image J software was used for plotting the distribution of DSas-4-GFP and Asl-GFP within centrosomes. Images were processed as maximum intensity projections; each pixel of the image was sub-divided into 10x10 pixels before the radial intensity profile was calculated from the centre of each centrosome to a 1μm radius; $n_{DSas\text{-}4\text{-}GFP} = 8$ centrosomes; $n_{Asl\text{-}GFP} = 24$ centrosomes. Note that in our analysis of DSas-4-GFP the improved resolution allowed us to visualize centriole pairs at virtually all stages of the cell cycle. For ease of presentation, however, we present an image in Figure 1G where one centriole was below the plane of the other centriole, allowing us to obtain a maximum intensity profile through a single centriole; the average fluorescence intensity profile presented in Figure 1H was obtained from 8 such centrioles. This was not necessary for our analysis of Asl-GFP, as the ring of Asl-GFP was only detectable around one centriole (the mother) in each pair. Note that this super-resolution imaging leads to very rapid bleaching of DSas-4-GFP and Asl-GFP, so we could not perform high quality time lapse super-resolution imaging.

In all experiments, cell cycle stage was determined based on the timing of centrosome separation (indicating the start of *S*-phase) and nuclear envelope breakdown (NEB) (indicating the start of mitosis).

With the exception of Figure 1G,I all fluorescent images shown were obtained after 3D rendering of image data in Volocity, and the Volocity 'smooth zoom filter' was applied to all images. Images shown in Figure 1G,I are maximum intensity projections generated in Image J software with no filter applied.

Antibody injections. Anti-DSas-4 [5] or anti-Asl [1] antibodies used for immuno-inhibition experiments were covalently coupled to Texas Red as described previously [6]. The antibodies were injected into embryos at the onset of mitosis. Embryos were imaged immediately following antibody injection using the spinning disc confocal system described above. For FRAP experiments 3-4 old centrosomes were bleached in *S*-phase both on the side of the embryo closest to the injection site (antibody-blocked) and the side furthest form the injection site (control). Data shown was collated from at least 3 embryos for each experiment (see image analysis section above). We have shown previously that the injection of control IgG antibodies does not detectably interfere with the centrosome cycle or with any other aspect of embryo development [6], and have also shown examples where injected anti-centrosomal antibodies that were bound to centrosomes did not detectably perturb centrosome function [1].

Analysis of protein levels in whole embryo lysates. Embryos were dechorionated by bleach and then fixed in methanol containing 2mM EGTA, incubated in methanol at 4^0C for at least 24h, then re-hydrated in PBS+0.1% Triton X-100. 20 embryos were selected manually and homogenized in a total volume of 25µl SDS sample buffer. 10µl of each sample was separated on 3-8% NuPAGE acrylamide gels (Invitrogen) and then transferred to nitrocellulose membranes (0.2µm pore size, BIO-RAD). Membranes were blocked for 1h at room temperature in blocking solution (PBS+4% milk powder+0.1% Tween-20) before incubation with the primary antibody for 1h at room temperature (antibodies were diluted to 1-5ng/ml in blocking solution). Membranes were washed in PBS+0.1% Tween-20 and incubated with horseradish peroxidase-conjugated secondary antibody (GE Healthcare, diluted 3000-fold in blocking solution) for 45 minutes at room temperature. Following washing in PBS+0.1% Tween-20 membranes were incubated with enhanced chemiluminescent substrate for 1 minute (Thermo Scientific, #34095, diluted 2-5 -fold) and exposed to X-ray film.

SUPPLEMENTAL REFERENCES:

S1. Conduit, P.T., Brunk, K., Dobbelaere, J., Dix, C.I., Lucas, E.P., and Raff, J.W. (2010). Centrioles regulate centrosome size by controlling the rate of Cnn incorporation into the PCM. Curr Biol *20*, 2178-2186.

S2. Dzhindzhev, N.S., Yu, Q.D., Weiskopf, K., Tzolovsky, G., Cunha-Ferreira, I., Riparbelli, M., Rodrigues-Martins, A., Bettencourt-Dias, M., Callaini, G., and Glover, D.M. (2010). Asterless is a scaffold for the onset of centriole assembly. Nature *467*, 714-718.

S3. Blachon, S., Gopalakrishnan, J., Omori, Y., Polyanovsky, A., Church, A., Nicastro, D., Malicki, J., and Avidor-Reiss, T. (2008). Drosophila asterless and vertebrate Cep152 Are orthologs essential for centriole duplication. Genetics *180*, 2081-2094.

S4. Lucas, E.P., and Raff, J.W. (2007). Maintaining the proper connection between the centrioles and the pericentriolar matrix requires Drosophila centrosomin. J Cell Biol *178*, 725-732.

S5. Basto, R., Lau, J., Vinogradova, T., Gardiol, A., Woods, C.G., Khodjakov, A., and Raff, J.W. (2006). Flies without centrioles. Cell *125*, 1375-1386.

S6. Gergely, F., Kidd, D., Jeffers, K., Wakefield, J.G., and Raff, J.W. (2000). D-TACC: a novel centrosomal protein required for normal spindle function in the early Drosophila embryo. EMBO J *19*, 241-252.